CHARACTERIZATION OF LOW MOLECULAR WEIGHT *C*-TYPE CYTOCHROMES IN CYANOBACTERIA AND PLANTS

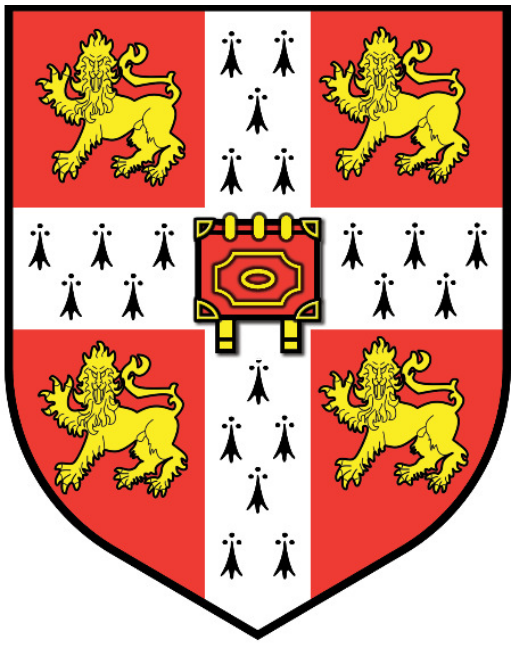

Ravendran Vasudevan

Darwin College

December 2018

This dissertation is submitted for the degree of Doctor of Philosophy

PREFACE

This dissertation is the result of my own work and includes nothing which is the outcome of work done in collaboration except as declared in the Preface and specified in the text. In chapter 4, 5 and 6, the Chlorophyll fluorescence measurements and $P700^{+}$ reduction kinetics were performed in collaboration with Dr. Iskander Ibrahim, in Professor John F Allen lab, Queen Mary University of London,

It is not substantially the same as any that I have submitted, or, is being concurrently submitted for a degree or diploma or other qualification at the University of Cambridge or any other University or similar institution except as declared in the Preface and specified in the text. I further state that no substantial part of my dissertation has already been submitted, or, is being concurrently submitted for any such degree, diploma or other qualification at the University of Cambridge or any other University of similar institution except as declared in the Preface and specified in the text.

It does not exceed the prescribed word limit for the relevant Degree Committee

Ravendran Vasudevan

ACKNOWLEDGEMENTS

I owe my deepest gratitude to Professor Christopher Howe for his constant support, encouragement, feedback and the opportunity to work his laboratory and for continued supervision and guidance throughout my Ph.D.

I would like to thank Professor John F. Allen, Professor P. Dayanandan, Dr Franklin Caesar Thomas, Dr Ellen Nisbet, Dr Paolo Bombelli, Dr. Mathias Soreul, Dr Iskander Ibrahim, Dr Stephen Rowden, and Dr Robert Bradley for invaluable discussion and their generous support. I thank everyone in the Howe laboratory for creating a wonderful working atmosphere.

Thank you to the Ministry of Social Justice and Empowerment Govt of India, selecting me for the National Overseas Scholarship to carry out this project.

And finally, I am eternally grateful to my family: Sudha Ravendran, Kabilan Vasudevan Ravendran, Vasudevan, Pavunammal, Ramesh, Babu, Sudhaker and Anitha, for encouragement and support.

ABSTRACT

Cytochrome c_6 (Cyt c_6) and Plastocyanin (Pc) are two well characterised redox carriers in the thylakoid lumen of cyanobacteria and algae. In cyanobacteria Cyt c_6 or Pc shuttles electrons from the Cyt b_6f complex to Photosystem I (PSI) or the terminal oxidase, and in plants Pc transfers electrons from the Cyt b_6f complex to PSI. Along with Pc or Cyt c_6, additional, poorly uncharacterized, low molecular weight electron carriers have recently been reported in cyanobacteria, algae and higher plants. These are Cyt c_M and Cyt c_{6C}/c_{6B} in cyanobacteria and Cyt c_{6A} in algae and higher plants.

The possible functions of these proteins were investigated using *Arabidopsis* strains in which the Cyt c_{6A} gene was inactivated, and over-expression lines constructed in this work, as well as strains of the cyanobacterium *Synechococcus elongatus* PCC7942 in which the Cyt c_M and Cyt c_{6C} genes had been inactivated, also constructed in this work. The phenotypes of the modified organisms were assessed in different physiological conditions, particularly with regard to their ability to withstand low or high light levels. In addition, chlorophyll fluorescence studies were performed, and transcriptomic analysis was carried out for the cyanobacterial strains.

Impaired growth of the ΔCyt c_{6C} strain was seen under extremely low light or extremely high light, and changes in levels of a large number of transcripts were detected in the mutant. Impaired growth of the ΔCyt c_M strain was also seen under extremely low light levels. Changes in transcript levels in the mutant were also assessed. Cyt c_{6C} and Cyt c_M transcripts were up regulated under high light intensities. ΔCyt c_{6A} *Arabidopsis* strains showed impaired growth at high light intensities, and strains overexpressing Cyt c_{6A} showed impaired growth at low light intensities. Cyt c_{6A}-EYFP fusion protein analysis by confocal microscopy indicated the localization of Cyt c_{6A} fusion protein in the chloroplast, and possibly in the thylakoid lumen.

The findings suggested the presence of possible alternative electron pathways from the plastoquinone (PQ) pool to PSI and/or to the respiratory complexes. These alternative electron pathways assist the organisms to withstand extreme light conditions. It is proposed that in cyanobacteria Cyt c_{6C} accepts electrons directly from the PQ pool and donates them to Pc or directly to PSI bypassing the Cyt b_6f complex, and Cyt c_M accepts electron directly

from the PQ pool, donating them to cytochrome oxidase. In plants, Cyt c_{6A} accepts electron directly from the PQ pool and donates them to Pc and thence to PSI or directly to PSI.

INDEX

LIST OF FIGURES

LIST OF TABLES

Appendices tables **P.No**

LIST OF ABBREVIATIONS

PSI	-	Photosystem I
PSII	-	Photosystem II
Cyt	-	cytochrome
Cyt b_6f complex	-	cytochrome b_6f complex
PQ pool	-	plasto quinol pool
Cyt c_6/*petJ1*	-	cytochrome c_6
PC/*petE*	-	plastocyanin
Cyt c_{6A}	-	cytochrome c_{6A}
Cyt c_{6C}/*petJ2*	-	cytochrome c_{6C}
Cyt c_M/*cytM*	-	cytochrome c_M
cydAB	-	cytochrome *bd* quinol oxidase
COX	-	Cytochrome oxidase
RTOs	-	Respiratory terminal oxidase
ARTOX	-	Alternative terminal oxidase
DNA	-	Deoxyribonucleic acid
PCR	-	Polymerase chain reaction
RT-PCR	-	Reverse transcription polymerase chain reaction
Fv	-	Variable fluorescence
Fm	-	Maximum fluorescence
F_0	-	Minimum fluorescence
qE	-	Heat dissipation
qI	-	Photoinhibition
qP	-	Photochemical quenching
qT	-	State transitions
ΦI	-	Yield of photosystem I
ΦII	-	Yield of photosystem II
Δ	-	knockout/mutant
kb	-	kilobytes
bp	-	base pairs
BG-11 medium	-	Blue green medium
pH	-	potential of hydrogen

°C	-	Degree celsius
OD	-	Optical density
g	-	Gram
µg	-	Microgram
ng/µl	-	nanogram per micro liter
mM	-	Millimolar
µl	-	Micro liter
µM	-	Micro molar
u	-	units
%	-	Percentage
X	-	Concentration
w/v	-	weight/volume
v/v	-	volume/volume
V	-	Volt
E_m value	-	Electromagnetic force value
mV	-	millivolt
µE m^{-2} s^{-1}	-	micro Einsteins per second per square meter
rpm	-	Revolution per minute
xg	-	Time gravity
min	-	minutes
h	-	hour
s	-	Second
UV	-	Ultra violet
WT	-	Wild type
K/O	-	knock out
ΔCyt c_{6C}	-	Cyt c_{6C} knockout
ΔCyt c_M	-	Cyt c_M knockout
ΔCyt c_{6A}	-	Cyt c_{6A} knockout
fig	-	Figure
ATP	-	adenosine triphosphate
$NADP^+$	-	Nicotinamide adenine dinucleotide phosphate oxidized

NADPH	-	Nicotinamide adenine dinucleotide phosphate
reduced		
NADH	-	Nicotinamide adenine dinucleotide
dH_2O	-	distilled water
ddH_2O	-	double distilled water
NH_4Cl	-	Ammonium chloride
$MnCl_2.4H_2O$	-	Manganese chloride
$CaCl_2.2H_2O$	-	Calcium chloride
MES	-	2-(*N*-morpholino) ethanesulfonic acid
$MgCl_2.6H2O$	-	Magnesium chloride
Tris	-	Tris (hydroxymethyl) aminomethane
EDTA	-	Ethylenediaminetetraacetic acid
CO_2	-	Carbon dioxide
$NaHCO_3$	-	Sodium bicarbonate
PBS	-	Phosphate buffer saline
PB	-	Phosphate buffer
(c)DNA	-	(complementary) Deoxyribonucleic acid
(m)RNA	-	(messenger) Ribonucleic acid
35S CaMV 35S	-	promoter of Cauliflower mosaic virus
ADP	-	Adenosine diphosphate
ATP	-	Adenosine triphosphate
P680	-	Photosystem II reaction center
P700	-	Photosystem I reaction center
PAGE	-	Polyacrylamide gel electrophoresis
PAM	-	Pulse-amplitude modulation
PCR	-	Polymerase chain reaction
RNAi	-	RNA-interference
T-DNA	-	Transfer-DNA
TL	-	Thermolysin
UTR	-	Untranslated region
VDE	-	Violaxanthin-de-epoxidase
Y2H	-	Yeast two hybrid assay
ZEP	-	Zeaxanthin-epoxidase

CHAPTER 1 INTRODUCTION

1.1 Photosynthesis

1.1.1 General aspects of Photosynthesis

Photosynthesis is a biological process where the sun's energy is captured by special pigments that convert it to chemical energy in plants, algae and photosynthetic bacteria such as cyanobacteria (Scholes *et al*., 2011; Lea-Smith *et al.*, 2015). This chemical energy is used to synthesize carbohydrates, with generation of reducing equivalents by oxidation of water, and producing oxygen as a by-product (Nelson and Yocum, 2006; Hohmann-Marriott and Blankenship, 2011). Oxygenic photosynthesis in plants, algae and cyanobacteria is accomplished by a series of chemical reactions that occur exclusively in specialized flattened vesicles called the thylakoids. The thylakoid membrane is able to convert the light energy into chemical energy, generating the high energy compound adenosine triphosphate (ATP), and reducing equivalents as nicotinamide adenine dinucleotide phosphate (NADPH). These chemical reactions are catalyzed by two distinct photosystems, photosystem II (PSII) and photosystem I (PSI). The cytochrome $b_6 f$ complex mediates electron flow from PSII to PSI and contributes to the proton gradient across the membrane resulting in the production by ATP synthase of ATP by means of the proton motive force (pmf).

In higher plants thylakoids are differentiated into two distinct membrane structures, the cylindrical stacked structures called grana and the interconnecting membrane regions known as stromal lamellae (Nelson and Ben-Shem, 2004; Nelson and Yocum, 2006). The four membrane protein complexes that function in the light-dependent reactions of photosynthesis are unevenly distributed in the thylakoid, PSI complex is located in the stromal lamellae and the grana margins and is segregated from PSII. PSII is exclusively found in the grana and the ATPase concentrates mainly in the stroma region (Nelson and Ben-Shem, 2004; Nelson and Yocum, 2006). In cyanobacteria the protein complexes are evenly distributed in the thylakoid membrane (there are no stromal lamellae cyanobacteria). Detailed organisation of the cyanobacterial membrane is described in sections 1.2.1 and 1.2.2).

1.2 Ultra structure and electron transport pathways in cyanobacteria

Cyanobacteria (blue green algae) are photoautotrophic and free-living Gram-negative bacteria (figure1.1). They are unusual in being among the very few groups that can perform oxygenic photosynthesis and respiration simultaneously in the same compartment, which may facilitate survival under varying environmental conditions (Vermaas, 2001). Two types of bioenergetically active membranes are found in cyanobacterial cells. The cytoplasmic membrane (CM) contains a respiratory electron transport pathway, although there are also reports of incompletely assembled components of the photosynthetic electron chain present (Smith *et al*., 1992).

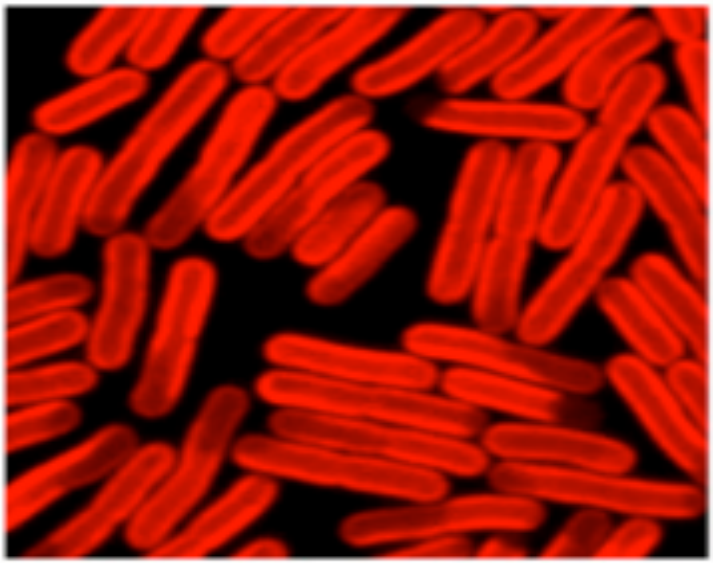

Figure 1.1: Morphology of cyanobacterial cell *Synechococcus elongatus* PCC 7942 (confocal image of chlorophyll autofluorescence, figure taken from Liu *et al*., 2012).

The thylakoid membrane (TM) contains interlinked photosynthetic and respiratory electron transport chains. Analysis of the distribution of terminal oxidases in the model organism *Synechocystis* sp. PCC 6803 indicates the presence of cytochrome *c* oxidase and a cytochrome *bd* quinol oxidase in the TM, and cytochrome *c* oxidase and an alternative respiratory terminal oxidase (ARTO) in the CM (Hart *et al*., 2005; Schultze *et al*., 2009) which function as discussed below. The cytochrome b_6f complex appears to be restricted to the TM (figure1.2).

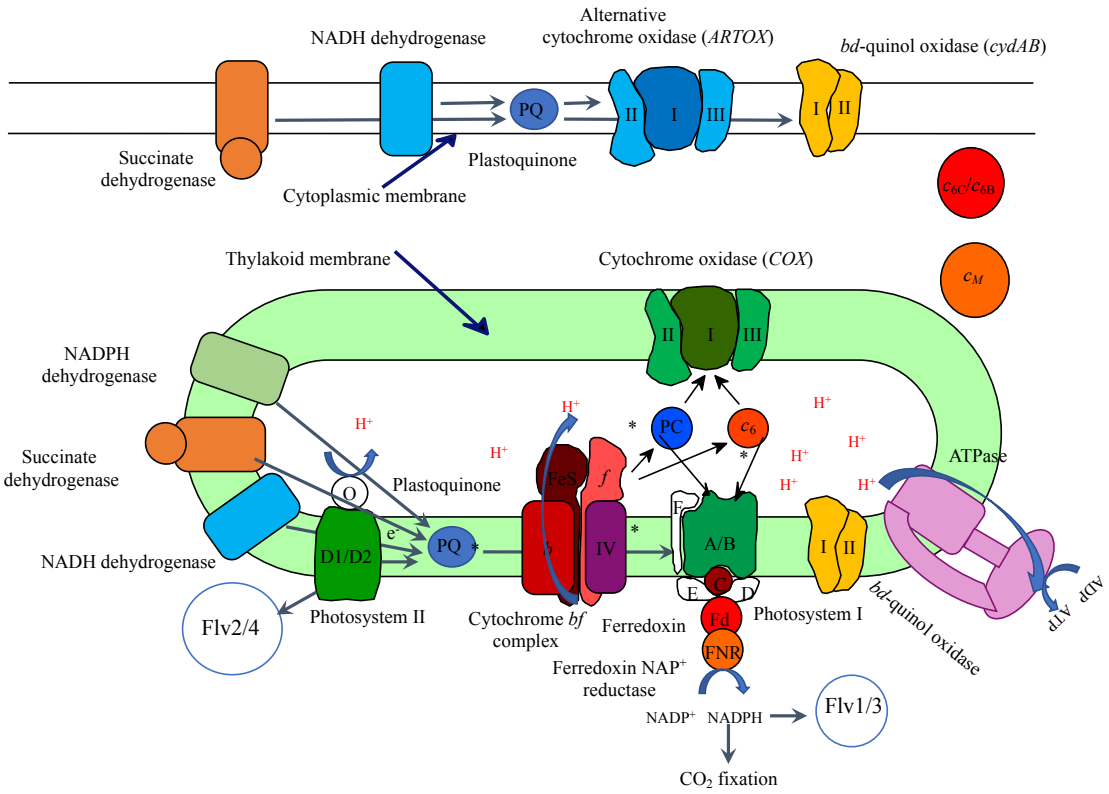

Figure 1.2: Schematic orientation of the photosynthetic and respiratory electron transport components in the membrane of cyanobacteria (Flv2/4: Flavo-diiron proteins 2 and 4, Flv1/3: Flavo-diiron proteins 1 and 3), PQ: Plastoquinone pool, c_M: Cytochrome c_M, c_{6C}/c_{6B}: Cytochrome c_{6C} and Cytochrome c_{6B}.

1.2.1 Photosynthetic electron transport pathway in cyanobacteria

The cyanobacterial thylakoid electron transport chain is more or less similar to that in the chloroplasts of eukaryotic algae and plants. Photosystem II (PSII) splits water molecules using light energy, to generate electrons, protons and oxygen. Electrons generated in PSII are transferred through the plastoquinone pool (PQ pool) to the cytochrome b_6f complex (Cyt b_6/f) and from there to a soluble electron carrier located in the thylakoid lumen (Bialek *et al.*, 2008). In cyanobacteria either plastocyanin (Pc) or cytochrome c_6 (Cyt c_6) may function as the electron carrier between the Cyt b_6/f complex and photosystem I (PSI). Cyt c_6 proteins that function in photosynthesis in cyanobacteria and algae have been largely conserved in their structure and function during the course of evolution. Cyt c_6 is a well-documented mobile carrier in the thylakoid lumenal side of many cyanobacteria and algae (Diaz-Quintana *et al.*, 2003; Lange *et al.*, 2003), and in several organisms under conditions of copper deprivation it may substitute for the copper containing Pc (Bovy *et*

al., 1992; Nakamura *et al*., 2011; Reyes-Sosa *et al*., 2011). Either Pc or Cyt c_6 reduces the oxidized PSI, and from PSI the electron is transferred to ferredoxin, which reduces $NADP^+$ to form NADPH (figure1.3). The photosynthetic electron transport mechanism leads to the formation of a proton gradient across the TM, which is used to generate ATP by ATP synthase (Vermaas, 2001). NADPH and ATP are utilized to fix CO_2 in the Calvin Benson cycle.

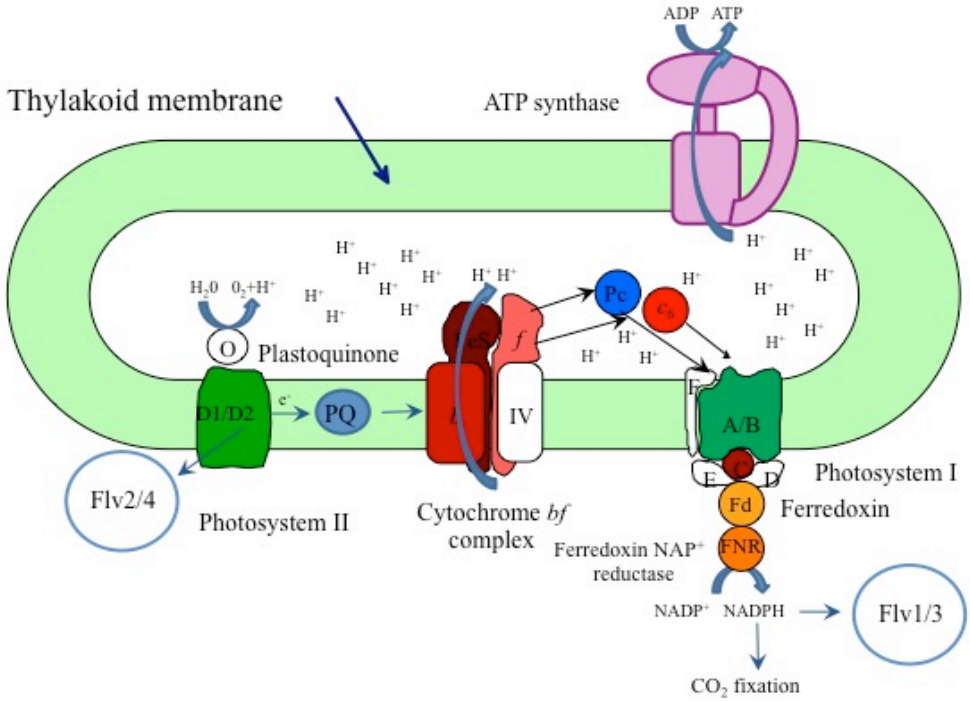

Figure 1.3: Photosynthetic electron transport chain in cyanobacteria. The cyanobacterial linear electron transport pathway shows electrons moving from PSII to PSI via the PQ pool, Cyt b_6f complex and to PSI. The soluble electron carriers in the lumen (cytochrome c_6 (c_6) and plastocyanin (Pc) shuttle electrons between Cyt b_6f complex and PSI. FLVs are the flavo-diiron proteins.

1.2.2 Respiratory electron transport chain in cyanobacteria

Cyanobacteria contain photosynthetic and respiratory electron transport chains in the TM, which imply that the two processes are associated. The model organism *Synechocystis* sp PCC 6803 strain has three classes of respiratory terminal oxidases (RTOs). These are cytochrome *c* oxidase (COX) localized in the TM, the alternative respiratory terminal oxidase (ARTO) in the CM and the cytochrome *bd* quinol oxidase (*cyd*) localized both in the thylakoid and CM (figure 1.4) (Hart *et al*., 2005; Schultze *et al*., 2009).

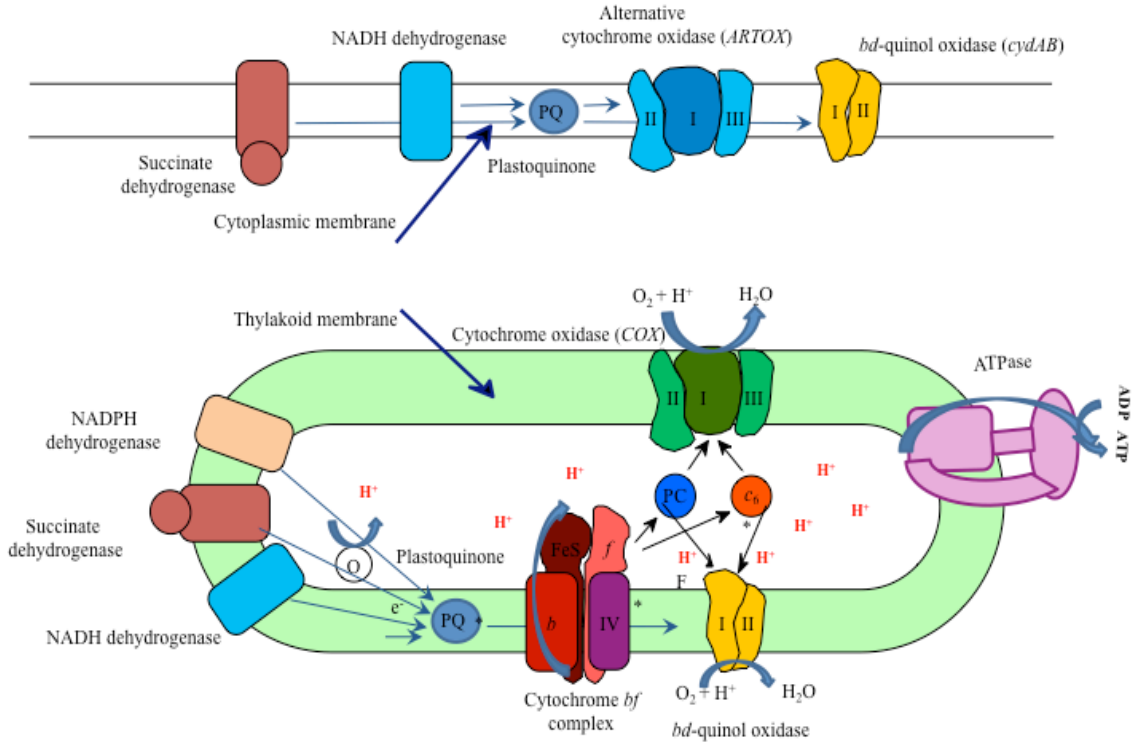

Figure 1.4: Respiratory electron transport chain in cyanobacteria. The respiratory electron transport chain is distributed in both thylakoid and cytoplasmic membrane.

In the cyanobacterial respiratory electron transport chain plastoquinone is the primary electron acceptor from the several dehydrogenase complexes that oxidize NADPH, NADH or succinate (Cooley *et al*., 2001). Electrons are transferred directly to the cytochrome *bd* quinol oxidase (*cyd*), encoded by *cydAB* (Berry *et al*., 2002) or to the alternative terminal oxidase (ARTO), encoded by *ctaII* in the cytoplasmic membrane. Electrons can also be transferred through the Cyt b_6/f and associated redox carrier to PSI or to cytochrome *c* oxidase (COX), encoded by *ctaI*, in the TM (Howitt *et al*., 1998). As previously described, the cytochrome *bd* quinol oxidase is present in both the thylakoid and cytoplasmic membrane, suggesting that the cytochrome *bd* quinol oxidase could be able to energize both thylakoid and cytoplasmic membranes. It has also been suggested that it may function as an addition to the COX to oxidize the over reduced PQ pool under high light condition (Lea-Smith *et al*., 2013). In addition it has been suggested that it may function under low oxygen tension (Hart *et al*., 2005). However, its functions are yet to be conclusively demonstrated.

1.3 Photosynthetic electron transport pathway in higher plants

In algae and plants, the electron transport pathways are compartmentalized in two distinct places, chloroplast and mitochondria. Photosynthesis takes place in the chloroplast and respiration in the mitochondria, although a plastid terminal oxidase, PTOX, is able to transfer photosynthetic electrons to oxygen. During plant photosynthetic electron transfer electrons are moved from PSII to the PQ pool and to Cyt b_6/f and PSI. Pc is the only lumenal electron carrier protein that transfers electron from Cyt b_6/f complex to PSI (figure1.5). However, Cyt c_6 also present in many algal chloroplasts and can substitute for plastocyanin (Allen *et al.*, 2011).

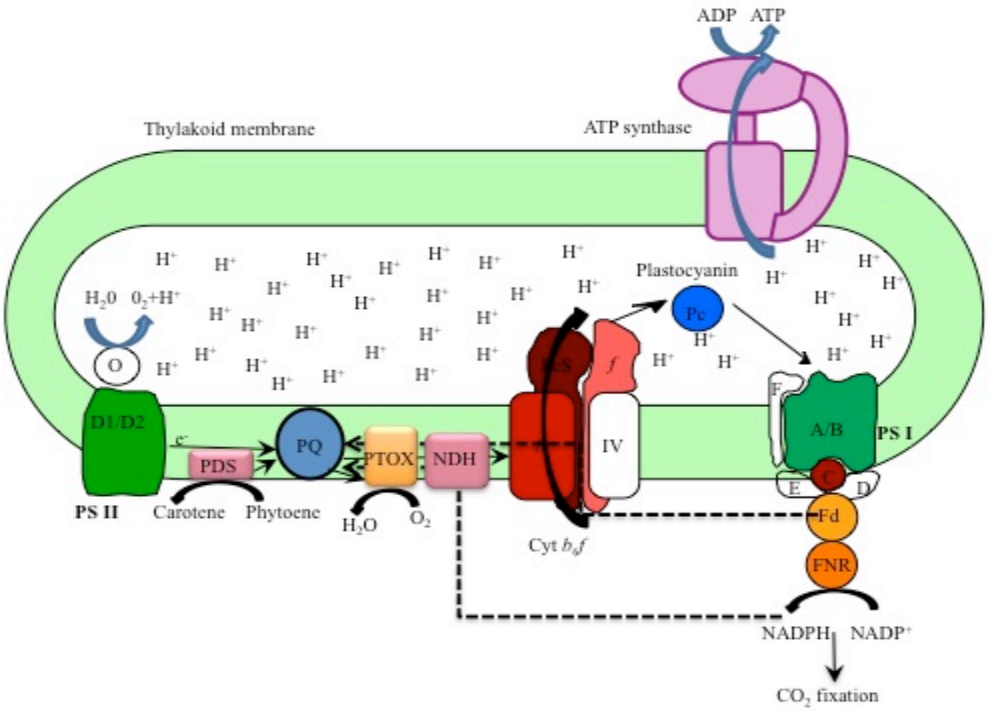

Figure 1.5: Plant photosynthetic electron transport chain shows cyclic and non-cyclic electron transport pathways. PSII: Photosystem II, PQ: Plastoquinone pool, PDS: Phytoene desaturase (Phytoene desaturase feeds electrons to PQ pool), PTOX: Plastid terminal oxidase, NDH: NADPH Dehydrogenase, Cyt b_6f: Cytochrome b_6f complex, FD: Ferredoxin, FNR: Ferredoxin-$NADP^+$ reductase, PSI: Photosystem I.

1.4 Light stress and photoprotection in photosynthetic organisms

Photosynthetic organisms require light energy to do photochemistry. However, absorption of excess light can lead to photo oxidative damage of the photosynthetic apparatus

(Erickson *et al*., 2015; Bailey and Grossman 2008; Thurotte *et al*., 2015). In the natural environment, sunlight can differ from extreme intensities (2000 μE m^{-2} s^{-2}) to heavily shaded conditions; these conditions can fluctuate in seconds. In limited light conditions, the rate of photosynthesis increases with the rate of light absorbtion. As the light intensity increases, a maximum photosynthetic rate (P_{max}) is achieved but light excess of what is required for the maximum photosynthetic rate is still absorbed (Erickson *et al*., 2015).

Organisms need to dissipate excess energy otherwise it can lead to the production of reactive oxygen species such as superoxide, hydroxyl radical ($OH^{\cdot}$), and the non-radical hydrogen peroxide (H_2O_2) and singlet oxygen. These molecules cause photo-oxidative damage to molecules including the photosystems II and I, and lipid bilayers (Erickson *et al*., 2015). The absorption of excess light results in photoinhibition which is defined as a decrease in the maximum efficiency and the rate of photosynthesis (Erickson *et al*., 2015; Adir *et al*., 2003). There are different types of short term and long-term response mechanisms that quench excess light energy, including qE (de-excitation quenching), qT (state transition dependent quenching), qZ (Zeaxanthin dependent quenching), and qI (photoinhibitory quenching) (Campbell *et al.*, 1998; Ebenhöh *et al.*, 2014).

1.4.1 Adaptation of photosynthetic organisms to varying light conditions

High light, and abrupt and rapid fluctuations in light intensity are the most damaging to PSII and PSI and the photosynthetic electron transport chain (Suorsa *et al*., 2012; Grieco *et al*., 2012; Allahverdiyeva *et al*., 2015b). To survive such changing environmental conditions, cyanobacteria, algae and plants have evolved sophisticated protective mechanisms with interesting evolutionary variations. Cyanobacteria have several regulatory mechanisms to allow the cells to cope with high light and rapidly fluctuating light conditions. In cyanobacteria these include; (i) having a high PSI/PSII ratio, enabling the rapid oxidisation of the PQ pool under high light conditions (Allahverdiyeva *et al*., 2015b), (ii) transfer of excess electrons to terminal oxidases (Lea-Smith *et al*., 2015; Allahverdiyeva *et al*., 2015b), (iii) presence of more lumenal electron carriers in cyanobacteria that enhance the electron flow between photosynthesis and respiration (Lea-Smith *et al*., 2015), (iv) redistribution of energy between PSII and PSI via phycobilisome mediated state transition mechanism during light fluctuation, (v) the Flv2/Flv4 and Flv1/Flv3 proteins which protect PSII and PSI respectively under fluctuating light conditions (Allahverdiyeva *et al*., 2015a), (vi) presence of Orange

Carotenoid Protein (OCP) which dissipates the excess energy as heat in PSII at high light conditions (Bailey and Grossman, 2008), and (vii) the presence of High Light Inducible Polypeptides (HLIPs) that are essential for survival under high light conditions.

Plants and algae have a number of other mechanisms to protect the photosynthetic apparatus under high light and fluctuating light. Cyt b_6f complex and ATP synthase are the predominant sites for photosynthetic flux control, and both react strongly to changing environmental conditions and metabolic status (Schöttler *et al.*, 2015). Under low light condition the thylakoid lumen pH value is in a range of 7.5 to a minimum of 6.5 (Takizawa *et al.*, 2007; Schöttler *et al.*, 2015). This is enough to drive ATP synthesis but Non Photochemical Quenching (NPQ) is weakly activated. When the light intensity increases resulting in saturation of photosynthesis or when the Calvin-Benson cycle slows down, and metabolic utilisation of ATP decreases, availability of ADP and free orthophosphate (P_i) becomes limiting for ATP synthase. (Schöttler *et al.*, 2015).

P_i limitation slows down proton efflux through ATP synthase, resulting in increasing acidification of thylakoid lumen. This signals multiple photoprotective mechanisms in response to photosynthetic ATP production and its consumption (Sharkey and Vanderveer, 1989; Kanazawa and Kramer, 2002; Kiirats *et al.*, 2009; Schöttler *et al.*, 2015). Excess absorbed light energy can be harmlessly dissipated via rapidly reversible NPQ in the PSII antenna. qE is activated by the protonation of two glutamate residues in the PsbS protein (Li *et al.*, 2004). Lumenal acidification below the threshold value of ~ 6.8-6.5 activates the violaxanthin de-epoxidase, which converts the accessary pigment violaxanthin into zeaxanthin (Takizawa *et al.*, 2007), and zeaxanthin protects and stabilises the PSII. Acidification of the thylakoid lumen reversibly slows down the linear electron flux at the level of plastoquinol re-oxidation at the Cyt b_6f complex (Schöttler *et al.*, 2015). When the lumenal pH value reaches <6.5 plastoquinol re-oxidation and proton pumping into the lumen become thermodynamically unfavourable (Takizawa *et al.*, 2007; Schöttler *et al.*, 2015). Specific amino acid protonation in the Cyt b_6f complex contributes to the inhibition of plastoquinol reoxidation (Nishio and Whitmarsh, 1993; Hope *et al.*, 1994; Kramer *et al.*, 1999; Takizawa *et al.*, 2007; Schöttler *et al.*, 2015). PGR5/PGRL1 related lumenal acidification via cyclic electron flow will be activated. An additional mechanism to protect against rapid changes in light intensity is STN7/Stt7-related

phosphorylation of Light Harvesting Complex II (LHCII) to allow state transitions to distribute energy between PSII and PSI. Dissipation of excess energy by cyanobacteria, algae and plants is illustrated in Figure 1.6 and the relative time scale of short term and long term responses to high light is in figure 1.7.

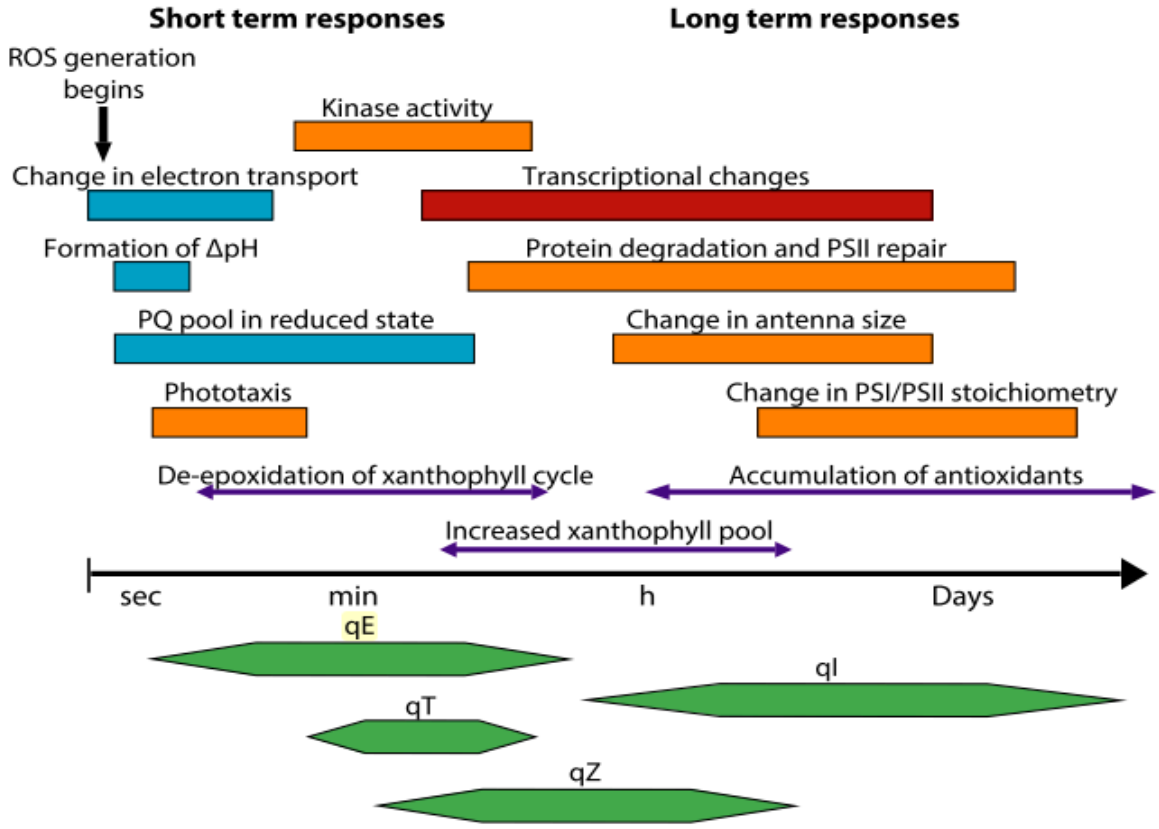

Figure 1.6: Relative time scale for long term and short term acclimation to excess high. Different types of non-photochemical quenching are shown in green, regulation of light harvesting components, reaction center stoichiometry, degradation and synthesis of proteins, PSII repair and activation kinase are shown in orange, transcriptional responses such as up and down regulation of high light induced, stress response genes are shown in red. qE: De-excitation quenching, qT: State transition dependent quenching, qZ: zeaxanthin dependant quenching, qI: Photoinhibitory quenching (figure taken from Erickson *et al.*, 2015).

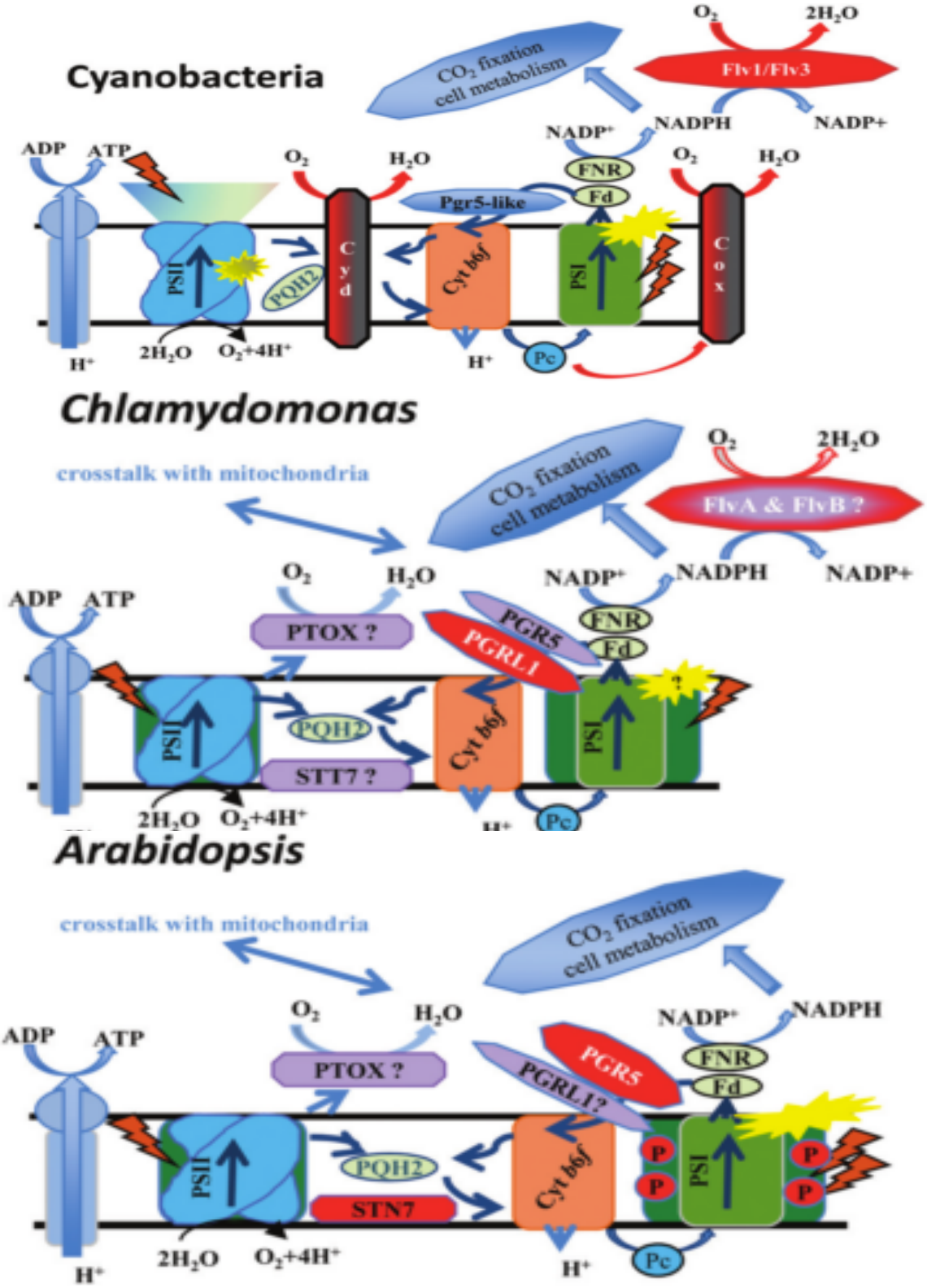
Cyanobacteria
CO2 fixation cell metabolism
O2
2H2O
Flv1/Flv3
NADPH
NADP+
ADP
ATP
O2
H2O
NADP+
FNR
Fd
Pgr5-like
PSII
PQH2
Cyd
Cyt b6f
PSI
Cox
H+
2H2O
O2+4H+
Pc
Chlamydomonas
crosstalk with mitochondria
CO2 fixation cell metabolism
FlvA & FlvB ?
PTOX ?
PGR5
PGRL1
STT7 ?
Arabidopsis
crosstalk with mitochondria
PTOX ?
PGR5
PGRL1?
STN7
P

Figure 1.7: Schematic view of electron-transfer components operating in different photosynthetic organisms under high and fluctuating light conditions (figure taken from Allahverdiyeva *et al*., 2015b). The main components of the photosynthetic electron transport chain participating in safeguarding the photosynthetic apparatus upon rapidly changing light conditions are marked with red. The target of the damage caused by fluctuating light is shown as a yellow explosion.

1.4.2 Energy redistribution by State transition

State transitions are a rapid physiological adaptation mechanism in photosynthetic organisms that adjusts the distribution of absorbed energy between photosystems (PSI and PSII). In plants and green algae, when light conditions favouring PSII result in excess stimulation of PSII compared to PSI this causes a high degree of reduction of the PQ pool that triggers the activation of a kinase (STN7 and STN8 in plants or Stt7 in *Chlamydomonas*), and the resulting phosphorylation of LHCII results in redistribution from PSII to PSI. Similarly when light favours PSI, oxidation of the PQ pool by PSI reverses this process (Bellafiore *et al*., 2005). This mechanisms occurs in response to an imbalance of PSI and PSII turnover (Mullineaux and Allen, 1990). In plants and green algae state transitions therefore result in redistribution of LHCII between the photosystems. In state 1, the LHCII is associated primarily with PSII. When the PQ pool gets reduced, a portion of the LHCII dissociates from PSII and migrates to PSI, resulting in increased energy transfer to PSI (Schönberg and Baginsky 2012; Shapiguzov *et al*., 2010; Mullineaux and Allen 1990). When the PQ pool gets oxidised, phosphorylated LHCII at state 2 is dephosphorylated by phospho-LHCII phosphatase PPH1/TAP38 and the dephosphorylated LHCII migrates from PSI to PSII (figure 1.8A). In cyanobacteria, the transitions determine efficiency of energy transfer from the phycobilisome to PSII. During state transition 2 a portion of PBS core complexes functionally detaches from the PSII (Mullineaux and Emlyn-Jones, 2005) (figure 1.8B).

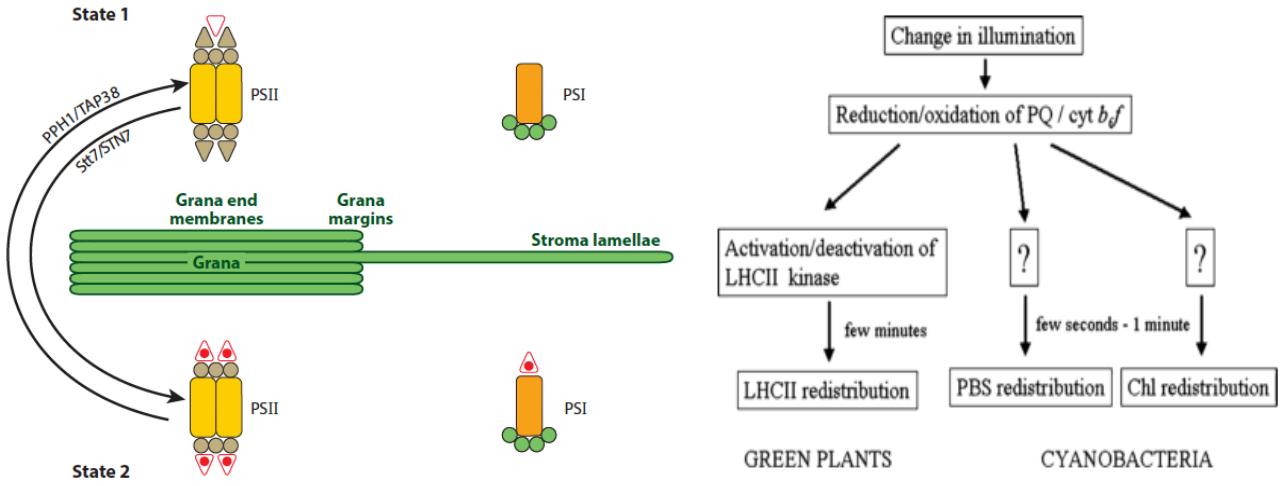

Figure 1.8: State transition mechanism in Plants (A) and in cyanobacteria (B) Photosystem I with its associated protein complexes and the electron transport route in PSI (figure from Mullineaux and Emlyn-Jones, 2005).

1.4.3 Electron dissipation via flavodiiron proteins

Flavodiiron proteins (FDPs), previously known as A-type flavoproteins (Flv), are a large family of enzymes that share sequence similarity (Helman *et al*., 2003; Bersanini *et al*., 2014). FDPs have been found mainly in anaerobic bacteria, in some aerobic prokaryotes including cyanobacteria, as well as in Archaea, and in protists. Genome sequence analysis suggested there are homologues of FDPs in some photosynthetic eukaryotes (Zhang *et al*., 2009; Helman *et al*., 2003; Bersanini *et al*., 2014; Allahverdiyeva *et al*., 2015a). FDPs share two conserved structural domains: the N-terminal metallo-β-lactamase-like domain, harbouring a non-heme diiron center where O_2 and/or NO reduction take place, and the C-terminal flavodoxin-like domain, containing a flavin mononucleotide (FMN) moiety (Allahverdiyeva *et al*., 2015a).

Genes encoding FDPs (*flv*) are found in most sequenced cyanobacteria. Some cyanobacterial strains contain several copies of *flv* genes, thus comprising a small family encoding different FDPs. FDPs found in oxygenic photosynthetic organisms can be grouped into two clusters (cluster A: Flv1 and Flv2, and cluster B: Flv3 and Flv4) and appear in pair(s) (Flv1-Flv3 or Flv2-Flv4) (Allahverdiyeva *et al*., 2015a). The Flv2/Flv4 and Flv1/Flv3 proteins in cyanobacteria are powerful safety valves which protect PSII and

PSI respectively under fluctuating light conditions (Allahverdiyeva *et al*., 2015a; Zhang *et al*., 2009; Bersanini *et al*., 2014; Shimakawa *et al*., 2015; Eisenhut *et al*., 2012; Helman *et al*., 2003; Chukhutsina *et al*., 2015).

1.4.4 Electron dissipation via terminal oxidases

Terminal oxidases play important roles in photosynthetic organisms in dissipating excess electrons. The functions of terminal oxidases were explained in section 1.2.2. Terminal oxidase knockouts in cyanobacteria are believed to result in over-reduction of the photosynthetic electron transfer chain, which in turn induces photoinhibition, and production of ROS (Lea-Smith *et al*., 2013)

1.5 Uncharacterized *c* type cytochromes in cyanobacteria, algae and higher plants

Cyt c_6 and Pc are the two conventional redox carriers in cyanobacteria and algae that shuttle electrons between the Cyt b_6f complex and PSI. A few other uncharacterized low molecular weight electron carriers have been reported in cyanobacteria (Malakhov *et al*., 1994; Bialek *et al*., 2008), algae and higher plants. They have a low redox midpoint potential and are Cyt c_M, Cyt c_{6C}/c_{6B} (in cyanobacteria) and Cyt c_{6A} in algae and higher plants (Wastl *et al*., 2002; Gupta *et al*., 2002).

1.5.1 Cytochrome $_6$ like proteins

1.5.1.1 Discovery of cytochrome c_6 like proteins in photosynthetic organisms

It was generally supposed that Cyt c_6 is absent from higher plants. However, in 2002 two groups independently discovered a homologue of Cyt c_6 in higher plants and algae that showed up to 30% similarity at the amino acid sequence level to other Cyt c_6 proteins. The protein is now designated Cyt c_{6A} and is found in higher plants and green algae. Homologues of *Arabidopsis* Cyt c_{6A}, (designated Cyt c_{6B}/c_{6C} and which are clearly different from the well-characterized Cyt c_6) have also been identified in several cyanobacteria (Gupta *et al*., 2002; Wastl *et al*., 2002; Wastl *et al*., 2004; Bialek *et al*., 2008; Reyes-Sosa *et al*., 2011). These discoveries generated great debate among the scientific community as to whether the Cyt $c_{6A/B/C}$ proteins can substitute for Pc in higher plants or Cyt c_6 and Pc in algae and cyanobacteria (Howe *et al*., 2006; Molina-Heredia *et al*., 2003).

1.5.1.2 Distribution of cytochrome c_6 like proteins

Bialek *et al*., 2008 constructed a sequence comparison and phylogenetic trees of Cyt c_6-like proteins, including the conventional Cyt c_6 and other related proteins. This analysis revealed discrete phylogenetic clusters of related proteins, including Cyt c_{550}, Cyt c_{555} of *Chlorobium*, Cyt c_6, the chloroplast Cyt c_{6A} and another Cyt *c* type protein, Cyt c_M. Interestingly, they found two deeply branching clusters branches within the tree, which they designated as Cyt c_{6B} and Cyt c_{6C} (figure 1.9A). Cyt c_{6C} and c_{6B} like proteins are highly similar at ca. 69% and 78% when compared with Cyt c_6 (Reyes-Sosa *et al*., 2011). It has been proposed that the use of the copper-containing plastocyanin as a redox carrier evolved in response to the declining availability of iron as the atmosphere became increasingly oxidizing, and figure 1.9B shows a simple evolutionary model for the acquisition of Cyt c_6, Pc, and cytochrome c_6-like proteins in response to such environmental changes (Bialek *et al*., 2008).

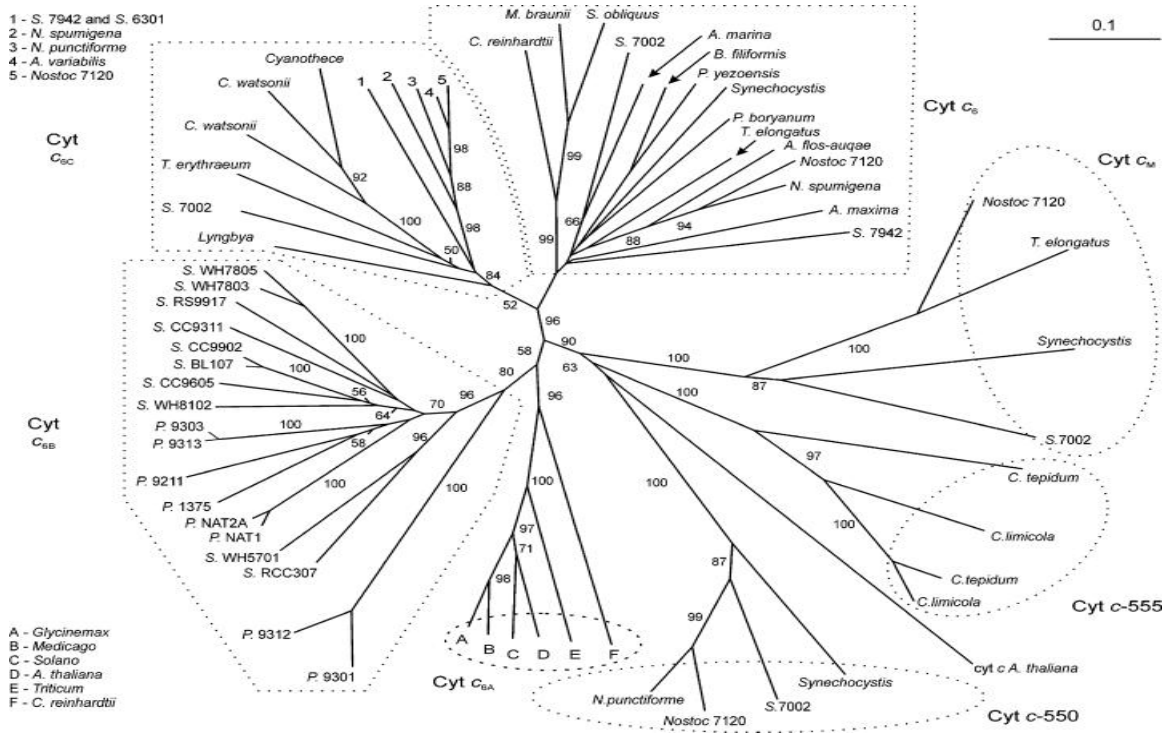

A

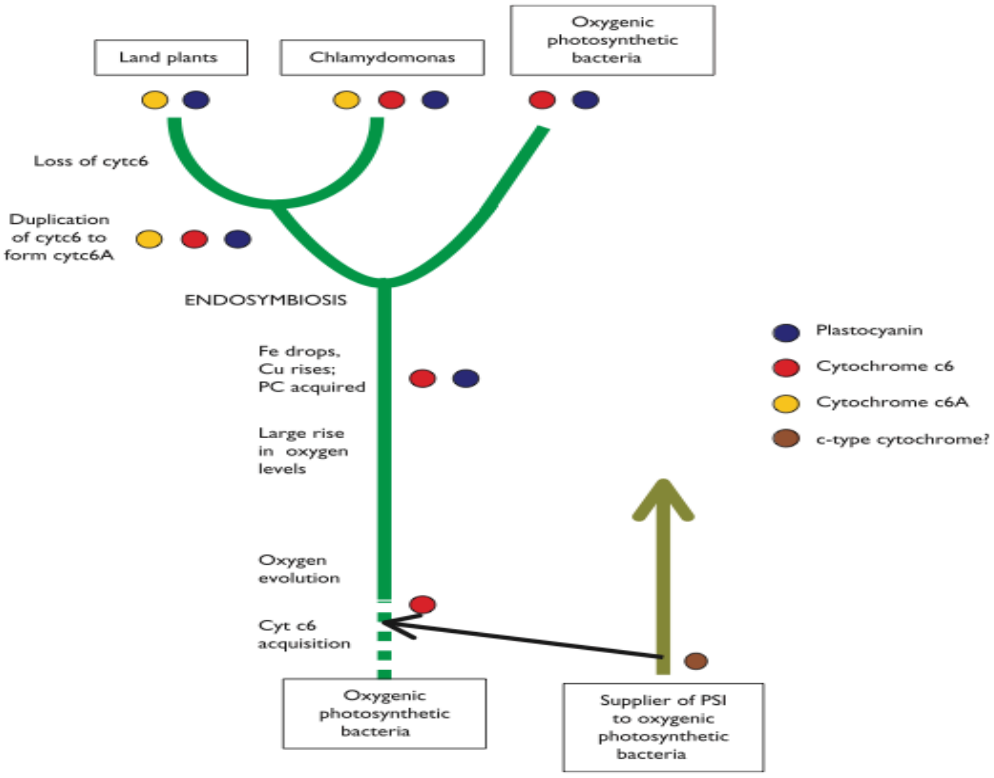

B

Figure 1.9: Unrooted tree showing distribution of *c* type cytochrome from cyanobacteria, algae and plants (A) (Figure from Bialek *et al*., 2008) and the distribution and evolution of c type cytochromes in cyanobacteria, algae and plants (B) (figure modified from Howe *et al*., 2006).

1.5.1.3 Structure Modeling and Circular Dichroism of cytochrome c_6 like proteins

A theoretical model for Arabidopsis c_{6A} was put forward in 2003 (Molina-Heredia, *et al*) based on the *Monoraphidium* Cyt c_6 structure. This indicated very different surface electrostatic properties. The structure was confirmed experimentally (Marcaida *et al*., 2006). Bialek *et al*., 2008, predicted structures of PetJ1 (Cyt c_6) and PetJ2 (Cyt c_{6C}) and Cyt c_{6A} based on known cyt c_6 structures and confirmed by CD that PetJ1 and PetJ2 had similar structures. Again, the structures indicated very different surface electrostatic potentials of the proteins.

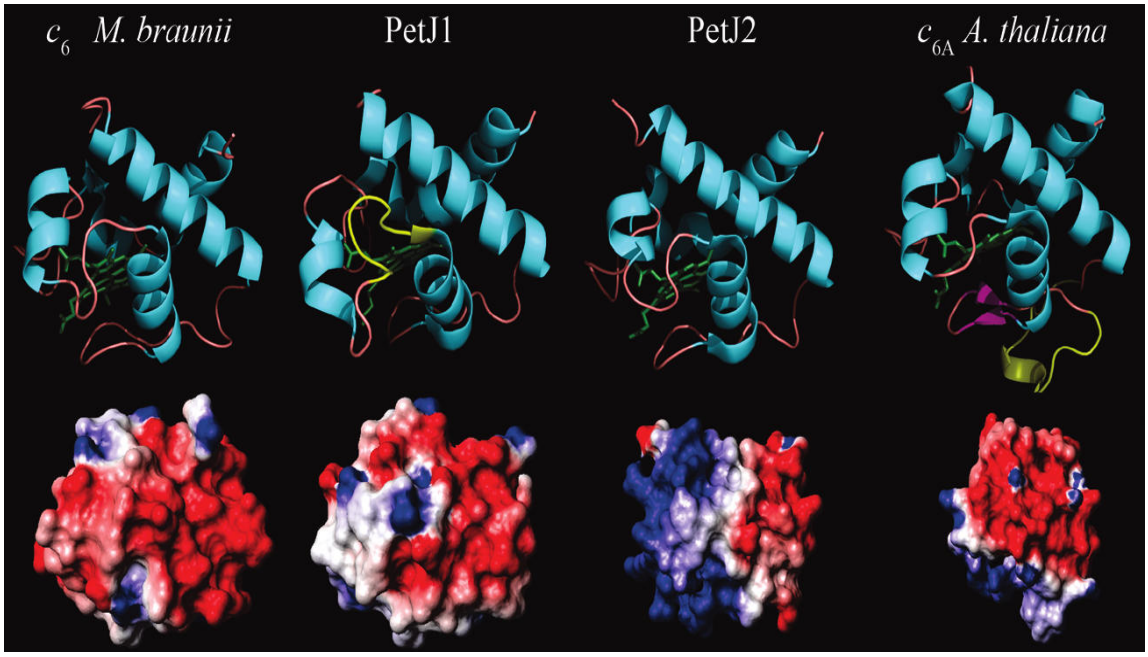

Figure 1.10: Structural model of Cyt c_6 and c_6 like protein with same orientation to known 3D structure of Cyt c_6 of M. braunii (*PetJ1*: Cyt c_6; *PetJ2*: Cyt c_{6C}, figure taken from Bialek *et al*., 2008).

1.5.1.4 Redox mid-point potential of cytochrome c_6 like proteins

The Cyt c_6 like proteins have a low redox midpoint potential when compared to the conventional Cyt c_6. For example *Synechococcus* sp. PCC 7002 Cyt c_6 has a redox midpoint potential ($E_{m.7}$) of 319 ± 1.6 mV (Bialek *et al*., 2008) which is typical of cyanobacterial Cyt c_6. Cyt c_6 accepts electrons from the Cyt b_6/f complex whose E_m at pH 7.0 is +334 mV (Albarran *et al*., 2005; Cho *et al*., 2000), to reduce oxidised PSI whose E_m is +500 mV (Brettel, 1997). On the other hand the midpoint redox potential of Cyt c_{6A} was reported as +140 mV (Molina-Heredia *et al*., 2003), which Worrall *et al*., 2007 later revised to +70 mV. That of Cyt c_{6C} from *Synechococcus* sp PCC 7002 is +148 ± 1.7 mV (Bialek *et al*., 2008) and from *Nostoc* is +199 mV (Reyes-Sosa *et al*., 2011). The low redox midpoint potential is one of the most important differences between Cyt c_6 like proteins and Cyt c_6 or Pc (Howe *et al*., 2016).

Cyt c_{6A} protein has a special insertion of 12 amino acids in a loop region which is designated as the Loop Insertion Peptide (LIP), which is unique feature of Cyt c_{6A} (Wastl *et al*., 2002; Marcaida *et al*., 2006; Schlarb-Ridley *et al*., 2006; Chida *et al*., 2006; Howe *et al*., 2006; Worrall *et al*., 2007; Worrall *et al*., 2008; Mason *et al*., 2012; Howe *et al*.,

2016). Deletion of LIP resulted in slight drop in the p*I* from 5.1 to 4.6 but the LIP is not directly responsible for the low redox midpoint potential or the low rate of reaction with PSI (Howe *et al*., 2016).

1.5.1.5 Expression of cyt c_6 like proteins in different physiological condition

Nearly 47 species of sequenced cyanobacteria have a Cyt c_{6C}/c_{6B} protein, along with conventional Cyt c_6 and/or Pc. Cyt c_{6C} was initially discovered in *Synechococcus* sp. PCC 7002 and the gene encoding Cyt c_{6C} was designated as *petJ2* to distinguish it from the *petJ1* gene for the conventional Cyt c_6 (Bialek *et al*., 2008). Expression of Cyt c_{6C} was not observed under typical laboratory condition at either the mRNA or protein level. However, Bialek *et al*., (2008) reported that in *S. elongatus* and *Nostoc punctiforme NPF1886* transcripts of the Cyt c_{6C} gene were observed at low but significant levels in nitrogen starved, sulfur starved, ammonia grown cells and in hormogonia and akinetes. Reyes-Sosa *et al*., 2011 reported expression of the Cyt c_{6C} transcript in *Nostoc* sp. PCC 7119 under standard growth conditions, with or without copper, and with or without nitrate. Wastl *et al*., noted the representation of Cyt c_{6A} in a wide range of cDNA libraries. Expression of the Cyt c_{6A} transcript was observed in *Arabidopsis* leaves and a negligible amount was detected in roots (Gupta *et al*., 2002). The transcript has also been reported from ripening tomatoes (Renato *et al*., 2014).

1.5.1.6 Cyt c_6 like proteins unable to replace Cyt c_6 or Pc

The controversial hypothesis was proposed by Gupta *et al*., 2002, that the Cyt c_6 like (Cyt c_{6A}) protein is a functional substitute for Pc in higher plants, but a number of later lines of evidence contradicted the hypothesis. Cyt c_{6A} was shown to be unable to substitute for Pc and Cyt c_6 in electron transfer to PSI *in vitro*, consistent with the redox midpoint potential of Cyt c_6 like proteins being too low to oxidize cytochrome *f* (Molina-Heredia *et al*., 2003; Weigel *et al*., 2003a; Bialek *et al*., 2008; Reyes-Sosa *et al*., 2011). However, in theory Cyt c_6 like proteins could potentially reduce PSI. Table 1 shows the physiochemical and functional properties of *Nostoc* sp PCC 7119 Cyt c_6, Cyt c_6 like protein, and Pc. Subsequently, Reyes-Sosa *et al*., 2011, proposed that the Cyt c_6 like protein in *Nostoc* sp PCC 7119, 'is an alternative photosynthetic soluble electron donor to PSI, which probably acts in an electron transfer pathway different to those from Cyt c_6 and Pc'.

Protein	Mass (kDa)	Isoelectric point (pI)	E_m (mV) at pH 7.0	k_{bim} (M^{-1} s^{-1})[a]	k_{inf} (M^{-1} s^{-1})[b]	k_{et} (s^{-1})[c]
Cyt c_6	9.7	9.0	+335	12.1×10^7	11.4×10^6	1.7×10^5
Cyt c_6-like	10.2	8.0	+199	3.2×10^7	4.0×10^6	
Pc	11.1	8.8	+357	7.6×10^7	5.9×10^6	

[a] k_{bim} is the second-order rate constant for PSI reduction

[b] k_{inf} is the k_{bim} extrapolated to infinite ionic strength

[c] k_{et} is the first-order electron transfer rate constant for PSI reduction

Table 1.1: Phytochemical and functional properties of Nostoc sp PCC 7119 Cyt c_6, Cyt c_6 like protein, and Pc (Reyes-Sosa *et al*., 2011).

The Cyt c_{6A} LIP region was analysed for its effect on the functionality of the protein. Site direct mutagenesis of cysteines in the LIP to serine or LIP deletion resulted in the conclusion that the disulfide bridge contributed to stability of the protein but not the functionality (Chida *et al.*, 2006; Mason *et al*., 2012; Howe *et al*., 2016).

1.5.2 Cytochrome c_M

1.5.2.1 Discovery, distribution and amino acid sequence among cyanobacteria

A gene encoding another *c* type cytochrome designated as *cytM* was discovered in the genome of *Synechocystis* sp PCC6803 (Malakhov etal., 1994). The gene *cytM* encodes a water soluble protein Cytochrome c_M (Cyt c_M) that is relatively short - about 76 amino acids compared to Cyt c_6 which is typically 90-115 amino acids - and with a predicted molecular weight of 8.3 kDa in the mature form (Ho *et al*., 2011). The amino acid sequence of Cyt c_M is about 40% similar to cyanobacterial cytochrome c_6 and 30% similar to the mitochondrial Cyt *c* (Malakhov etal., 1994; Malakhov *et al*., 1999). Cyt c_M shows the conserved heme binding motif (CXXCH) with C representing the cysteines involved in heme to protein linkage and the histidine and a methionine being the other heme ligands (Bernroitner *et al*., 2009; Malakhov etal., 1994; Malakhov *et al*., 1999).

Cyt c_M is distributed among almost all cyanobacterial strains except *Prochlorococcus marinus* MIT 9515 (Bernroitner *et al*., 2009; Ho *et al*., 2011). Figure 1.11 shows full-length amino acid sequences from 49 species of cyanobacteria. Other than the conserved heme binding site, and some individual conserved residues, all the sequences show two highly conserved motifs: Thr-Pro-Pro-Met-Pro, (127-131) and LL (143-144).

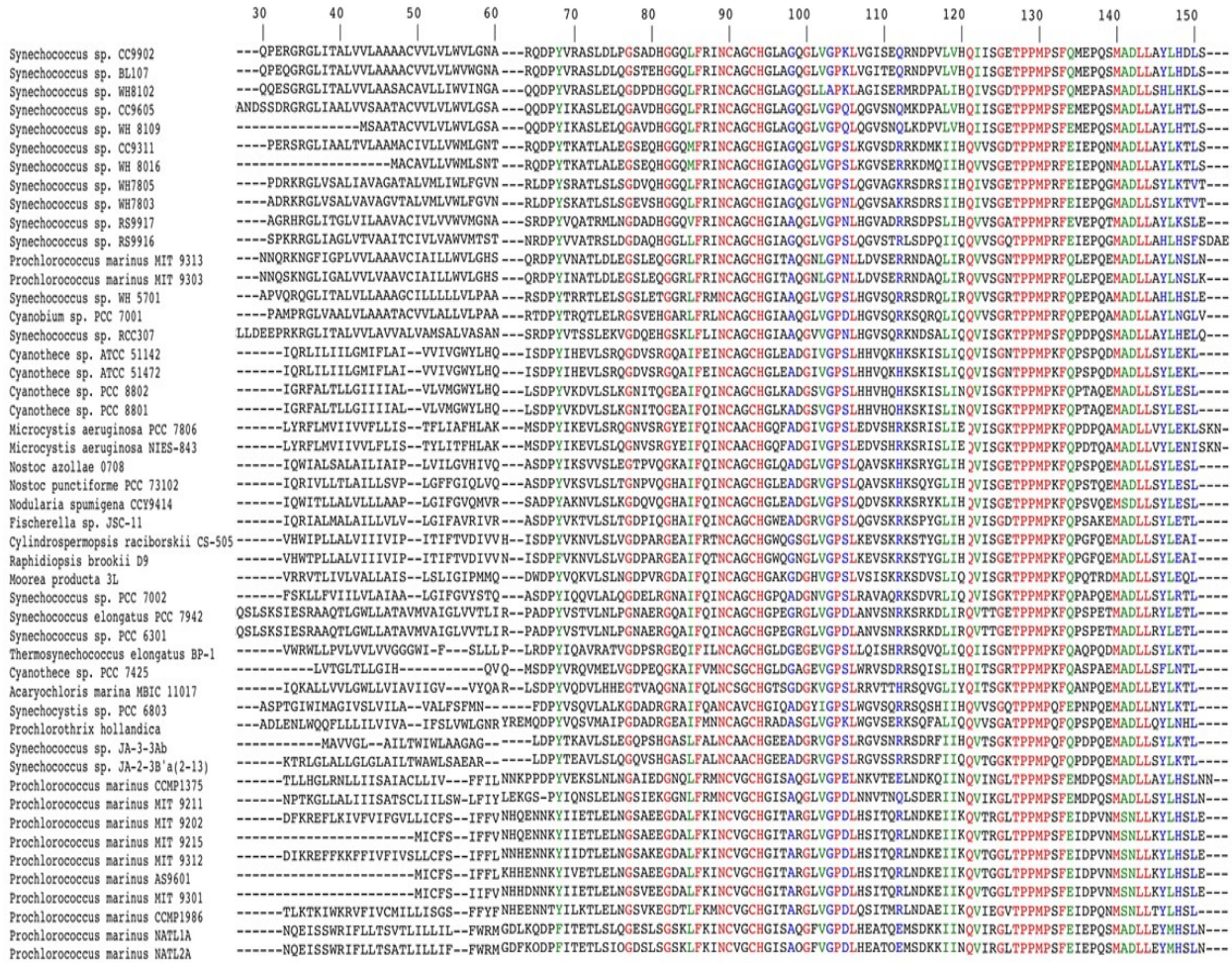

Figure 1.11: Sequence alignment of cytochrome c_M proteins in cyanobacteria. The conserved residues of the heme binding motif (CXXCH) are at 90-94. Other highly conserved motifs Thr-Pro-Pro-Met-Pro, (127-131) and LL (143-144) are indicated in red. The online tool ClustalW (http://www.ebi.ac.uk/Tools/msa/clustalw2) was used to align the sequences.

1.5.2.2 Structure and redox midpoint potential of Cyt c_M

The Cyt c_M gene *of Synechocystis sp*. PCC6803 has been cloned and expressed in *E. coli* (Malakhov *et al*., 1994; Ho *et al*., 2011). Cho *et al*., (2000) reported that Cyt c_M has an alpha peak at 550 nm and calculated the pI value as 5.6, which was lower than that previously reported (7.3) by Malakhov *et al*., 1994. The redox midpoint potential of Cyt c_M is +151 mV (Cho *et al*., 2000).

1.5.2.3 Possible function of Cyt c_M

Northern blot analysis revealed a Cyt c_M transcript was barely detectable under normal physiological conditions for *Synechocystis* sp. PCC6803, but its level was increased when the culture was exposed to low temperature (22°C rather than 34°C) or under high light intensity (2000 μmol photons m^{-2} s^{-1}). In contrast, levels of conventional Cyt c_6 and Pc transcripts were lower under low temperature and in high light conditions (Malakhov *et al*., 1999). These observations suggested that Cyt c_M could potentially replace Cyt c_6 or Pc under stress conditions (Malakhov *et al*., 1999). Thermodynamically it seems very unlikely that Cyt c_M with a low redox mid-point potential (+151 mV) could oxidize Cyt *f* with a significantly higher redox mid-point potential (+350 mV) (Cho *et al*., 2000). Cho *et al.,* also reported detection of Cyt c_M *in vivo* in *Synechocystis* sp PCC6803 using western blot analysis of cells grown under normal physiological conditions (Cho *et al*., 2000).
A double knockout of Cyt c_6 and Pc to assess the role of Cyt c_M in photosynthesis could not be achieved. The photosynthetic electron flow rate from PSII was measured by chlorophyll fluorescence yield in *Synechocystis,* and found to be decreased in the Cyt c_6 or Pc knockout lines. However, Cyt c_M could not be deleted in a PSI-less background (Manna and Vermaas, 1997).

Cyt c_M protein has some degree of similarity with the Cyt *c* docking site of the Cyt caa_3-type oxidase from *Bacillus* spp and *Thermus thermophilus*. These findings led Manna and Vermaas (1997) to suggest that Cyt c_M is a part of the Cyt oxidase complex in cyanobacteria that could function as a redox intermediate between the conventional redox carriers Pc/Cyt c_6 and cytochrome *c* oxidase. P700 oxidation and reduction kinetics studies in *Synechocystis* suggested that Cyt c_M could donate electrons to PSI under stress conditions (Shuvalov *et al*., 2001), but comparative laser flash induced kinetic analysis of P700 reduction in *Synechocystis* failed to prove the involvement of Cyt c_M in PSI reduction, and the bimolecular rate constant reaction was 100 times lower for Cyt c_M than Cyt c_6 or Pc (Molina-Heredia *et al*., 2002). On the other hand, the intermolecular electron transfer rate between Cyt c_M and the Cu domain of Cyt oxidase demonstrated that Cyt c_M could potentially donate electron to Cyt oxidase as efficiently as Cyt c_6 but more effectively than Pc (Bernroitner *et al*., 2009). The distribution of surface electrostatic potential of Cyt c_M is different from Cyt c_6 and Pc, so Cyt c_M cannot function in exactly the same way as those proteins (Molina-Heredia *et al*., 2002). Recently, Hiraide *et al*., (2015) observed that a Cyt c_M knockout mutant of *Synechocystis* showed enhanced

heterotrophic growth in the dark or in light limited conditions compared to wild type. Until now no other growth characterization studies have been published to assess the role of Cyt c_M in cell physiology.

1.6 Genetic manipulation techniques

Natural transformation of cyanobacteria was reported long ago (Shestakov and Khyenn 1970; Shestakov *et al*., 1982). However, although very few species have a natural ability to engulf exogenous DNA, the efficiency of DNA uptake is very high in several species, including *Synechococcus elongatus* PCC7942, *Synechococcus* sp. PCC 7002 and *Synechocystis* sp PCC 6803 (Chauvat *et al*., 1986). The availability of transformation, together with genomic sequences of some species of cyanobacteria, provides a great opportunity to use them for photosynthesis research at the molecular level. *Synechococcus elongatus* PCC 7942 is particularly useful as a model system, as it offers the possibility to construct marked and unmarked gene knockouts (Dexter, 2009; Vermaas, 1996; Lea-Smith *et al*., 2016). For plant transformation we used the simple and non-laborious *Agrobacterium*-mediated floral dip transformation system (Clough and Bent 1998; Zhang *et al*., 2006).

1. 7 Aims of the current study

The goal of this study is to investigate the functions of the lower molecular weight redox proteins Cyt c_{6C} (encoded by *petJ*2), and cytochrome c_M (encoded by *cytM*) in *Synechococcus elongatus* PCC 7942 and Cyt c_{6A} (encoded by AT5G45040) in *A. thaliana*.

The initial aim was to knock out the genes for each of these proteins (Cyt c_{6C} and Cyt c_M) by replacing the coding sequence with a cassette conferring kanamycin resistance and sucrose sensitivity (*kan*^{R}*sacB*) or one conferring kanamycin resistance alone (*kan*^{R}). Mutants would be identified by selection for kanamycin resistance and then assessed for phenotypes under a range of different growth conditions. We would assess the rate of photosynthesis and respiration of these mutants using an oxygen electrode, and chlorophyll fluorescence measurements to assess deficiencies in photosynthetic electron transfer machinery. We would also carry out transcriptomic studies on the mutants.

For Cyt c_{6A}, publicly available mutants in *A. thaliana* would be used. We would assess growth phenotypes under different light conditions and use chlorophyll fluorescence

measurements to identify effects on photosynthetic electron transfer. We would also use reporter genes for localization studies.

CHAPTER 2 MATERIALS AND METHODS

2.1 Strains and maintenance

2.1.1 Maintenance of *Synechococcus elongatus* PCC7942, *E. coli* and *Agrobacterium* strains

Wild type *Synechococcus elongatus* PCC 7942 (*S. elongatus*) was taken from our laboratory stock. For liquid culture *S. elongatus* strains were grown on BG-11 (Appendix-B) medium (Rippka, *et al*., 1979) with 10 mM $NaHCO_3$, with continuous shaking in a Multitron II incubator (Infors) at 160 rpm in 100 ml flasks in moderate light (ML) 40 µE m^{-2} s^{-1} condition at 30°C. Cultures were bubbled with sterile air as required. Cultures were also grown on BG-11 agar (Appendix-A) plates containing (1.5% w/v) Bacto™ agar (Scientific Laboratory Supplies) with 1 mM TES-NaOH (pH 8.2) and 3 g l^{-1} $Na_2S_2O_3$ (sodium thiosulphate, SIGMA) in an Innova 4230 incubator with 40 µE m^{-2} s^{-1} illumination (New Brunswick Scientific). When required, sucrose was added at 5% (w/v) and kanamycin at 60 µg/ml

Escherichia coli (*Ecoli*) DH5α and *E. coli dam*$^-$ competent cells were kindly provided by Dr. Mathias Sorieul, (Department of Biochemistry, University of Cambridge) were routinely grown at 37 °C in liquid LB medium (ForMedium) with shaking at 220 rpm or on LB-agar plates (1.5% agar). Where added, supplements were used at the following final concentrations: ampicillin 100 µg ml^{-1}; spectinomycin 50 µg ml^{-1}; kanamycin 60 µg ml^{-1}; isopropyl β-D-1-thiogalactopyranoside (IPTG) 150 µM; 5-bromo-4-chloro-3-indolyl-beta-D-galactopyranoside (X-Gal) 30 µg ml^{-1}.

Agrobacterium tumefaciens [(GV 3101) (*Agrobacterium*) strain was grown at 30 °C in liquid LB medium with shaking at 160 rpm or on LB-agar plates (1.5% agar) with appropriate antibiotics at the following final concentrations: kanamycin 50 µg ml^{-1}, tetracycline 25 µg ml^{-1}, and rifampicin 5 µg ml^{-1}.

2.1.2 *Arabidopsis* seed sterilization, storage and growth

Arabidopsis thaliana (*A. thaliana*) WT (Colombia) seeds were kindly provided by Dr. Mathias Sorieul, (Department of Biochemistry, University of Cambridge). Two independent *Arabidopsis* T-DNA insertion lines of cytochrome c_{6A} SALK_060652

(hereafter 652), and SALK 011266C (hereafter 66C) were purchased from the European Arabidopsis Stock Center. Different overexpression lines of cytochrome c_{6A} were generated in the lab. All the seeds were stored at 4 °C for long-term viability.

A. thaliana WT and mutant seeds were sterilized with a series of ethanol washes. About 300 mg of seeds from different lines were dispensed into 1.5 ml microcentrifuge tubes. 30 ml of 85% ethanol, 100 µl lipsol detergent and 100 µl of Tween20 were mixed and 1 ml of the mixture was added to tubes containing 300 mg seeds. Tubes were agitated for 7 min at 2,500 rpm in a Vibrax VXR shaker (IKA) and subjected to centrifugation, after which the supernatant was removed. One ml of 65% ethanol was added to each of the tubes, after which the tubes were tilted a few times and the supernatant was removed. One ml of 85 % ethanol was then added, tubes tilted and the supernatant was again removed. Finally one ml of 100% ethanol was added, the tubes were taken into a sterile flow hood, the supernatant was removed completely and the tubes left opened in the hood for ~2-3 hrs for complete evaporation. Dried sterile seeds were stored at 4 °C for further processing. *A. thaliana* seeds were grown either in ½ MS (Murashige and Skoog) agar plates or in soil. To grow in MS agar plates 2.25 g of ½ MS salt (Sigma Aldrich) was mixed with 1000 ml of Milli-Q water (Milli-Q, Millipore), stirred well to mix and the pH raised to pH 5.8 with 0.1 M sodium hydroxide solution. 8 g of plant agar (Duchefa Biochemie) was added and the mixture was autoclaved (Omega media) for 15 min at 121 °C. Sterilized medium was then placed in a water bath (~55 °C) to reduce the temperature. In a sterile flow hood, about 50 ml of the medium was dispensed into each sterile culture plate. Culture plates were left in the flow hood until the agar solidified, after which the plates were transferred to a cold room (4 °C) until further use.

Sterile seeds from each line were carefully transferred onto ½ MS Plates under aseptic conditions. Then the plates were left at 4 °C for 2 days for stratification and homogeneous germination. After the incubation, plates were shifted to appropriate conditions for growth assessment (see section 2.7 for more details).

2.1.3 Storage of cyanobacteria

Cultures were prepared by harvesting a 50 ml culture at mid-log growth phase by centrifugation at 5000 rpm (Hettich Universal 32 Hettich Zentrifugen) for 5 minutes and washing twice with 2 ml of freshly made BG-11 medium. The pellet was resuspended in

1.73 ml BG-11 medium and split into two aliquots. DMSO was added to one (930 µl cells, 70 μl DMSO), and glycerol to the other [(800 µl cells, 200 µl filter-sterilized (0.2 μ Minisart single use filter unit non pyrogenic by Sartorius Stedim biotech) 80% glycerol in dH_2O)]. Samples were snap frozen in liquid N_2 and stored at -80 ºC. Strains were revived by streaking a loop of frozen cells onto a BG-11-agar plate with appropriate antibiotics and incubating at 30 °C with continuous moderate light.

2.2 Molecular biology

2.2.1 Water

Autoclaved ultrapure (Milli-Q, Millipore) water was used for molecular biology applications. Autoclaved ddH_2O (double distilled water) was used for all other applications.

2.2.2 Plasmids

The pUC19, pUC19-*kan*^{RT}, pUC4K (ref), pKMOBsacB (Lea-Smith *et al*., 2016) plasmids were laboratory stocks. A plasmid pGreen binary vector (Shimada *et al*., 2010) derivative containing a sequence encoding an *A. thaliana* seed coat protein oleosin fused at its C-terminus with Green Fluorescent Protein coding sequence (GFP), cauliflower mosaic virus promoter sequence (p35S), Enhanced Yellow Fluorescent Protein coding sequence (EYFP) and a transcription terminator, frequently used for plant genetic engineering to terminate the expression of the insert gene (NosT) (hereafter referred to as oleosin:GFP:p35S:EYFP:NosT) (figure 2.1A) and a second pGreen vector derivative having Oleosin:GFP and a 4x myc epitope tag coding sequence (hereafter oleosin:GFP:4xmyc:NosT) (figure 2.1B) plasmids were kindly provided by Dr. Mathias Sorieul (Department of Biochemistry, University of Cambridge, United Kingdom).

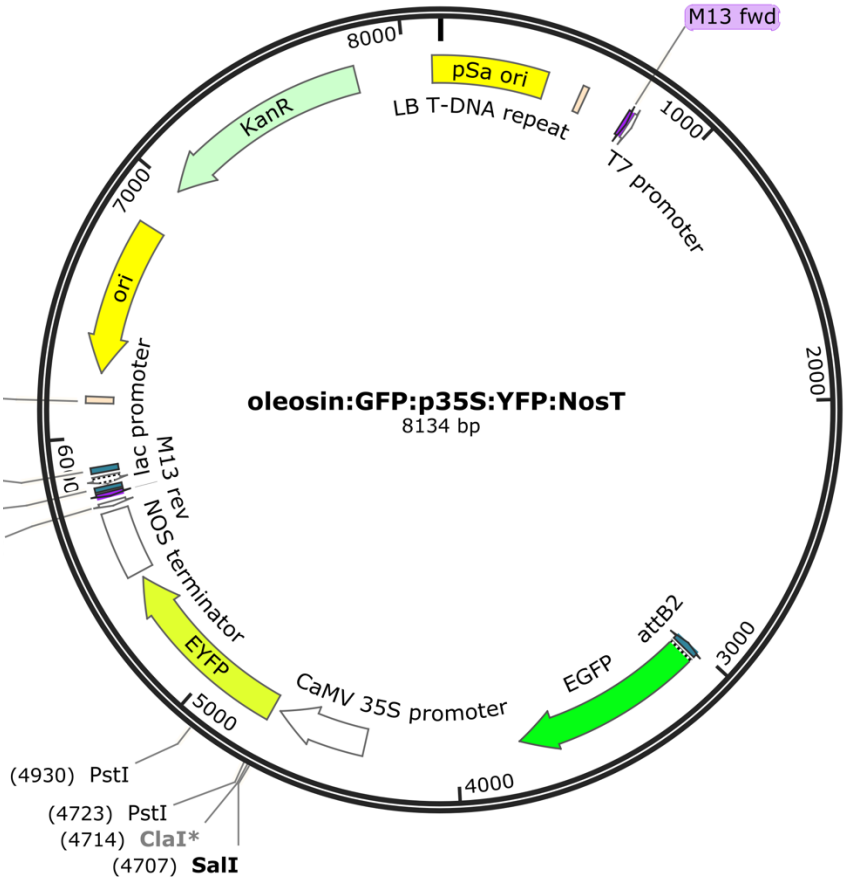
M13 fwd
8000
pSa ori
LB T-DNA repeat
1000
T7 promoter
KanR
7000
ori
2000
oleosin:GFP:p35S:YFP:NosT
8134 bp
lac promoter
M13 rev
60
NOS terminator
EYFP
attB2
3000
CaMV 35S promoter
EGFP
5000
4000
(4930) PstI
(4723) PstI
(4714) ClaI*
(4707) SalI

A

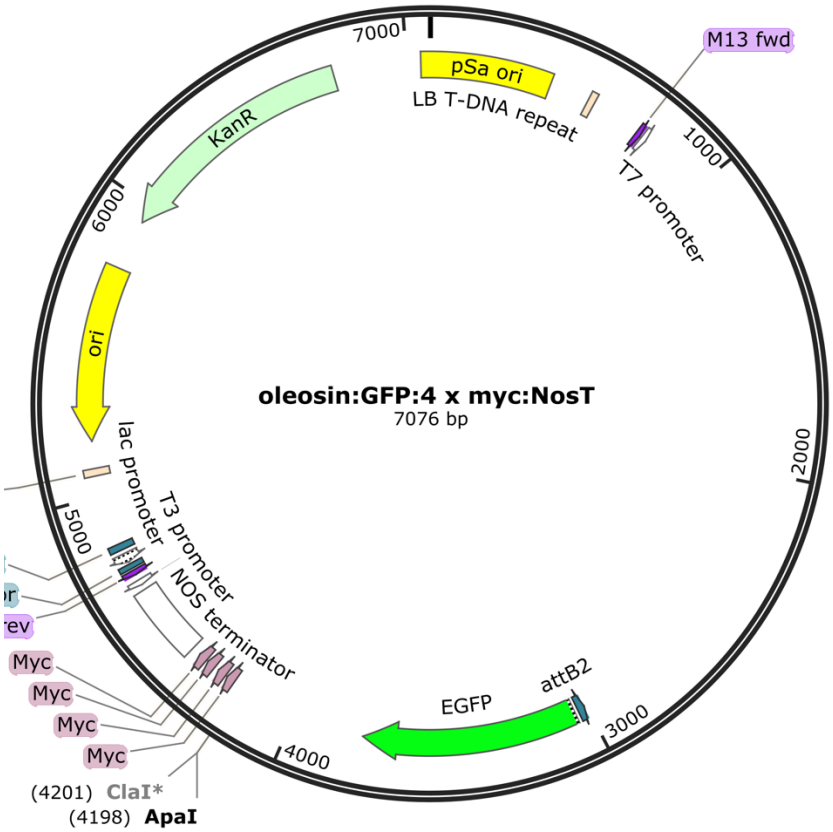
7000
M13 fwd
pSa ori
LB T-DNA repeat
1000
T7 promoter
KanR
6000
ori
2000
oleosin:GFP:4 x myc:NosT
7076 bp
lac promoter
5000
T3 promoter
NOS terminator
Myc
Myc
Myc
Myc
attB2
EGFP
3000
4000
(4201) ClaI*
(4198) ApaI

B

Figure 2.1: Plasmid oleosin:GFP:p35S:EYFP:NosT and plasmid oleosin:GFP:4xmyc:NosT maps. Plasmid oleosin:GFP:p35S:EYFP:NosT (A) was used for cyt c_{6A} protein localization study and the plasmid oleosin:GFP:4xmyc:NosT (B) was used for protein pull-down analysis.

2.2.3 Plasmid purification

Plasmids were purified from 2 ml of overnight grown *E. coli* cultures bearing the relevant plasmids, using a GeneJet Plasmid Miniprep Kit (Fermentas), according to the manufacturer's protocol.

2.2.4 Genomic DNA purification from cyanobacteria

Five milliliters of a mid-log phase *S. elongatus* culture was harvested by centrifugation at 14,000 rpm (Eppendorf centrifuge 5415 R) for 5 minutes and washed twice in 500 µl ddH_2O to remove BG-11 salts. Genomic DNA was then extracted using a GeneJet Genomic DNA Purification Kit (Fermentas) according to the manufacturer's instructions).

2.2.5 Polymerase Chain Reaction

The Primer3 tool (http://frodo.wi.mit.edu/) was used to design primers. Primer pairs were designed to have melting temperatures as close as possible to 60 °C. All primers for PCRs were re-suspended in ddH_2O to a stock concentration of 100 µM and a working concentration of 10 µM or 20 µM as appropriate. All primers used in this investigation are listed in Appendix-B. Phusion High-Fidelity DNA polymerase (Finnzymes) was used to amplify DNA fragments for all cloning strategies for *S. elongatus* and *Arabidopsis*. The total volume of the PCR reaction mixture was 20 µl, consisting of

0.25 µl / 0.5 µl	plasmid / gDNA (template)
4 µl	5x HF buffer/GC buffer (Thermoscientific)
0.5 µl	10 µM forward primer
0.5 µl	10 µM reverse primer
0.4 µl	dNTP mix, 10 mM each (Company)
0.2 µl	Phusion DNA Polymerase (2 U μl^{-1}) (Thermoscientific)
0.4 µl	DMSO (optional – included with GC buffer)
To 20 µl	Water

GoTaq polymerase (Promega) was used for *S. elongatus* colony PCR. To prepare template DNA from *S. elongatus* strains for colony PCR, a small amount of cells was picked from plates and suspended in 50 µl ddH_2O containing 15-20 425-600 µm acid-washed glass beads (Sigma). The cells were broken by vibration for 10 min at 2,500 rpm in a Vibrax VXR (IKA). Broken cells were centrifuged at 14,000 rpm (Eppendorf centrifuge 5415 R) for 5 min and the supernatant was transferred into a new sterile tube and placed on ice until use. Five µl of the supernatant was used as a template for a typical 50 µl reaction.

5 µl	boiled cell supernatant (template)
10 µl	5x Green GoTaq reaction buffer (Promega)
5 µl	25 mM $MgCl_2$ (Promega)
1 µl	20 µM forward primer
1 µl	20 µM reverse primer
1 µl	dNTP mix, 10 mM each
0.25 µl	GoTaq DNA Polymerase (5 U μl^{-1}) (Promega)
To 50 µl	ddH_2O

PCR cycling profiles are listed in Appendix-B.

GoTaq polymerase was used to check *Arabidopsis* knockouts. 50 µl of CTAB (Cetyltrimethyl ammonium bromide) buffer was added to each PCR tube. Aseptically growing *Arabidopsis* plates were shifted to a flow hood, the seal was carefully removed under aseptic conditions, and, using sterile forceps, single leaves from each plants were transferred individually into PCR tubes containing CTAB buffer. Culture plates were sealed and placed back in growth room. Leaves were individually ground using blunt 200 µl pipette micro tip. 5 µl of the ground supernatant of each leaf was used as a template for a typical 50 µl reaction.

5 µl	ground leaf supernatant (template)
10 µl	5x Green GoTaq reaction buffer
5 µl	25 mM $MgCl_2$
1 µl	20 µM forward primer
1 µl	20 µM reverse primer
1 µl	dNTP mix, 10 mM each
0.25 µl	GoTaq DNA Polymerase (5 U μl^{-1})
To 50 µl	ddH_2O

PCR cycling profiles are listed in Appendix-B.

2.2.6 Gel electrophoresis

Tris-boric acid-EDTA (TBE buffer Appendix-A) mediated agarose gel electrophoresis was used to separate DNA fragments. 100 ml of 1% (W/L) agarose (Melford) was used for the majority of electrophoresis gels and 5 µl of 10 mg ml^{-1} ethidium bromide solution (Sigma-Aldrich) was added. DNA samples were mixed with 6x DNA loading dye (Appendix-A) prior to loading. Gels were run at 100 V for 60 min, viewed and photographed on a UV transilluminator fitted with photographing facilities (U:Genius, SYNGENE)

2.2.7 Purification of PCR products

PCR products (section 2.2.6) were purified in a final volume of 20 µl using the Ultra Clean ™ DNA purification kit from Mo-Bio Laboratories Inc according to the manufacturer's instructions. Where required, the PCR products were purified from electrophoresis gels using the same kit. Appropriate bands were visualized with a UV transilluminator and excised using a razor blade.

2.2.8 Restriction endonuclease digestion

All the restriction endonucleases used in this work were purchased from New England Bio-labs. A typical 20 µl restriction digest was incubated for 1 h at 37 °C and was made up of:

7 µl	DNA PCR product /plasmid at approx. 100 ng μl^{-1}
2 µl	10x Buffer
1 µl	each enzyme
0.5 µl	20x BSA (if required)
To 20 µl	Water

Partial digests normally used a minimal incubation period of 1 min at 37 °C.

2.2.9 Ligation

Purified inserts and vector were ligated using 5 U of T4 DNA ligase (Fermentas). A typical 20 µl ligation mixture included:

5 µl	Vector
12 µl	Insert
2 µl	T_4 DNA ligase buffer (10X)
1 µl	T_4 DNA ligase
To 20 µl	Water

The ligation mixture was incubated at room temperature (20~22 °C) for 1 hour or overnight at 4°C.

2.2.10 Plasmid transformation of *E.coli* competent cells

5 µl of ligation mixture was incubated with 50 µl of heat shock competent DH5α cells prepared by the Burr method (Appendix-A) for 45 min on ice. The mixture was heat shocked in a 42°C water bath for 90 s and incubated on ice for a further 2 min. 1 ml of sterile LB medium was then added and the cells incubated for 1h in a shaker at 160 rpm at 37°C. 200 µl of the transformation mix was spread on LB agar plates (section 2.1.1) and the plates were incubated overnight at 37°C.

Colonies were picked using sterile wooden toothpicks, and inoculated individually into 2 ml of LB liquid medium containing appropriate antibiotics. Cultures were then incubated overnight in a shaker rotating at 160 rpm at 37°C. Cells were then harvested via centrifugation at 14,000 rpm (Eppendorf centrifuge 5415 R) for 15 min. Harvested cells were used to isolate plasmids using a Gene Jet ™ Plasmid miniprep kit from Fermentas. Isolated constructs were confirmed as correct by sequencing using the in-house facility, Department of Biochemistry, University of Cambridge.

2.3 Cyanobacterial transformation

Fifty ml of *S. elongatus* culture was grown in 100 ml conical flasks with BG-11 (Rippka, *et al*., 1979) medium in a shaker rotating at 160 rpm at 30°C under low light (15 μE m^{-2} s^{-2}). Cells were harvested at mid-log phase (OD_{750} of 0.3-0.5 using HeλIOS Y from Thermo Spectronic) using a bench top centrifuge at 4000 rpm (Hettich Universal 32 Hettich Zentrifugen) for 15 min. Pellets were re-suspended in 1 ml of sterile fresh BG-11 medium and centrifuged at 4000 rpm (eppendrorp centrifuge 5415 R) for 15min. Pellets were again re-suspended in 100 µl of sterile fresh BG-11 medium.

About 10 µg of marker plasmid (derived from chapter 4) containing the flanking regions of the target gene and a marker cassette *kan*^{R}, or *kan*^{R}*sacB* was transferred into a 15 ml Falcon tube (CELLSTAR®) and mixed with 100 µl of the re-suspended culture by pipetting. The incubation tube was then sealed with sterile cotton wool and placed horizontally in an incubator for 6 h at 30°C in dark conditions. This mixture was gently agitated at 50 rpm to stop the cells sedimenting. 30 and 50 µl of the incubated culture was then spread separately on BG-11 agar plates with half the usual concentration of antibiotic, i.e. kanamycin (30 µg ml^{-1}) which were then incubated at 30°C under moderate light (40 µE m^{-2} s^{-1}).

Transformant colonies could be seen after 8-10 days. Four individual transformants were re-streaked 6-8 times on BG-11 agar plates containing kanamycin (60 µg ml^{-1}). One to four individual colonies were analysed by PCR using the knockout check primers (Appendix-C)

2.4 Agrobacterium transformation

Three to 5 µl of recombinant plasmid (chapter 4) was added to competent *Agrobacterium* cells of 50 µl, then the tube containing the mixture was snap frozen in liquid nitrogen, followed by incubation in a 37 °C water bath for 3 min. One ml of sterile LB medium was added to the mixture and incubated for 5 h in a shaker at 160 rpm and 30 °C. One ml of the incubated cells was spread on LB agar plate containing kanamycin (50 µg ml^{-1}), rifampicin (25 µg ml^{-1}) and tetracycline (50 µg ml^{-1}). Plates were then incubated at 30 °C for 3 days until transformants were visible. A few individual colonies were selected for liquid seed culture, from which 1 ml was used to prepare glycerol stocks for long-term storage.

2.5 Arabidopsis transformation

Col-0 wild type seeds were grown on ½ MS agar plates in a growth chamber 16/8 light dark condition and 22 °C for 10-15 days, then seedlings were transferred on to compost (Levington Advance Solution) in 4 inch x 4 inch plastic pots, and transferred into a plant growth chamber with long day conditions (16 h light/8 h dark) at 22 °C with 60% humidity. Watering was done every other day for healthy growth. After 3 weeks, the plants were ready for the floral dip transformation (Zhang, *et al*., 2006; Clough and Bent 1998). Two days before the transformation, additional watering of the plants was performed to

maintain humidity. About 5 ml of *Agrobacterium* seed culture (section 2.4) was transferred into a 1 L flask containing 250 ml of LB medium supplemented with kanamycin (50 μg ml^{-1}), rifampicin (25 μg ml^{-1}) and tetracycline (50 μg ml^{-1}).

The culture was kept in a shaker at 200 rpm at 30 °C for ~6-8 h or until OD_{620} ~0.6-0.8. After the incubation the culture was centrifuged at 5000 rpm (Hettich Universal 32 Hettich Zentrifugen) for 10 min at 22 °C. Pellets were re-suspended in 5% sucrose (w/v) containing 0.02% surfactant (Silvet L-77) (v/v) solution by micropipetting. Plants were dipped in the sucrose solution for ~1-2 mins. The plants were then sealed and kept under dark conditions for 24 h. After dark incubation, the plants were unsealed and transferred to a plant growth chamber under long day conditions (16 h light/8 h dark) at 22 °C and 60% humidity. About the time the siliques matured, watering was stopped. Once the plant had completely dried, the seeds were harvested; transformed seeds (ones that fluoresced) were picked under a fluorescent binocular microscope (OLYMPUS SZX12) with GFP filter.

2.6 Cyanobacterial growth studies

S. elongatus mutant strains were grown as a stock for cell growth studies in 50 ml sterile BG-11 medium in a shaker rotating at 160 rpm at 30 °C under moderate light {(ML) (40 μE m^{-2} s^{-1})}. Measured the OD of the stock and used it to set up subcultures of 50 ml in BG-11 medium using a Thermo-spectronic spectrophotometer. For each treatment three replicates of both mutant and WT were grown. Cultures were grown at a range of different conditions, including varying light conditions; extreme low light {(ELL) (2-5 μE m^{-2} s^{-1})}, low light {(LL) (15 μE m^{-2} s^{-1})}, ML , and high light {(HL) (150 μE m^{-2} s^{-1})}. Growth of the cultures under different environmental conditions was assessed by measurement at OD_{750}. 500 ml cultures were also grown under higher light conditions, including 300, 500, and 700 μE m^{-2} s^{-1} using a Algem photobioreactor (Algenuity) with auto cell density measurement at OD_{740}.

2.7 Arabidopsis growth study

2.7.1 Root and leaf phenotype assessment in culture plate

For root measurement and leaf morphology studies different mutants of *A. thaliana* seeds were sterilized (Chapter 2.1.2) and inoculated on MS agar plates. Culture plates were kept under 100 μE m^{-2} s^{-1} light intensity. Growth room temperature was maintained at 22 °C,

humidity was controlled to 60%, and illumination was maintained at 16 h light /8 h dark cycles. After every 24 hrs the plants were scanned (SHARP MX5070v). Scanning was performed for 13 days. Fourteen individual plant roots from each line were measured and the experiments were repeated twice. After the experiment, the leaves were harvested and counted and the leaf areas were measured. All the measurements were done using the image software.

2.7.2 Plant growth phenotype characterization in soil

Mutant and WT seeds were sterilized and plated on ½ MS agar plate and incubated at 4°C for 2 days (Chapter 2.1.2). Then the plates were incubated under 100 μE m^{-2} s^{-1} light for 2 weeks. Seedlings were carefully removed from the agar plates and planted in separate pots 4 inch 4 inch containing compost (Levington Advance Solution) mixed with Vermiculite. Planted seedlings were grown in controlled Plant Growth Facilities (PGF) provided by the Department of Plant Sciences, University of Cambridge. Potted plants were then placed under 2 different light conditions for growth characterization studies. One set of plants (5 plants from each line) was kept under 150 μE m^{-2} s^{-1} light intensity and another set under 300 μE m^{-2} s^{-1} light intensity. The temperature was maintained at 22 °C, the humidity was controlled to 60% and the illumination was maintained at 16 h light /8 h dark cycles. Plats were watered regularly with automated irrigation facility. Plant growth was monitored and photographs taken every 10 days. Plant growth was measured using ImageJ software.

2.8 Transcript analysis study

2.8.1 RNA Isolation

50 ml cultures of *S. elongatus* WT cells were grown under LL, ML, HL, HL/D (high light dark cycle), 300, 500 and 700 µE m^{-2} s^{-1} light conditions respectively. Total RNA was isolated from 2 ml of cultures from each treatment. RNA was isolated using RNeasy mini kit (Qiagen). Isolated RNA was treated with DNaseI (Thermo Scientific) to remove residual genomic DNA and the RNA quality and quantity were assessed using Nano drop (Thermo scientific) at A260/A280. RNA preparations were directly used for experiments or stored at -80 °C for future analysis.

2.8.2 Complementary DNA (cDNA) synthesis

To investigate transcript abundance under different physiological conditions, isolated RNA was converted into cDNA. First-strand synthesis of cDNA was performed using 100 ng of total RNA. SuperScript™ III First-Strand Synthesis System (Life Technologies) and random primers were used for cDNA synthesis. Controls without reverse transcriptase were used to investigate potential gDNA contamination. First-strand cDNA was synthesised according to the manufacturer's specification. Synthesised cDNA was diluted 10 fold prior to qRT-PCR.

2.8.3 Relative quantification of transcript levels by real time qPCR (RT-qPCR)

Primers used for real-time qRT-PCR are listed in Appendix-C. The amplification efficiency of the primers was initially tested using gDNA in conventional PCR using Go Taq DNA polymerase enzyme (Promega). 16S ribosomal RNA gene was used as a reference transcript (Filipe, *et al*., 2012).

Gene expression studies were carried out in order to investigate the relative transcript abundance of the redox carriers cytochrome c_{6C} (PetJ2) and cytochrome c_M (CytM). qRT-PCR measurements were performed using the Rotor gene Q (Qiagen) Real-Time Detection System. qRT-PCR reactions were prepared in triplicate in a total volume of 20 µl using the SYBR® Green JumpStart™ *Taq* ReadyMix™ master mix containing each gene specific primer at 0.4 µM and 1/25 volume of 10X-diluted cDNA**.** The following PCR cycling conditions were used:

Thermocycler parameters

Initial Denaturation	95°C	10 min	1 cycle
Denaturation	95°C	15 sec	
Annealing	60°C	1 min	40 cycle
Extension	72°C	1 min/kb	
Hold	4°C	Indefinite	1 cycle

Final melt-curve analysis of 55-95°C. Controls without template and without reverse transcriptase were included in all qRT-PCR experiments. Transcript expression levels were calculated by the comparative quantification method using the endogenous control gene encoding 16S rRNAs in *S. elongatus* as a reference.

2.9 Northern Blotting: Probe Labelling

The T7 promoter in the reverse primer was preceded by the *Bam*HI site and the forward primer had the *Eco*RI site. A template for a digoxygenin (DIG)-labeled RNA probe for Northern hybridization experiments was generated by amplifying the coding sequence for cyt c_{6C} with gene specific primers. The reverse primer had a *Bam*HI site followed by a T7 promoter sequence, and the forward primer had an *Eco*RI site. The amplified sequence was cloned into pUC19. One µg of plasmid was linearized with *Eco*RI and the products purified (section 2.2.8) and the probe was generated according to the manufacturer's instructions (Roche Diagnostics GmbH).

2.9.1 RNA Gel electrophoresis

The gel tank, 100 ml gel casting trays and gel combs were soaked in 3% (v/v) hydrogen peroxide solution (H_2O_2). Areas for gel electrophoresis were also cleaned with the same solution. Fresh TBE buffer was used for RNA electrophoresis and made by dissolving 5.49 g of TRIZMA base, 2.7 g of boric acid and 2 ml of 0.5 M EDTA in 1 litre of DEPC H_2O. Guanidine thiocyanate (60 mg ml^{-1}) was added to a 1% agarose gel. A total volume of 50 µl loading mixture was loaded into each well containing 3 µg (~200ng/ µl) of total RNA in 15µl) with 35 µl of formamide solution, 5 µl of RNA loading dye in 45 µl of formamide and 50 µl of formamide as a negative control. All the loading mixtures were incubated at 65° C for 5 min, loaded directly into the set gel and analysed by electrophoresis at 100 V for 30-40 min.

After electrophoresis, the gel was trimmed and soaked in 20x SSC (Appendix-A) solution. The RNA was subsequently transferred to a positively charged nylon membrane (Roche) according to the capillary transfer method (Sambrook *et al*., 1989). After overnight transfer, the RNA was cross-linked to the nylon by exposing the membrane to ultraviolet light (UV cross-linker, UV Stratalinker®, STRATAGENE®) for 10 minutes.

Nylon membranes were initially pre-hybridised in 50 ml of blocking solution (12.5 ml 2xSSC (Appendix-A), 0.05g lauroyl sarcosinate, 0.1 ml 10% (w/v) SDS, 0.5 g skim milk powder and 36.9 ml distilled water) at 65°C in a Robbins Scientific model 1000 hybridization incubator for 2 hours, with rotation. After this incubation, the pre-hybridization solution was discarded and the membrane was incubated in 30 ml of

hybridization solution (identical to blocking solution, except with the addition of the DIG-labelled probe). The membrane and probe were allowed to hybridise overnight at 65°C.

After hybridization, the membrane was subjected to a series of washes. These were as follows: 2 × SSC, (3 washes of 5 minutes at room temperature); 0.5 × SSC, (2 washes of 20 minutes at 65°C). Following equilibration in washing buffer, the membrane was incubated with blocking solution for 30 minutes. This solution was removed and replaced with blocking solution containing 1:20000 diluted anti-DIG antibody from sheep (Roche). Following incubation for 30 minutes, the membrane was washed twice for 15 minutes with washing buffer before being equilibrated in detection buffer. CDP-Star (Roche), a chemiluminescent substrate, was diluted 1:100 in detection buffer and added to the membrane. The result was visualised in a G-BOX (SYNGENE) and the images were captured frequently.

2.10 Immunoblotting techniques.

2.10.1 Sample preparation

Different mutant lines of plants were grown in 100 μE m^{-2} s^{-1} light, and a single leaf from each of the different knockouts was snap frozen in liquid N_2 and stored at -80°C for later use or kept on ice for immediate homogenization. About 3 mg of sample (about 2 leaves) was used for immunoblot analysis. 100 μl lysis buffer (Appendix-A) was added to the sample tube, and homogenized with a plastic pestle. Homogenized samples were centrifuged for 20 minutes at 14,000 rpm (Eppendrorp Centrifuge 5415 R) at 4°C and placed on ice. The supernatant was transferred to a pre-chilled fresh tube.

Cyanobacterial cultures were grown at different light conditions in 100 ml conical flasks. Cells were harvested at mid log phase and centrifuged for 10 min at 500 rpm (Hettich Universal 32 Hettich Zentrifugen). 100 μl of phosphate buffered saline ((PBS) Appendix-A)) was added and the cultures were snap frozen and stored at -80ºC for later use or kept on ice for immediatelysis. 5x SDS loading buffer (Appendix-A) was directly added to the samples, which were boiled for 5 min, followed by centrifugation for 5 min at 14000 rpm (Eppendorf centrifuge 5415 R). Cell lysate was gently removed and transferred to a new tube.

2.10.2 SDS-PAGE (Polyacrylamide Gel Electrophoresis)

About 20-50 µl of lysate was used to perform SDS-PAGE electrophoresis. To the volume of plant cell lysate, an equal volume of 2x Laemmli Sample Buffer (Appendix-A) was added and boiled at 100°C for 5 minutes prior to loading on an SDS-polyacrylamide gel. Cyanobacterial cell lysate was mixed with 2x Laemmli Sample Buffer and directly loaded onto an SD-polyacrylamide gel. Equal amounts of lysate were loaded into the SDS mini protein precast gels 4-20% (BIO RAD), with molecular weight markers PageRuler^{TM}) The gel was run in SDS tank (BIO RAD) with 1 X SDS-PAGE Running Buffer (Appendix-A), about 1 hr at 100 V or until the dye front reached the bottom of the gel, with power supplied by a Biorad PowerPac Junior power supply. If not to be used for Western blotting, gels were stained with InstantBlue (Expedeon) according to the manufacturer's instructions.

2.10.3 Protein transfer to the membrane

Wet electro-blotting was performed in a Mini Protean II tank for 75 min at 100 V onto PVDF membrane (Amersham Hybond-LFP), with power supplied by a Biorad PowerPac Junior power supply, in a 4 °C room. The gel was soaked in 4 °C transfer buffer (Appendix-A) for at least 10 minutes prior to blotting. The PVDF membrane was soaked in methanol for 20 s, followed by mqH_2O for 20 s, then 4 °C transfer buffer for at least 5 min prior to blotting. A blotting sandwich was constructed of a layer of 3 mm sponge, two layers of blotting paper (Sartorius), membrane, gel, two layers of blotting paper, and sponge. Sponge and blotting paper were soaked in 4 °C transfer buffer and had all air bubbles removed prior to use.

2.10.4 Protein transfers and antibody detection

The membrane was blocked for 1 hour at room temperature or overnight at 4°C using 5% dried milk (Marvel original dried milk) in phosphate buffered saline Tween 20 (PBST) (Appendix-A) solution. The membrane was then incubated with appropriate dilutions of primary antibody, anti-c-Myc (A-14) rabbit polyclonal IgG, [(1:1000 dilution) Santa Cruz Biotechnology, Inc], anti-polyhistidine mouse monoclonal IgG [(1: 3000) SIGMA], or anti-GFP mouse monoclonal IgG1 [(1:3000), Cell Biolabs Inc] PBST containing 1% milk for 1 hour at room temperature or overnight at 4°C. After the incubation, the membrane was washed five times with wash buffer (PBST) for periods of 5 minutes. The membrane was then labeled with the secondary antibody, either goat anti-rabbit IgG (H+L)-HRP

conjugate, [(1:10,000 dilution) ThermoFisher] or goat anti-mouse IgG HRP conjugate [(1: 10,000) ThermoFisher], in 1% Milk-PBST at room temperature for 1 hour. The membrane was then washed five times with PBST. For signal development, the WesternBright ™ Western blotting detection kit was used. A total volume of 2-4 ml of reagent mix was added to the membrane, followed by incubation in the dark for 5 min. Excess reagent was removed and the membrane was covered in transparent plastic wrap prior to exposure. Chemiluminescence was recorded using a GBOX gel scanner with Genesnap software (Syngene) taking cumulative images for total exposure times of up to 80 min (no illumination, no filter).

2.11 Oxygen electrode measurements

2.11.1 Photosynthesis and respiration measurements

Photosynthetic O_2 evolution rates (photosynthesis) and O_2 depletion rates (respiration) were determined using cell cultures (~4 nmol Chl ml^{-1}) in a oxygen electrode system (Rank Brothers Instruments Hansatech) maintained at 30 °C. Following dark equilibration (10 min), O_2 exchange rates were recorded for 5 min at increasing light intensities (0, 10, 25, 50, 100, 250, 500, 1000 and 2000 μE m^{-2} s^{-1}), using MR16 white LED lamps (Deltech UK, London). Each light period was followed by 10 min dark periods in order to measure respiration rates. The respiration rate following illumination at each light intensity was subtracted to estimate the real rate of photosynthetic O_2 evolution.

2.11.2 Photoinhibition measurements

To measure photoinhibition, cell cultures (approximately 1 nmol chlorophyll mL^{-1}) were first dark equilibrated (10 min), and the rate of oxygen evolution was recorded for 80 min at a light intensity of 2,000 μE m^{-2} s^{-1}. All measurements were standardized to the initial rate. Photoinhibition experiments were conducted either in the absence or presence of lincomycin (250 mg mL^{-1}). A Student's paired t test was used for all comparisons, $P<0.05$ being considered statistically significant.

To measure photoinhibition, cell cultures (~1 nmol Chl ml^{-1}) were first dark equilibrated (30 min), and the rate of O_2 evolution was recorded for 80 mins at a light intensity of 1200 µE m^{-2} s^{-1}. All measurements were standardized to the initial rate. Photosynthetic oxygen evolution rates and oxygen depletion rates (respiration) were determined on cell cultures (approximately 4 nmol chlorophyll mL^{-1}) using an oxygen electrode system (Rank

Brothers Instruments) maintained at 30°C. Following dark equilibration (10 min), oxygen-exchange rates were recorded for 10 min at increasing light intensities (10, 25, 60, 150, 350, 900, and 2,000 mmol photons m^{-2} s^{-1}) using MR16 white LED lamps (Deltech). Each light period was followed immediately by 10 min in darkness to calculate the respiration rates. The respiration rate following illumination at each light intensity was subtracted to estimate the real rate of photosynthetic oxygen evolution.

Numbers of cells per unit of volume were measured by counting the cells directly using a Beckman Coulter 2Z particle counter. Measurements were performed using 20 mL of O.D. (750 nm) = 0.5 cells diluted in 10 mL of measuring buffer. Cell diameter was directly measured using the same instrument. Cell volume was calculated from these measurements. The amount of chlorophyll was measured by subtracting the 750-nm O.D. value from the 680-nm O.D. value and multiplying by 10.854, as described previously (Bombelli *et al.*, 2011; Lea-Smith *et al.*, 2013).

2.12. Fluorescence measurements

Fluorescence measurements were made using a Walz PAM 101 fluorometer with the 101-ED emitter-detector unit. A Walz Optical Unit ED-101US was used for cell suspension. All samples were grown to an OD_{750} of ~ 0.5 and bubbled with air. Actinic light for state-2 to state-1 transitions was provided using Flexilux 150 HL white lights behind a blue Corning 4-96 glass filter. State-2 to state-1 transitions were provided by using a PAM-102 Far-red light source. Prior to measurements, cells were dark adapted for 40 min. Minimum fluorescence (F_0) (Maxwell and Johnson, 2000) was determined by illuminating with measuring light (0.01 μEm^{-2} s^{-1}). Maximum fluorescence (F_m) in the dark-adapted state was determined using 0.8 second long saturation (6500 μE m^{-2} s^{-1}) pulses delivered by a Schott KL 1500 white light source. The actinic light was then turned on and a second saturation pulse was applied after 20 min (F'_m). At the end of state transition measurements, actinic light was turned off to obtain F_0. Finally, maximum fluorescence (F_m) was determined by injecting 10 µM of DCMU ((3,4-dichlorophenyl)-1, 1-dimethylurea) with the actinic light kept on. Maximum quantum yield of PSII (F_v/F_m) was calculated as the ratio of variable fluorescence (F_v) to maximum fluorescence (F_m) obtained with DCMU and was calculated as (F_m-F_0)/ F. The effective quantum yield of PSII (Φ_{PSII}) was calculated as (F'_m–F_t)/ F'_m. Photochemical quenching (qP) was calculated

as $(F'_m - F_t)/(F'_m - F'_0)$. Non-photochemical quenching (NPQ) was calculated as $(F'_m - F_{m1})/F_{m1}$.

2.13 P700 reduction kinetics

$P700^+$ reduction kinetic was preformed with PAM-100 (Walz, Effeltrich, Germany) equipped with an emitter-detector unit 101 ED (Schreiber *et al.*, 1986). A modulated non-actinic 1.6 kHz measuring beam was used to measure fluorescence. PSI was excited for 5 min period of far-red light (10 μE m^{-2} s^{-1}) using PAM-102. Far-red light was switched off and immediately flowed by100 ms saturating pulses (4500 μmol m^{-2} s^{-1}) to complete oxidation $P700^+$. Dark reduction of $P700^+$ was then monitored.

2.14 Microscopic studies of protein localization

The Green Fluorescent Protein variant Enhanced Yellow Fluorescent Protein (EYFP) from the jellyfish *Aequorea victoria* (Tsien, 1998) was used as reporter to determine the intracellular localization of proteins in plants. cDNA of cyt c_{6A} was amplified and cloned in frame upstream of the sequence of EYFP as described in chapter 3.3.1 and 3.3.3. 10-day old transgenic seedlings grown on MS agar plates were used for confocal fluorescence microscopy (Leica SP8-iPhox). Transgenic cyanobacteria were grown to an OD_{750} of ~ 0.5 and used for confocal microscopy as above.

2.15 RNA extraction, cDNA library construction, sequencing and bioinformatics analysis of *Synechococcus elongatus* PCC 7942 transcriptome samples

Synechococcus elongatus PCC 7942 wild type and mutant cells were lysed by resuspension in RLT buffer and subsequent bead beating in a Mini-Beadbeater-16 (BioSpec Products) for 5 minutes. Total RNA was then isolated using RNeasy Plant Mini Kit (Qiagen), including an on the column digest, according to the manufacturer's protocol. All RNA samples had A260/A280 ratios higher than 1.8. The concentration and quality of each RNA preparation was determined using a Agilent 2100 Bioanalyzer, which provides sizing, quantitation and quality control. RNA-seq libraries were constructed from independent biological duplicates in each condition by the sequencing facility in the Biochemistry Department, University of Cambridge. The cDNA libraries were constructed using TruSeq Stranded RNA library preparation (Illumina) in combination with Ribo-Zero Magnetic Kit (Bacteria) (Illumina), according to manufacturers' instructions. The cDNA libraries obtained were sequenced using a NextSeq500 machine

(Illumina) in single-read mode, running 150 cycles by the sequencing facility in the Biochemistry Department, University of Cambridge. The alignment of reads, coverage calculation, gene-wise read quantification and differential gene expression were performed with READemption (Forstner *et al*., 2014), using segemehl version X and DESeq version V (Anders and Huber, 2013; Otto *et al*., 2014). Segmehl and DESeq interfaced with Python 3.0 and R (3.2.2), respectively (Ripley, 2001; Summerfield, 2011). A visual inspection of the coverage was performed using the Integrative Genomics Viewer (IGV) (Robinson *et al*., 2011). The reference sequences and gene annotations were retrieved from the EnsemblBacteria database. Genes with a fold-change of at least 2.0 and an adjusted p-value ≤ 0.05 were considered differentially expressed.

2.16 Bioinformatics

BLAST searches (http://genome.microbedb.jp/CyanoBase) and (http://blast.ncbi.nlm.nih.gov/Blast.cgi) for homologues of genes or proteins were run using standard parameters. Performing virtual digests with NEBcutter V2.0 (http://tools.neb.com/NEBcutter2/) (Vincze, 2003) was helpful when designing cloning strategies and checking expected sizes for restriction digests. BPROM(http://linux1.softberry.com/berry.phtml?topic=bprom&group=programs&subgroup=gfindb) (Solovyev and Salamov, 2010) was used to search for possible bacterial promoter sites. TransTermHP (http://transterm.cbcb.umd.edu/) (Kingsford *et al*., 2007) was used to predict bacterial rho-independent transcription terminators. SignalP (http://www.cbs.dtu.dk/services/SignalP/) (Petersen *et al*., 2011), SignalBLAST (http://sigpep.services.came.sbg.ac.at/signalblast.html) (Frank and Sippl, 2008), TatP (http://www.cbs.dtu.dk/services/TatP/) (Bendtsen *et al*., 2005) and LipoP (http://www.cbs.dtu.dk/services/LipoP/) (Rahman *et al*., 2008) were used to check protein sequences for possible Sec or TAT signal sequences, or lipid modification motifs. ClustalW2 (http://www.ebi.ac.uk/Tools/msa/clustalw2/) (Larkin *et al*., 2007) and Clustal Omega (http://www.ebi.ac.uk/Tools/msa/clustalo/) (Sievers *et al*., 2011) were used for creating multiple alignments of DNA sequences with the default settings. Snapgene free software (http://www.snapgene.com/) was downloaded and used to design plasmids. ImageJ (http://imagej.nih.gov/ij/) software was used to measure the root and shoot lengths and the leaf area of different lines of *A. thaliana*. Mendeley Desktop (www.mendeley.com) was used as a reference manager.

CHAPTER 3 CONSTRUCTION OF GENETICALLY MODIFIED STRAINS

3.1 Results of cyt c_{6C} mutant strain construction in *S. elongates*

3.1.1 Amplification of flanking regions for disruption of cytochrome c_{6C}

The strategy used for disruption of the cytochrome c_{6C} (cyt c_{6C}) gene is shown in figure 3.1. Upstream and downstream flanking regions of the cyt c_{6C} gene were amplified from *S. elongatus* PCC 7942 genomic DNA with gene specific primers containing *Xba*I+*Hin*dIII and *Eco*RI+*Kpn*I sites (Appendix-C) and cloned into pUC19. These primers would amplify 885 bp of the upstream flanking region and 976 bp of the downstream flanking region. PCR products from reactions using primers for downstream and upstream flanking sequences were analysed by gel electrophoresis. Bands corresponding to the sizes of the expected products were seen (data not shown). These bands were excised from the gels and the DNA purified.

3.1.2 Cloning of flanking sequences into pUC19 vector

Gel purified upstream flanking region and pUC19 vector were digested with *Xba*I+*Hin*dIII simultaneously, and downstream flanking region and pUC19 vector were digested with *Eco*RI+*Kpn*I simultaneously and the products were purified from the digestion reaction. Purified inserts and cut vector were ligated using T4 DNA ligase in separate reactions for the upstream and downstream flanking regions. pUC19 + upstream and the pUC19 + downstream flanking sequence ligation mixtures were added to competent *E. coli* DH5α cells for transformation. After overnight incubation of the transformation products on agar plates containing ampicillin, Xgal and IPTG, four white colonies were picked for each construct for plasmid isolation. Isolated plasmids were digested with *Xba*I+*Hin*dIII and *Eco*RI+*Kpn*I as appropriate. The digested products were analysed by gel electrophoresis. Plasmid DNA corresponding to one example of each construct showing the expected digest pattern was sent for DNA sequencing which confirmed the nature of the insert.

3.1.3 Cloning of upstream and downstream flanking sequences together

The plasmid pUC19 containing the upstream flank confirmed by sequencing was designated as pRV1 and that pUC19 containing the downstream flank was designated pRV2. Samples of each were digested with *Eco*RI+*Kpn*I. The pRV1 digestion mixture

was fractionated by gel electrophoresis and the upstream flank was gel purified, but the cut pRV2 was directly purified from the restriction digestion mixture. Gel purified upstream flank was then ligated with *Eco*RI+*Kpn*I cut pRV2, and the ligation products introduced into competent DH5α cells by transformation. Four individual white colonies were picked for plasmid purification and the plasmid was digested with *Eco*RI+*Hin*dIII followed by electrophoresis to confirm the insertion of both flanks. A plasmid generating the expected digestion products of 3.5 kb was designated pRV3.

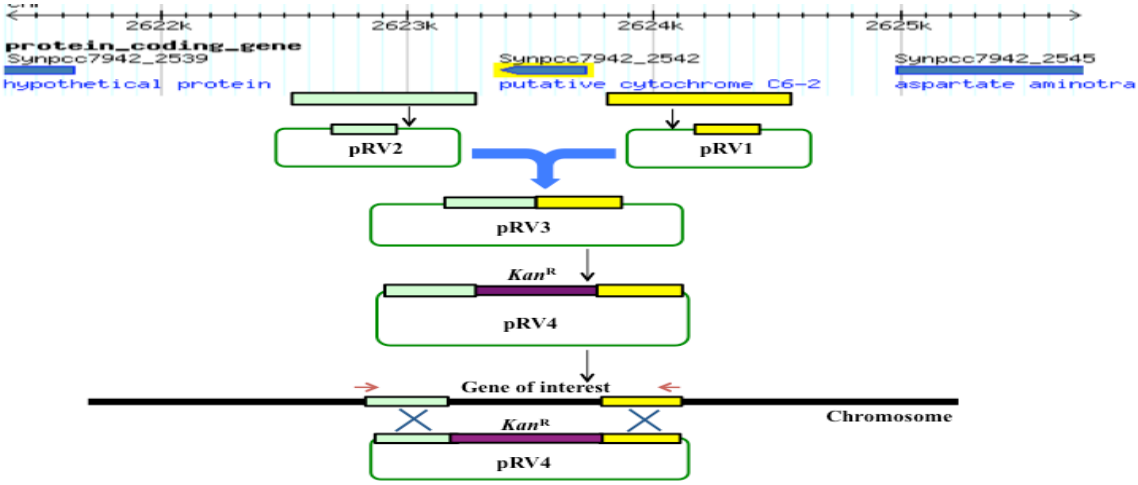

Figure 3.1: Schematic diagram for cyt c_{6C} knockout strategy. This diagram indicates the different steps involved in generating plasmids for construction of the cyt c_{6C} knockout mutant. (Not drawn to scale).

3.1.4 Cloning of *kan*^{R} cassette into the pRV3 plasmid

Plasmid pUC4K contains a kanamycin resistance cassette *kan*^{R} flanked by *Bam*HI sites. Hence the pUC4K plasmid was digested with *Bam*HI to excise the kanamycin resistance cassette. The digestion products were fractionated by gel electrophoresis and the kanamycin resistance cassette was gel purified. The pRV3 plasmid was digested with *Bam*HI and purified directly from the restriction reaction. The *kan*^{R} cassette was incubated with the *Bam*HI cut pRV3 vector and T4 DNA ligase, and the ligation products were introduced into competent DH5α cells by transformation. The transformed cells were spread on kanamycin supplemented LB agar plates to select for colonies containing the *kan*^{R} gene. Purified plasmid DNA from four colonies was then digested with *Bam*HI and electrophoresis to confirm the presence of the *kan*^{R} cassette, and a plasmid generating the

expected restriction pattern (data not shown) was designated pRV4. pRV4 was now ready to transfer into *S. elongatus*.

3.1.5 Cyt c_{6C} knockout segregation

S. elongatus PCC 7942 cells were transformed by incubating with 10 μg of plasmid pRV4 DNA. (See section 2.3 in chapter 2 for the detailed method of transformation). Recombination occurring between the upstream and downstream flanking regions replaces the target gene with the kan^R. Successfully transformed cells resulted in individual colonies; two individual colonies were taken for segregation and were analysed by PCR using gene-specific flanking primers to confirm the segregation (figure 3.2).

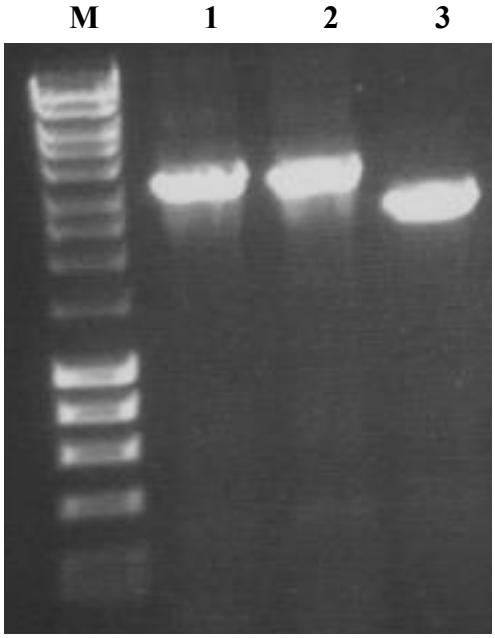

Figure 3.2: Analysis of segregation of cytochrome c_{6C} of *S. elongatus* PCC 7942. Lane 1: M: (Marker, Bioline hyper Ladder™ I), Lane 2&3: Cyt c_{6C} mutant (1&2), lane 4: WT (3).

3.2 Results of construction of plasmids for cyt c_M mutant strains

3.2.1 Amplification and cloning of cyt c_M flanking regions together

Disruption of the cytochrome c_M gene was similar to the strategy used for cyt c_{6C} as explained in section 3.1, except that a disruption cassette also containing a levansucrase gene *sacB* was used. Upstream and downstream flanking regions of the cyt c_M gene were amplified with gene specific primers containing *Eco*RI+*Bam*HI and *Bam*HI+*Xba*I sites

(Appendix-C) and cloned into pUC19. The plasmid containing the upstream flank as confirmed by sequencing was designated pRV18, and that containing the downstream flank was designated pRV19. Samples of each were digested with *Eco*RI+*BamH*I. The pRV18 digestion mixture was fractionated by electrophoresis and the upstream flank was gel purified, but the cut pRV19 was directly purified from the restriction digestion mixture. Gel purified upstream flank was then ligated with *Eco*RI+*Bam*HI cut pRV19, the ligation products were introduced into competent cells, and plasmid was isolated from 4 colonies obtained after plating on ampicillin. A plasmid generating the expected pattern on digestion with the Cyt c_M upstream and downstream flanking region in pUC19 was designated pRV20. Plasmid construction strategies are depicted in figure 3.3.

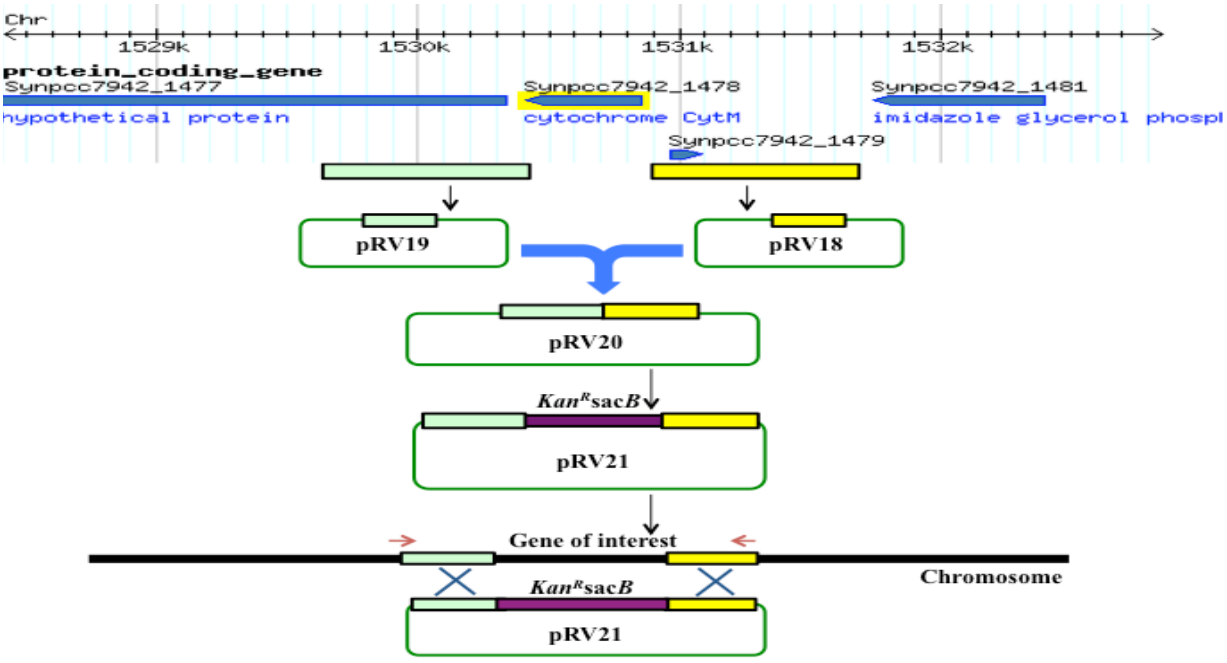

Figure 3.3: Schematic diagram showing different stages of plasmid construction for inactivation of cyt c_M. The *kan*^{R}*sacB* cassette was used for selection of transformed colonies.

3.2.2 Cloning of *kan*^{R} *sacB* cassette into the pRV18 plasmid

The plasmid contains a kanamycin resistance and sucrose sensitivity cassette (*kan*^{R}*sacB*) inserted into a *Bam*HI site. Hence the plasmid was digested with *Bam*HI to excise the *kan*^{R}*sacB* resistance cassette. The restriction mixture was electrophoresed, and the kanamycin resistance cassette was gel purified. The pRV20 plasmid was digested with

*Bam*HI and purified directly from the restriction reaction. The *kan*^{R}*sacB* cassette was incubated with the *Bam*HI cut pRV20 vector, ligation buffer and T4 DNA ligase, and this ligation mixture was introduced into competent DH5α cells by transformation. The transformed cells were spread on kanamycin supplemented LB agar plates to select for colonies containing the *kan*^{R}*sacB* gene. Purified plasmid DNA from four colonies was then digested with *Bam*HI to confirm the presence of the *kan*^{R}*sacB* cassette, and a plasmid generating the expected restriction pattern was designated as pRV21 (figure 3.4) and introduced into *S. elongatus* WT background by transformation.

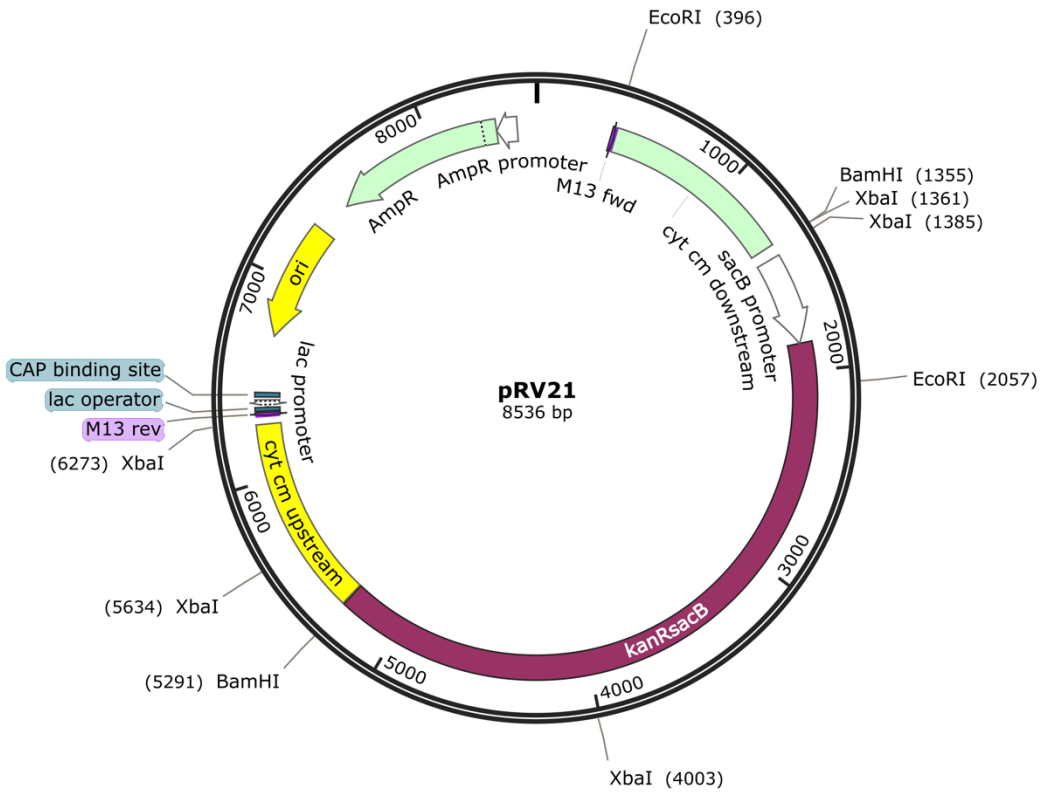

Figure 3.4: Plasmid pRV21. pRV21 has upstream and downstream flanking regions of cyt c_M gene, with the *kan*^{R}*sacB* cassette cloned between the flanking regions. This plasmid was used to knock out the cyt c_M gene.

3.2.3 Cyt c_M knockout segregation

S. elongatus PCC 7942 cells were transformed by incubating with 10 µg of plasmid pRV21 DNA. (See section 2.3 in chapter 2 for the detailed method of transformation). Successfully transformed cells resulted in individual colonies, which were seen after 8-10 days of incubation. Individual colonies were analyzed by PCR using gene-specific primers

to confirm for segregation (figure 3.5 shows a representative example). Although additional faint bands were seen, they did not correspond to the wild type patterns.

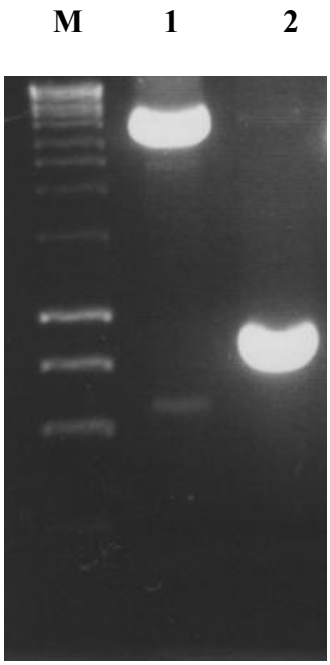

Figure 3.5: Analysis of segregation of knockout strains of cytochrome c_M of *S. elongatus* PCC 7942. Lane 1: M: (Marker, Bioline hyper Ladder^{TM} I), Lane 2: Cyt c_M knockout (1), Lane 3: WT (2).

3.3 Results of strain construction in *Arabidopsis thaliana*

3.3.1 Construction of cyt c_{6A} overexpression plasmids for protein localization

Cyt c_{6A} cDNA was amplified from *A. thaliana* cDNAs using gene specific primers (Appendix-C) that introduced *Eco*RI:*Sal*I+*Pst*I:*Cla*I sites and placed immediately upstream to the EYFP coding sequence in the plasmid oleosin:GFP:p35S:EYFP:NosT. PCR products were fractionated by gel electrophoresis and the product corresponding to the cDNA was purified. Purified PCR product and the plasmid oleosin:GFP:p35S:EYFP:NosT were digested with *Sal*I+*Cla*I, and recovered from the restriction digestion reaction and ligated together. The ligation mixture was then introduced into competent *dam*$^{-}$ DH5α *E. coli* cells. Plasmid was purified from four individual colonies obtained by plating cells onto LB medium containing kanamycin the antibiotics. Isolated plasmid was digested to confirm the nature of insert and the insert was sequenced from two plasmids. Sequence-confirmed plasmid was designated as

pRV33 (figure 3.6). Plasmid pRV33 was introduced into *Agrobacterium* by transformation and then into *A. thaliana* Col-0 wild type background by floral dipping.

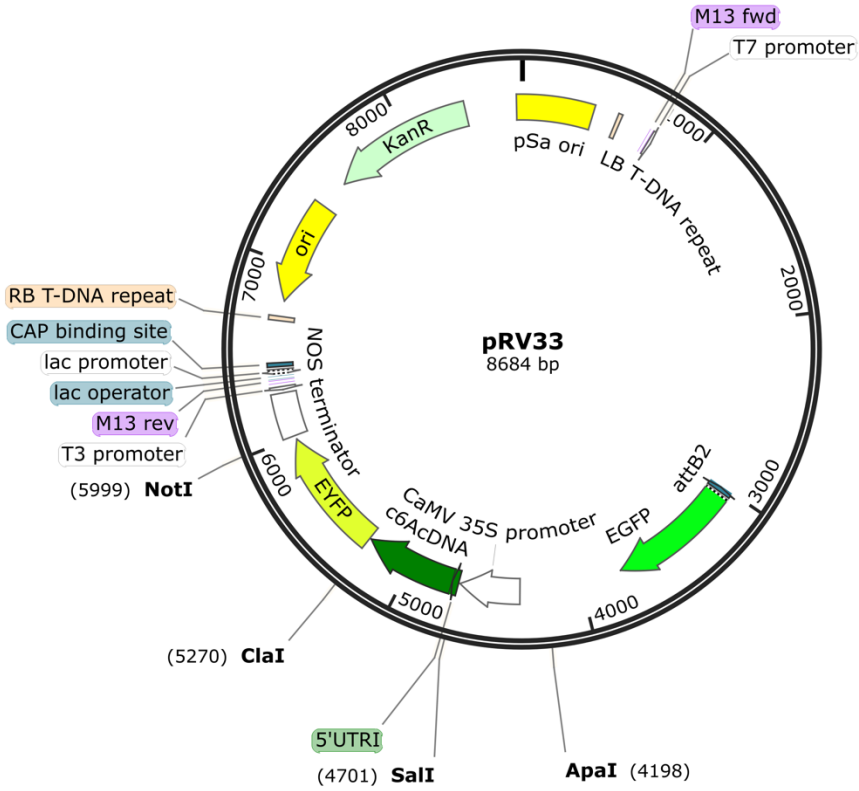

Figure 3.6: Overexpression of cytochrome c_{6A} using p35S promoter. The cyt c_{6A} coding sequence was fused to a sequence encoding EYFP for localization studies. Cyt c_{6A} cDNA was expressed under Cauliflower Mosaic Virus promoter p35S. The plasmid was used to transform *A. thaliana* by Agrobacterium-mediated floral dipping.

3.3.2 Construction of plasmid for overexpression of cyt c_{6A}-myc tag for pull down and immunoblot analysis

Plasmid pRV33 and the plasmid oleosin:GFP:4 x myc:NosT were digested individually with *Apa*I+*Cla*I. The pRV33 digestion products were fractionated by gel electrophoresis. A single band corresponding to a fragment containing the p35S promoter and cyt c_{6A} cDNA was gel purified and ligated to oleosin: 4x myc epitope-tag: NosT plasmid cut with *Apa*I+*Cla*I, that would result in a region encoding a 4x-myc tag on the 3' end of the cDNA. The ligation products were then introduced into competent *dam*$^-$ DH5α *E. coli* cells.

Plasmid DNA was recovered from colonies from transformed cells and verified by restriction digestion and then sent for plasmid sequencing to confirm the nature of insert. The resulting plasmid was designated as pRV34 (figure 3.7). Plasmid pRV34 was introduced into *Agrobacterium* by transformation, which was then that was used for T-DNA transfer into *A. thaliana* Col-0 wild type.

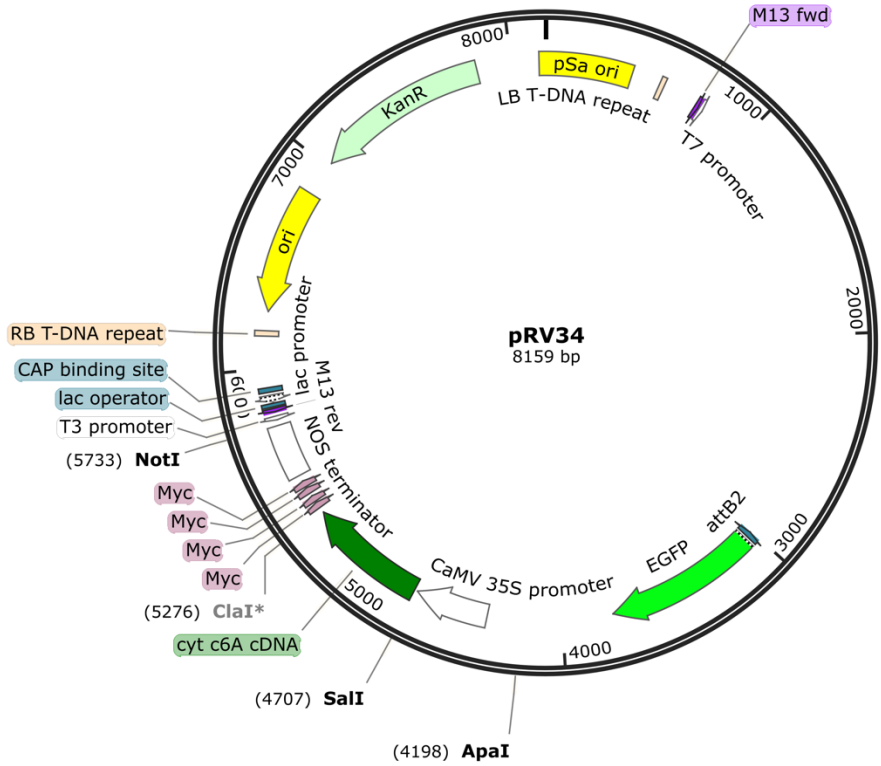

Figure 3.7: Plasmid for overexpression of cytochrome c_{6A} fused to a 4x myc epitope tag for pull down analysis. Cyt c_{6A} cDNA cloned in to a plasmid pGreen:GFP:4xmyc:nosT plasmid.

3.3.3 Construction of plastocyanin:EYFP plasmid as a positive control for cyt c_{6A}

In higher plants plastocyanin (Pc) is the sole lumenal redox carrier that shuttles electrons between the cytochrome b_6f complex and PSI (reference). It was decided to use a Pc:EYFP fusion as a control for studies on the targeting of cyt c_{6A}. The plant *A. thaliana* has two Pc coding genes *petE1* (*At1g76100*) and *petE2* (*At1g20340*). *PetE1* encodes the Pc minor isoform and *petE2* encodes the Pc major isoform. *PetE2* is expressed under normal physiological condition to perform electron carrier activities in the lumen (Salah Esmat Abdel-Ghany, 2009; Weigel *et al*., 2003a). Hence a EYFP cassette was fused to the 3'

end of the cDNA for the Pc major isoform *petE2*. cDNA of the Pc major isoform was amplified from *A.thaliana* cDNA library with gene specific primers (Appendix-C) that introduced *Eco*RI:*Sal*I+*Pst*I:*Cla*I sites. The PCR product was gel purified and both it and the Oleosin-GFP: p35S: EYFP: NosT plasmid were digested with *Sal*I+*Cla*I and ligated together. The ligation mixture was then introduced into competent *dam*$^{-}$ DH5α *E. coli* cells. Plasmid DNA was recovered from colonies growing on LB medium containing kanamycin, and the plasmid verified by restriction digestion and the insert was sequenced and confirmed and designated as pRV35 (figure 3.8).

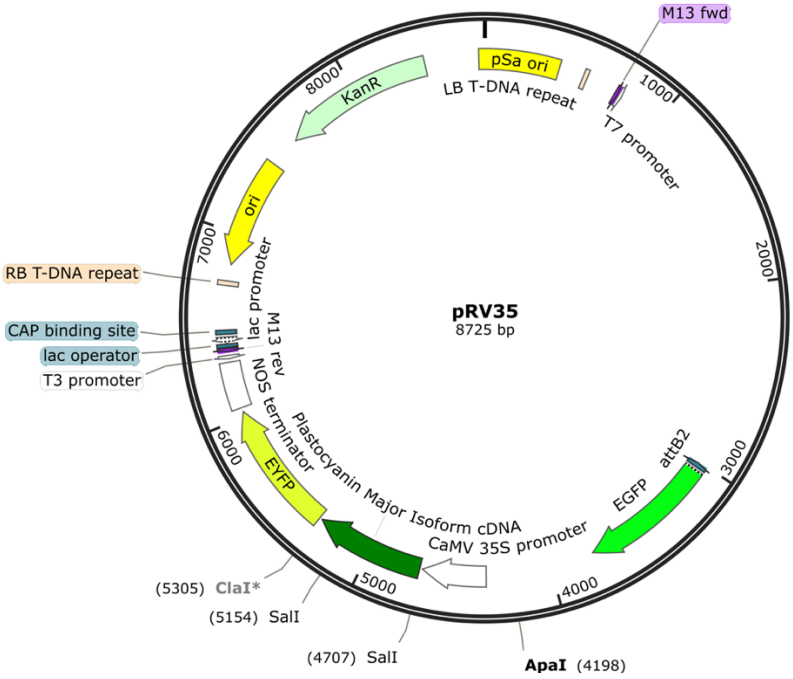

Figure 3.8: Plasmid for overexpression of plastocyanin major isoform cDNA (*petE2*) fused to EYFP coding sequence. Plastocyanin major isoform cDNA was amplified and cloned in into pGreen plasmid for localization studies.

3.4 Plant transformation and homozygous seeds production

Transgenic *Agrobacterium* strains were used to transform *A. thaliana* Col-0 wild type plants via the floral dip method (section 2.5). Transformed transgenic generation 1 (T_1) line fluorescent seeds were collected from 3.3.31, 3.3.2 and 3.3.3, and five highly fluorescent individual T_1 lines were selected for producing the T_2 generation. In the T_2 generation about 75% of the seeds were fluorescent. Five most fluorescent seeds from each T_2 line (five seeds from each of five lines) were selected for T_3 generation. One

hundred % of the T_3 generation seeds were fluorescent, indicating the T_3 transgenic lines were homozygous in nature. T_3 generation seeds were used for all further experiments on protein localization, chlorophyll fluorescence, and measurement. For growth analysis, T_3 lines were grown along with *A. thaliana* Col-0 wild type and the seeds were harvested at the same time. Harvested seeds were then used for growth characterization and root measurement analysis.

CHAPTER 4 CHARACTERIZATION OF CYT c_{6C}

4.1 General introduction

It was generally believed that Cyt c_6 is absent from higher plants. However, in 2002 two groups independently discovered a homologue of Cyt c_6 in higher plants and green algae that showed up to 30% identity at the amino acid sequence level to other Cyt c_6 proteins. This was later designated Cyt c_{6A} (chapter 6 for more details). Bialek and co workers (Bialek *et al*., 2008) subsequently identified two new groups of Cyt c_6 like proteins in cyanobacteria, which are homologous to Cyt c_{6A}. These groups are named analogously as Cyt c_{6C} and Cyt c_{6B}, and are proposed to have different functions. It is plausible that Cyt c_{6C} and Cyt c_{6B} donate electrons to PSI and/ or one of the terminal oxidases (Bialek *et al.*, 2008; Reyes-Sosa *et al.*, 2011). Cyt c_{6B}/c_{6C} are low molecular weight redox proteins and around 47 species of cyanobacteria are annotated to contain Cyt c_{6C}, along with conventional Cyt c_6 and or Pc. Cyt c_{6C} was initially discovered in *Synechococcus* sp PCC 7002 (*Synechococcus*) and the gene encoding Cyt c_{6C} is designated as *pet*J2 (Bialek *et al*., 2008). Expression of Cyt c_{6B}/c_{6C} was not observed under typical laboratory conditions at either the mRNA or protein level, however, Bialek *et al*., (2008) reported that in *S. elongatus* and *Nostoc punctiforme* expression of the Cyt c_{6C} gene (*NpF1886* in *N. punctiforme*) was observed at low but significant levels in nitrogen starved, sulphur starved and ammonia grown cells. Having a low redox midpoint potential, Cyt c_{6B}/c_{6C} could not perform the same role as Cyt c_6 or Pc in the cyanobacterial photosynthetic electron transport chain (Bialek *et al*., 2008; Worrall *et al*., 2008; Reyes-Sosa *et al*., 2011), hence Pc or Cyt c_6 are strictly required for thylakoid membrane electron transport (Durán *et al*., 2004). Both Bialek *et al*., 2008 and Reyes-Sosa *et al*., 2011 proposed that Cyt c_{6B}/c_{6C} could possibly donate electrons to PSI or terminal oxidase, however, laser kinetic experiments suggested that Cyt c_{6B}/c_{6C} reacts with PSI but 3.8 times slower than Cyt c_6 and 2.4 times slower than Pc (Reyes-Sosa *et al*., 2011).

When photosynthetic organisms are exposed to high light intensities which are enough to saturate the photosynthetic electron transport chain, excess light energy could potentially damage the photosynthetic machinery (Roach and Krieger-Liszkay, 2012). Cyanobacteria have developed numerous mechanisms to reduce this photoinhibitory damage (see chapter one for detailed information). We propose here a new photoprotective mechanism; that

Cyt $c_{6C}/_{6B}$ functions as an electron sink under high light intensity to avoid over reduction of the PQ pool and thus to decrease PSII photodamage. We propose that Cyt c_{6C} accepts electrons directly from the PQ pool during high light intensities, or over-reduced PQ conditions, and donates them directly to Pc/PSI, thereby bypassing the Cyt b_6f complex. To test this hypothesis in cyanobacteria we studied the model organism *S. elongatus* PCC 7942, using mutant lines of Cyt $c_{6C}/_{6B}$ and measuring their growth performances under different light intensities, especially under high light conditions. Photosynthesis efficiencies were also measured using a PAM fluorimeter. We used $P700^+$ reduction kinetics experiments to measure the rate of PSI reduction in ΔCyt $c_{6C}/_{6B}$ line compared to wild type. Finally we used RNA-Seq analysis to investigate the effects of the mutation on transcript levels using RNA-Seq.

4.2 Growth phenotype of ΔCyt c_{6C} under different light intensities

Previous studies from our lab have demonstrated that siRNA knockdown lines of Cyt c_{6A} in *Chlamydomonas reinhardtii* have slower growth rates compared to wild type under constant HL conditions, suggesting that the Cyt c_{6A} has a role in protection against high light intensities. The possibility that Cyt c_{6C} might have a similar role in cyanobacteria was tested using a *S. elongatus* ΔCyt c_{6C} mutant and wild type strains, grown under different light intensities to assess the phenotype.

4.2.1 Growth phenotype under low, moderate and high light

In order to investigate the effect of different light intensities on the growth rate, cultures were diluted to an OD_{750} of 0.1 from a starter liquid culture grown under ML conditions (section 2.1.1). Each treatment consisted of three biological replicates of both mutant and WT. In LL the *S. elongatus* cultures grew more slowly than cultures incubated in ML or HL. The faster growth rate seen in ML and HL conditions suggested that cultures were not carbon limited in LL conditions; however, in ML and HL conditions, bubbling with sterile air was performed in order to provide additional carbon dioxide. Cultures were grown at a range of different light intensities; growth of the mutants along with wild type was assessed by measurement of OD_{750} of samples in a spectrophotometer, and in the Algem photobioreactor by measurement of OD_{740} with the inbuilt facility.

Under constant LL conditions, a growth difference between the knockout and wild type was clearly apparent after two days of growth. The difference in growth rate persisted

until the end of the experiment (figure 4.1 A). However, under constant ML and HL conditions, no visible growth difference was observed between wild type and the mutant (figure 4.1 B&C). The LL grown culture was not bubbled with sterile air so it was inappropriate to compare with ML or HL as they were bubbled with sterile air.

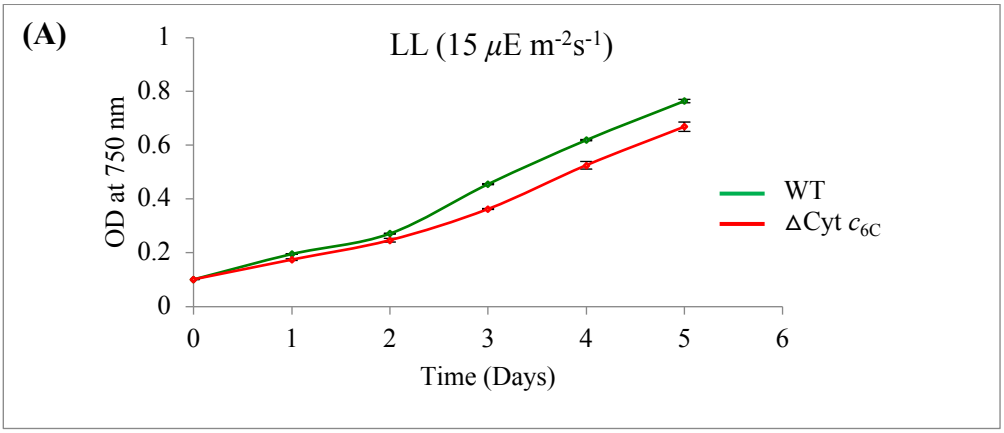

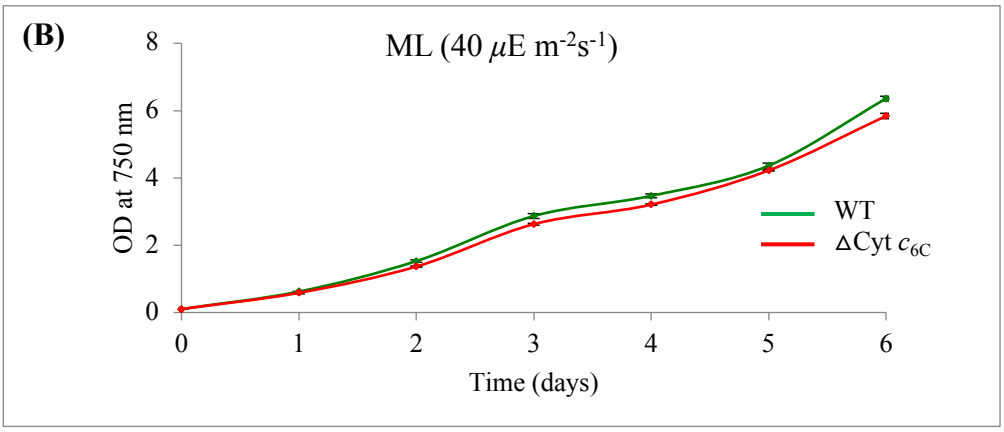

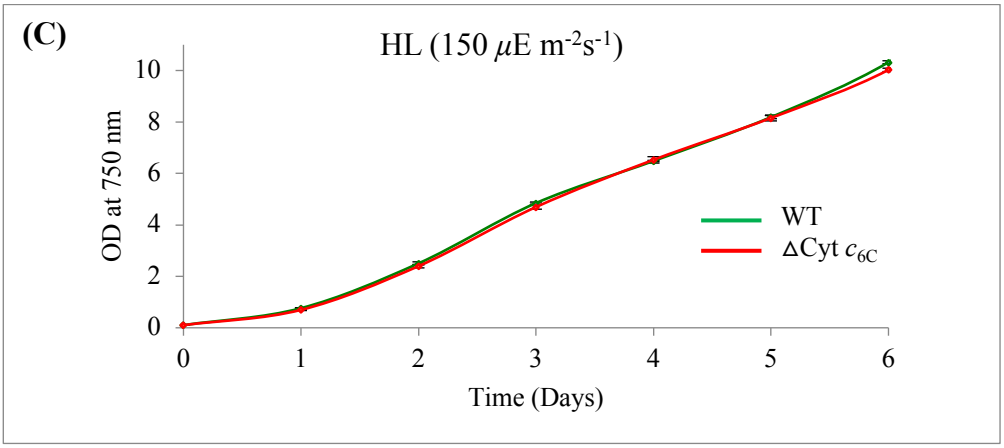

Figure 4.1: Growth of Cyt c_{6C} mutant and wild type under different light intensities. Under LL conditions impaired growth was seen compared to wild type (A). Under ML and HL conditions no growth difference was observed between wild type and the mutant (B&C).

Given the lack of a growth phenotype under HL the cultures were exposed to even higher light intensities using an Algem photobioreactor. The light intensities used were 300 μE m^{-2} s^{-1} (300) and 500 μE m^{-2} s^{-1} (500), and cultures were bubbled with sterile air. Under 300 light intensity, the wild type culture grew at a similar rate to the mutant for the first 20 hrs, with a growth difference clearly apparent between 30 hrs and 55 hrs (figure 4.2 A). Interestingly, no growth was observed in the mutant culture for the first 1 hr at 500 light intensity, in contrast to the wild type, The mutant gradually increased to an OD_{740} 1.1 after 40 hrs but the wild type showed OD_{740}. 1.9 by this stage (figure 4.2 B).

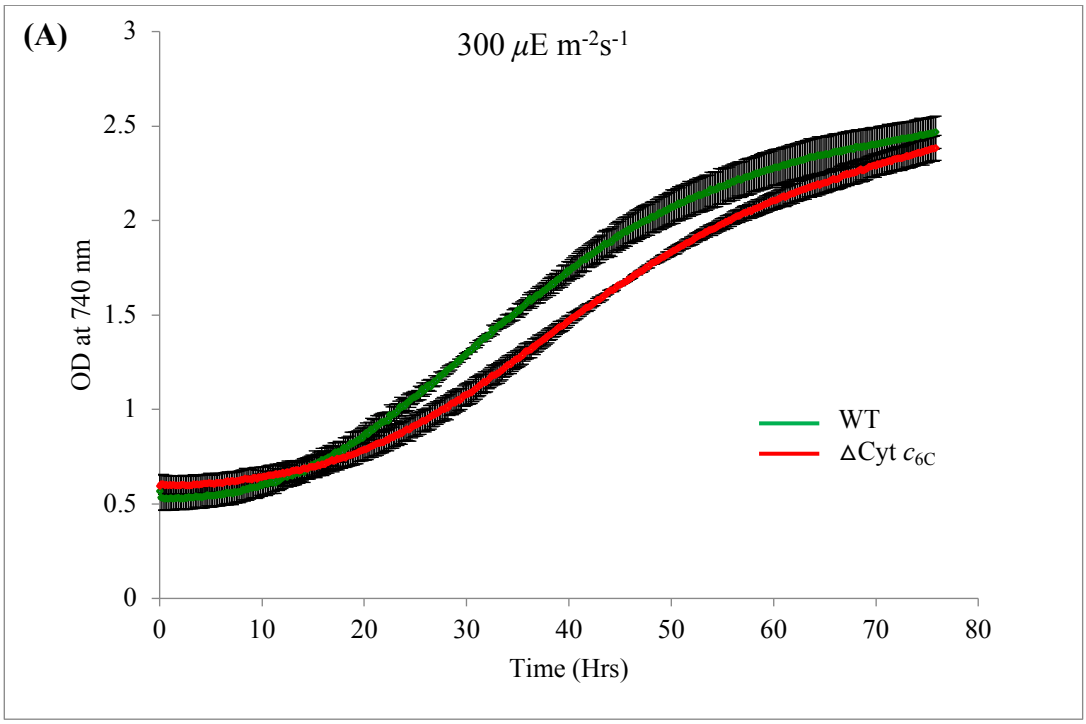

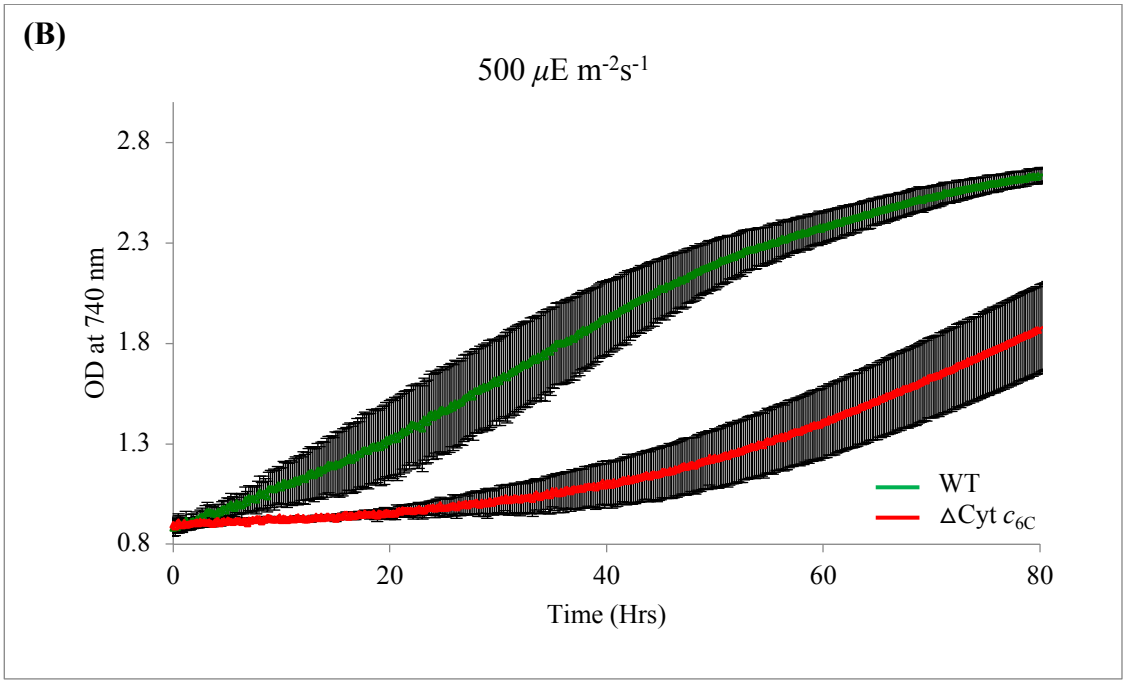

Figure 4.2: Growth curve analysis of Cyt c_{6C} mutant and wild type culture at light intensities of 300 - 500 μE m^{-2} s^{-1}. A & B show growth at 300 μE m^{-2} s^{-1} and 500 μE m^{-2} s^{-1} light intensities, respectively. A. Cyt c_{6C} mutant shows similar growth to wild type for the first 20 hrs, followed by decreased growth subsequently. B shows a clear growth phenotype between wild type and mutant from the start of experiment.

4.2.2 Growth phenotype under extreme light intensities

Given the growth phenotypes observed at the lowest and highest light intensities used, Cyt c_{6C} mutant and wild type cultures were incubated under extreme low light (ELL, 2 μE m^{-2} s^{-1}) and extreme high light (EHL, 1200 μE m^{-2} s^{-1}) intensities to assess growth phenotype. Given the slow growth rates of both strains under ELL conditions, cultures were shifted to ELL conditions after growth under ML conditions. Interestingly, partial chlorophyll bleaching was observed in the Cyt c_{6C} mutant kept under ELL conditions for 15-20 days (figure 4.3 A). When cultures with OD_{750} of 0.1 were exposed to EHL conditions, bleaching was observed in the mutant after 48 hrs (figure 4.3 B).

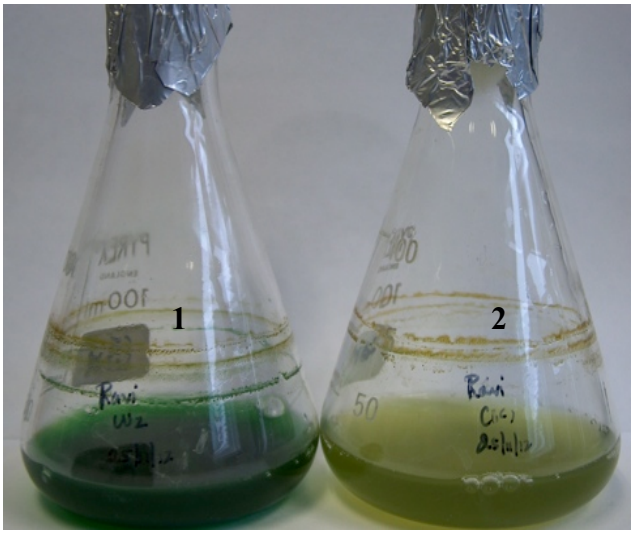

A

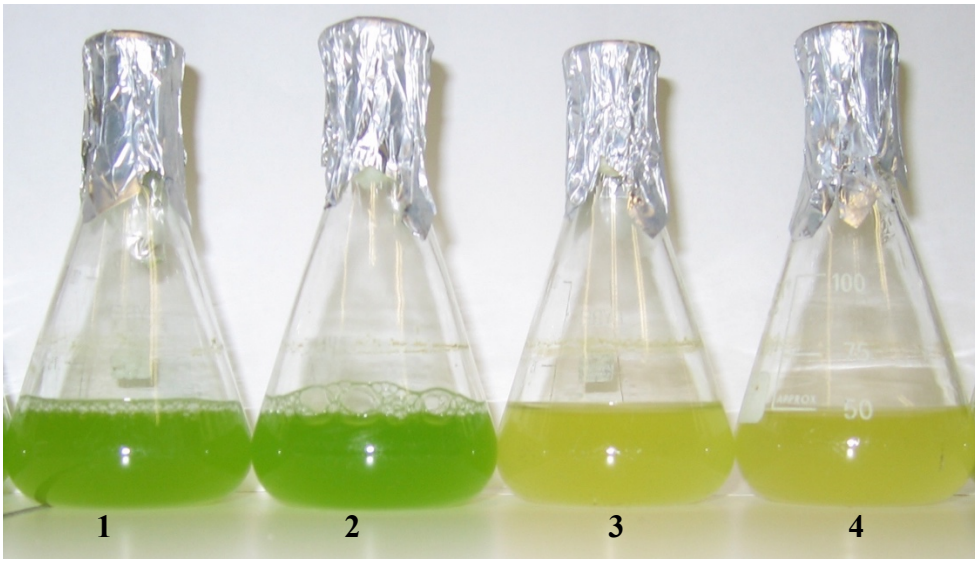

B

Figure 4.3: Cyt c_{6C} mutant phenotype under extreme light intensities. Under ELL conditions chlorophyll bleaching occurred in mutant (A-2) when the cultures were shifted to ELL condition for 15-20 days compared to wild type (A-1). Under EHL conditions more pronounced chlorophyll bleaching was observed in the mutant (B 3&4) after 48 hrs when compared to wild type (B 1&2).

4.3 Cyt c_{6C} expression analysis by northern blot and qRT PCR techniques

Expression of the Cyt c_{6C} transcript was analysed using two different techniques: Northern blot analysis and qRT-PCR. Wild type culture was exposed to two different light intensities and the total RNA was isolated and used for northern blot analysis. For the qRT-PCR, a wild type culture was exposed to different light intensities and total RNA was isolated (section 2.8.1) and the qRT-PCR showed that the relative transcript abundance of Cyt c_{6C} increased at higher light intensities in wild type cultures (data not shown). We therefore went on to use RNA-Seq analysis.

4.3.1 Northern blot analysis of Cyt c_{6C} transcript levels

Cyt c_{6C} has not yet been detected under typical laboratory conditions at either mRNA or protein level, although Bialek *et al*., (2008) reported that in *S. elongatus* and *Nostoc punctiforme*, Cyt c_{6C} transcripts were observed at low but significant levels in nitrogen starved, sulphur starved and ammonia grown cells. The work presented here (growth phenotype of mutant and WT) revealed that Cyt c_{6C} is required under high light intensities. Hence, the wild type culture was exposed to 300 and 1200 μE $m^{-2}s^{-1}$, RNA was isolated and a northern blot was probed for Cyt c_{6C} using DIG labeled Cyt c_{6C} DNA (section 2.9). A single smeared band of approximately 350 nucleotides was detected on the membrane (figure 4.4). This would be consistent with a transcript containing the coding sequence of Cyt c_{6C} (348 nucleotides) but no adjacent sequences. The band seen in RNA isolated from cells grown at 1200 μE $m^{-2}s^{-1}$ light appeared more intense than that in RNA isolated from cells grown at 300 μE $m^{-2}s^{-1}$ light, suggesting Cyt c_{6C} is expressed under high light intensities (figure 4.4), but it is inappropriate to draw any conclusions on the relative levels of Cyt c_{6C} transcripts without having a proper control.

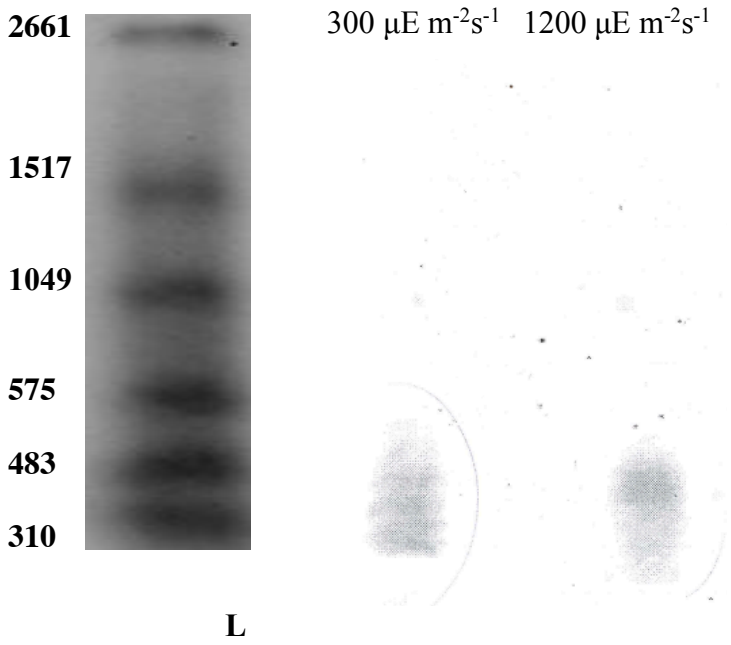

Figure 4.4 : Northern blot analysis for Cyt c_{6C} transcript. Total RNA was isolated from wild type cultures grown under 300 and 1200 μE m^{-2} s^{-1} light intensities, and a northern blot was made and probed wtih DIG labeled Cyt c_{6C} DNA. Cyt c_{6C} transcript was detected in both the conditions (approximately 350 nucleotides) L: Marker.

4.4 Physiological characterization of ΔCyt c_{6C}

4.4.1 Oxygen electrode study

The rate of photosynthesis, respiration and photoinhibition were measured using a Clark oxygen electrode. A sample of 2 ml of (~ 4 nmol Chl ml^{-1}) culture from each strain was used for measuring the rate of photosynthesis and respiration (Section 2.11.1). The overall O_2 evolution rate of the ΔCyt c_{6C} was only 40% of the rate of the wild type (figure 4. 5A). The average rate of respiration (measured as oxygen consumption) was higher in the ΔCyt c_{6C} than wild type (figure 4.5B), although the difference was not statistically significant. These results suggested an involvement of Cyt c_{6C} in photosynthesis. The extent of photoinhibition was measured using 2 ml of (~1 nmol Chl ml^{-1}) culture of wild type and ΔCyt c_{6C} (section 2.11.2). Wild type and the mutant showed a similar rate of oxygen evolution in initial 5 min. However, in the following minutes, the mutant showed reduced oxygen evolution comparable to wild type up to 30 min, but then the oxygen evolution from the wild type decreased faster than the mutant (figure 4. 5C).

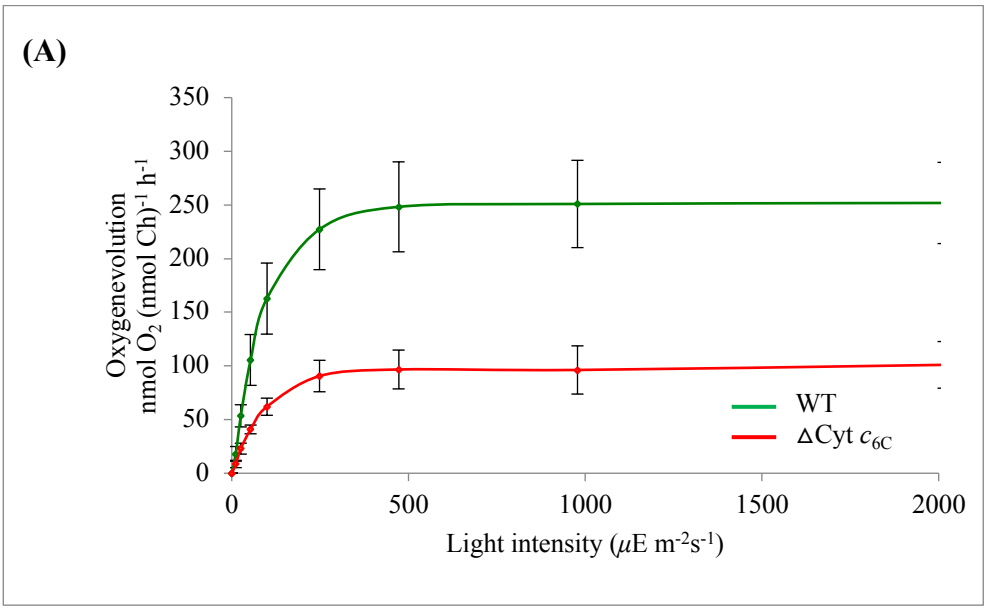
(A)
Oxygenevolution
nmol O2 (nmol Ch)-1 h-1
350
300
250
200
150
100
50
0
0
500
1000
1500
2000
Light intensity (μE m-2s-1)
WT
ΔCyt c6C

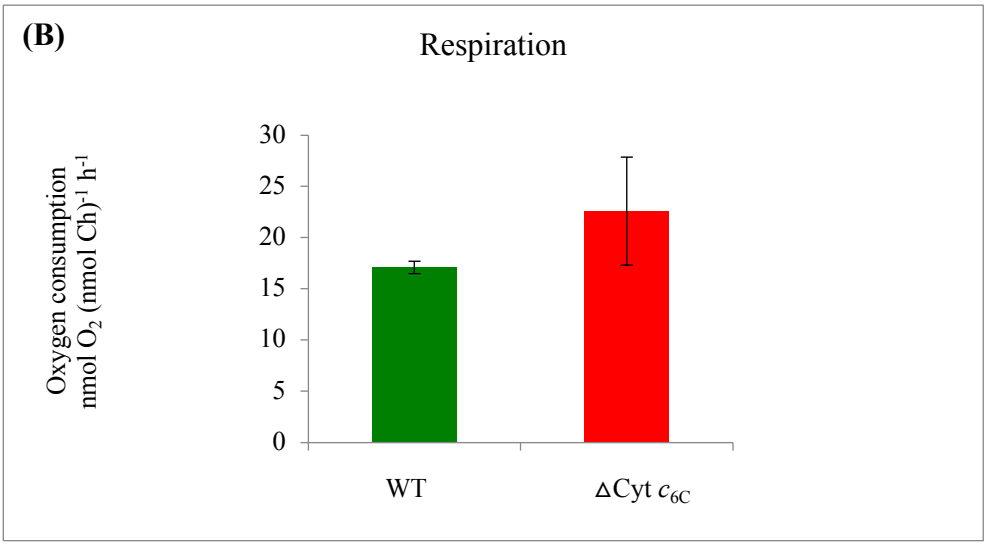
(B)
Respiration
Oxygen consumption
nmol O2 (nmol Ch)-1 h-1
30
25
20
15
10
5
0
WT
ΔCyt c6C

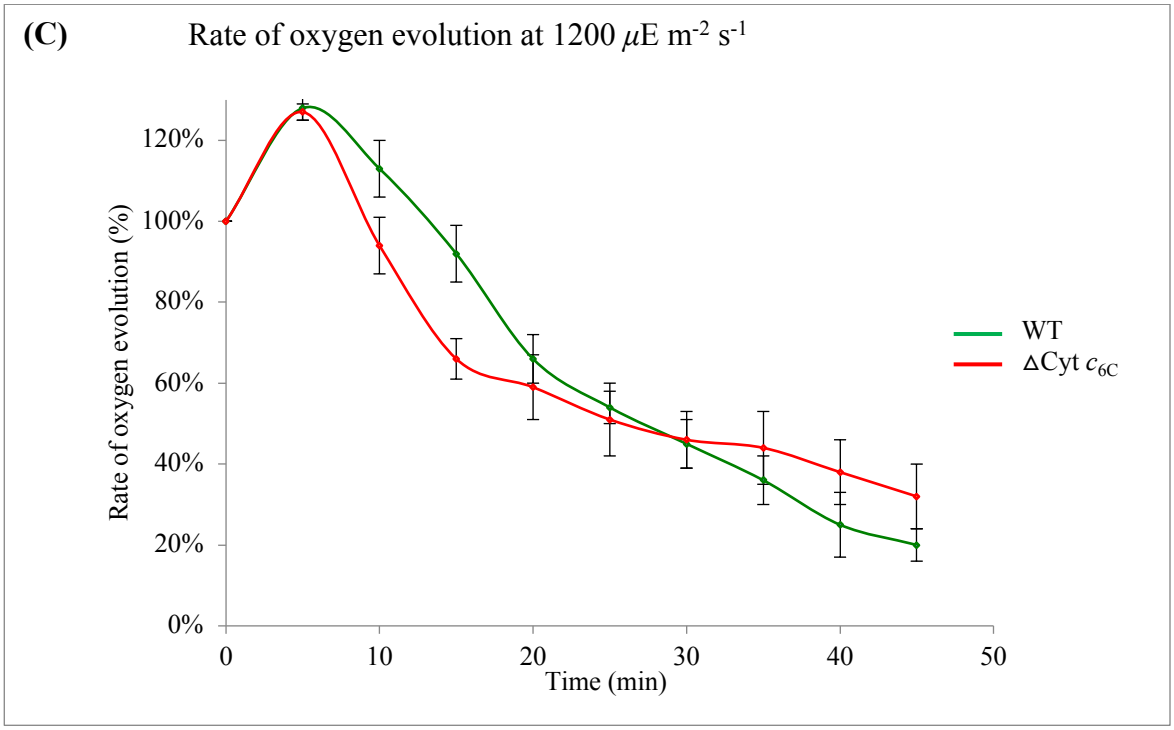

Figure 4.5: Relative rate of photosynthesis, respiration and photoinhibition of Cyt c_{6C} mutant and wild type. The ΔCyt c_{6C} showed a relatively reduced rate of overall oxygen evolution compared to wild type (A) No difference in rate of respiration was seen in Cyt c_{6C} mutant to wild type (B). Greater photoinhibition was seen in the mutant compared to wild type from 5 to 20 min (C).

4.4.2 Chlorophyll fluorescence measurement

Chlorophyll fluorescence measurements provide information on the photosynthetic electron transfer chain and its performance in the light reactions of photosynthesis (Baker, 2008). Pulse Amplitude Modulated (PAM) fluorescence measurements of PSII reaction centres provide information about the distribution of photosynthetic energy between Photochemical (PQ) and Non-Photochemical Quenching (NPQ). During photosynthesis, light energy collected by the antenna proteins (phycobilisomes (PBs)) in cyanobacteria and Light Harvesting Complexes ((LHC) in higher plants) can be used to drive the photosynthetic electron transport chain, resulting in photochemical quenching. Due to the susceptibility of PSII to photodamage in high light intensities, the electron transport components in the electron transport chain are not sufficient to utilise the high amount of energy that is transported. Furthermore, high light leads to over reduction of the

plastoquinone pool, thus activating dissipation of excess light via NPQ (Eberhard *et al*., 2008).

The efficiency of the light energy capturing ability of ΔCyt c_{6C} was assessed and compared to that of WT. Fv/Fm describes the PSII maximum efficiency in the dark adapted state in chloroplasts or with DCMU plus light treatment in cyanobacteria. ΦPSII specifies the effective quantum yield of PSII in light. qP is related to photochemical quenching, qT is photochemical quenching associated with state transitions and NPQ is collective non photochemical quenching including heat dissipation and photoinhibition. A relatively reduced Fv/Fm was observed in the ΔCyt c_{6C} compared to WT, indicating the ΔCyt c_{6C} has a lower fraction of open PSII reaction centres in dark adaptation. ΦPSII yield was significantly (about 33 %) higher in ΔCyt c_{6C} (0.27) compared to wild type (0.18). The values of qP and qT in ΔCyt c_{6C} were similar to the wild type culture indicating similar levels of photochemical quenching. Interestingly, the value of NPQ in the ΔCyt c_{6C} was significantly reduced, by about 45%, compared to WT, (figure 4.6).

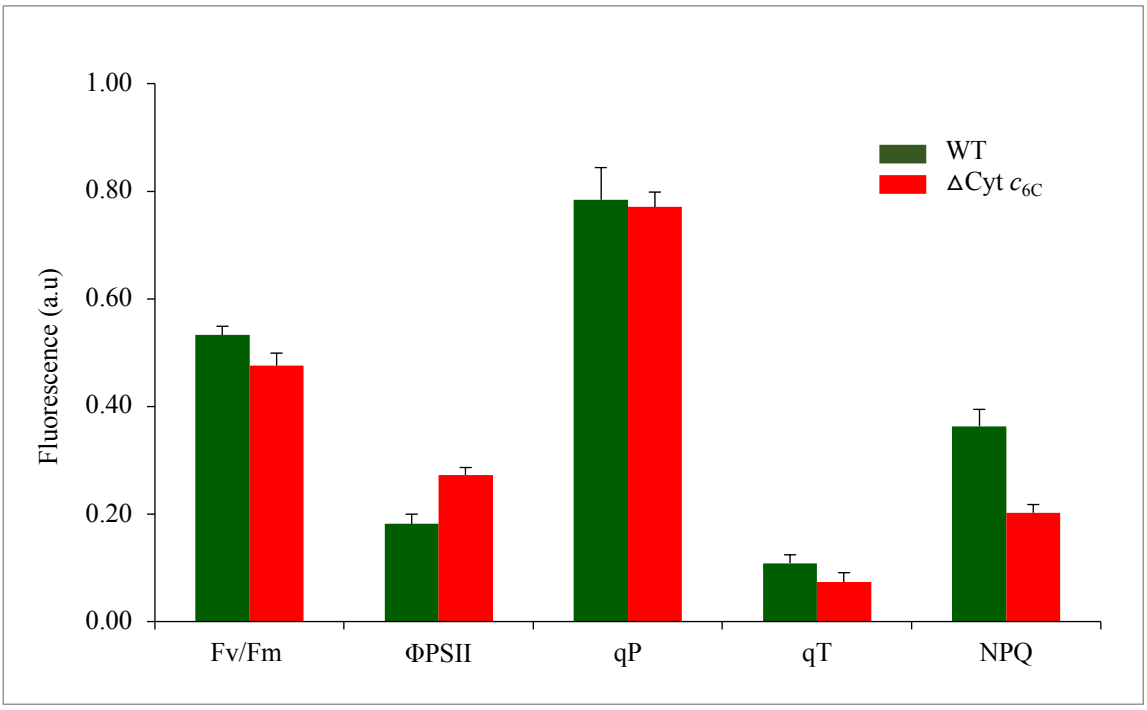

Figure 4.6: Chlorophyll fluorescence measurement ΔCyt c_{6C} and WT. ΔCyt c_{6C} mutant chlorophyll measurements parameters such as maximum chlorophyll fluorescent yield in dark with DCMU (Fv/Fm), PSII quantum yield or efficiency of PSII (ΦPSII), photochemical quenching (qP), photochemical quenching associated with state transition (qT) and non photochemical quenching (NPQ) were measured from dark adapted ΔCyt c_{6C} and wild type cultures. These data were generated in collaboration with Dr. Iskander Ibrahim in Professor John F Allen lab, Queen Mary University of London, UK.

4.4.3 $P700^+$ Reduction kinetics

$P700^+$ dark reduction kinetics of wild type and ΔCyt c_{6C} culture were measured with under the following condition. PSI was excited for 5 mins using far-red light. The light was switched off and immediately followed by 100 msec of saturating pulse (4500 μmol m^{-2} s^{-1}) to complete oxidation of $P700^+$. Dark reduction of $P700^+$ was then recorded (section 2.13). Figure 4.7 shows the dark reduction rate of $P700^+$ for wild type and ΔCyt c_{6C} cultures. The reduction rate of $P700^+$ for ΔCyt c_{6C} culture was significantly slower than in the wild type. We observed only about 50% reduction in 10 sec compared to about 80% reduction in the wild type. Complete reduction (100%) of $P700^+$ was observed in the wild type in 14 sec, but only about 60% reduction was observed in ΔCyt c_{6C} in the same timeframe (figure 4.7). This suggests that Cyt c_{6C} donates electrons (directly or indirectly) to PSI or regulates the transfer of electrons.

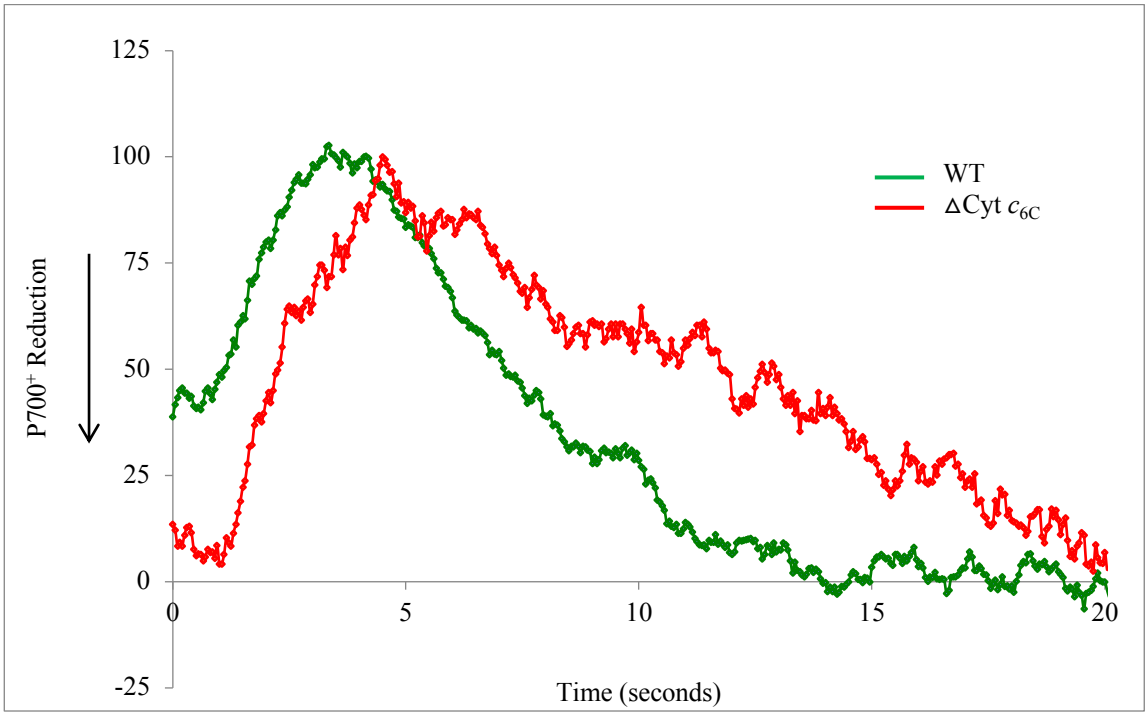

Figure 4.7: $P700^+$ reduction kinetics: ΔCyt c_{6C} and WT. A value of 100% indicates complete oxidation of P700. Lower values indicate the amount remaining oxidized at a given time. P700 reduction kinetics of WT was significantly faster than for the ΔCyt c_{6C} strain. Each data point represents at least four independent biological replicates. This data was generated in collaboration with Dr. Iskander Ibrahim in Professor John F Allen lab, Queen Mary University of London, UK.

4.5 Transcriptomic analysis of cyt c_{6C} mutant

We demonstrated in the growth phenotype study that ΔCyt c_{6C} has impaired growth under 300 and severely impaired growth at 500 $\mu Em^{-2}s^{-1}$ light intensity. This result suggested that Cyt c_{6C} is important under elevated light conditions. This was further supported using qRT-PCR, which showed that transcript abundance of Cyt c_{6C} increases at increased light intensities in wild type cultures. Similarly, the northern blot analysis suggested that Cyt c_{6C} was expressed in 300 $\mu Em^{-2}s^{-1}$ light and at higher levels in 1200 $\mu Em^{-2}s^{-1}$ light, which represents an extremely high light intensity for this organism.

In this section we used RNA-Seq, a powerful high throughput sequencing approach, to understand the global impact on the transcriptome of deleting the Cyt c_{6C} coding gene (*petJ2*) in *S. elongatus* PCC 7942. Such an investigation allows a global measurement of transcript abundance in ΔCyt c_{6C} culture under certain physiological conditions. We used 6 samples (3 ΔCyt c_{6C} biological replicates and 3 wild type controls) at 150 $\mu E\ m^{-2}\ s^{-1}$ light intensity, where there is little or no growth impairment) and 6 samples (biological replicates and 3 wild type controls) from 500 $\mu E\ m^{-2}\ s^{-1}$ light intensity, where there is a significant growth impairment. The transcript levels of photosynthesis and related genes of ΔCyt c_{6C} culture are compared here with those of wild type in the two different light intensities. We also compared the ΔCyt c_{6C} at 500 vs 150 $\mu Em^{-2}s^{-1}$ light intensity and likewise for the wild type.

4.5.1 RNA-Seq data quality

Total RNA was extracted from the 12 samples referred to above. The quality of the RNA was determined using an Agilent Bioanalyzer. RNA samples with RNA Integrity Numbers (RIN) of 8.1, 8.4, 8.2, 8.4, 8.1, 8.5 (150 $\mu Em^{-2}s^{-1}$ light intensity) and 9.0, 9.2, 8.9, 9.3, 9.7, 9.3 (500 $\mu Em^{-2}s^{-1}$ light intensity) were used in TruSeq cDNA library preparation, combined with a Bacterial Ribo-Zero Magnetic Kit to remove rRNA. The cDNA libraries were sequenced using a NextSeq500 machine with single-read.

A total of 151 million raw sequence reads (150 bp) were obtained from RNA-Seq transcriptomic analysis of the 12 samples, with an average number of 12.6 million reads per sample. The sequence quality of the reads was determined by FastQC bioinformatics tool and the quality was extremely high. Filtering steps were not performed in sample preparation, sequencing and analyses to reduce any imposed bias. The alignment of reads, coverage calculation, genewise read quantification and differential gene expression analysis was performed with READemption using segemehl version X and DESeq version V. A total of 138 million reads aligned to the *S. elongatus* genome, with an average number of 11.5 million aligned reads per sample, representing an average of 627 times coverage of the genome in each sample. Transcriptomic analysis conformed that knockout of the Cyt c_{6C} coding gene did not statistically significantly alter the regulation of its upstream genes (Synpcc7942_2543, Phage SP01 DNA polymerase related protein and hypothetical protein, Synpcc7942_2544.

4.5.2 Transcript levels for PSII genes in ΔCyt c_{6C} cultures under different light intensities

S. elongatus has 3 *psbA* genes and encodes two distinct D1 protein isoforms D1:1 encoded by *psbA*1 and D1:2 encoded by *psbA2* and *psbA3* (Mulo *et al.*, 2009). RNA-Seq demonstrated that knocking out of Cyt c_{6C} coding gene (*petJ2*) did not significantly alter the transcript levels of PSII components in 150 $\mu Em^{-2}s^{-1}$ light intensity compared to wild type, with the exception of *psbA*1, which was up regulated in ΔCyt c_{6C} culture. At 500 $\mu Em^{-2}s^{-1}$ light in ΔCyt c_{6C} culture transcript levels for *psbI, psbQ,* and *psbV,* genes were down regulated and *psbA3, psbM*, and *psbP*, genes transcript levels were up regulated compared to wild type.

When the ΔCyt c_{6C} culture was grown at 500 $\mu Em^{-2}s^{-1}$ light intensity, up regulation of the transcript levels for *psbA2, psbA3, psbB, psbC, psbD1, psbD2, psbN, psbO, psbP, psbQ, psbT, psbU, psbW, psb*27*, psb*29*, psb*30*, ftsH* isoforms *ftsH*1, *ftsH*2, *ftsH*3and *ftsH*4 genes and down regulation of the transcript levels for *psbA1, psbH, psbI, psbK, psbM, psbX, psbY,* and *psbZ* genes were seen compared to the mutant culture grown at 150 $\mu Em^{-2}s^{-1}$ light. Similar results were also observed when the wild type culture at 500 $\mu E\ m^{-2}\ s^{-1}$ light intensity was compared to the culture grown at 150 $\mu Em^{-2}s^{-1}$ light, however, PSII D1 degradation protease FtsH encoding *ftsH*3 transcript was not significantly regulated (figure 4.8 and Appendix table 4.1). Assuming the protein levels reflect transcript levels, these data may indicate relatively similar PSII in the mutant compared to wild type, although few individual genes were differentially regulated.

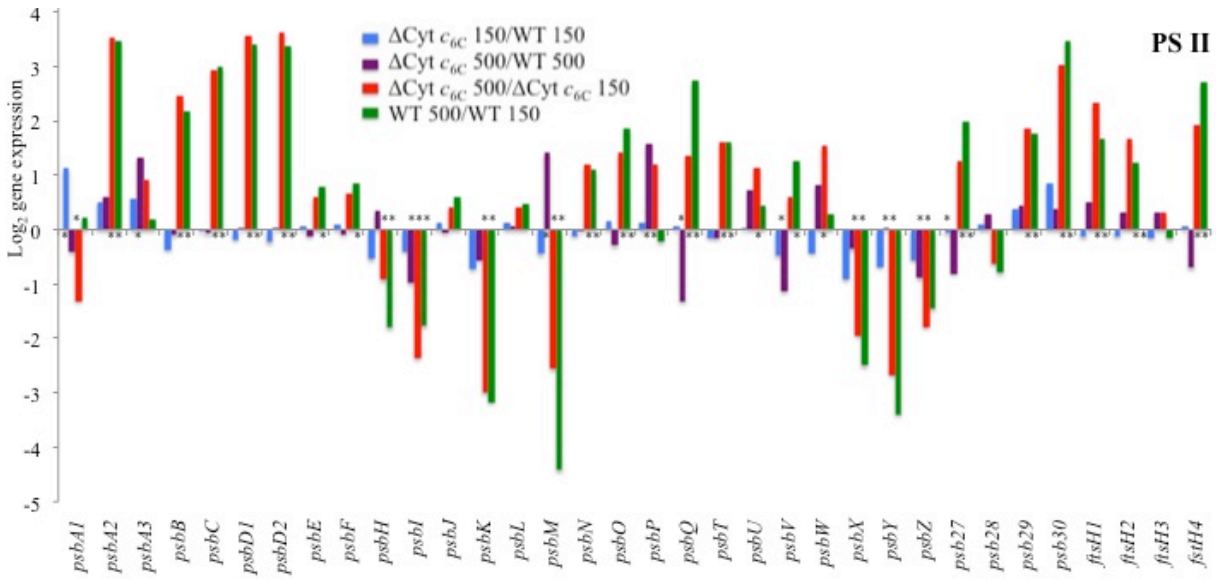

Figure 4.8: Comparative PSII transcript expression levels in ΔCyt c_{6C} and wild type under 150 and 500 $\mu Em^{-2}s^{-1}$ light intensities. Asterisks indicated significant differences in transcript abundance between ΔCyt c_{6C} 150/WT 150, ΔCyt c_{6C} 500/WT 500, ΔCyt c_{6C} 500/ ΔCyt c_{6C} 150 and WT 500 vs WT 150 $\mu Em^{-2}s^{-1}$ light intensity ($p < 0.05$). Changes in transcript abundance are given in $\log_2$ values in y-axis.

4.5.3 Transcript levels for PSI genes in ΔCyt c_{6C} cultures under different light intensities

RNA-Seq demonstrated that under 150 μE m^{-2} s^{-1} light intensity, transcript levels for PSI components were not significantly altered compared to the wild type, however, transcript levels for *psaK*1 and *psaK*2 which are implicated in state transition (Fujimori *et al*., 2005) were up regulated in the mutant compared to the wild type (figure 4.9). At 500 $\mu Em^{-2}s^{-1}$ light intensity, in ΔCyt c_{6C} culture, the transcript levels for *psaA*, *psaB*, *psaD*, *psaF*, *psaJ*, *psaL*, and *ycf*3 were down regulated in the ΔCyt c_{6C} culture compared to the wild type.

When the ΔCyt c_{6C} culture was grown at 500 $\mu Em^{-2}s^{-1}$ light intensity, chlorophyll *a* apoproteins *psaA* & *psaB* and the photosystem I assembly protein *ycf4* transcript levels were significantly up regulated and down regulation of the transcript levels for *psaD*, *psaE*, *psaI*, *psaJ*, *psaK*1, was seen compared to the mutant culture grown at 150 $\mu Em^{-2}s^{-1}$ light intensity (figure 4.9 and Appendix table 4.1). For the wild type culture grown at 500 $\mu Em^{-2}s^{-1}$ light intensity, transcript levels for *psaA, psaB, psaF, psaL, ycf*3 *and ycf*4 were significantly up regulated and other genes transcript levels were not significantly regulated compared to the wild type culture grown at 150 $\mu Em^{-2}s^{-1}$ light intensity. Assuming the protein levels reflect transcript levels, these data may imply the presence of less PSI in the ΔCyt c_{6C} compared to the wild type at 150 $\mu Em^{-2}s^{-1}$ light intensity (figure 4.9 and Appendix table 4.1).

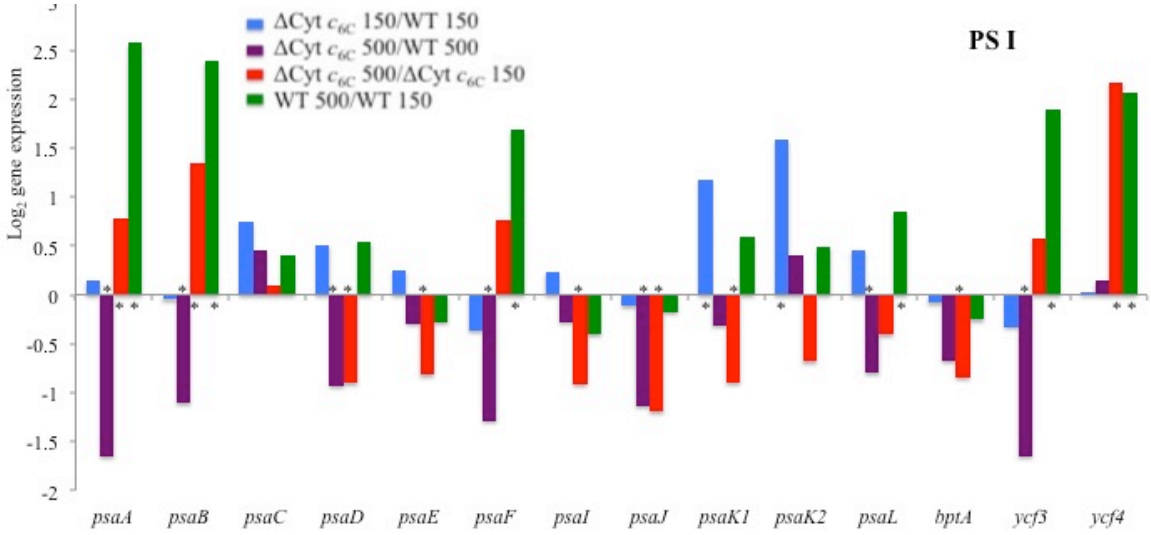

Figure 4.9: Comparative PSI transcript expression levels in ΔCyt c_{6C} and wild type under 150 and 500 $\mu Em^{-2}s^{-1}$ light intensities. Asterisks indicated significant differences in transcript abundance between ΔCyt c_{6C} 150/WT 150, ΔCyt c_{6C} 500/WT 500, ΔCyt c_{6C} 500/ ΔCyt c_{6C} 150 and WT 500 vs WT 150 $\mu Em^{-2}s^{-1}$ light intensity ($p < 0.05$). Changes in transcript abundance are given in log_2 values in y-axis.

4.5.4 Transcript levels for Cyt b_6f genes in ΔCyt c_{6C} cultures under different light intensities

RNA-Seq analysis revealed that knocking out Cyt c_{6C} did not significantly change the transcript levels of Cyt b_6f complex components under 150 $\mu Em^{-2}s^{-1}$ light intensity compared to wild type. At 500 $\mu Em^{-2}\,s^{-1}$ light intensity, significant up regulation of the transcript levels for cytochrome b_6 (*petB*) and *petM* was seen compared to the wild type, however, other genes transcript levels were not significantly regulated (figure 4.10 and table 4.1).

When the ΔCyt c_{6C} culture was grown at 500 $\mu E\ m^{-2}\ s^{-1}$ light intensity, transcript levels for cytochrome *f* (*petA*), *petB* and the Rieske iron-sulfur protein (*petC*) were increased, and down regulation of *petG* and *petM* transcript was observed compared to the wild type. For the wild type grown at 500 $\mu E\ m^{-2}\ s^{-1}$ light intensity, elevated transcript levels for *petA*, *petB* and *petC* were also seen, as well as down regulation of the transcript levels for *petG* and *petM* compared to the culture grown at 150 $\mu E\ m^{-2}\ s^{-1}$ light intensity (figure 4.10 and table 4.1). Assuming the protein levels reflect transcript levels, these data may imply that there more or less similar amounts of Cyt b_6f complex in the ΔCyt c_{6C} compared to the wild type (figure 4.10 and Appendix table 4.1).

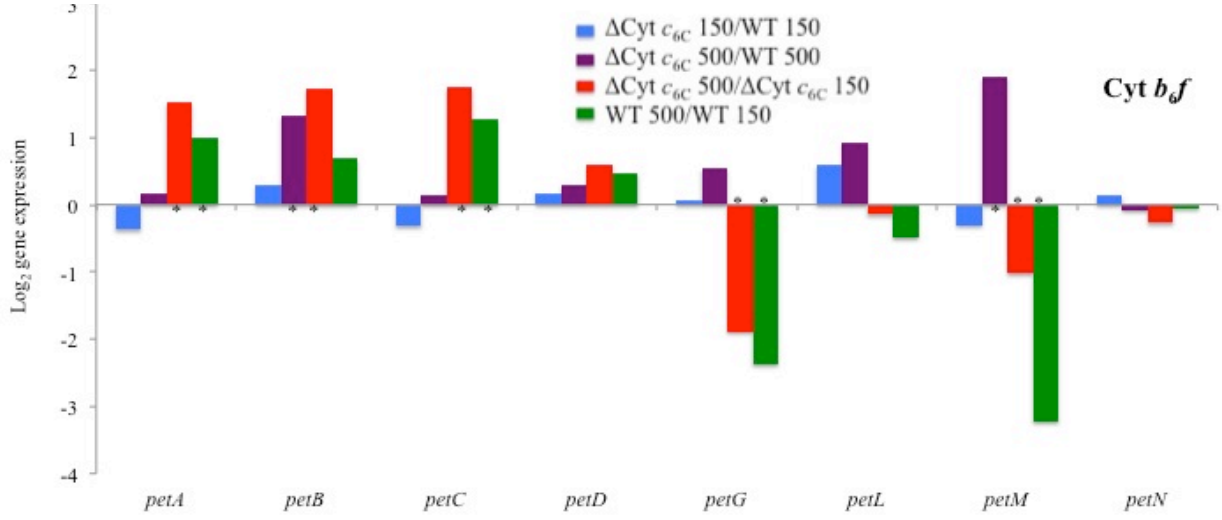

Figure 4.10: Comparative Cyt b_6f complex transcript expression levels in ΔCyt c_{6C} and wild type under 150 and 500 μEm^{-2}s^{-1} light intensities. Asterisks indicated significant differences in transcript abundance between ΔCyt c_{6C} 150/WT 150, ΔCyt c_{6C} 500/WT 500, ΔCyt c_{6C} 500/ ΔCyt c_{6C} 150 and WT 500 vs WT 150 μEm^{-2}s^{-1} light intensity ($p < 0.05$). Changes in transcript abundance are given in $\log_2$ values in y-axis.

4.5.5 Transcript levels for ATP synthase genes in ΔCyt c_{6C} cultures under different light intensities

RNA-seq analysis demonstrated that knocking out Cyt c_{6C} did not significantly change the transcript levels of ATP synthase components under 150 μEm^{-2}s^{-1} light intensity compared to wild type. At 500 μEm^{-2}s^{-1} light intensity, ATP synthase components transcript levels for *atpA*, *atpB*, *atpC/E*, *atpD*, *atpF*, *atpG*, and *atpH* were up regulated in the mutant compared to the wild type. Consistent with this, when the ΔCyt c_{6C} culture was shifted from 150 to 500 μEm^{-2}s^{-1} light intensity, ATP synthase component transcripts *atpA*, *atpB*, *atpC/E*, *atpD*, *atpF*, *atpG*, and *atpH* were up regulated, but when the wild type shifted from 150 to 500 μE m^{-2} s^{-1} light intensity, few significant changes were observed (figure 4.11 and table 4.1). Assuming the protein levels reflect transcript levels, these data may imply presence of more ATP synthase in the ΔCyt c_{6C} compared to the wild type at 500 μEm^{-2}s^{-1} light intensity (figure 4.11 and Appendix table 4.1).

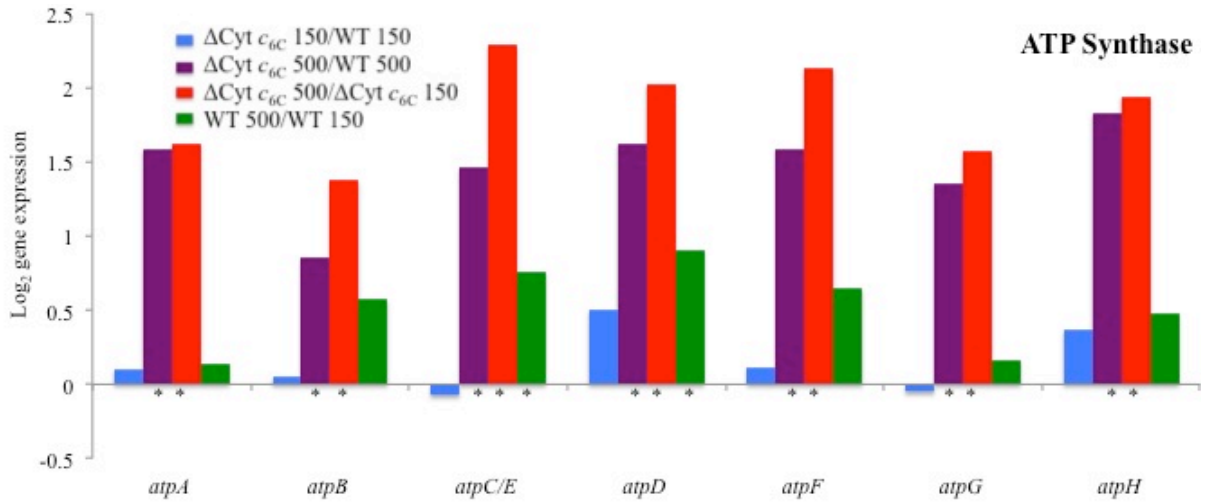

Figure 4.11: Comparative ATP synthase transcript expression levels in ΔCyt c_{6C} and wild type under 150 and 500 $\mu Em^{-2}s^{-1}$ light intensities. Asterisks indicated significant differences in transcript abundance between ΔCyt c_{6C} 150/WT 150, ΔCyt c_{6C} 500/WT 500, ΔCyt c_{6C} 500/ ΔCyt c_{6C} 150 and WT 500 vs WT 150 $\mu Em^{-2}s^{-1}$ light intensity ($p < 0.05$). Changes in transcript abundance are given in log_2 values in y-axis.

4.5.6 Transcript levels for phycobilisome genes in ΔCyt c_{6C} cultures under different light intensities

In cyanobacteria grown iron replete conditions the phycobiliproteins (PBPs) attach to the cytoplasmic surface of the thylakoid membrane and transiently move between PSII and PSI and are responsible for capturing the majority of the light for photosynthesis. Based on bilin energy level PBS are mainly classified into three types: phycoerythrins (PEs) or phycoerythrocyanin at the end of the rod distal to the core, (absorb high energy light), phycocyanins (PCs), the portion of the rods adjacent to the core (absorb the intermediate energy light) and the allophycocyanins (APCs), major components of the core ((absorb low energy light) (Lea-Smith *et al*., 2014; Chang *et al*., 2015)).

RNA-seq analysis revealed that knocking out of Cyt c_{6C} did not significantly alter the expression of light harvesting phycobilisomes components under 150 $\mu E\ m^{-2}s^{-1}$ light intensity compared to wild type, whereas under 500 $\mu E\ m^{-2}s^{-1}$ light intensity the APCs, PCs and linker proteins transcripts were down regulated in the mutant compared to the wild type. The significantly down regulated components were *apcA*, *cpcA1*, *cpcA2*, *cpcB1*, *cpcB2*, *cpcE*, *cpcH*, and *cpcl1*. (figure 4.12 and table 4.1). When the ΔCyt c_{6C}

culture was shifted from 150 to 500 μEm^{-2}s^{-1} light intensity the APC transcripts were not significantly regulated, but the PCs and linker proteins transcript were significantly regulated. PCs components *cpcA1*, *cpcA2*, but, the PCs and linker proteins transcript were significantly down regulated. PCs components *cpcA1*, *cpcA2*, *cpcB1*, *cpcB2* and the linker protein transcript *cpcH* and *cpcl1* were down regulated (figure 4.12 and Appendix table 4.1).

When the wild type cells were grown at 500 μE m^{-2}s^{-1} light intensity rather than 150 μE m^{-2}s^{-1} light, the APC transcripts were generally up regulated with the *cpc* transcripts showing a mixture of up- and down-regulation. Assuming the protein levels reflect transcript levels, these data may imply the presence of fewer phycobilisomes in the ΔCyt c_{6C} compared to the wild type at 500 μEm^{-2}s^{-1} light intensity.

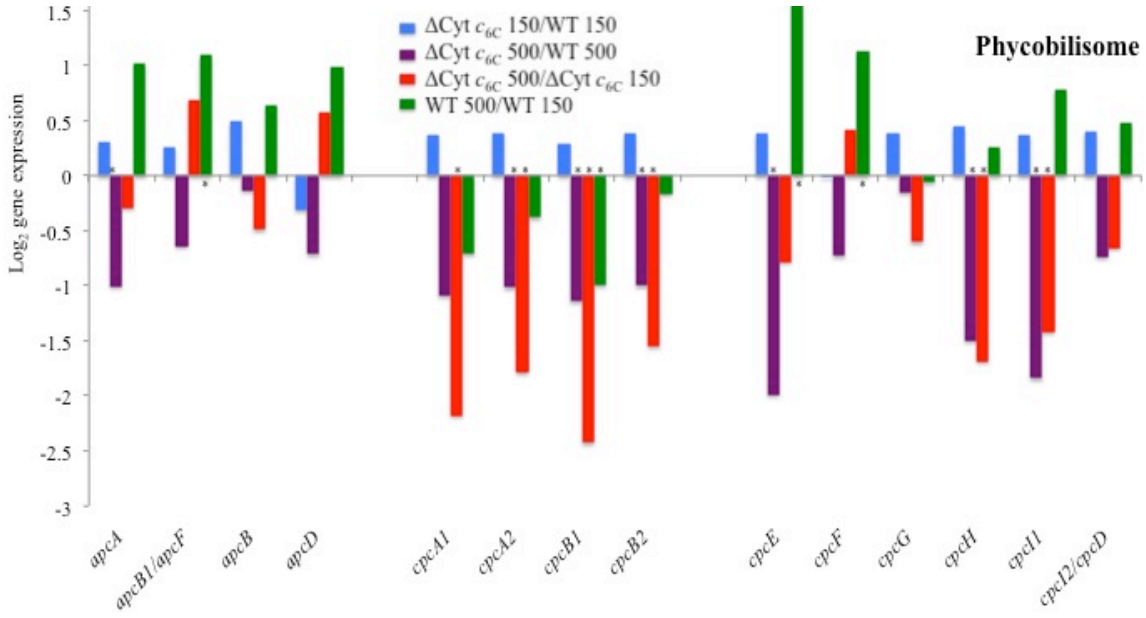

Figure 4.12: Comparative phycobilisome protein complex transcript expression levels in ΔCyt c_{6C} and wild type under 150 and 500 μEm^{-2}s^{-1} light intensities. Asterisks indicated significant differences in transcript abundance between ΔCyt c_{6C} 150/WT 150, ΔCyt c_{6C} 500/WT 500, ΔCyt c_{6C} 500/ ΔCyt c_{6C} 150 and WT 500 vs WT 150 μEm^{-2}s^{-1} light intensity ($p < 0.05$). Changes in transcript abundance are given in $\log_2$ values in y-axis.

4.5.7 Transcript levels for high light inducible proteins in ΔCyt c_{6C} cultures under different light intensities

RNA-seq analysis demonstrated that knocking out Cyt c_{6C} did not significantly change the transcript levels of high light inducible protein components under 150 $\mu Em^{-2}s^{-1}$ light intensity compared to wild type, although the non bleaching phenotype (*nblA1*) transcript was up regulated by 2.3 fold. At 500 $\mu E\ m^{-2}s^{-1}$ light intensity, however all the high light inducible transcript were up regulated in the mutant. These were the transcripts of *nbA1, hliA, hliC, hliP* isoforms 1 and 2, and *isiA/cp43*' genes which were upregulated compared to wild type. When the ΔCyt c_{6C} culture was shifted from 150 to 500 $\mu Em^{-2}s^{-1}$ light intensity, up regulation of *nblA1*, *nblB2, hliC, hliP* isomers 1 and *isiA/cp43'* genes was seen. Interestingly, when the wild type culture was shifted from 150 to 500 $\mu Em^{-2}s^{-1}$ light intensity up regulation of, *nblB*, *hliC* and *isiA/cp43'* genes was seen. Assuming the protein levels reflect transcript levels, these data may imply the presence of more phycobilisome degradation protein (*nblA1*) in ΔCyt c_{6C} culture at 150 $\mu Em^{-2}s^{-1}$ light intensity and even greater abundance at 500 $\mu Em^{-2}s^{-1}$ light intensity compared to the wild type. The high light excess energy dissipation protein (*hliA*) concentration was relatively higher in ΔCyt c_{6C} culture at 500 $\mu Em^{-2}s^{-1}$ light intensity compared to the wild type, however, unexpectedly, it was down regulated in the wild type at 500 $\mu Em^{-2}s^{-1}$ light intensity compared to the wild type culture grown at 150 $\mu Em^{-2}s^{-1}$ light intensity. Iron stress response regulated protein protein CP 43' (*isiA*) was relatively higher in the ΔCyt c_{6C} culture at 500 $\mu Em^{-2}s^{-1}$ light intensity compared to wild type. (figure 4.13 and Appendix table 4.1).

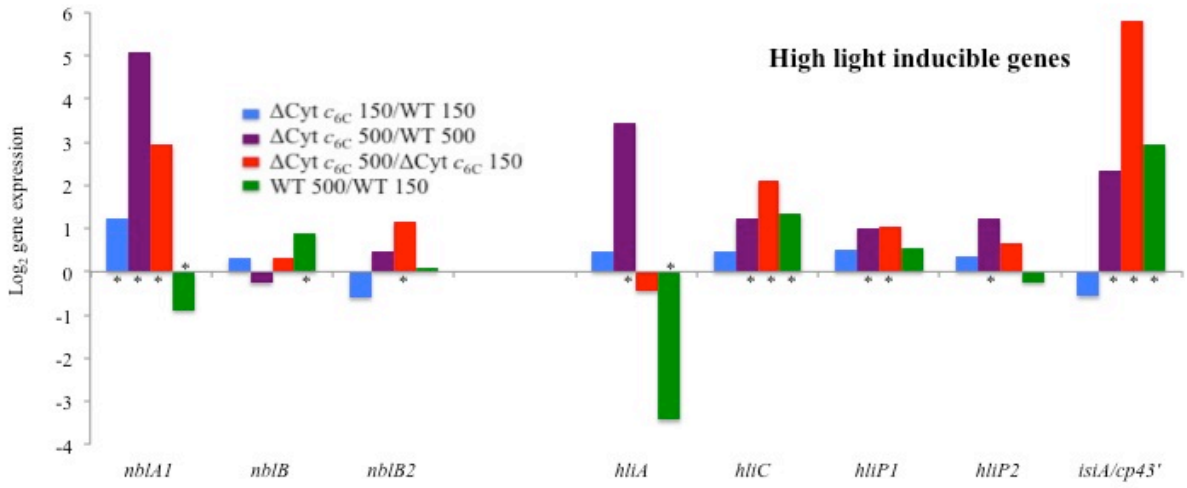

Figure 4.13: Comparative high light inducible protein complex transcript expression levels in ΔCyt c_{6C} and wild type under 150 and 500 $\mu Em^{-2}s^{-1}$ light intensities.Asterisks indicated significant differences in transcript abundance between ΔCyt c_{6C} 150/WT 150, ΔCyt c_{6C} 500/WT 500, ΔCyt c_{6C} 500/ ΔCyt c_{6C} 150 and WT 500 vs WT 150 $\beta Em^{-2}s^{-1}$ light intensity ($p < 0.05$). Changes in transcript abundance are given in log_2 values in y-axis.

4.5.8 Transcript levels for soluble electron carriers in ΔCyt c_{6C} cultures under different light intensities

RNA-seq analysis demonstrated that knocking out of Cyt c_{6C} significantly changed the transcript levels of different electron carriers under different light intensities. *S. elongatus* has two regular electron carriers, Cyt c_6 and Pc. Either one can function as an electron carrier from the Cyt b_6f complex to PSI (Bialek *et al*., 2008; Reyes-Sosa *et al*., 2011; Ho *et al*., 2011; Zatwarnicki *et al.*, 2014). Along with the Cyt c_6 (*petJ1*) and Pc (*petE*), the presence of a Cyt c_6 isoform (*petJ1iso*) and low molecular weight low redox potential electron carriers Cyt c_{6C} (*petJ2*) and Cyt c_M (*cytM*) were also reported in *S. elongatus* (Bialek *et al*., 2008; Reyes-Sosa *et al*., 2011; Ho *et al*., 2011; Zatwarnicki *et al*., 2014; Cho, Pakrasi *et al*., 2000; Lucini, 2008; Hiraide *et al*., 2015; Bernroitner *et al*., 2009). When the ΔCyt c_{6C} culture was grown in 150 $\mu Em^{-2}s^{-1}$ light intensity, up regulation of *petJ*1 gene transcript levels encoding Cyt c_6 protein (conventional Cyt c_6) was observed compared to wild type.

When the ΔCyt c_{6C} culture was grown at 500 $\mu Em^{-2}s^{-1}$ light none of the conventional Cyt c_6/Pc (*petJ1/petE*) were significantly regulated compared to wild type, although interestingly the *cytM* transcript encoding Cyt c_M protein was up regulated compared to wild type at the same light intensity. When the ΔCyt c_{6C} culture was grown at 500 $\mu Em^{-2}s^{-1}$ light intensity, up regulation of Cyt c_6 isoform (*petJ1iso*), and Pc (*petE*) genes was seen compared to 150 $\mu Em^{-2}s^{-1}$ was seen (figure 4.14 and Appendix table 4.1). When the wild type culture was grown at 500 $\mu Em^{-2}s^{-1}$ light intensity, up regulation of transcripts of *petJ1, petJ1iso, petE* and *petJ*2 and down regulation of the transcript of *cytM* gene was observed compared to cells grown at 150 $\mu Em^{-2}s^{-1}$ light intensity (figure 4.14 and Appendix table 4.1). Assuming the protein levels reflect transcript levels, these data indicate the presence of significantly more Cyt c_6, in ΔCyt c_{6C} culture, compared to the wild type at 150 $\mu Em^{-2}s^{-1}$ light, however Cyt c_6 isoform, Pc and Cyt c_M transcripts were

not significantly regulated. At 500 $\mu Em^{-2}s^{-1}$ light intensity, there is presence of more Cyt c_M in the ΔCyt c_{6C} culture compared to the wild type. Interestingly Cyt c_6, Cyt c_6 isoform and Pc also present but not significantly altered compared to the wild type. At 500 $\mu Em^{-2}s^{-1}$ light, there is more Pc and Cyt c_6 isoform in the mutant compared to the culture grown at 150 $\mu Em^{-2}s^{-1}$ light. For the wild type at 500 $\mu Em^{-2}s^{-1}$ light, there is also more, Cyt c_{6C} compared to the culture grown at 150 $\mu Em^{-2}s^{-1}$ light, consistent with the preliminary indication from the northern blot and qPCR earlier.

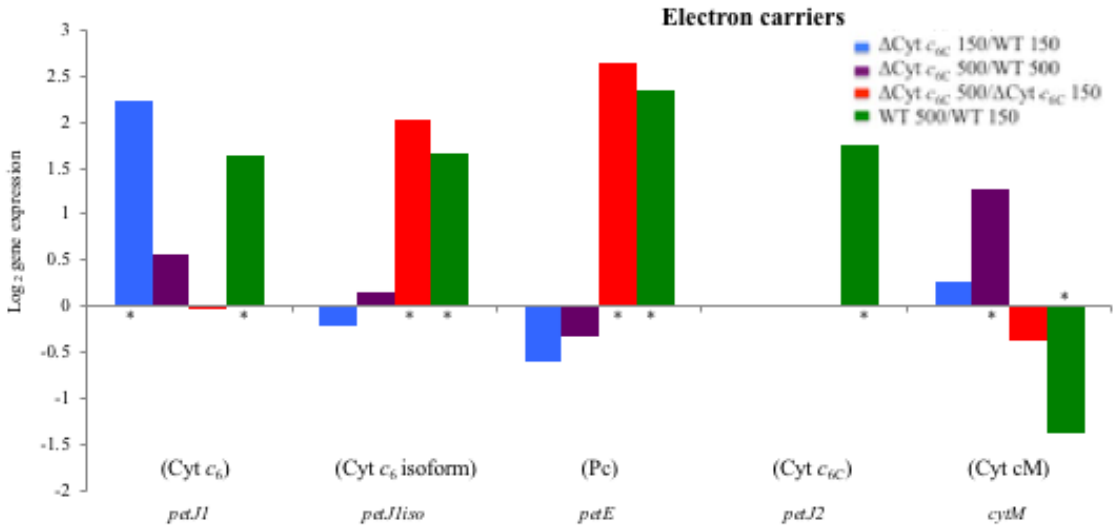

Figure 4.14: Comparative lumenal redox carriers transcript expression levels in ΔCyt c_{6C} and wild type under 150 and 500 $\mu Em^{-2}s^{-1}$ light intensities. Asterisks indicated significant differences in transcript abundance between ΔCyt c_{6C} 150/WT 150, ΔCyt c_{6C} 500/WT 500, ΔCyt c_{6C} 500/ ΔCyt c_{6C} 150 and WT 500 vs WT 150 $\mu Em^{-2}s^{-1}$ light intensity ($p < 0.05$). Changes in transcript abundance are given in log_2 values in y-axis.

4.5.9 Transcript levels for terminal oxidase, Ndb and Sdh complexes in ΔCyt c_{6C} cultures under different light intensities

RNA-seq analysis demonstrated that knocking out Cyt c_{6C} did not significantly change the transcript levels of Cyt *bd* quinol oxidase subunit 1 (*cydA*) and subunit 2 (*cydB*) genes, NDH II dehydrogenase (*ndbA, ndbB* and *ndbC*) genes and succinate dehydrogenase (*sdhA* and *sdhB*) genes under 150 $\mu Em^{-2}s^{-1}$ light intensity compared to wild type, although there was down regulation of transcripts of Cyt oxidase subunit 1 (*cox*) and subunit 3 (*ctaE*) genes in the mutant compared to wild type (figure 4.15 and Appendix table 4.1). At 500

$\mu Em^{-2}s^{-1}$ light intensity significant up regulation of transcripts of *cydA* and *cydB* genes was seen in the mutant compared to the wild type,. Up regulation of *ndbB* transcript was observed. Downregulation of cytochrome oxidase transcripts in the mutant was also seen compared to the wild type, as at 150 $\mu Em^{-2}s^{-1}$. When the ΔCyt c_{6C} culture was shifted from 150 to 500 $\mu Em^{-2}s^{-1}$ light intensity, up regulation of the transcripts of Cyt *bd* quinol oxidase (*cydA* and *cydB*) genes and up regulation of *cox,* and Cyt oxidase subunit 2 (*ctaC*) transcripts was seen. Up regulation of NDH II dehydrogenase (*ndbA, ndbB* and *ndbC)* transcripts and up regulation of the succinate dehydrogenase (*sdhA*) transcript and down regulation of the *sdhB* transcript were observed. Similar results were also observed in the wild type when the culture was shifted from 150 to 500 $\mu Em^{-2}s^{-1}$ light intensity.

Assuming the protein levels reflect transcript levels, these data indicate the presence of less Cyt oxidase in the mutant compared to the wild type at 150 $\mu Em^{-2}s^{-1}$ and 500 $\mu Em^{-2}s^{-1}$ light intensity. There is moderately more Cyt *bd* quinol oxidase and possibly NDH II in the mutant compared to the wild type at 500 $\mu Em^{-2}s^{-1}$ light intensity. Both mutant and wild type show similar increases in Cyt *bd* quinol oxidase, Cyt oxidase, and NDH II at 500 $\mu Em^{-2}s^{-1}$ compared to 150 $\mu Em^{-2}s^{-1}$ light intensity. (figure 4.15 and Appendix table 4.1).

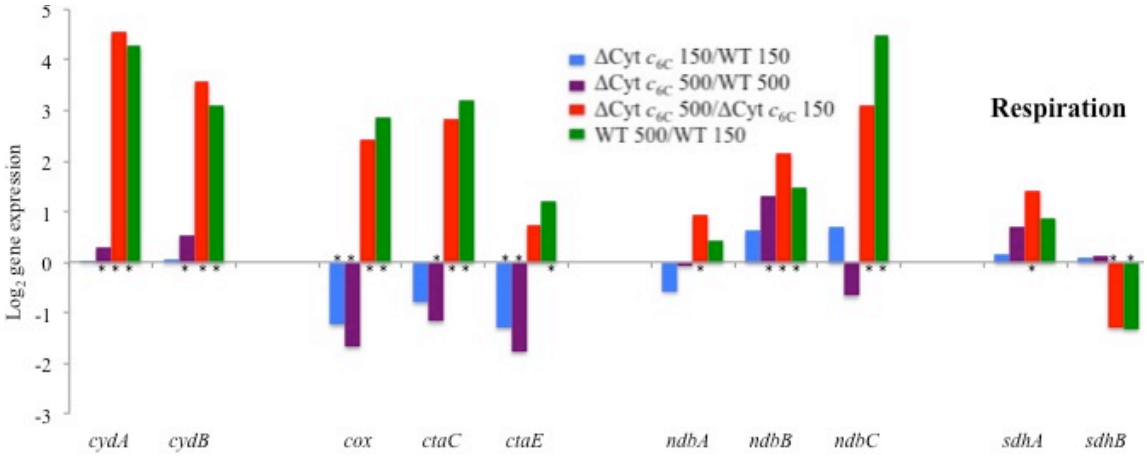

Figure 4.15: Comparative terminal oxidase, Ndb and Sdh transcript expression levels in ΔCyt c_{6C} and wild type under 150 and 500 $\mu Em^{-2}s^{-1}$ light intensities. Asterisks indicated significant differences in transcript abundance between ΔCyt c_{6C} 150/WT 150, ΔCyt c_{6C} 500/WT 500, ΔCyt c_{6C} 500/ ΔCyt c_{6C} 150 and WT 500 vs WT 150 $\mu Em^{-2}s^{-1}$ light intensity ($p < 0.05$). Changes in transcript abundance are given in log_2 values in y-axis.

4.5.10 Transcript levels for type 1 NAD(P)H dehydrogenase subunits in ΔCyt c_{6C} cultures under different light intensities

RNA-Seq analysis demonstrated that knocking out of Cyt c_{6C} did not significantly alter the transcript levels of NDH I dehydrogenase components at 150 $\mu Em^{-2}s^{-1}$ light intensity compared to wild type, although up regulation of the transcript levels for *ndhD2*, *ndhF3* genes was observed. At 500 $\mu Em^{-2}s^{-1}$ light intensity, up regulation of the transcripts levels for *ndhA, ndhB, ndhC, ndhD2, ndhD3, ndhD4, ndhD5, ndhF1, ndhF3, ndhK, ndhL,* and *ndhM,* genes and down regulation of the transcript of *ndhD* gene was observed compared to the wild type.

When the ΔCyt c_{6C} culture was grown at 500 $\mu Em^{-2}s^{-1}$ light intensity, up regulation of the transcript levels for *ndhA, ndhB, ndhC, ndhD3, ndhD4, ndhE, ndhF1, ndhF3, ndhF4, ndhG, ndhH, ndhI, ndhJ, ndhK, ndhL, ndhM, cmpR, cupA, cupB* genes was observed compared to the culture grown at 150 $\mu Em^{-2}s^{-1}$ light intensity. Similar results were also observed in the wild type when the culture was grown at 500 $\mu Em^{-2}s^{-1}$ light intensity, although the fold changes were relatively lower compared to ΔCyt c_{6C} culture grown at 500 $\mu Em^{-2}s^{-1}$ light intensity (figure 4.16 and Appendix table 4.1). Assuming the protein levels reflect transcript levels these data indicate the presence of more NDH I dehydrogenase in the mutant compared to the wild type at 500 $\mu Em^{-2}s^{-1}$ light intensity.

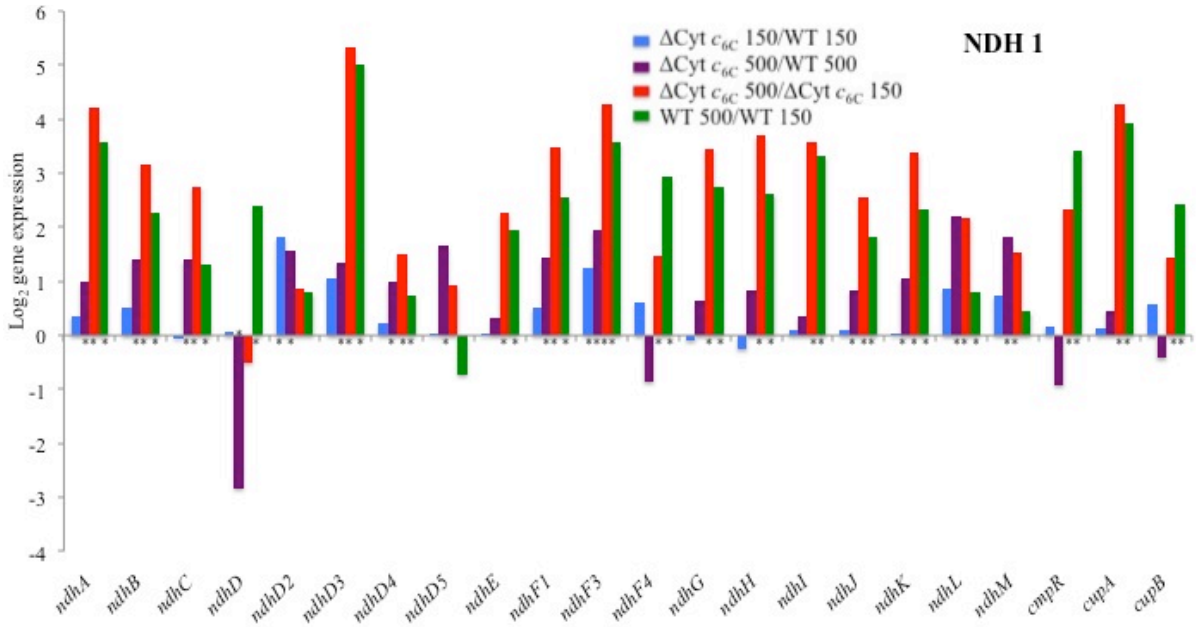

Figure 4.16: Comparative type 1 NAD(P)H dehydrogenase transcript expression levels in ΔCyt c_{6C} and wild type under 150 and 500 $\mu Em^{-2}s^{-1}$ light intensities. Asterisks indicated significant differences in transcript abundance between ΔCyt c_{6C} 150/WT 150, ΔCyt c_{6C} 500/WT 500, ΔCyt c_{6C} 500/ ΔCyt c_{6C} 150 and WT 500 vs WT 150 $\mu Em^{-2}s^{-1}$ light intensity ($p < 0.05$). Changes in transcript abundance are given in log_2 values in y-axis.

4.5.11 Overview of transcript changes

MapMan analysis (figure 4.17) and RNA-Seq analysis demonstrated that loss of the *petJ2* gene encoding Cyt c_{6C} in *S. elongatus* did not significantly alter the expression of PSII, PSI, Cyt b_6f complex, ATP synthase, phycobilisomes, high light inducible proteins, and the respiratory complexes Cyt *bd* quinol oxidase, Cyt oxidase, NDH I and NDH II dehydrogenase, succinate dehydrogenase under 150 $\mu Em^{-2}s^{-1}$ light intensity compared to wild type. However, *nblA*1 was more abundant in the mutant compared to the wild type. At 500 $\mu Em^{-2}s^{-1}$ light intensity, transcript levels for the PSII, Cyt b_6f complex were more or less similar to the wild type, transcript levels for PSI were down regulated compared to the wild type and the transcript levels for ATP synthase were more abundant compared to the wild type. High light inducible protein transcript levels were up regulated in the mutant compared to the wild type, phycobilisome proteins transcript levels were less abundant in the mutant. Transcript levels for Cyt *bd* quinol oxidase, NDH I and NDH II dehydrogenase were up regulated in the mutant, transcript levels for Cyt oxidase were down regulated in the mutant and succinate dehydrogenase was not significantly regulated compared to wild type.

When the ΔCyt c_{6C} culture was grown at 500 $\mu Em^{-2}s^{-1}$ light intensity, transcript levels for PSII, Cyt b_6f complex, ATP synthase, high light inducible proteins, Cyt *bd* quinol oxidase, Cyt oxidase, NDH I and NDH II dehydrogenase, succinate dehydrogenase were more abundant in the mutant compared to the mutant culture grown at 150 $\mu Em^{-2}s^{-1}$ light intensity, however the transcript levels for PSI, phycocyanin and phycobilisome linkers were down regulated and allophycocyanin transcript levels were not significantly altered. For the wild type culture grown at 500 $\mu Em^{-2}s^{-1}$ light intensity, similar changes in transcript levels were seen compared to 150 $\mu Em^{-2}s^{-1}$ light intensity, except that PSI transcripts were generally upregulated.

Knocking out of Cyt c_{6C} significantly influenced the expression of the lumenal redox carriers in *S. elongatus*. When ΔCyt c_{6C} culture was grown under 150 $\mu Em^{-2}s^{-1}$ light intensity, the transcript level for Cyt c_6 (*petJ1*) was up regulated, and none of the other redox carriers was significantly affected compared to wild type. At 500 $\mu Em^{-2}s^{-1}$ light intensity, the Cyt c_M (*cytM*) transcript was significantly upregulated, and others were un-affected (figure 4.14).

When ΔCyt c_{6C} culture was grown at 500 $\mu Em^{-2}s^{-1}$ light intensity, up regulation of the transcript levels for Cyt c_6 isoform (*petJ1 iso*), and Pc (*petE*) genes was seen compared to the ΔCyt c_{6C} culture grown at 150 $\mu Em^{-2}s^{-1}$ light intensity. The same changes were seen in wild type culture grown at 500 $\mu Em^{-2}s^{-1}$ light intensity, together with significant increases in the transcript levels for Cyt c_6 (*petJ1*) and Cyt c_{6C} (*petJ2*) and a decrease in the transcript level for Cyt c_M.

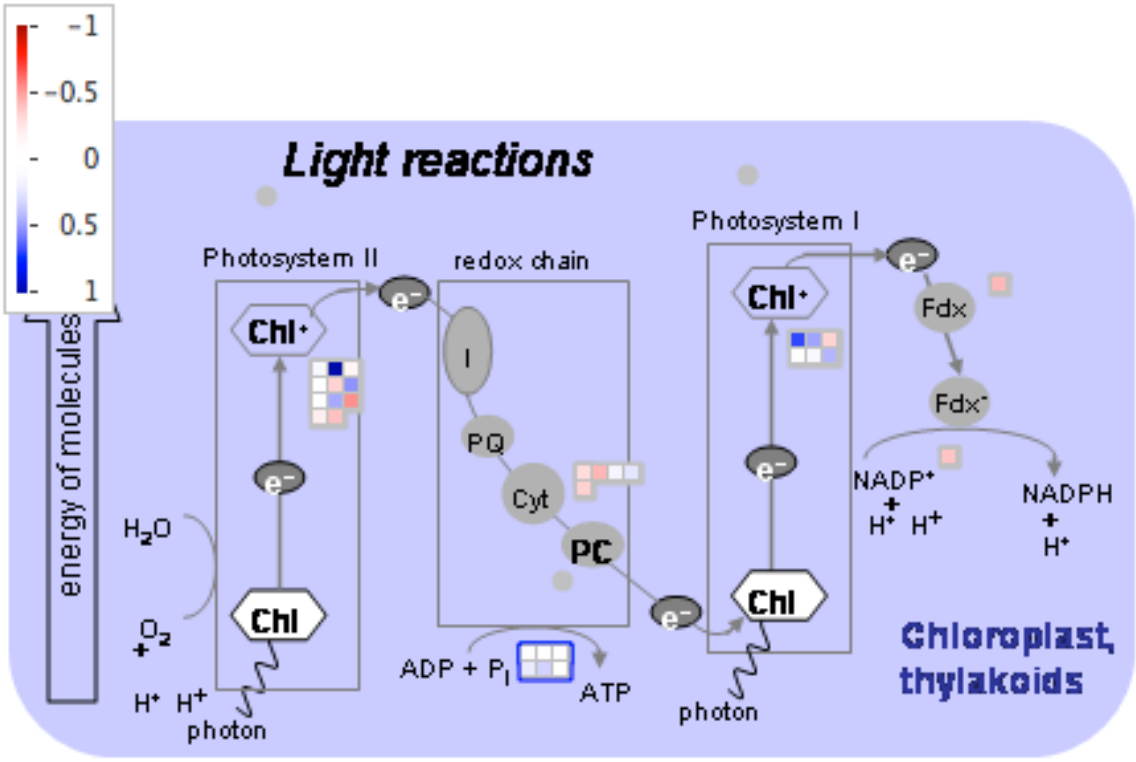

A

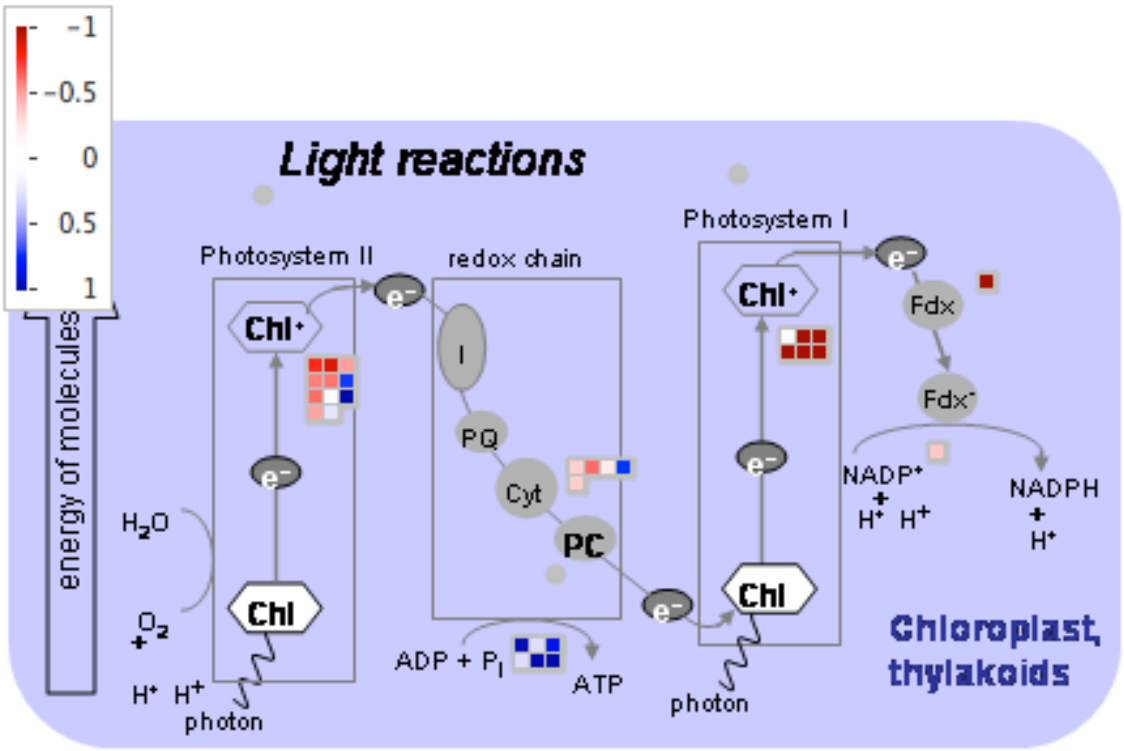
-1
-0.5
0
0.5
1
energy of molecules
Light reactions
Photosystem II
redox chain
Photosystem I
Chl*
Chl
e⁻
I
PQ
Cyt
PC
Fdx
Fdx⁻
NADP⁺ + H⁺ H⁺
NADPH + H⁺
H₂O
O₂ +
H⁺ H⁺
photon
ADP + Pi
ATP
Chloroplast, thylakoids

B

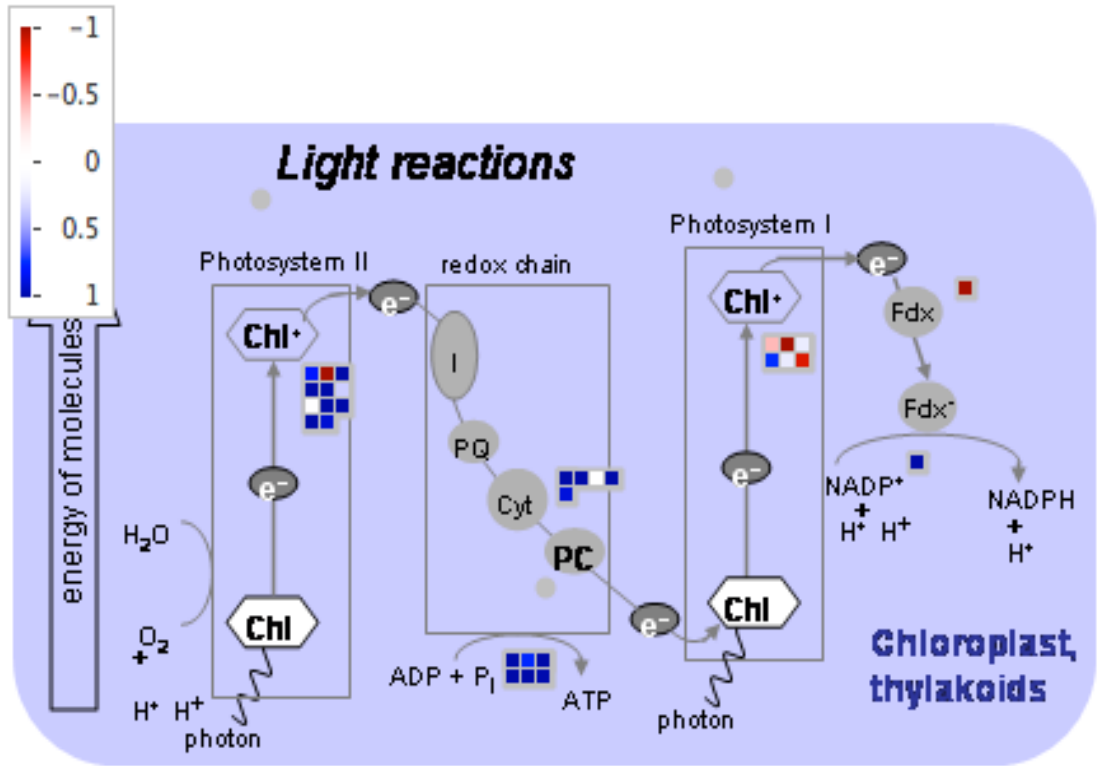
-1
-0.5
0
0.5
1
energy of molecules
Light reactions
Photosystem II
redox chain
Photosystem I
Chl*
Chl
e⁻
I
PQ
Cyt
PC
Fdx
Fdx⁻
NADP⁺ + H⁺ H⁺
NADPH + H⁺
H₂O
O₂ +
H⁺ H⁺
photon
ADP + Pi
ATP
Chloroplast, thylakoids

C

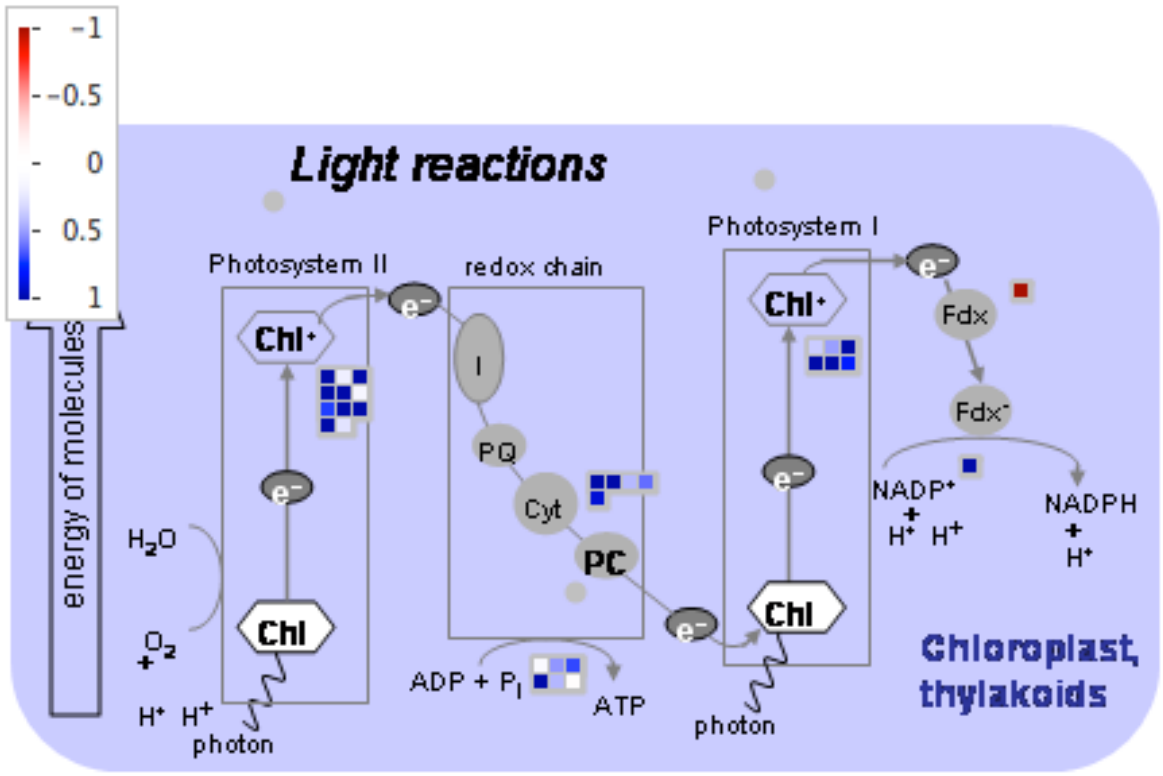

D

Figure 4.17: MapMan comparison of the transcripts of photosynthetic gene expression under different light conditions. Differences in transcript abundance between ΔCyt c_{6C} 150/WT 150 (A), ΔCyt c_{6C} 500/WT 500 (B), ΔCyt c_{6C} 500/ΔCyt c_{6C} 150 (C) and WT 500 vs WT 150 $\mu Em^{-2}s^{-1}$ light intensity (D). Changes in transcript abundance in log_2 values from Dark red (down regulation) to white (no regulation) and Dark blue (up regulation).

4.6 General Discussion of about Cyt c_{6C} function

The growth phenotypes observed are summarised in table 4.1.

S.No	Light (µE)	Other conditions	Mutant phenotype
1	2 (ELL)	No bubbling (Incubator)	Bleaching
2	15 (LL)	No bubbling (Incubator)	Slight growth impairment
3	40 (ML)	Bubbling (Incubator)	No growth impairment
4	150 (HL)	Bubbling (Incubator)	No growth impairment
5	300	Bubbling (Algem Photobioreactor)	Some growth impairment
6	500	Bubbling (Algem Photobioreactor)	Severe growth impairment
7	1200 (EHL)	Bubbling (Incubator)	Rapid bleaching

Table 4.1: Summary of the growth characterization of ΔCyt c_{6C} at different light conditions.

These data indicate growth impairment at very low and very high light levels in the ΔCyt c_{6C} culture, although comparison between ELL or LL and other data should be treated with caution, as the ELL and LL cells were not bubbled with sterile air. The northern blot, qRT-PCR and transcriptomic data all indicated increased transcript levels for Cyt c_{6C} under elevated light levels, consistent with the appearance of a phenotype in the mutants at elevated light levels.

Physiological characterisation studies indicate impaired oxygen evolution, especially at high light levels, and possibly increased photoinhibition. The respiration rate was increased but not statistically significantly compared to the wild type. The chlorophyll fluorescence analysis data indicated the mutant shows less NPQ and somewhat greater Φ PSII in ΔCyt c_{6C} culture with other parameters little affected. ΔCyt c_{6C} showed slower rates of P700+ reduction kinetics compared to wild type.

Transcriptomic analysis data indicated the presence of a similar amount of PSII and less PSI in the mutant compared to the wild type at 500 μE m^{-2} s^{-1} light intensity. The data also suggested increased abundance of ATP synthase, and Cyt *bd* quinol oxidase and less abundance of Cyt oxidase in the mutant compared to the wild type at 500 μE m^{-2} s^{-1} light

intensity. The mutant also showed less abundance of phycocyanin compared to the wild type at 500 μE m^{-2} s^{-1} light intensity, with highly increased abundance of *nblA*, associated with phycobilisome degradation, which also showed increased transcript levels at 150 μE m^{-2} s^{-1} light intensity. Similarly *hliA* and *isiA* were more abundant in the mutant compared to the wild type at 500 μE m^{-2} s^{-1} light intensity.

The transcriptomic data also indicated the presence of more Cyt c_6, in the ΔCyt c_{6C} culture, compared to the wild type at 150 $\mu Em^{-2}s^{-1}$ light, and more Cyt c_M at 500 $\mu Em^{-2}s^{-1}$. Interestingly significant increases in Cyt c_6, Cyt c_6 isoform and Pc seen in the wild type at 500 $\mu Em^{-2}s^{-1}$ light compared to 150 $\mu Em^{-2}s^{-1}$ were not seen in the mutant, and a decrease in Cyt c_M was seen in contrast to the mutant.

Cyanobacteria have two types of bioenergetically active membranes; the CM contains a respiratory electron transport pathway and the TM contains interlinked photosynthetic and respiratory electron transport chains. This interlinked system supports the survival of cyanobacteria under different physiological conditions. We interpret the data in terms of a model in which Cyt c_{6C} serves to transfer electrons from the plastoquinone pool to PSI (if this is mediated by Cyt c_6 or Pc, transfer to cytochrome oxidase would also presumably be possible), and Cyt c_M serves to transfer electron from the plastoquinone pool to cytochrome oxidase (if this is mediated by Cyt c_6 or Pc, transfers to PSI would also possible). In growth in moderate light conditions (40 - 150 μE m^{-2} s^{-1} light), even though the light energy was below the saturation of photosynthetic electron flow, respiratory electrons were also redirected to the PQ pool from NDHI, NAD(P)H, and SHD. The redox state of PQ pool was in moderately steady state; linear electron flow occurred in wild type cultures through Cyt b_6f complex to PSI and to the terminal oxidase, there was no growth phenotype in the ΔCyt c_{6C} culture. The increased level of the phycobilisome degradation protein NblA1 transcript observed in the mutant may suggest that knocking out Cyt c_{6C} moderately alters the redox state of PQ pool at 150 μE m^{-2} s^{-1} light with upregulation of *NblA1* and degradation of PBS.

Upon increasing the light intensity to 500 or 1200 μE m^{-2} s^{-1} the ΔCyt c_{6C} culture showed a phenotype of slower growth, and rapid bleaching respectively (figure 4.2 and 4.3B respectively). When the culture is exposed to high light intensity the photosynthetic electron transport chain becomes saturated and the excess light energy needs to be

dissipated in different ways (Erickson *et al*., 2015). Photosynthetic organisms have multiple strategies to prevent oxidative damage by high light stress or fluctuating light conditions. These include reducing the antenna size, energy redistribution to photosystems by state transition mechanism and NPQ. In plants and algae, the excess light absorbed by the antenna proteins of PSII can dissipated as heat through psbS-mediated NPQ in response to low lumenal pH, or redistributed between the photosystems by state transition mechanisms or decrease in antenna size (King *et al.*, 2014). Cyanobacteria posses several short term regulation mechanisms to dissipate excess energy harvested by the PBS antenna, as heat with Orange Carotenoid Protein (OCP, Bailey and Grossman 2008; Zhang *et al*., 2014; Thurotte *et al*., 2015) and via state transitions (Chukhutsina *et al*., 2015). Other mechanisms of photoprotection involve induction of alternative electron transfer routes to flavodiiron proteins Flv2/Flv4 that protect PSII against photodamage, and Flv1/Flv3 that protect PSI against photodamage (Chukhutsina *et al*., 2015; Allahverdiyeva *et al*., 2015a; Bersanini *et al*., 2014; Latifi *et al*., 2009; Zhang *et al*., 2009) or to the Cox and Cyd terminal oxidases (Hart *et al*., 2005, Lea-Smith *et al*., 2013). Given the absence of the OCP pathway in *S. elongatus* the mechanism of thermal dissipation is not well understood, however, presence of Flv1/3 and Cyd & Cox could potentially be involved in excess energy dissipation in *S. elongatus*. Under high light conditions, in wild type cells, cyclic electron flow will occur to prevent photoinhibition to the photosynthetic apparatus as well as providing ATP, using the proton gradient established by coupled cyclic electron transport through PGR5 protein.

According to the model proposed here, under these circumstances, Cyt c_{6C} and Cyt c_M would remove excess electrons directly from the reduced PQ pool to Pc/PSI or to terminal oxidase bypassing Cyt b_6f complex. However in the ΔCyt c_{6C} strain, this alternative Cyt c_{6C} pathway would be disrupted and the Cyt c_M pathway would get saturated, which is consistent with the observed reduction in rate of $P700^+$and more abundance of Cyt c_M. If loss of Cyt c_{6C} reduced the rate of cyclic electron transfer, and consequently the acidification of the lumen, it would be expected to result in lower NPQ (figure 4.6) compared to wild type. The PQ pool would also be expected to be more reduced, and these two effects, may create higher levels of reactive oxygen species that would damage the photosystems and other components of the cell, leading to reduced growth compared to wild type at high light intensities. Transcriptomic studies suggested higher levels of ATP synthase in the mutant compared to the wild type at high light intensity (figure 4.11). A

similar result was also observed in the Arabidopsis *pgr*5 mutant (impaired in cyclic electron flow) at fluctuating and high light levels ((Suorsa *et al*., 2012; Wang *et al*., 2015). Increased abundance of transcripts for high light inducible proteins, phycobilisome degradation protein (NblA1) and chlorophyll-binding antenna protein (IsiA/CP43') were seen in the mutant under high light compared to the wild type. Similar results were also observed in *Synechocystis* and other cyanobacteria at high light conditions (Muramatsu and Hihara 2012; Golden 1995; Waasbergen *et al*., 2002; Bailey and Grossman 2008). These are consistent with increased photoprotection under high light conditions with down regulation of the light harvesting machinery and PSII function. The reasons for the changes in terminal oxidases are less clear, but the increase in Cyt *bd* quinol oxidase and decrease in cytochrome oxidase may reflect a shift in the source of electrons towards PQ.

Under extreme low light conditions (ELL, 2 μE m^{-2} s^{-1} light) the Cyt c_{6C} knockout showed chlorophyll bleaching, with impaired growth at Low light (LL, 15 μE m^{-2} s^{-1} light). Significant down regulation of Cyt b_6f complex electron transfer efficiency has been observed in plants at low light condition (Laisk *et al*., 2005), probably due to inactivation of carbon reduction cycle enzymes. This result is consistent with our hypothesis. The lack of Cyt c_{6C} when the Cyt b_6f complex is inhibited might lead to damage from over-reduced PQ, or a simple inability to maintain a suitable level of ATP synthesis. Schematic model showing different routes of electron transfer chain in the WT, and ΔCyt c_{6C} line in a range of light conditions is given in Figure 4.18.

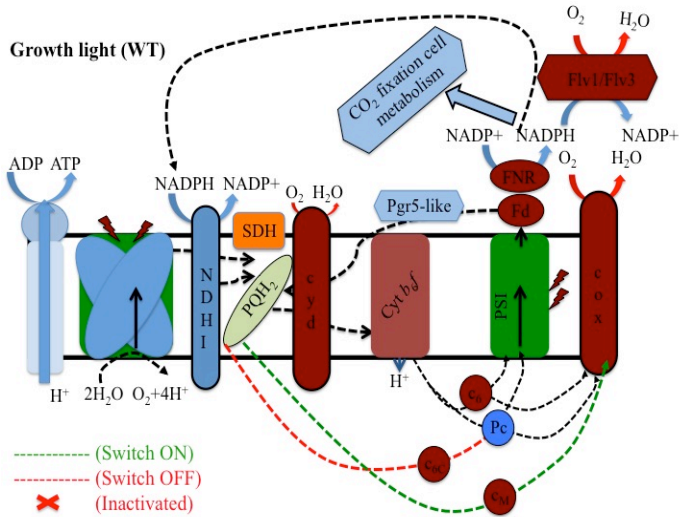
Growth light (WT)
CO_2 fixation cell metabolism
Flv1/Flv3
O_2 H_2O
NADP+ NADPH NADP+
ADP ATP
NADPH NADP+
SDH
FNR
Fd
Pgr5-like
NDHI
PQH_2
cyd
Cyt b_6f
PSI
cox
H^+ $2H_2O$ O_2+4H^+
c_6
Pc
c_{6C}
c_M
---------- (Switch ON)
---------- (Switch OFF)
(Inactivated)

(A)

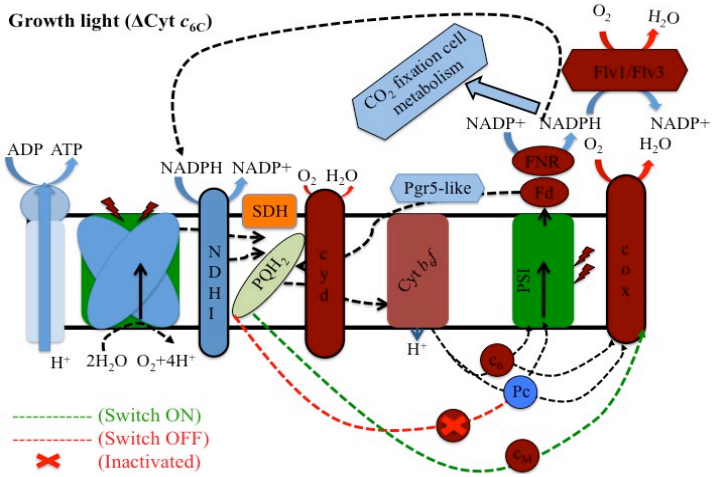
Growth light (ΔCyt c_{6C})
CO_2 fixation cell metabolism
Flv1/Flv3
O_2 H_2O
NADP+ NADPH NADP+
ADP ATP
NADPH NADP+
SDH
FNR
Fd
Pgr5-like
NDHI
PQH_2
cyd
Cyt b_6f
PSI
cox
H^+ $2H_2O$ O_2+4H^+
c_6
Pc
c_M
---------- (Switch ON)
---------- (Switch OFF)
(Inactivated)

(B)

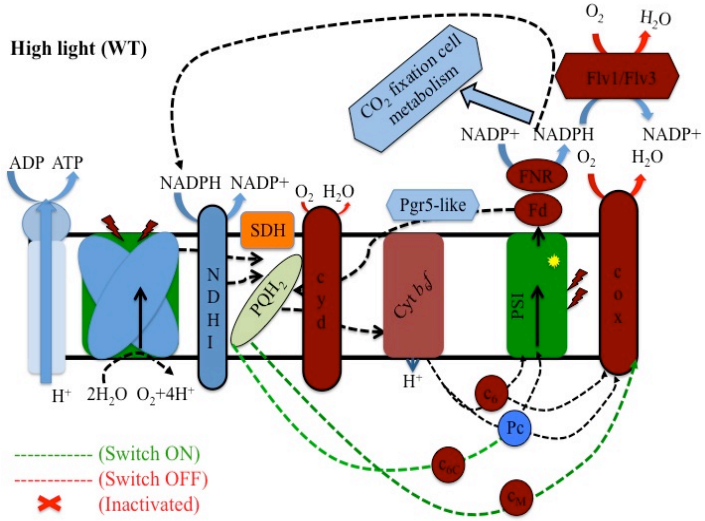
High light (WT)
CO_2 fixation cell metabolism
Flv1/Flv3
O_2 H_2O
NADP+ NADPH NADP+
ADP ATP
NADPH NADP+
SDH
FNR
Fd
Pgr5-like
NDHI
PQH_2
cyd
Cyt b_6f
PSI
cox
H^+ $2H_2O$ O_2+4H^+
c_6
Pc
c_{6C}
c_M
---------- (Switch ON)
---------- (Switch OFF)
(Inactivated)

(C)

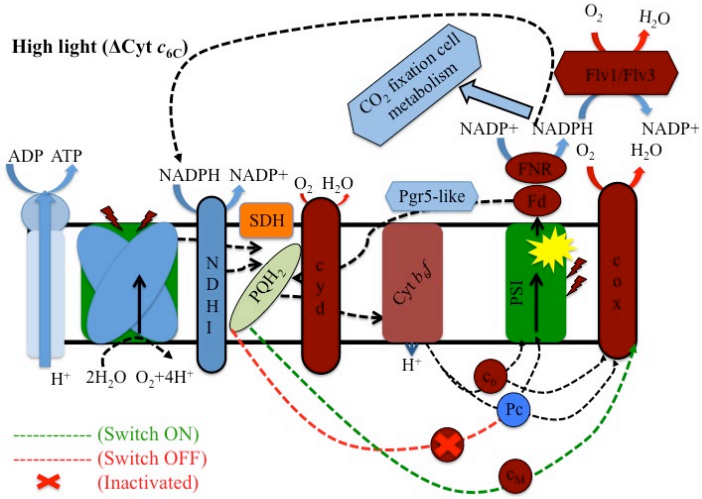
High light (ΔCyt c_{6C})
CO_2 fixation cell metabolism
Flv1/Flv3
O_2 H_2O
NADP+ NADPH NADP+
ADP ATP
NADPH NADP+
SDH
FNR
Fd
Pgr5-like
NDHI
PQH_2
cyd
Cyt b_6f
PSI
cox
H^+ $2H_2O$ O_2+4H^+
c_6
Pc
c_M
---------- (Switch ON)
---------- (Switch OFF)
(Inactivated)

(D)

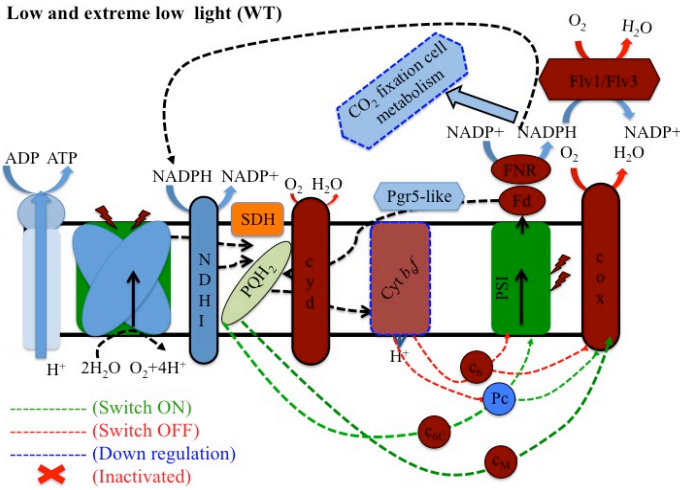
Low and extreme low light (WT)
CO_2 fixation cell metabolism
Flv1/Flv3
O_2 H_2O
NADP+ NADPH NADP+
ADP ATP
NADPH NADP+
SDH
FNR
Fd
Pgr5-like
NDHI
PQH_2
cyd
Cyt b_6f
PSI
cox
H^+ $2H_2O$ O_2+4H^+
c_6
Pc
c_{6C}
c_M
---------- (Switch ON)
---------- (Switch OFF)
---------- (Down regulation)
(Inactivated)

(E)

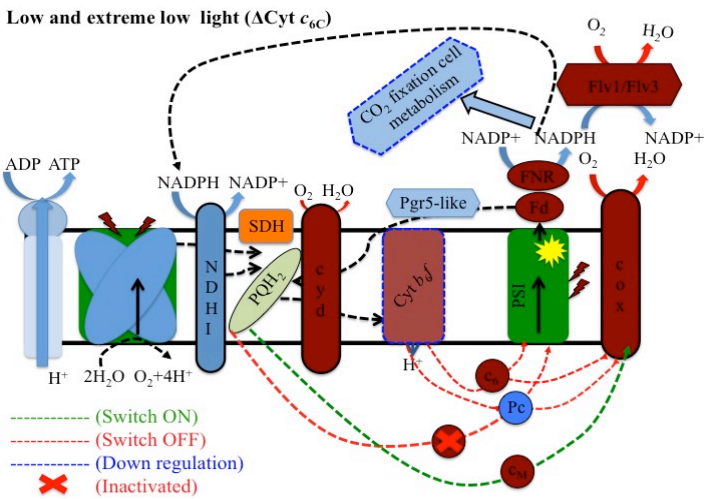
Low and extreme low light (ΔCyt c_{6C})
CO_2 fixation cell metabolism
Flv1/Flv3
O_2 H_2O
NADP+ NADPH NADP+
ADP ATP
NADPH NADP+
SDH
FNR
Fd
Pgr5-like
NDHI
PQH_2
cyd
Cyt b_6f
PSI
cox
H^+ $2H_2O$ O_2+4H^+
c_6
Pc
c_M
---------- (Switch ON)
---------- (Switch OFF)
---------- (Down regulation)
(Inactivated)

(F)

Figure 4.18: Schematic model showing different routes of electron transfer chain in WT and ΔCyt c_{6C} strain in growth light (40-150 μE m^{-2} s^{-1} light intensities), high light intensities (300, 500 and above μE m^{-2} s^{-1} light intensities) and low and extreme low light (2-15 μE m^{-2} s^{-1} light intensities). At growth light or below the growth light intensity WT (A), ΔCyt c_{6C} (B) can keep the intersystem electron transfer chain optimally oxidized and Cyt c_6 and Pc function as electron carriers in WT, along with Cyt c_6 and Pc, Cyt c_M function as electron carriers in the mutant. Increase in light intensity enhances ΔpH in WT (C) and Cyt c_6, Pc, function as normal electron carriers. Cyt c_{6C} and Cyt c_M function as electron sinks, directly accepting electrons from the PQ pool and Cyt c_{6C} donating electrons to Pc/PSI and Cyt c_M donating electron to Cyt oxidase, bypassing Cyt b_6f complex. In the mutant (D), Cyt c_6 and Pc function as normal electron carriers, and Cyt c_M functions as an alternative electron carrier from the PQ pool to Cyt oxidase. Under low and extreme low light conditions electron transfer through Cyt b_6f complex is severely inhibited. As a result Cyt c_{6C} and Cyt c_M function as electron carriers in WT (E), directly from PQ pool and to Pc/PSI or to Cyt oxidase respectively. In the mutant (F) Cyt c_M functions as an electron carrier directly from PQ pool to Cyt oxidase.

CHAPTER 5 CHARACTERIZATION OF CYT c_M

5.1 General Introduction

Cyt c_6 and Pc are the two conventional redox carriers in cyanobacteria that shuttle electrons between the Cyt b_6f complex and PSI or Cyt *c* oxidase. Along with Pc or Cyt c_6, a few other uncharacterized low molecular weight, low redox midpoint point potential electron carriers have been reported in cyanobacteria, including those designated as Cyt $c_{6B/C}$ and Cyt c_M. The gene encoding Cyt c_M was initially identified in *Synechocystis* (Malkova *et al*., 1994); the amino acid sequence exhibits about 40% sequence identity to Cyt c_6 of other cyanobacteria and nearly 30% identity to mitochondrial *c* type cytochrome of *Tetrahymena pyriformis* (Malkova *et al*., 1999). Interestingly, Cyt c_M is present in all sequenced cyanobacteria except *Prochlorococcus marinus* MIT 9515 (Bernroitner *et al*., 2009; Hiraide *et al*., 2015). It is a small water soluble protein with molecular mass of 8 kDa, isoelectric point (p*I*) of 6 and redox midpoint potential of + 151 mV at pH 7 (Molina-Heredia *et al*., 2002).

The protein was detected in *Synechocystis* wild type cells (Cho *et al*., 2000), and the protein was localized in both cytoplasmic (CM) and intracytoplasmic membranes (ICM) (Bernroitner *et al*., 2009). However, its location remains controversial, and detailed studies need to be done to confirm it. Northern blot analysis revealed the Cyt c_M transcript was barely expressed under normal physiological conditions, however, its expression was increased when the culture was exposed to low temperature (22°C) or under high light intensity (2000 μmol photons m^{-2} s^{-1}). In contrast, expression of conventional Cyt c_6 and Pc transcripts was suppressed under low temperature and in high light conditions. These observations suggested that Cyt c_M might replace Cyt c_6 or Pc under stress conditions (Malakhov *et al*., 1999). Thermodynamically, however, it does not seem possible, that Cyt c_M with a low redox mid point potential (+151 mV) could potentially oxidize the Cyt b_6f complex with high redox mid point potential (+350 mV) (Cho *et al*., 2000). A double knockout of Cyt c_6 and Pc could not be achieved to assess a role for Cyt c_M in photosynthesis in their absence. Photosynthetic electron flow rate from of PSII was measured by measuring chlorophyll fluorescence yield in *Synechocystis*, and found to be decreased in a Cyt c_6 or Pc knockout mutant, and Cyt c_M could not be deleted in a PSI-less background (Manna and Vermaas, 1997).

Cyt c_M protein has some degree of similarity with the Cyt *c* docking site of the Cyt caa_3-type oxidase from *Bacillus* spp and *Thermus thermophilus*. This finding led Manna and Vermaas (1997) to suggest that Cyt c_M is a part of the Cyt *c* oxidase complex in cyanobacteria and functions as a redox intermediate between the conventional redox carriers Pc/Cyt c_6 and Cyt *c* oxidase. However, a study of the kinetics of P700 oxidation and reduction in *Synechocystis* suggested that Cyt c_M could donate electrons to PSI under stress conditions (Shuvalov *et al*., 2001), although comparative laser flash induced kinetic analysis of P700 reduction in *Synechocystis* failed to prove the involvement of Cyt c_M in PSI reduction, and the bimolecular rate constant for the reaction is 100 times lower for Cyt c_M than Cyt c_6 or Pc (Molina-Heredia *et al*., 2002). On the other hand, measurement of the intermolecular electron transfer rate between Cyt c_M and the Cu domain of Cyt *c* oxidase demonstrated that Cyt c_M could potentially donate electrons to Cyt *c* oxidase as efficiently as Cyt c_6 and more effectively than Pc (Bernroitner *et al*., 2009). Distribution of the surface electrostatic potential of Cyt c_M is different from Cyt c_6 and Pc, therefore Cyt c_M cannot function in the same way as Cyt c_6 and Pc (Molina-Heredia *et al*., 2002). Recently, Hiraide *et al*., (2015) observed that a Cyt c_M knockout mutant of *Synechocystis* had improved heterotrophic growth in the dark or in light limited conditions compared to wild type.

When photosynthetic organisms are exposed to high light intensities which are enough to saturate the photosynthetic electron transport chain, excess light energy could potentially damage the photosynthetic machinery (Roach and Krieger-Liszkay, 2012). Cyanobacteria have developed numerous mechanisms to reduce this photoinhibitory damage (see chapter one for detailed information). We propose here a new photoprotective mechanism; that Cyt c_M functions as an electron sink under high light intensity to avoid over reduction of the PQ pool and thus to decrease PSII photodamage. We propose that Cyt c_M accepts electrons directly from the PQ pool during high light intensities, or over-reduced PQ conditions, and donates electrons directly to Cyt *c* oxidase, thereby bypassing the Cyt b_6f complex. To test this hypothesis in cyanobacteria we studied the model organism *S. elongatus* PCC 7942, using mutant lines of Cyt c_M and measuring their growth performances under different light intensities, especially under high light conditions. Photosynthesis efficiencies were also measured using a PAM fluorimeter. We used $P700^+$ reduction kinetics experiments to measure the rate of PSI reduction in a ΔCyt c_M line

compared to wild type. Finally, we used RNA-Seq analysis to investigate the effects of the mutation on transcript levels.

5.2 Growth phenotype of Cyt c_M knockout

Cyt c_M knockout and the wild type cultures were grown under different light conditions to assess the role of Cyt c_M under different physiological conditions.

5.2.1 Response of Cyt c_M knockout mutant under different light conditions

Under constant low light (LL, 15 μE m^{-2} s^{-1} light) conditions, growth differences between the ΔCyt c_M and wild type were apparent from day 2, with the wild type showing faster growth, and this difference in growth rate persisted until the end of the experiment (figure 5.1A). Under moderate light (ML, 40 μE m^{-2} s^{-1} light) conditions, a clear growth difference between wild type and ΔCyt c_M was observed, which also persisted till the experiment was over (figure 5.1B). Under constant high light (HL, 150 μE m^{-2} s^{-1} light) conditions a clear growth difference was also observed between the wild type and ΔCyt c_M from the start of the experiment (figure 5.1C).

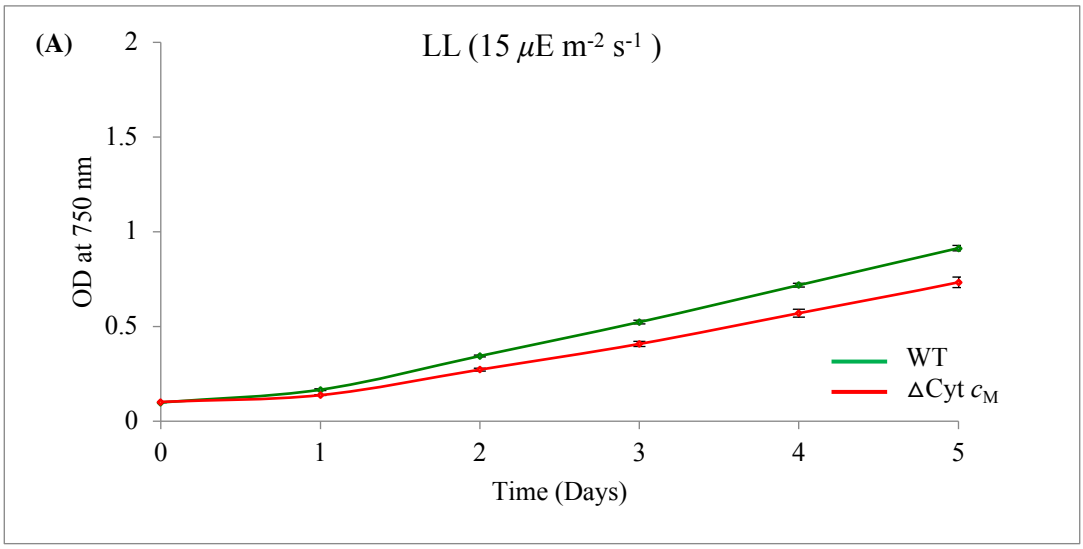

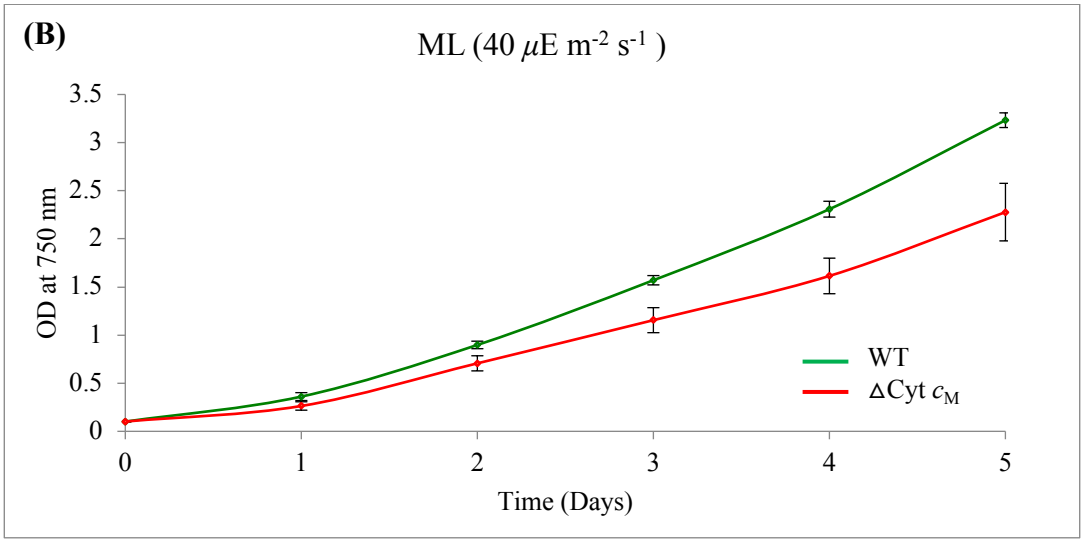

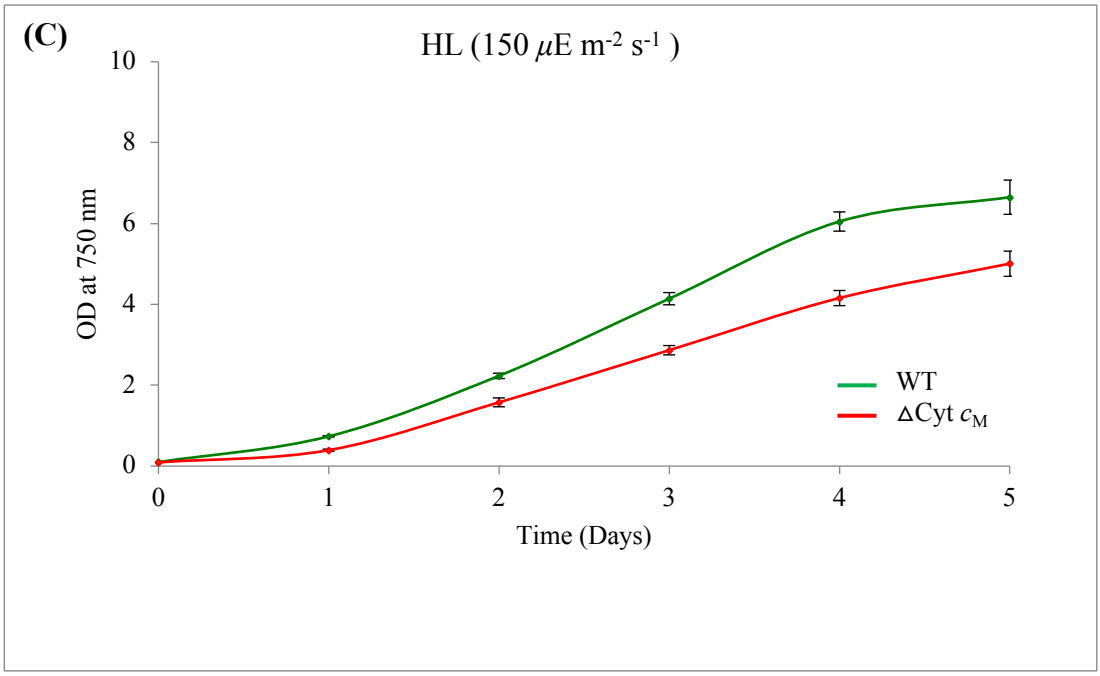

Figure 5.1: Growth phenotype of Cyt c_M mutant under different light conditions: Under low light (A) moderate light (B) and high light intensity (C) a clear growth phenotype was observed in the mutant compared to WT.

5.2.2 Growth phenotype under 300 and 700 μE m^{-2} s^{-1} light intensity

The growth phenotype was assessed under higher light intensities using the Algem photobioreactor (Algenuity UK) with sterile air bubbling. Under 300 μE m^{-2} s^{-1} light conditions, a growth difference between the wild type and ΔCyt c_M was seen clearly by 40 hrs of growth, with the wild type growing faster, and which persisted throughout the

experiment (figure 5.2A). Interestingly, when the light intensity was further increased, the mutant showed more dramatically retarded growth compared to WT. Under 700 μE m^{-2} s^{-1} light intensity both the wild type and ΔCyt c_M cultures showed no growth for a period of ~ 20 hrs, after which the wild type culture showed significant growth, but the ΔCyt c_M strain did not show any sign of growth throughout the experiment (figure 5.2B).

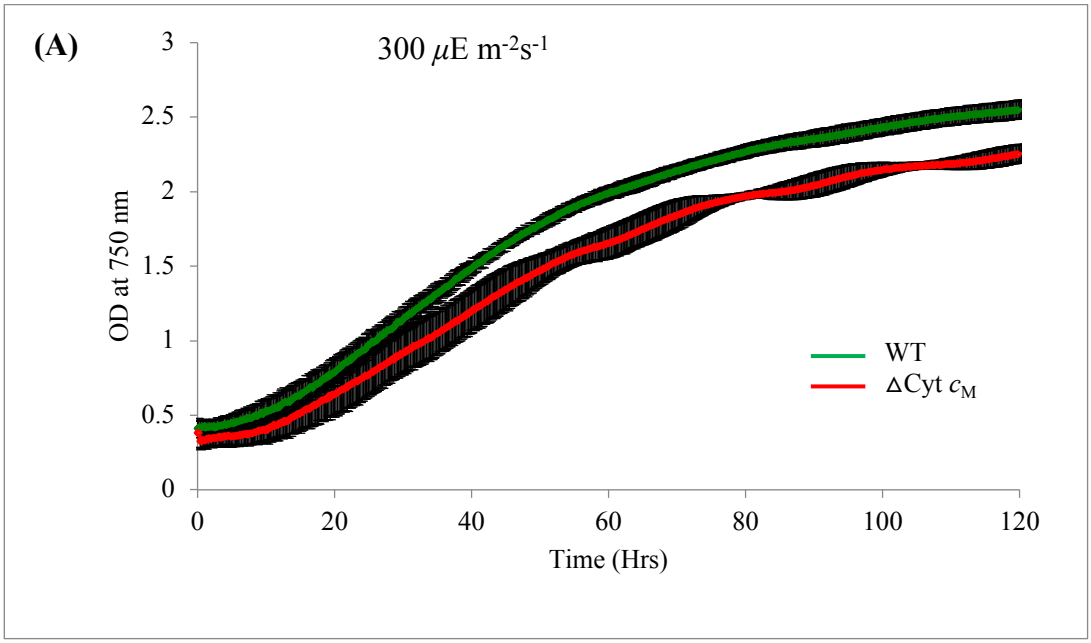

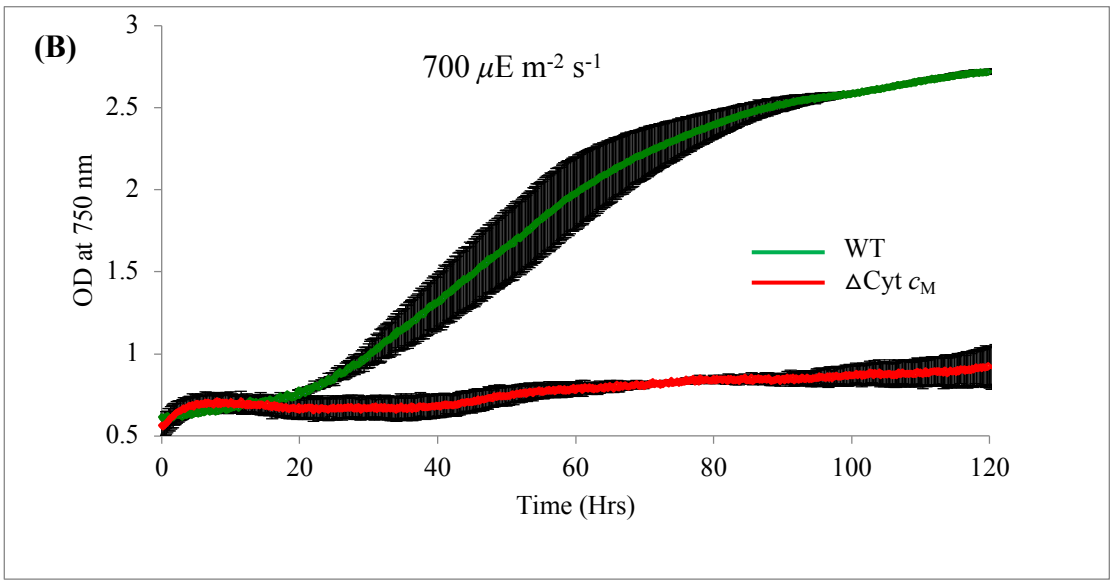

Figure 5.2: Growth characterization of Cy c_M knockout and wild type cultures in a photobioreactor in different light conditions. Cyt c_M and wild type cultures were grown in 300 μE m^{-2} s^{-1} light (A) or 700 μE m^{-2} s^{-1} light intensities (B).

5.2.3 Growth phenotype under extreme light intensity

We tested the role of Cyt c_M in *S. elongatus* PCC 7942 by growing the Cyt c_M knockout under extremely low light. Liquid and solid cultures of different mutants were incubated in an incubator at ELL (figure 5.3C, and E) and on the bench (figure 5.3A, B and D). ΔCyt c_M showed complete chlorophyll bleaching in both conditions in 10-15 days (compare 5.3C3 to 5.3C4 and 5.3 E right to 5.3E left for liquid culture and compare 5.3A6 with 5.3B1 and 5.3D right to 5.3D left). This bleaching phenomenon was also seen in ΔCyt c_M of *Synechocystis sp* 6803 on the bench (figure: 5.3B2, compare 5.3B2with 5.3B4).

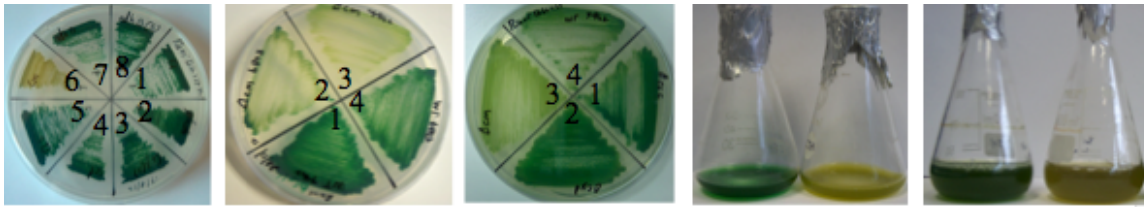

Figure: 5.3: ΔCyt c_M growth phenotype in liquid culture as well as on culture plates under low light conditions: ΔCyt c_M and other redox carrier mutant strains of *S. elongatus* grown on a plate A (ΔCyt c_6 (1), ΔPc (2), ΔCyt c_6 isoform (3), ΔCyt *bd* quinol oxidase (4), ΔCyt c_{6C} (5), ΔCyt c_M (6), ΔndbA (7) and ΔndbB (8)) and B (*S. elongatus* wild type (1), ΔCyt c_M of *Synechocystis* 6803 (2), ΔCyt c_{6M} of *S. elongatus* (3) and wild type of *Synechocystis* 6803 (4) and C (wild type of *Synechocystis* 6803 (1), ΔCyt *bd* quinol oxidase (2), ΔCyt c_M (3), and *S. elongatus* wild type (4)) and in liquid culture (D (left wild type and right ΔCyt $c_{M)}$ & E (left wild type and right ΔCyt c_M) under ELL condition for growth phenotype study, ΔCyt c_M shows complete chlorophyll bleaching in both liquid as well as in plate; a similar phenotype is also observed in *Synechocystis* sp 6803 (B).

5.3 Physiological characterization of ΔCyt c_M mutant

5.3.1 Oxygen electrode study to investigate photosynthetic efficiency

The oxygen electrode is widely used to measure oxygen (O_2) evolution in photosynthetic organisms. During photosynthesis O_2 is produced and released to the environment. Quantification of oxygen production in the presence of light, and oxygen consumption in the dark by photosynthetic organisms is an excellent approach to measure the rate of photosynthesis and respiration (González *et al*., 2003). The rates of oxygen evolution in the light and consumption in the dark were measured using a Clark type oxygen electrode.

5.3.2 Oxygen electrode study

Using 2 ml of (~ 4 nmol Chl ml^{-1}) culture from each strain the rates of photosynthesis and respiration were measured (section 2.11.1). The rate of oxygen evolution in Cyt c_M knockout was not significantly different from that of WT, indicating an essential involvement of Cyt c_M in photosynthesis is unlikely (figure 5.4A). Interestingly the rate of dark respiration in ΔCyt c_M was significantly higher than in wild type (figure 5.4B). This result suggests the involvement of Cyt c_M in respiration.

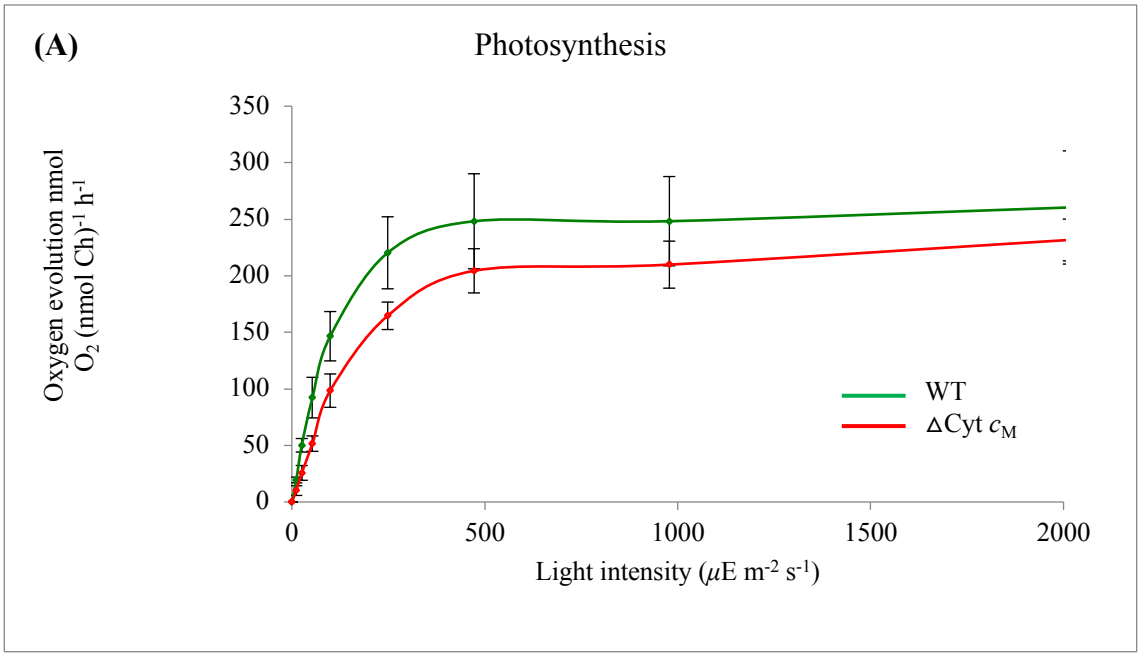

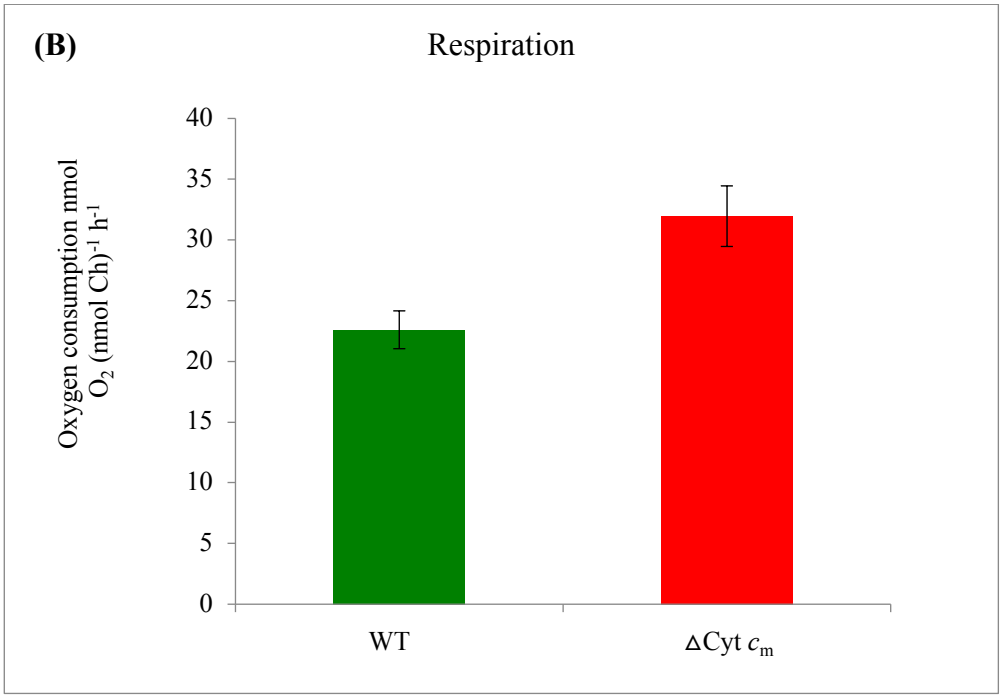

Figure 5.4: Rates of photosynthesis and respiration in Cyt c_M knockout and WT: the Cyt c_M knockout showed a relatively similar rate of oxygen evolution compared to wild type cultures (A). The rate of oxygen consumption in the dark in Cyt c_M knockout was significantly higher compared to wild type culture (B).

5.4 Chlorophyll fluorescence experiment

Chlorophyll fluorescence measurements were made for ΔCyt c_M and wild type strains with a PAM (section 2.12). Parameters used in this section are explained in section 2.3.2. A relatively higher Fv/Fm was observed in ΔCyt c_M compared to WT, but the ΦPSII, qP and qT of ΔCyt c_M were not significantly different from the wild type culture (figure 5.5). Interestingly, NPQ was significantly higher (more than 40%) in ΔCyt c_M compared to wild type (figure 5.5).

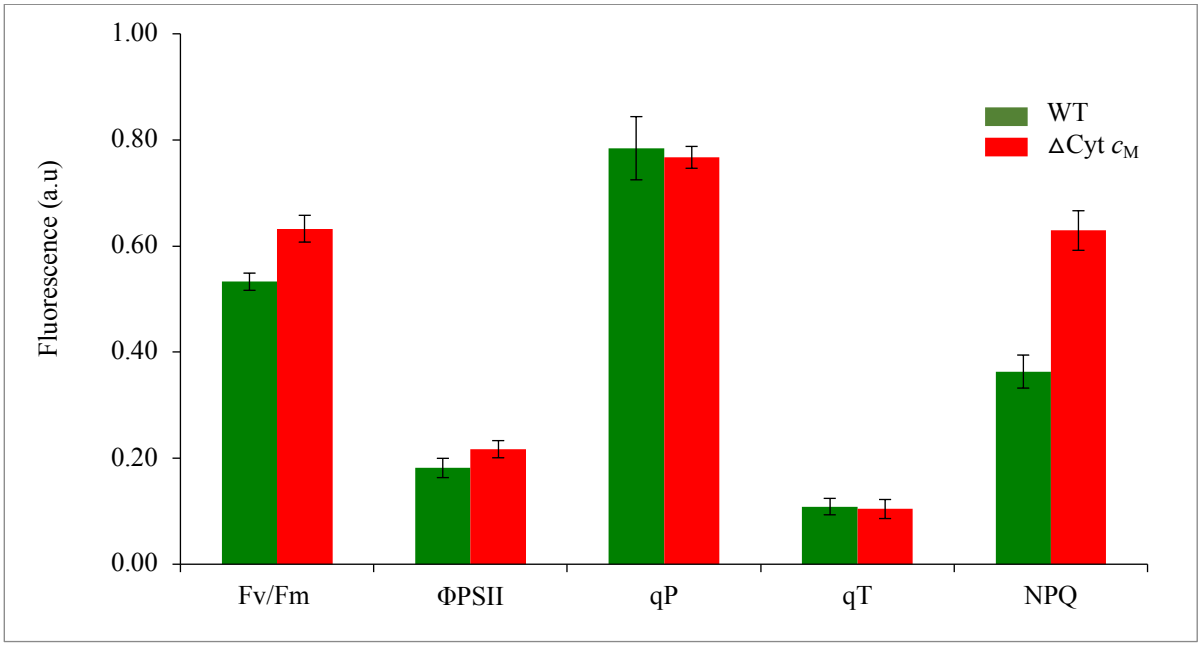

Figure 5.5: Chlorophyll fluorescence measurements of Cyt c_M knockout and WT. Measurements of maximum chlorophyll fluorescence yield in dark with DCMU (Fv/Fm), PSII quantum yield or efficiency of PSII (ΦPSII), photochemical quenching (qP), photochemical quenching associated with state transitions (qT) and non photochemical quenching (NPQ) were made from dark adapted Cyt c_M and wild type cultures. These data were generated in collaboration with Dr. Iskander Ibrahim in Professor John F Allen lab, Queen Mary University of London, UK.

5.4.1 P700 Reduction experiment

Similar to what was seen for the Cyt c_{6C} mutant, $P700^+$ dark reduction in the ΔCyt c_M mutant was also slow when compared to wild type ((section 4.4.3) (figure 5.6)).

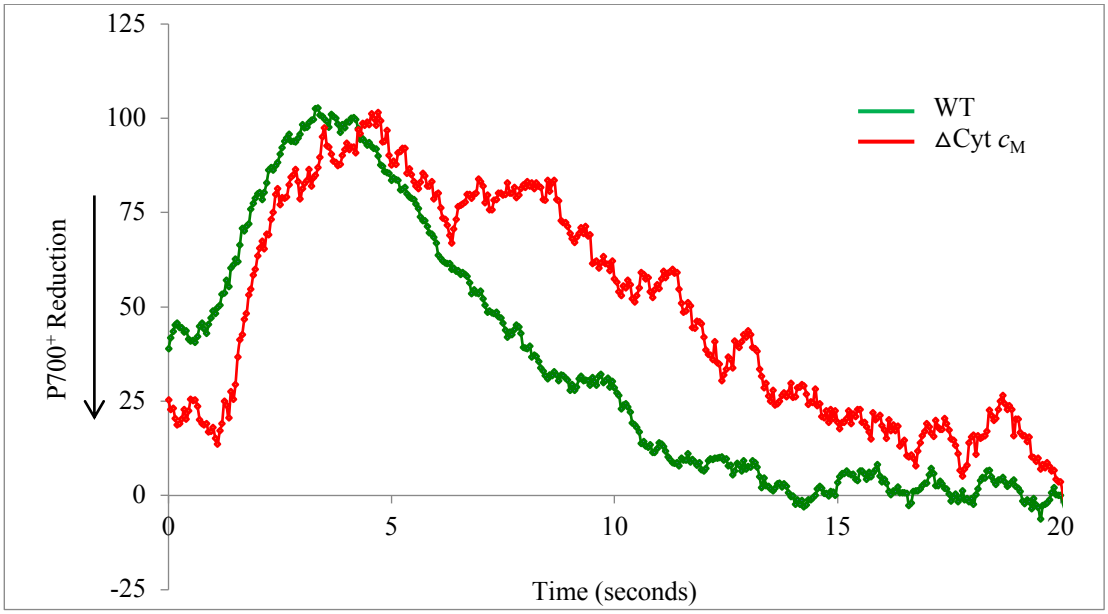

Figure 5.6: $P700^+$ reduction kinetics of ΔCyt c_M and WT: PSI reduction rate was slower in ΔCyt c_M than wild type. A value of 100% indicates complete oxidation of P700. Lower values indicate the amount remaining oxidized at a given time. Each data point represents at least four biological replicates. This data was generated in collaboration with Dr. Iskander Ibrahim in Professor John F Allen lab, Queen Mary University of London, UK.

5.5 Transcriptomic analysis of cyt c_M mutant

We demonstrated in the growth phenotype study that ΔCyt c_M showed impaired growth under LL, ML, HL and 300 $\mu Em^{-2}s^{-1}$ light intensities, and severe growth impairment at 700 $\mu Em^{-2}s^{-1}$ light intensity. Consistent with this, initial experiments using qRT-PCR showed that the relative transcript abundance of Cyt c_M increased at higher light intensities in wild type cultures (data not shown). We therefore went on to use RNA-Seq analysis.

In this section we used RNA-Seq to determine the global impact on the transcriptome of deleting the Cyt c_M gene (*cytM*) in *S. elongatus* PCC 7942. Such an investigation allows for global measurement of transcript abundance in ΔCyt c_M culture under certain physiological conditions and comparison with wild type. We used 6 samples (1 experiment containing 3 ΔCyt c_M biological replicates and 3 wild type controls) of the HL (150 $\mu Em^{-2}s^{-1}$ light intensity) and 6 samples (1 experiment containing 3 ΔCyt c_M biological replicates and 3 wild type controls) from 600 $\mu Em^{-2}s^{-1}$ light intensity. We observed no growth of ΔCyt c_M at 700 $\mu Em^{-2}s^{-1}$ light intensity, so we decide to grow the mutant at 600

$\mu Em^{-2}s^{-1}$ light intensity and perform the RNA-Seq analysis. The transcript levels of photosynthesis and related genes in a ΔCyt c_M culture were compared with those of wild type in the two different light intensities. We also compared the ΔCyt c_M and wild type 600 vs 150 $\mu Em^{-2}s^{-1}$ light intensity and the results are described.

5.5.1 RNA-Seq data quality

Total RNA of *S. elongatus* was extracted from 6 samples (3 ΔCyt c_M biological replicates and 3 wild type replicate controls) grown in 600 $\mu Em^{-2}s^{-1}$ light intensity and 3 samples (of ΔCyt c_M) grown in HL (150 $\mu Em^{-2}s^{-1}$). Data for three wild type samples grown at 150 $\mu Em^{-2}s^{-1}$ were available from the Cytc_{6C} experiments. The quality of the RNA was determined using Agilent Bioanalyzer. RIN numbers for samples grown at 150 $\mu Em^{-2}s^{-1}$ were 9.6, 9.6, 9.5 and for samples grown at 600 $\mu Em^{-2}s^{-1}$ were 9.4, 9.2, 9.1 (wild type) and 9.3, 9.0, 9.3 (ΔCyt c_M). The samples were used in TruSeq RNA library preparation, combined with a Bacterial Ribo-Zero Magnetic Kit. RNA with RIN above 6.0 is considered good enough for RNA-Seq analysis. RNA with RIN above 9.0 is the gold standard. The cDNA libraries were sequenced using a NextSeq500 machine with single-read mode.

A total of 243 million raw sequence reads (150 bp) were obtained from RNA-Seq transcriptomic analysis of the 9 samples, with an average number of 20.2 million reads per sample. The sequence quality of the reads was determined by the FastQC bioinformatics tool and the quality was extremely high. Filtering steps were not performed in sample preparation, sequencing and analyses to reduce any imposed bias. The alignment of reads, coverage calculation, gene wise read quantification and differential gene expression determination were performed with READemption using segemehl version X and DESeq version V. A total of 228 million reads aligned to the *S. elongatus* genome, with an average number of 19.0 million aligned reads per sample, representing an average of 1040 times coverage of the genome in each sample.

5.5.2 Transcript levels for PSII genes in ΔCyt c_M cultures under different light intensities.

RNA-Seq analysis revealed that knocking out of Cyt c_M significantly altered the transcript levels of several PSII components or related proteins under 150 $\mu E\ m^{-2}s^{-1}$ light intensity compared to wild type. Upregulated transcript levels for *psbA2, psbA3, psbC, psbD*1,

*psbD*2*, psbN, psbO, psb*29*, psb*30*, ftsH*1, and *ftsH*2, and significantly down regulated transcript levels for *psbE, psbF, psbH, psbI, psbJ, psbK, psbL, psbM, psbP, psbT, psbU, psbV, psbW, psbX, psbY, psbZ, psb*27*, psb*28*, ftsH*3*, ftsH*4 were seen in the mutant compared to wild type. Under 600 μE $m^{-2}s^{-1}$ light, all the PSII components were down regulated compared to wild type, apart from *psbA*1*, psbA*2*, psbA*3 and *psb*28, which were upregulated but not significantly. Significantly down regulated transcript levels compared to the wild type were seen for *psbE, psbF, psbH, psbJ, psbL, psbP, psbQ, psbT, psbU, psbV, psbX, psbY, psbZ, psb*27*, psb*29*, ftsH*3 and *ftsH*4 (figure 5.7 and Appendix table 5.1).

When the ΔCyt c_M culture was grown at 600 $\mu Em^{-2}s^{-1}$ light, down regulation of most of the transcripts of PSII components compared to the culture grown at 150 $\mu Em^{-2}s^{-1}$ light was observed, although a few components were upregulated but none of them significantly. The significantly down regulated transcript levels compared to ΔCyt c_M 150 $\mu Em^{-2}s^{-1}$ light were for *psbA*1*, psbA*2*, psbA*3. For the wild type culture grown at 600 $\mu Em^{-2}s^{-1}$ light, significantly elevated transcript levels compared to 150 $\mu Em^{-2}s^{-1}$ light were seen for *psbA*2*, psbC, psbD*1*, psbD*2*, psbN, psb*29*, psb*30*, psb*27*, ftsH*1 and *ftsH*2. In addition, *psbO, psbP, psbW* and *ftsH*3 were present at elevated levels but not statistically significantly so. Significantly down regulated transcript levels compared to wild type 150 $\mu Em^{-2}s^{-1}$ light were observed for *psbA*1*, psbE, psbF, psbH, psbI, psbJ, psbK, psbL, psbM, psbQ, psbT, psbV, psbW, psbY, psbZ,* and *psb*28. Down regulation was also seen for *psbA*3*, psbU,* and *FtsH*4*,* but was not significant. Assuming the protein levels reflect transcript levels, these data may indicate the presence of less PSII in in the ΔCyt c_M mutant compared to the wild type at 600 $\mu Em^{-2}s^{-1}$ light and less PSII in mutant on elevation from 150 to 600 $\mu Em^{-2}s^{-1}$ light (figure 5.7 and Appendix table 5.1).

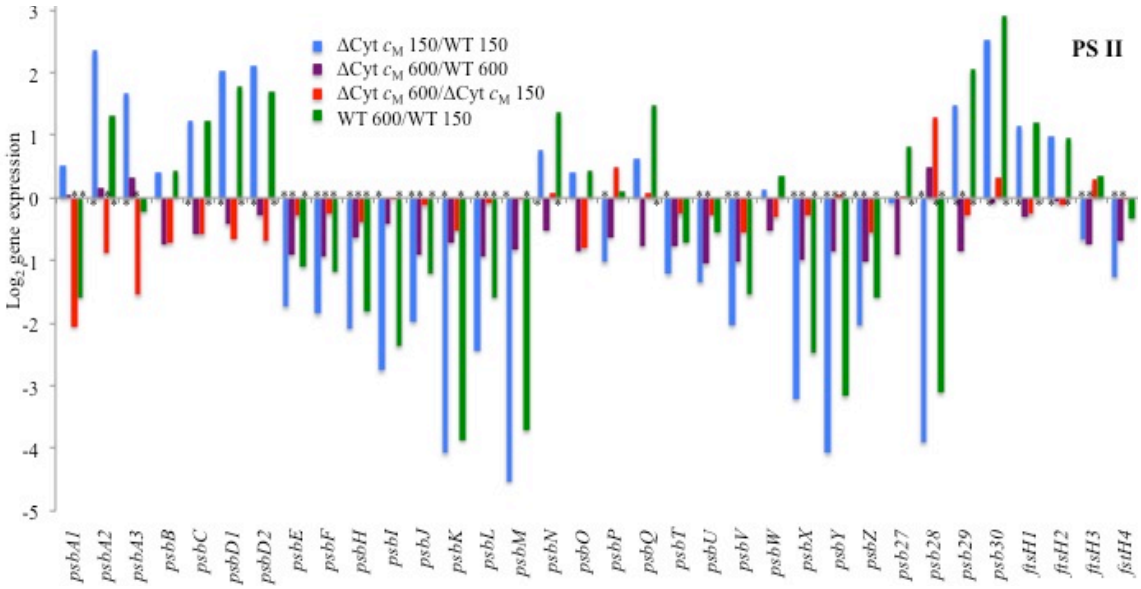

Figure 5.7: Comparative PSII transcript expression levels in ΔCyt c_M and wild type under 150 and 600 $\mu Em^{-2}s^{-1}$ light intensities. Asterisks indicate significant differences in transcript abundance between ΔCyt c_M 150/WT 150, ΔCyt c_M 600/WT, ΔCyt c_M 600/ ΔCyt c_M 150 and WT 600/WT 150 $\mu Em^{-2}s^{-1}$ light intensity ($p < 0.05$). Changes in transcript abundance are given in log_2 values in y-axis.

5.5.3 Transcript levels for PSI genes in ΔCyt c_M cultures under different light intensities.

RNA-Seq analysis demonstrated that knocking out Cyt c_M resulted in down regulation of transcript levels for PSI components compared to wild type cells under 150 $\mu Em^{-2}s^{-1}$ light, although transcript levels for *psaK*1, *bptA*, and *ycf*4 were elevated in the mutant. At 600 $\mu Em^{-2}s^{-1}$ light, interestingly, all the PSI component transcript levels were down regulated compared to wild type.

When the mutant was grown at 600 $\mu Em^{-2}s^{-1}$ light, down regulation of transcript levels was seen for all the PSI components compared to the culture grown at 150 $\mu Em^{-2}s^{-1}$ light, although the transcript level for *ycf*4 was elevated but not significantly. For the wild type culture grown at 600 $\mu Em^{-2}s^{-1}$ light, transcript levels for *psaC, psaF*, and *psaK*2, were elevated but not significantly and transcript levels for *psaK*1*, bptA* and *ycf*4 were significantly elevated compared to culture grown at 150 $\mu Em^{-2}s^{-1}$ light. Assuming that the protein levels reflect transcript levels, these data may indicate the presence of less PSI in the ΔCyt c_M culture compared to wild type at 600 $\mu Em^{-2}s^{-1}$ light, and similarly less in the

mutant at 600 μEm^{-2}s^{-1} light compared to 150 μEm^{-2}s^{-1} light. In summary, lower levels of PSI were seen in the mutant at 150 μEm^{-2}s^{-1} light compared to wild type and lower levels in wild type at 600 μEm^{-2}s^{-1} light compared to grown at 150 μEm^{-2}s^{-1} light (figure 5.8 and Appendix table 5.1).

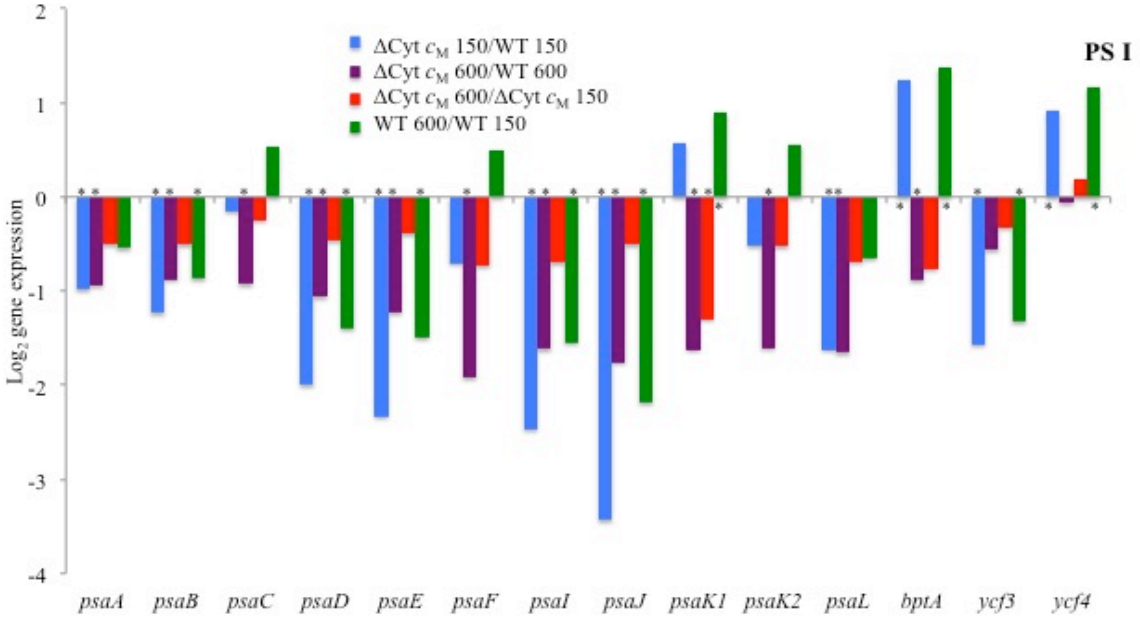

Figure 5.8: Comparative PSI transcript expression levels in ΔCyt c_M and wild type under 150 and 600 μEm^{-2}s^{-1} light intensities. Asterisks indicated significant differences in transcript abundance between ΔCyt c_M 150/WT 150, ΔCyt c_M 600/WT 600, ΔCyt c_M 600/ ΔCyt c_M 150 and WT 600/WT 150 μEm^{-2}s^{-1} light intensity ($p < 0.05$). Changes in transcript abundance are given in $\log_2$ values in y-axis.

5.5.4 Transcript levels for Cyt *b*$_6$*f* genes in ΔCyt c_M cultures under different light intensities.

RNA-Seq analysis demonstrated that in the ΔCyt c_M culture under 150 μEm^{-2}s^{-1} light elevated levels of transcript for Cyt *b*$_6$*f* complex components *petA, petB, petC,* and *petN* were observed compared to wild type, although significant upregulation was seen only for *petB*, and *petC*. At 600 μEm^{-2}s^{-1} light, down regulation of all Cyt *b*$_6$*f* transcripts was observed compared to the wild type culture (figure 5.9 and Appendix table 5.1).

When the mutant culture was grown at 600 μEm^{-2}s^{-1} light, down regulation of all the Cyt *b*$_6$*f* transcripts was seen compared to the culture grown at 150 μEm^{-2}s^{-1} light. For the wild

type grown at 600 μEm^{-2}s^{-1} light, transcript levels for *petA, petB, petC* and *petN* were elevated, and those for *petD, petG, petL, petM* and *petN* were lower compared to the culture grown at 150 μEm^{-2}s^{-1} light. The changes in levels of *petA*, *petD*, *petL*, and *petN* transcripts were not statistically significant (figure 5.9 and table 5.1). Assuming that the protein levels reflect the transcript levels, these data may indicate the presence of less Cyt b_6f complex in the ΔCyt c_M at 600 μEm^{-2}s^{-1} light compared to the wild type, and less Cyt b_6f in ΔCyt c_M at 600 μEm^{-2}s^{-1} light compared to 150 μEm^{-2}s^{-1} light.

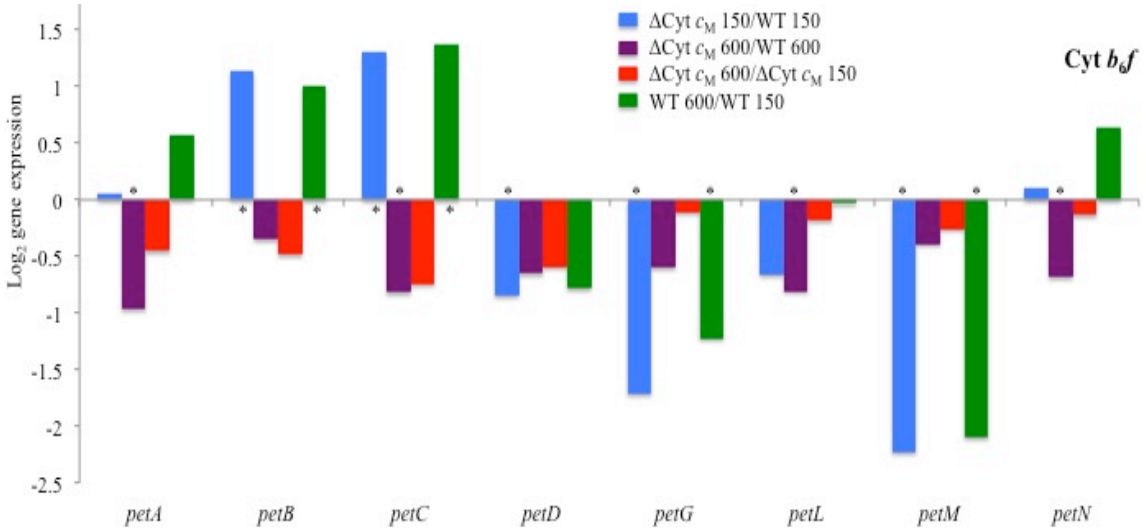

Figure 5.9: Comparative Cyt b_6f complex transcript expression levels in ΔCyt c_M and wild type under 150 and 600 μEm^{-2}s^{-1} light intensities. Asterisks indicated significant differences in transcript abundance between ΔCyt c_M 150/WT 150, ΔCyt c_M 600/ WT 600, ΔCyt c_M 600/ ΔCyt c_M 150 and WT 600/ WT 150 μEm^{-2}s^{-1} light intensity ($p < 0.05$). Changes in transcript abundance are given in $\log_2$ values in y-axis.

5.5.5 Transcript levels for ATP synthase genes in ΔCyt c_M cultures under different light intensities.

RNA-Seq analysis demonstrated that in the ΔCyt c_M culture under 150 μEm^{-2}s^{-1} light, transcript levels for *atpC/E, atpD, atpF, atpG* and *atpH* were elevated compared to wild type, although transcript levels for *atpA* and *atpB* were lower but not significantly so. At 600 μEm^{-2}s^{-1} light, the component transcript levels were all down regulated compared to wild type.

When the mutant culture was grown at 600 $\mu Em^{-2}s^{-1}$ light, down regulation of all the transcript levels of ATP synthase was observed compared to the cells grown at 150 $\mu Em^{-2}s^{-1}$ light. For the wild type culture grown at 600 $\mu Em^{-2}s^{-1}$ light transcript levels of ATP synthase components were all up regulated compared to cells grown at 150 $\mu Em^{-2}s^{-1}$ light. Assuming the protein levels reflect transcript levels, these data may indicate the presence of more ATP synthase in the ΔCyt c_M culture compared to the wild type at 150 $\mu Em^{-2}s^{-1}$ but statistically significantly lower levels of ATP synthase in the ΔCyt c_M culture compared to wild type at 600 $\mu Em^{-2}s^{-1}$ light. The wild type showed a significant increase in ATP synthase levels at 600 $\mu Em^{-2}s^{-1}$ compared to 150 $\mu Em^{-2}s^{-1}$, and this increase was not seen in the mutant (figure 5.10 and Appendix table 5.1).

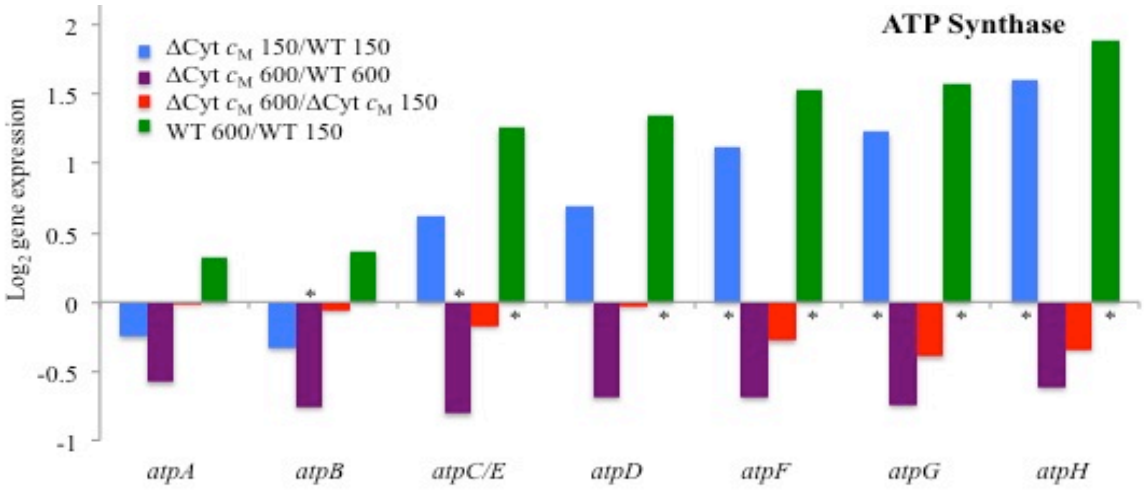

Figure 5.10: Comparative ATP synthase transcript expression levels in ΔCyt c_M and wild type under 150 and 600 $\mu Em^{-2}s^{-1}$ light intensities. Asterisks indicated significant differences in transcript abundance between ΔCyt c_M 150/WT 150, ΔCyt c_M 600/WT 600, ΔCyt c_M 600/ ΔCyt c_M 150 and WT 600/WT 150 $\mu Em^{-2}s^{-1}$ light intensity ($p < 0.05$). Changes in transcript abundance are given in fold change in text and log_2 values in y-axis.

5.5.6 Transcript levels for phycobilisome genes in ΔCyt c_M cultures under different light intensities.

RNA-Seq analysis demonstrated that in the ΔCyt c_M culture under 150 $\mu Em^{-2}s^{-1}$ light, the allophycocyanin component transcript levels for *apcA, apcB1/apcF* and *apcD* were elevated but not significantly, and *apcB* was significantly down regulated compared to

wild type. Phycocyanin polypeptide transcripts (*cpcA1, A2, B1, B2*) were uniformly down regulated in ΔCyt c_M strain compared to wild type, although the phycobilisome linker protein transcripts *cpcE* and *cpcF* were elevated, but not significantly. Transcripts for phycobilisome rod core linker polypeptide (*cpcG*), phycobilisome rod linker polypeptide (*cpcH*), phycobilisome linker polypeptide 9K (*cpcl1* and *cpcl2/cpcD*) were down regulated compared to wild type. At 600 $\mu Em^{-2}s^{-1}$ light, allophycocyanin, phycocyanin and the linker proteins transcript levels were all down regulated compared to wild type (figure 5.11 and Appendix table 5.1).

When the mutant culture was grown at 600 $\mu Em^{-2}s^{-1}$ light, consistent down regulation of the transcripts for allophycocyanin, phycocyanin and phycobilisome linker was observed compared to the mutant culture grown at 150 $\mu Em^{-2}s^{-1}$ light. For the wild type culture grown at 600 $\mu Em^{-2}s^{-1}$ light, transcript levels for allophycocyanin subunits *apcA, apcB/apcF* were upregulated, *apcB* and *apcD* were down regulated, transcripts for phycocyanin were all down regulated, phycobilisome linker protein transcript levels for *cpcE* and *cpcF* were elevated and *cpcG, cpcH, cpcl1,* and *cpcl2/cpD* were down regulated compared to 150 $\mu Em^{-2}s^{-1}$ light. Assuming the protein levels reflect transcript levels, these data may indicate the presence of less allophycocyanin, phycocyanin and phycobilisome linker proteins in the mutant compared to the wild type at 600 $\mu Em^{-2}s^{-1}$ light.

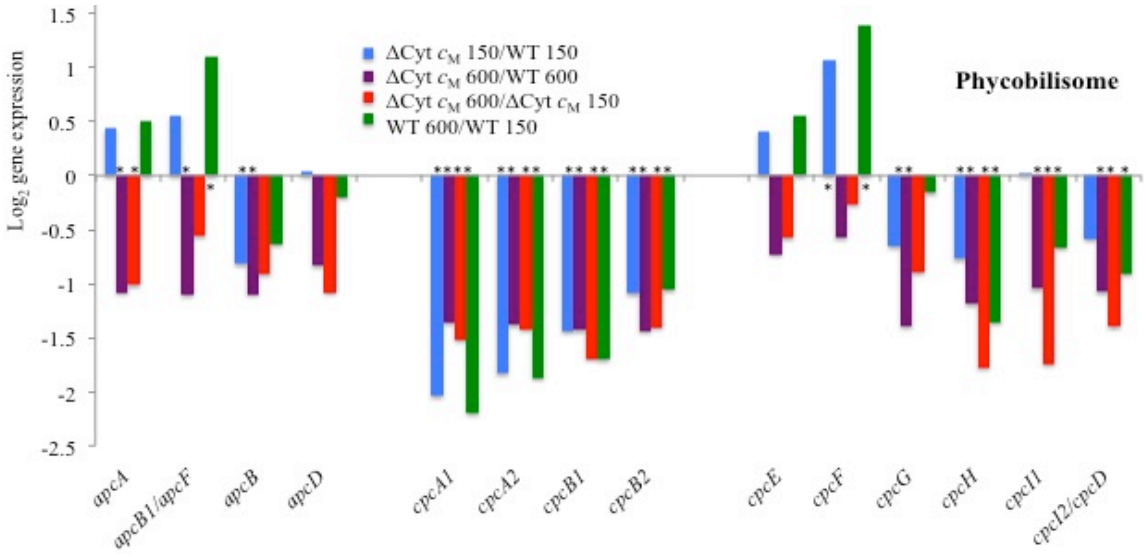

Figure 5.11 Comparative phycobilisome protein complex transcript expression levels in ΔCyt c_M and wild type under 150 and 600 $\mu Em^{-2}s^{-1}$ light intensities. Asterisks indicated significant differences in transcript abundance between ΔCyt c_M 150/WT 150, ΔCyt c_M 600/WT 600, ΔCyt c_M 600/ ΔCyt c_M 150 and WT 600/WT 150 $\mu Em^{-2}s^{-1}$ light intensity ($p < 0.05$). Changes in transcript abundance are given in fold change in text and log_2 values in y-axis.

5.5.7 Transcript levels for high light inducible proteins in ΔCyt c_M cultures under different light intensities.

RNA-Seq analysis demonstrated that in the ΔCyt c_M culture under 150 $\mu Em^{-2}s^{-1}$ light intensity, there were elevated transcript levels for *nblA*1*, nblB, hliP*1 and *isiA* and lower levels of the transcripts for *nblB2, hliA, hliC* and *hliP*2 compared to the wild type. At 600 $\mu Em^{-2}s^{-1}$ light, down regulation of the transcript levels was seen for *nblA*1*, nblB, nblB2,* and *hliP*2 and upregulation of transcript levels was seen for *hliA, hliP*1, and *isiA* compared to wild type. However, these changes were not statistically significant (figure 5.12 and Appendix table 5.1).

When the mutant culture was grown at 600 $\mu Em^{-2}s^{-1}$ light, elevated transcript levels were seen for *nblA*1*, hliA, hliC, hliP*2 and *isiA* compared to the culture grown at 150 $\mu Em^{-2}s^{-1}$ light intensity. For the wild type culture grown at 600 $\mu Em^{-2}s^{-1}$ light, elevated transcript levels for *nblA*1*, nblB, hliC, hliP*1 and *isiA* and lower levels of the transcripts for *nblB2, hliA,* and *hliP*2 were seen compared to culture grown at 150 $\mu Em^{-2}s^{-1}$ light intensity. Assuming the protein levels reflect transcript levels, these data may indicate the presence of elevated levels of phycobilisome degradation protein (*nblA*1) and iron stress induced chlorophyll-containing protein CP43' (encoded by *isiA*) at 600 $\mu Em^{-2}s^{-1}$ light in mutant and wild type culture.

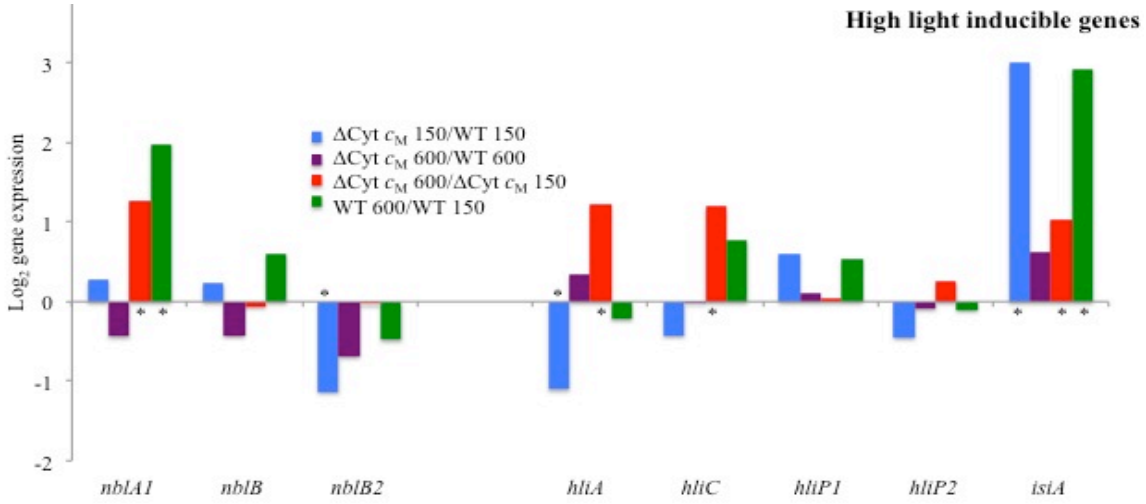

Figure 5.12: Comparative high light inducible protein complex transcript expression levels in ΔCyt c_M and wild type under 150 and 600 $\mu Em^{-2}s^{-1}$ light intensities. Asterisks indicated significant differences in transcript abundance between ΔCyt c_M 150/WT 150, ΔCyt c_M 600/WT 600, ΔCyt c_M 600/ ΔCyt c_M 150 and WT 600/WT 150 $\mu Em^{-2}s^{-1}$ light intensity ($p < 0.05$). Changes in transcript abundance are given in fold change in text and log_2 values in y-axis.

5.5.8 Transcript levels for soluble electron carriers in ΔCyt c_M culture under different light intensities.

RNA-Seq analysis demonstrated that in the ΔCyt c_M culture under 150 $\mu Em^{-2}s^{-1}$ light, elevated transcript levels were seen for *petE, petJ1, petJ1iso* and *petJ2* compared to wild type. At 600 $\mu Em^{-2}s^{-1}$ light, down regulation of the transcripts for *petE, petJ1*and *petJ1iso* and upregulation of the transcript for *petJ2* was seen compared to the wild type although the last was not statistically significant (figure 5.13 and Appendix table 5.1).

When the mutant culture was grown at 600 $\mu Em^{-2}s^{-1}$ light, down regulation of the transcripts for *petE*, *petJ1* and *petJ1iso* and upregulation of the transcripts for *petJ2* was seen compared to culture grown at 150 $\mu Em^{-2}s^{-1}$ light. For the wild type culture grown at 600 $\mu Em^{-2}s^{-1}$ light, elevated transcript levels for *petE, petJ1, petJ1iso, petJ2* and *cytM* were seen compared to growth at 150 $\mu Em^{-2}s^{-1}$ light intensity. Assuming the protein levels reflect transcript levels, these data may indicate the presence of more Cyt c_6, Cyt c_6 isoform and Cyt c_{6C} in ΔCyt c_M culture compared to the wild type at 150 $\mu Em^{-2}s^{-1}$ light intensity and presence of more Pc, Cyt c_6, Cyt c_6 isoform and Cyt c_{6C} in wild type at 600

$\mu Em^{-2}s^{-1}$ light intensity compared to the wild type culture grown at 150 $\mu Em^{-2}s^{-1}$ light intensity. (figure 5.13 and Appendix table 5.1).

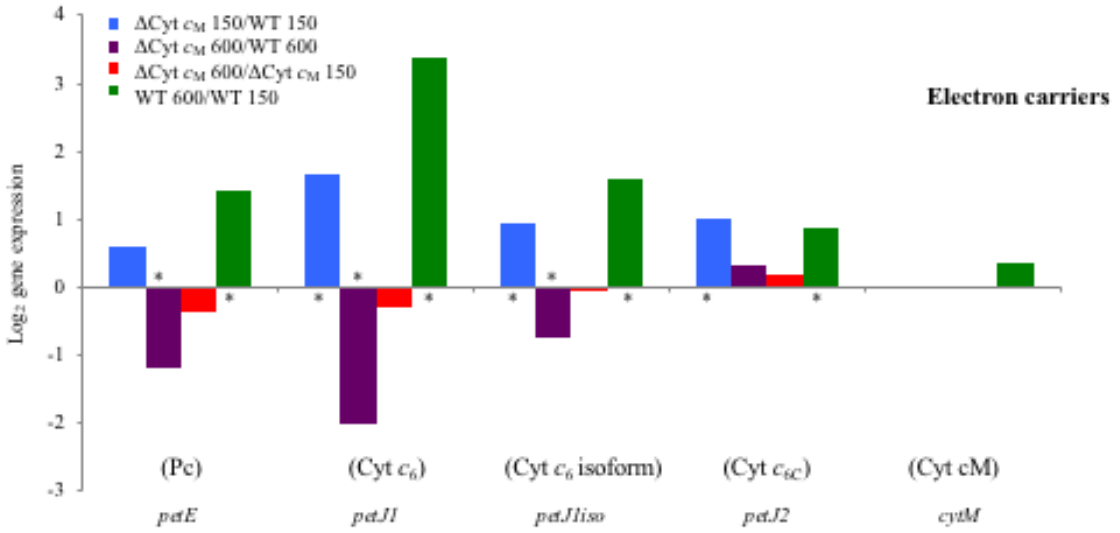

Figure 5.13: Comparative lumina redox carriers transcript expression levels in ΔCyt c_M and wild type under 150 and 600 $\mu Em^{-2}s^{-1}$ light intensities. Asterisks indicated significant differences in transcript abundance between ΔCyt c_M 150/WT 150, ΔCyt c_M 600/WT 600, ΔCyt c_M 600/ ΔCyt c_M 150 and WT 600/WT 150 $\mu Em^{-2}s^{-1}$ light intensity ($p < 0.05$). Changes in transcript abundance are given in fold change in text and log_2 values in y-axis.

5.5.9 Transcript levels for terminal oxidase, Ndb and Sdh complexes in ΔCyt c_M culture under different light intensities.

RNA-Seq analysis demonstrated that, in the ΔCyt c_M culture under 150 $\mu Em^{-2}s^{-1}$ light, elevated transcript levels for Cyt *bd* quinol oxidase subunit CydA were seen compared to wild type, although the subunit CydB transcript was down regulated but not significantly so. Interestingly, consistent down regulation of the transcripts for Cyt *c* oxidase (*ctaA, cox, ctaC* and *ctaE*) was seen compared to wild type. Type 2 NADH dehydrogenase showed elevated transcript levels for *ndbB,* and *ndbC* compared to wild type, although *ndhA* was down regulated but not significantly. Succinate dehydrogenase showed elevated transcript levels for *sdhA* compared to wild type, although significant down regulation of the transcript for *sdhB* was also seen. At 600 $\mu Em^{-2}s^{-1}$ light, elevated transcript levels were seen for Cyt *bd* quinol oxidase (not significant) and Cyt *c* oxidase subunits in the mutant compared to wild type. The type 2 NDH dehydrogenase transcript level for *ndhA* was

down regulated, whereas transcript levels for *ndhB* and *ndhC* were not regulated statistically significantly. Succinate dehydrogenase transcript levels were also down regulated but not statistically significantly (figure 5.14 and Appendix table 5.1).

When the mutant culture was grown at 600 $\mu Em^{-2}s^{-1}$ light, elevated transcript levels were seen for Cyt *bd* quinol oxidase, Cyt *c* oxidase and type 2 NADH dehydrogenase compared to the culture grown at 150 $\mu Em^{-2}s^{-1}$ light. Interestingly succinate dehydrogenase transcript levels were not significantly regulated. For the wild type grown at 600 $\mu Em^{-2}s^{-1}$ light elevated transcript levels for Cyt *bd* quinol oxidase subunit *CydA*, were seen compared to wild type grown at 150 $\mu Em^{-2}s^{-1}$ light. However, the *cydB* transcript was down regulated but not significantly. Interestingly consistent down regulation of the transcripts for Cyt *c* oxidase (*ctaA, cox, ctaC* and *ctaE*) was seen for the wild type at grown at 600 $\mu Em^{-2}s^{-1}$ light compared to 150 $\mu Em^{-2}s^{-1}$ light, whereas type 2 NADH dehydrogenase showed elevated transcript levels compared to wild type grown at 150 $\mu Em^{-2}s^{-1}$ light. Succinate dehydrogenase showed elevated transcript levels for *sdhA* in wild type cells grown at 600 $\mu Em^{-2}s^{-1}$ light, however significant down regulation of the transcript for *sdhB* was also seen compared to growth at 150 $\mu Em^{-2}s^{-1}$ light intensity. Assuming the protein levels reflect transcript levels, these data may indicate the presence of less Cyt *c* oxidase in the mutant compared to wild type at 150 $\mu Em^{-2}s^{-1}$ light, but more in the mutant at 600 $\mu Em^{-2}s^{-1}$ light compared to the mutant at 150 $\mu Em^{-2}s^{-1}$ light and also compared to the wild type at 600 $\mu Em^{-2}s^{-1}$ (figure 5.14 and Appendix table 5.1).

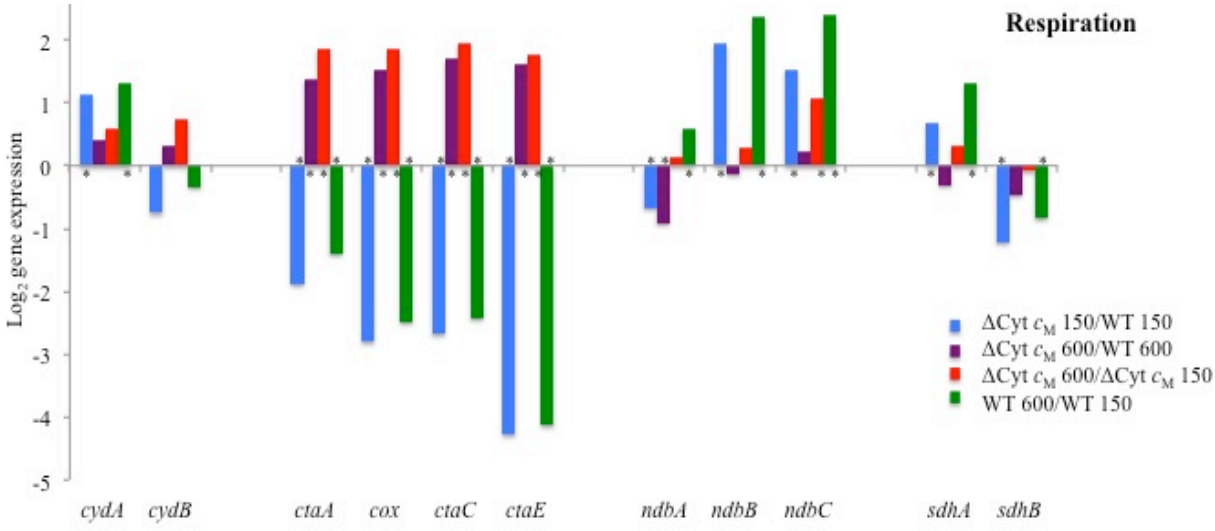

Figure 5.14: Comparative terminal oxidase, Ndb and Sdh transcript expression levels in ΔCyt c_M and wild type under 150 and 600 $\mu Em^{-2}s^{-1}$ light intensities. Asterisks indicated significant differences in transcript abundance between ΔCyt c_M 150/WT 150, ΔCyt c_M 600/WT 600, ΔCyt c_M 600/ ΔCyt c_M 150 and WT 600/WT 150 $\mu Em^{-2}s^{-1}$ light intensity ($p < 0.05$). Changes in transcript abundance are given in fold change in text and log_2 values in y-axis.

5.5.10 Transcript levels for type 1 NAD(P)H dehydrogenase subunits in ΔCyt c_M cultures under different light intensities

RNA-Seq analysis demonstrated that, in ΔCyt c_M culture under 150 $\mu Em^{-2}s^{-1}$ light, significantly elevated transcript levels for *ndhA, ndhC, ndhD2, ndhD3, ndhF1, ndhF3, ndhF4, ndhH, ndhI, ndhJ, ndhK* and *ndhL* were seen, and significantly lower transcript levels for *ndhD5* and *ndhE* were seen compared to the wild type. At 600 $\mu Em^{-2}s^{-1}$ light, only a few genes were significantly regulated compared to wild type. A significantly elevated transcript level for *ndhD5* was seen and a significantly lower transcript level for *ndhD2* was seen compared to the wild type (figure 5.15 and Appendix table 5.1).

When the mutant culture was grown at 600 $\mu Em^{-2}s^{-1}$ light, significantly elevated transcript levels for *ndhA, ndhC, ndhD2, ndhD5, ndhE, ndhG, ndhH, ndhI,* and *ndhJ* were seen compared to the culture grown at 150 $\mu Em^{-2}s^{-1}$ light. For the wild type culture grown at 600 $\mu Em^{-2}s^{-1}$ light, significantly elevated transcript levels for *ndhA, ndhB, ndhC, ndhD*2*, ndhD*3*, ndhF*1*, ndhF*3*, ndhF*4*, ndhG, ndhH, ndhI,* and *ndhJ ndhK, ndhL, ndhM* and *cupA* were seen and lower transcript levels for *ndhD*, and *ndhD5* were seen compared to the culture grown at 150 $\mu Em^{-2}s^{-1}$ light. Assuming the protein levels reflect transcript levels, these data may indicate the presence of high levels of type 2 NADH dehydrogenase in the mutant compared to the wild type at 150 $\mu Em^{-2}s^{-1}$ light intensity (figure 5.15 and Appendix table 5.1).

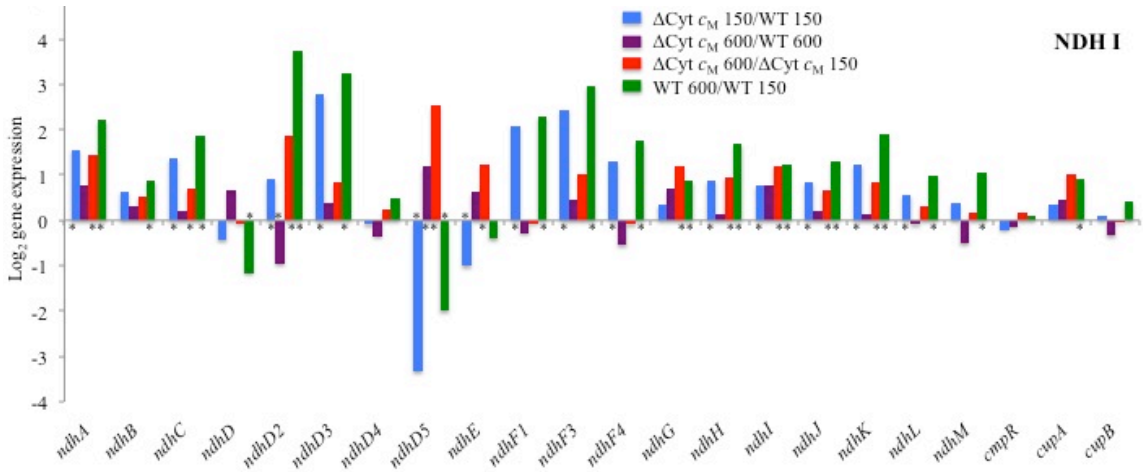

Figure 5.15: Comparative type 1 NAD(P)H dehydrogenase transcript expression levels in ΔCyt c_M and wild type under 150 and 600 $\mu Em^{-2}s^{-1}$ light intensities. Asterisks indicated significant differences in transcript abundance between ΔCyt c_M 150/WT 150, ΔCyt c_M 600/WT 600, ΔCyt c_M 600/ ΔCyt c_M 150 and WT 600/WT 150 $\mu Em^{-2}s^{-1}$ light intensity ($p < 0.05$). Changes in transcript abundance are given in fold change in text and log_2 values in y-axis.

5.5.11 Overview of transcript changes

MapMan analysis (figure 5.16) of the RNA-Seq data demonstrated that loss of the *cytM* gene encoding Cyt c_M protein in *S. elongatus* significantly altered the transcript levels of PSII, PSI, Cyt b_6f complex, ATP synthase, phycobilisomes, high light inducible proteins, and the respiratory proteins Cyt *bd* quinol oxidase, Cyt *c* oxidase, type 1&2 NAD(P)H dehydrogenase and succinate dehydrogenase genes under 150 $\mu Em^{-2}s^{-1}$ light intensity compared to wild type. Assuming the protein levels reflect transcript levels, these data may indicate the presence of similar PSII, Cyt b_6f complex, less PSI, more ATP synthase, less PBS proteins, more Cyt *bd* quinol oxidase, less Cyt *c* oxidase, more type II NDH dehydrogenase, and more type I NDH dehydrogenase in the mutant compared to the wild type at 150 $\mu Em^{-2}s^{-1}$ light intensity

Assuming the protein levels reflect transcript levels, at 600 $\mu Em^{-2}s^{-1}$ light intensity, transcript data may indicate the presence of less PSII, PSI, Cyt b_6f complex, ATP synthase, phycobilisome proteins and more Cyt *c* oxidase in the mutant compared to the wild type. When the mutant culture was grown at 600 $\mu Em^{-2}s^{-1}$ light intensity, the presence of less PSII, PSI, Cyt b_6f complex, a similar amount of ATP synthase, less phycobilisome

proteins, similar amounts of high light inducible proteins, more Cyt *c* oxidase, and more type 2 NDH dehydrogenase were seen compared to the culture grown at 150 $\mu Em^{-2}s^{-1}$ light intensity. For the wild type culture grown at 600 $\mu Em^{-2}s^{-1}$ light intensity, moderately similar levels of PSII, moderately high levels of some subunits of Cyt b_6f complex, and moderately less PSI, more ATP synthase, more allophycocyanin but less phycocyanin, more phycobilisome degradation protein, iron stress induced PSI protection protein IsiA, more Cyt *bd* quinol oxidase, less Cyt *c* oxidase, more type 1 NDH dehydrogenase and more type 2 NDH dehydrogenase were seen compared to the wild type culture grown at 150 $\mu Em^{-2}s^{-1}$ light intensity.

Knocking out of Cyt c_M significantly influenced the regulations of the lumenal redox carriers in *S. elongatus*. The data may indicate the presence of more Cyt c_6, Cyt c_6 isoform and Cyt c_{6C} in the mutant compared to the wild type at 150 $\mu Em^{-2}s^{-1}$ light intensity. At 600 $\mu Em^{-2}s^{-1}$ light intensity, there was less Pc, Cyt c_6, Cyt c_6 isoform in the mutant compared to the wild type. When the mutant culture was grown at 600 $\mu Em^{-2}s^{-1}$ light intensity, redox carriers expression levels were unchanged compared to the mutant culture grown at 150 $\mu Em^{-2}s^{-1}$ light intensity. For the wild type culture grown at 600 $\mu Em^{-2}s^{-1}$ light intensity, there was more Pc, Cyt c_6, Cyt c_6 isoform, Cyt c_{6C} compared to the wild type culture grown at 150 $\mu Em^{-2}s^{-1}$ light intensity.

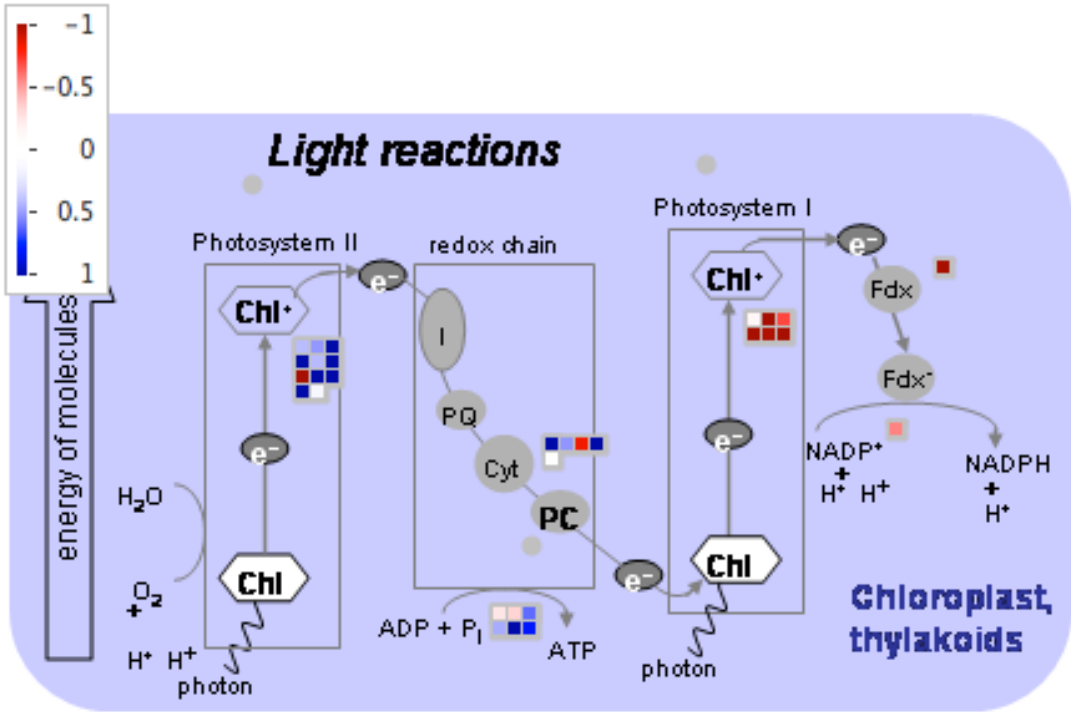
-1
-0.5
0
0.5
1
energy of molecules
Light reactions
Photosystem II
redox chain
Photosystem I
Chl*
Chl
e⁻
I
PQ
Cyt
PC
Fdx
Fdx⁻
H₂O
O₂
H⁺ H⁺
photon
ADP + Pi
ATP
NADP⁺ + H⁺ H⁺
NADPH + H⁺
Chloroplast, thylakoids

A

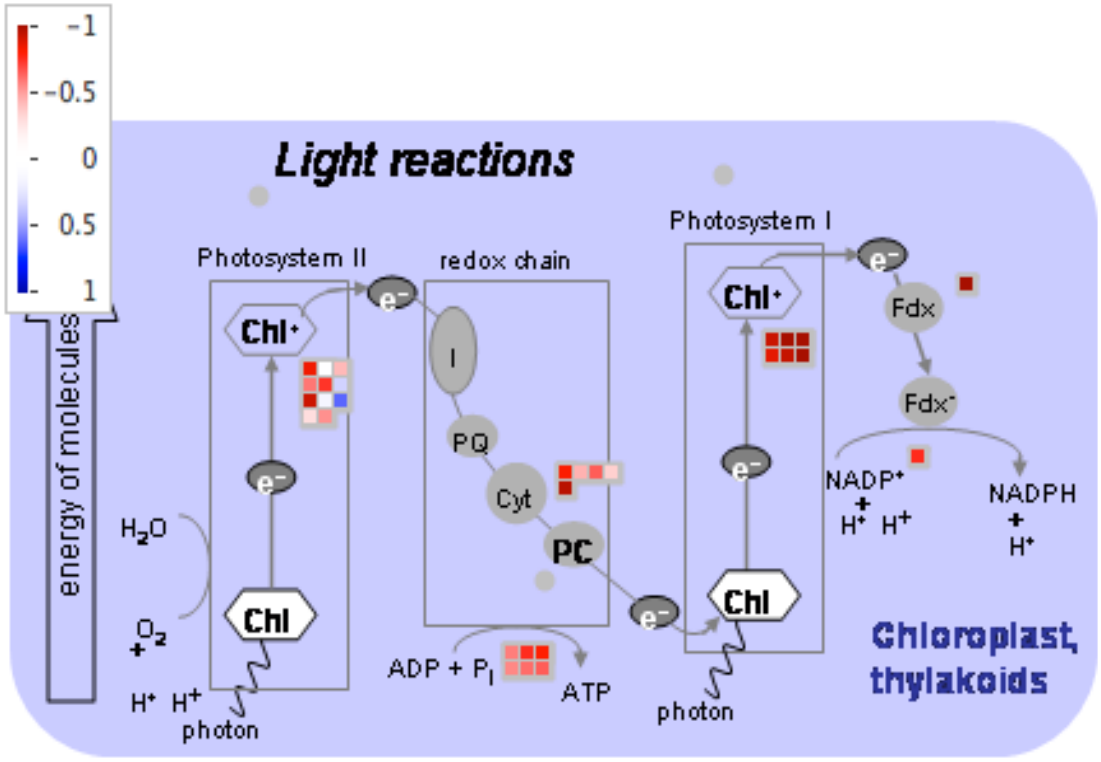
-1
-0.5
0
0.5
1
energy of molecules
Light reactions
Photosystem II
redox chain
Photosystem I
Chl*
Chl
e⁻
I
PQ
Cyt
PC
Fdx
Fdx⁻
H₂O
O₂
H⁺ H⁺
photon
ADP + Pi
ATP
NADP⁺ + H⁺ H⁺
NADPH + H⁺
Chloroplast, thylakoids

B

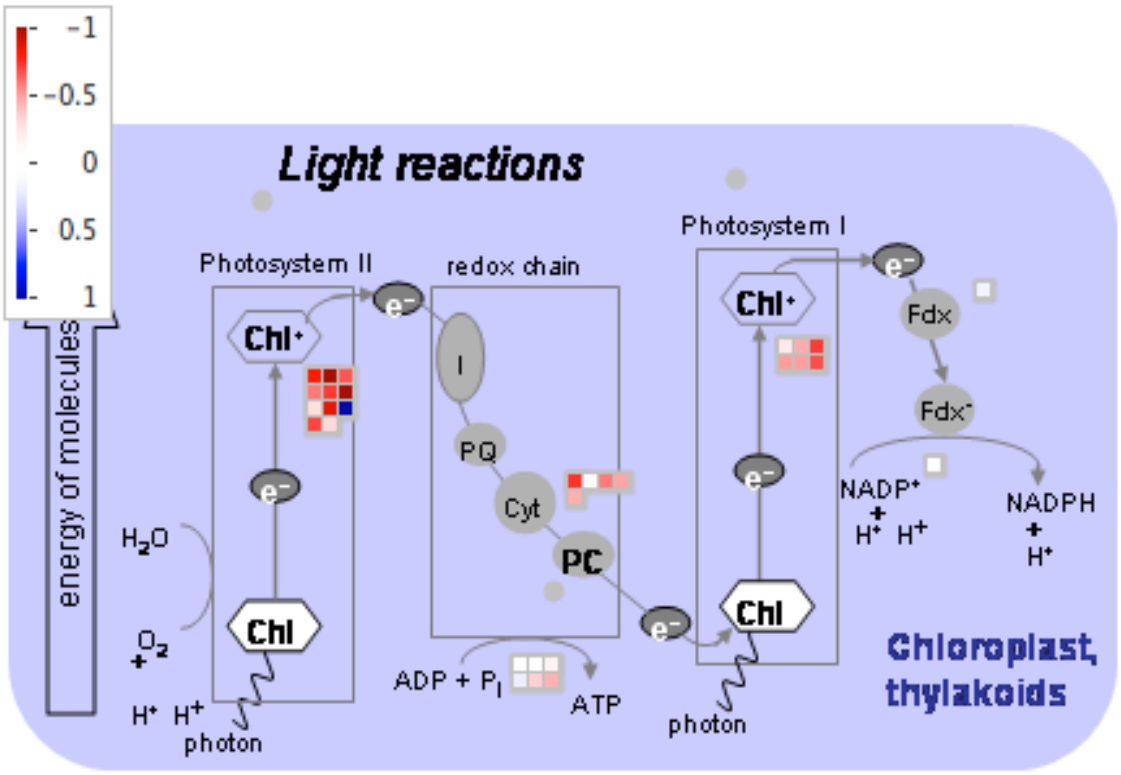
-1
-0.5
0
0.5
1
energy of molecules
Light reactions
Photosystem II
redox chain
Photosystem I
Chl*
Chl
e⁻
I
PQ
Cyt
PC
Fdx
Fdx⁻
H2O
O2
H+ H+
photon
ADP + PI
ATP
NADP+ + H+ H+
NADPH + H+
Chloroplast, thylakoids

C

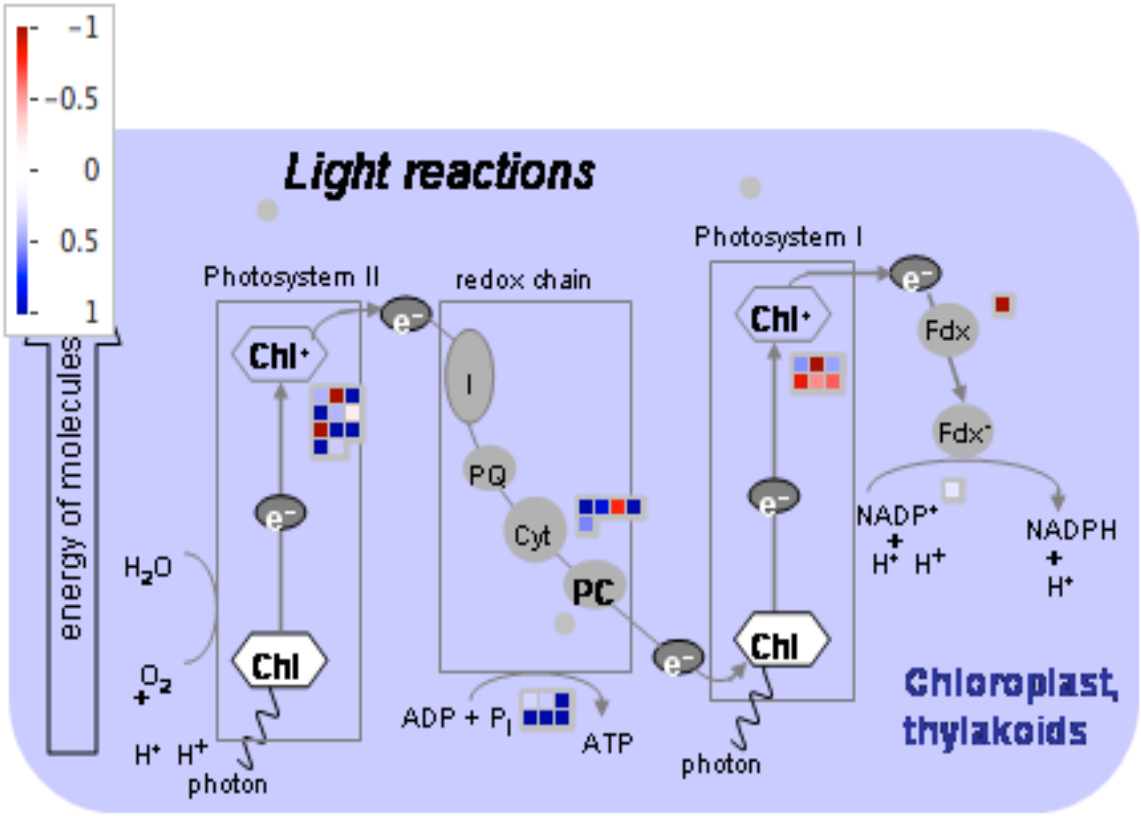
-1
-0.5
0
0.5
1
energy of molecules
Light reactions
Photosystem II
redox chain
Photosystem I
Chl*
Chl
e⁻
I
PQ
Cyt
PC
Fdx
Fdx⁻
H2O
O2
H+ H+
photon
ADP + PI
ATP
NADP+ + H+ H+
NADPH + H+
Chloroplast, thylakoids

D

Figure 5.16: MapMan comparison of the transcript of photosynthetic gene expression in ΔCyt c_M under different light conditions. Differences in transcript abundance between ΔCyt c_M 150/WT 150 (A), ΔCyt c_M 600/WT 600 (B), ΔCyt c_M 600/ΔCyt c_M 150 (C) and WT 600 vs WT 150 $\mu Em^{-2}s^{-1}$ light intensity (D). Changes in transcript abundance in log_2 values from Dark red (down regulation) to white (no regulation) and Dark blue (up regulation). Although the diagrams refer to 'chloroplasts' this is a consequence of the program used and should be ignored.

5.6 General Discussion of Cyt c_{6M} function

The growth phenotypes observed are summarized in table 5.1.

S.No	Light (μE)	Other conditions	Mutant phenotype
1	2 (ELL)	No bubbling (Incubator)	Bleaching
2	2 (ELL)	(Incubator and on the bench)	Bleaching, also in ΔCyt c_M of 6803
3	15 (LL)	No bubbling (Incubator)	Slight growth impairment
4	40 (ML)	Bubbling (Incubator)	Growth impairment
5	150 (HL)	Bubbling (Incubator)	Growth impairment
6	300	Bubbling (Algem Photobioreactor)	Some growth impairment
7	700	Bubbling (Algem Photobioreactor)	Severe growth impairment

Table 5.1: Summary of the growth characterization of ΔCyt c_M at different light conditions.

These data indicate growth impairment at all tested light levels in the ΔCyt c_M culture, although comparison between ELL or LL and other data should be treated with caution, as the ELL and LL cells were not bubbled with sterile air. The qRT-PCR (not shown) and transcriptomic data all indicated increased transcript levels for Cyt c_M under elevated light levels, consistent with the appearance of a phenotype in the mutants at elevated light levels.

Physiological characterisation studies indicated elevated oxygen consumption, especially at high light levels, and the overall rate of oxygen evolution was increased but not statistically significantly compared to the wild type. The chlorophyll fluorescence analysis data indicated the mutant shows high NPQ and somewhat greater Fv/Fm and Φ PSII in

ΔCyt c_M culture with other parameters little affected (figure 5.5). ΔCyt c_M showed slower rates of P700+ reduction kinetics compared to wild type (figure 5.6). Transcriptomic analysis data are summarized in table 5.2 and 5.3.

PSII		**PSI**		**ATP**	
psbA2	+	bptA	+	atpF	+
psbC	+	ycf4	+	atpG	+
psbD1	+			atpH	+
psbD2	+				
psbN	+				
psb29	+	**Cyt *b*$_6$*f***		**RESP. CHAIN**	
psb30	+	petB	+	cydA	+
ftsH1	+	petC	+	ndbB	+
ftsH2	+			ndbC	+
				ndbA	+
				sdhA	+
PBS		**E. CARRIERS**		ndhA	+
cpcF	+	petJ1	+	ndhC	+
cpcH	+	petJ1iso	+	ndhD2	+
petJ2	+			ndhD3	+
PROTECTION				ndhF1	+
isiA	+			ndhF3	+
				ndhH	+
				ndhI	+
				ndhJ	+
				ndhJ	+
				ndhK	+
				ndhL	+

Table 5.2: Upregulated transcript levels in ΔCyt c_M 150/WT 150 μEm^{-2}s^{-1} light intensity were also upregulated in WT 600/WT 150 μEm^{-2}s^{-1} light intensity. PSII (Photosystem II), PBS (Phycobilisome), PROTECTON (Photo protection), PSI (Photosystem I), Cyt *b*$_6$*f* (Cyt *b*$_6$*f* complex), E. CARRIERS (Electron carriers), ATP (ATP synthase), RESP.CHAIN (Respiratory Electron transport complexes). + (Upregulated in both conditions).

PSII		**PSI**		**ATP**	
psbE	-	psaB	-		
psbF	-	psaD	-	**RESP. CHAIN**	
psbH	-	psaE	-	ctaA	-
psbI	-	psaI	-	cox	-
psbJ	-	psaJ	-	ctaC	-
psbK	-	ycf3	-	ctaE	-
psbL	-			sdhB	-
psbM	-			ndhD5	-
psbV	-	**Cyt *b*$_6$*f***			
psbX	-	petG	-		
psbY	-	petM	-		
psbZ	-				
psb28	-				
PBS		**E CARRIERS**			
cpcA1	-	**PROTECTION**			
cpcA2	-				

Table 5.3: Down regulated gene transcript levels in ΔCyt c_M 150/WT 150 μEm^{-2}s^{-1} light intensity were also down regulated in WT 600/WT 150 μEm^{-2}s^{-1} light intensity. PSII (Photosystem II), PSI (Photosystem I), PBS (Phycobilisome), Cyt *b*$_6$*f* (Cyt *b*$_6$*f* complex), E. CARRIER (Electron carriers), ATP (ATP synthase), RESP.CHAIN (Respiratory Electron transport complexes). - (Down regulated).

Overall of 38 genes whose transcripts are significantly upregulated in the ΔCytc_M compared to the wild type (both at 150 μEm^{-2}s^{-1}), all are also upregulated in the WT at 600 μEm^{-2}s^{-1}light compared to 150. And of 32 genes whose transcripts are significantly downregulated in the ΔCytc_M compared to the wild type (both at 150 μEm^{-2}s^{-1}), 31 are also downregulated in the WT at 600 μEm^{-2}s^{-1} light compared to 150 μEm^{-2}s^{-1}. This is true even when subunits of the same complex go in different directions (eg for PSII and associated polypeptides 9 go up in both cases and 13 go down in both cases). In other words, the effect of the mutation at 150 μEm^{-2}s^{-1} is similar to subjecting wild type cells to a light stress of 600 μEm^{-2}s^{-1}.

Cyanobacteria have two types of bioenergetically active membranes and the TM contains interlinked photosynthetic and respiratory electron transport chains. This interlinked system allows excess electrons to flow from photosynthesis to respiration resulting in survival under certain stressful physiological conditions especially under fluctuating light

conditions (Lea-Smith *et al.*, 2013). We interpret the data in terms of a model in which Cyt c_M serves to transfer electrons from the PQ pool to Cyt *c* oxidase. (If this is mediated by Cyt c_6 or PC, transfer to PSI would also presumably be possible.) Under moderate light conditions (40 - 150 μE m^{-2} s^{-1} light) although the illumination was below the saturation of photosynthetic electron flow, respiratory electrons would also be directed to the PQ pool from NAD(P)H dehydrogenase, and succinate dehydrogenase. Thus the lack of Cyt c_M to assist in transfer of electrons to cytochrome oxidase may mimic light stress, accounting for the transcriptomic data and the mild growth phenotype observed in Cyt c_M mutant cultures. It is possible that increased cyclic electron flow occurred round PSI, causing a reduction in lumenal pH and thus increased NPQ. The increased expression of Cyt c_{6C} might have been an additional response to a more reduced PQ pool, but if Cyt c_{6C} were less effective at transferring reducing equivalents from the PQ pool compared to Cyt c_M, the increased expression of the former might not have been sufficient to compensate for the lack of Cyt c_M. The increased expression of *isiA* is also seen under elevated light intensity in the wild type strain, and may indicate stress.

Upon increasing the light intensity to 700 μE m^{-2} s^{-1}, the ΔCyt c_M culture showed a phenotype of clear growth inhibition (figure 5.2). Transcriptomic data have suggested that the ΔCyt c_M culture is already under severe stress even under normal light, so similar results were also observed in in wild type at high light conditions. The impaired growth of the mutant at very low light intensities would be consistent with the cells relying more on respiration, which could not be met under low light. However, the model does not readily explain the enhanced growth of the *Synechocystis* mutant under dark heterotrophic conditions reported by Hiraide *et al*., 2015. It is also not clear why the reduction of PSI was slower in the ΔCyt c_M knockout. It may be that plastocyanin and/or Cyt c_6 had been preferentially directed to cytochrome oxidase. The model is summarized in Figure 5.17.

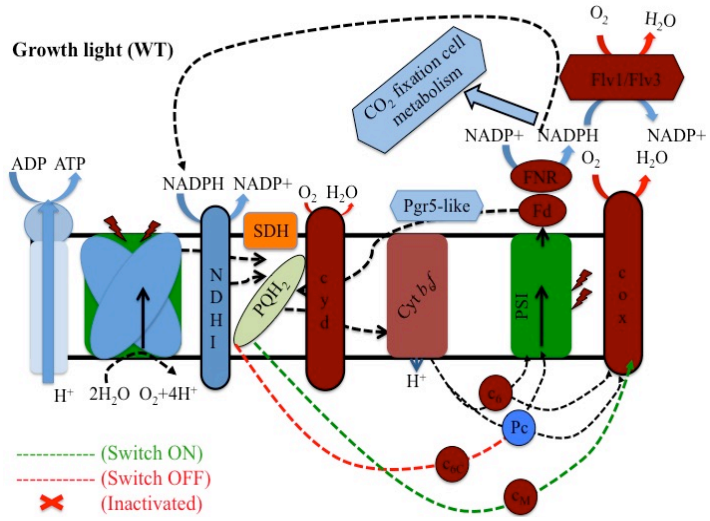
Growth light (WT)
CO_2 fixation cell metabolism
Flv1/Flv3
NADP+ NADPH NADP+
O_2 H_2O
ADP ATP
NADPH NADP+
SDH
FNR
Fd
Pgr5-like
NDHI
PQH_2
cyd
Cyt b_6f
PSI
cox
H^+ $2H_2O$ O_2+4H^+
c_6
Pc
c_{6C}
c_M
(Switch ON)
(Switch OFF)
(Inactivated)

(A)

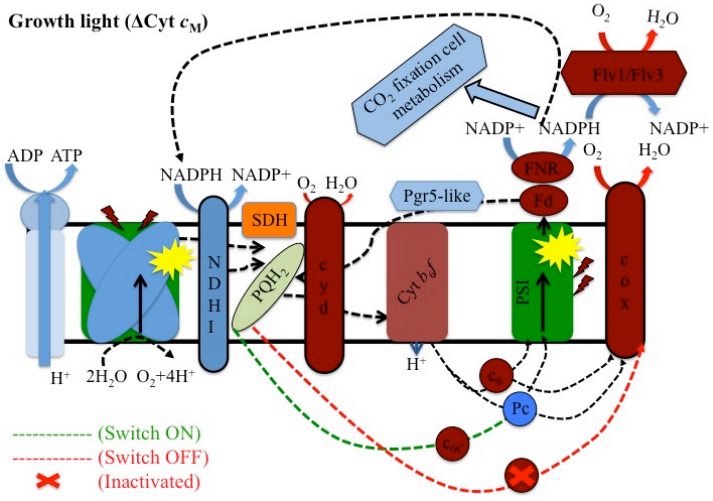
Growth light (ΔCyt c_M)
CO_2 fixation cell metabolism
Flv1/Flv3
NADP+ NADPH NADP+
O_2 H_2O
ADP ATP
NADPH NADP+
SDH
FNR
Fd
Pgr5-like
NDHI
PQH_2
cyd
Cyt b_6f
PSI
cox
H^+ $2H_2O$ O_2+4H^+
c_6
Pc
c_{6C}
(Switch ON)
(Switch OFF)
(Inactivated)

(B)

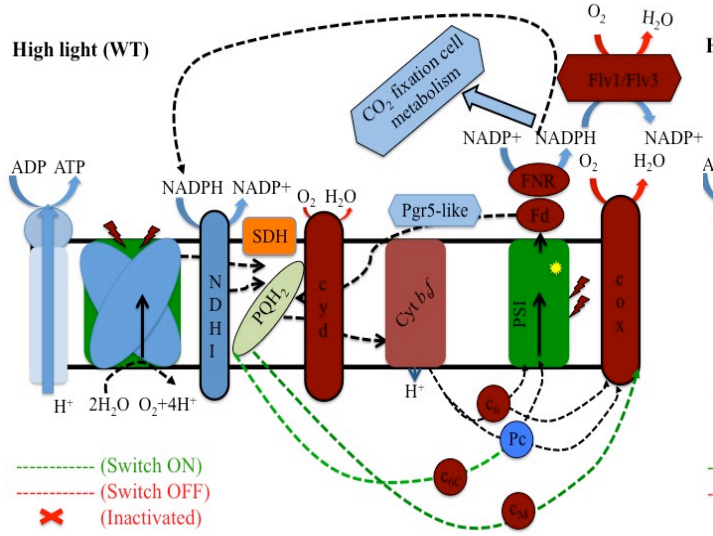
High light (WT)
CO_2 fixation cell metabolism
Flv1/Flv3
NADP+ NADPH NADP+
O_2 H_2O
ADP ATP
NADPH NADP+
SDH
FNR
Fd
Pgr5-like
NDHI
PQH_2
cyd
Cyt b_6f
PSI
cox
H^+ $2H_2O$ O_2+4H^+
c_6
Pc
c_{6C}
c_M
(Switch ON)
(Switch OFF)
(Inactivated)

(C)

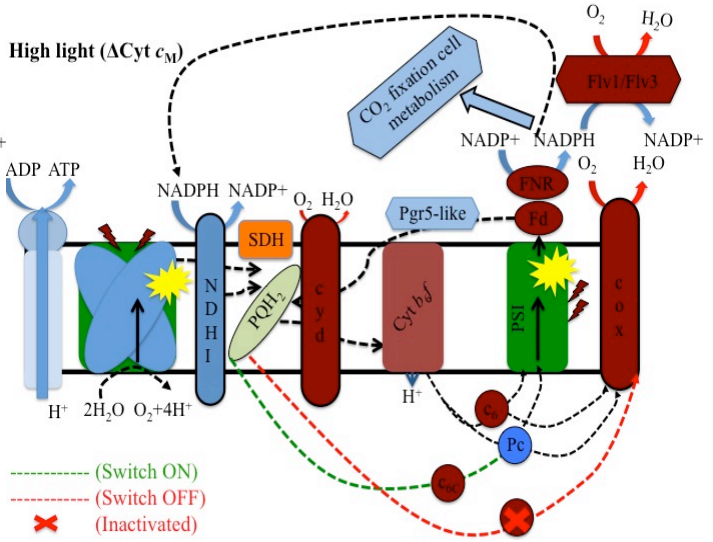
High light (ΔCyt c_M)
CO_2 fixation cell metabolism
Flv1/Flv3
NADP+ NADPH NADP+
O_2 H_2O
ADP ATP
NADPH NADP+
SDH
FNR
Fd
Pgr5-like
NDHI
PQH_2
cyd
Cyt b_6f
PSI
cox
H^+ $2H_2O$ O_2+4H^+
c_6
Pc
c_{6C}
(Switch ON)
(Switch OFF)
(Inactivated)

(D)

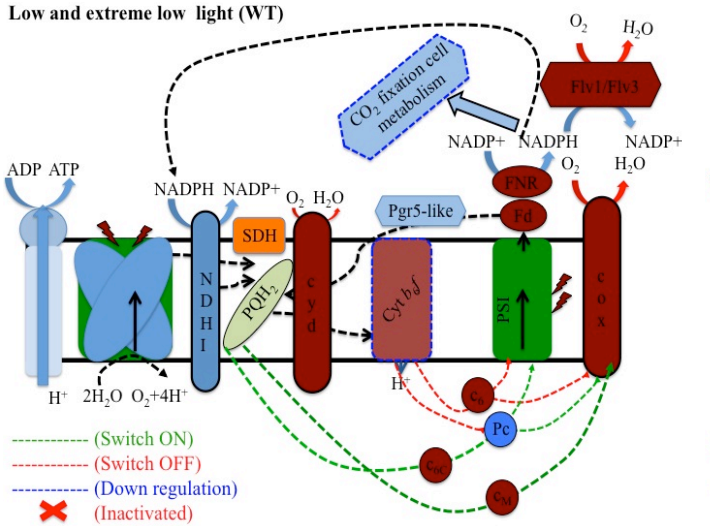
Low and extreme low light (WT)
CO_2 fixation cell metabolism
Flv1/Flv3
NADP+ NADPH NADP+
O_2 H_2O
ADP ATP
NADPH NADP+
SDH
FNR
Fd
Pgr5-like
NDHI
PQH_2
cyd
Cyt b_6f
PSI
cox
H^+ $2H_2O$ O_2+4H^+
c_6
Pc
c_{6C}
c_M
(Switch ON)
(Switch OFF)
(Down regulation)
(Inactivated)

(E)

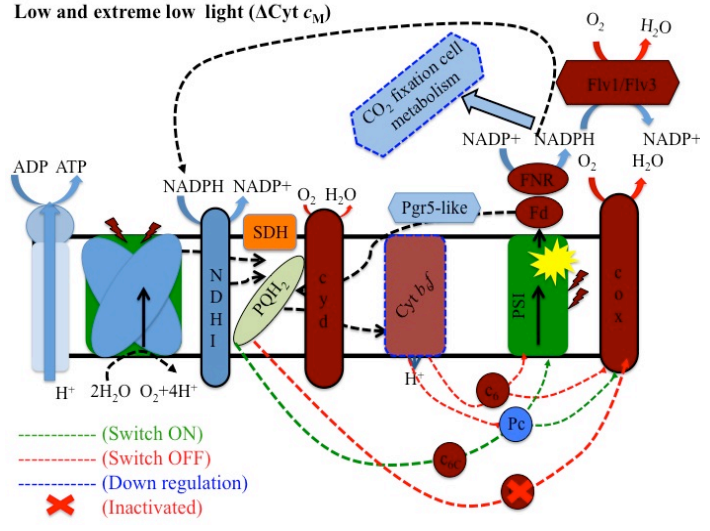
Low and extreme low light (ΔCyt c_M)
CO_2 fixation cell metabolism
Flv1/Flv3
NADP+ NADPH NADP+
O_2 H_2O
ADP ATP
NADPH NADP+
SDH
FNR
Fd
Pgr5-like
NDHI
PQH_2
cyd
Cyt b_6f
PSI
cox
H^+ $2H_2O$ O_2+4H^+
c_6
Pc
c_{6C}
(Switch ON)
(Switch OFF)
(Down regulation)
(Inactivated)

(F)

Figure 5.17: Schematic model showing different routes of electron transfer chain in WT and ΔCyt c_M strain in growth light (40-150 μE m^{-2} s^{-1} light intensities), high light intensities (300, 700 and above μE m^{-2} s^{-1} light intensities) and low and extreme low light (2-15 μE m^{-2} s^{-1} light intensities). At growth light or below the growth light intensity WT (A), ΔCyt c_M (B) can keep the intersystem electron transfer chain optimally oxidized and Cyt c_6 and Pc function as electron carriers in WT, along with Cyt c_6 and Pc, Cyt c_{6C} function as electron carriers in the mutant. Increase in light intensity enhances ΔpH in WT (C) and Cyt c_6, Pc, function as normal electron carriers. Cyt c_{6C} and Cyt c_M function as electron sinks, directly accepting electrons from the PQ pool and Cyt c_{6C} donating electrons to Pc/PSI and Cyt c_M donating electron to Cyt *c* oxidase, bypassing Cyt b_6f complex. In the mutant (D), Cyt c_6 and Pc function as normal electron carriers, and Cyt c_{6C} functions as an alternative electron carrier from the PQ pool to PSI. Under low and extreme low light conditions electron transfer through Cyt b_6f complex is severely inhibited. As a result Cyt c_{6C} and Cyt c_M function as electron carriers in WT (E), directly from PQ pool and to Pc/PSI or to Cyt *c* oxidase respectively. In the mutant (F) Cyt c_{6C} function as an electron carrier directly from PQ pool to PSI/to Cyt *c* oxidase via Pc.

CHAPTER 6 CHARACTERISATION OF CYT c_{6A} IN A. THALIANA

6.1 General introduction about the role of Cyt c_{6A} in *A. thaliana*

Since the discovery of Cyt c_{6A} in higher plants and algae, several hypotheses were proposed about the function of the protein. In 2002 it was proposed that Cyt c_{6A} was an alternative electron carrier to Pc, and shuttles electrons from the Cyt b_6f complex to the PSI complex during photosynthesis (Gupta *et al*., 2002). However, the aforementioned hypothesis was disproved when a double knockout of Pc isoforms (*petE1*& *petE2*) in *Arabidopsis thaliana* failed to grow under photoautotrophic conditions (Weigel *et al*., 2003b). This clearly demonstrated that Cyt c_{6A} does not simply replace Pc as an electron carrier. Furthermore, the redox midpoint potential of Cyt c_{6A} (initially estimated at + 140 mV) is too low to oxidise Cyt b_6f, which has a midpoint potential of + 320 mV (Molina-Heredia *et al*., 2003; Bialek *et al*., 2008). Despite the low midpoint potential of Cyt c_{6A}, it could potentially donate electrons to the PSI complex. However, laser-flash induced kinetics experiments in *Arabidopsis* demonstrated that the rate of electron transfer by Cyt c_{6A} to the PSI complex *in vitro* was 100 times slower compared with Pc (Molina-Heredia *et al*., 2003). Hence electron transfer from Cyt c_{6A} to the PSI complex is unlikely to be favourable in *in vivo* conditions.

The fact that Cyt c_{6A} is conserved in most higher plants and the presence of the LIP (Loop Insertion Peptide) and cysteine residues led to the proposal of a new model that Cyt c_{6A} could potentially catalyse the formation of disulphide bridges in the thylakoid lumen (Schlarb-Ridley *et al*., 2006; Howe *et al*., 2006). Oxidised Cyt c_{6A} could potentially interact with lumenal proteins that contain reduced disulphides, donating electrons to Cyt c_{6A} through the mechanism of disulphide exchange. The electrons from reduced cysteine residues of Cyt c_{6A} could then be transferred to Pc. Scharfenberg, 2009, later argued against this hypothesis, as he failed to detect interaction between Cyt c_{6A} and Pc in a yeast two-hybrid system. However, transient interactions resulting in electron transfer could not be ruled out.

When plants are exposed to high light intensities which are enough to saturate the photosynthetic electron transport chain, excess light energy could damage the

photosynthetic machinery (Roach and Krieger-Liszkay, 2012). Plants have developed numerous mechanisms to reduce this photoinhibitory damage (see chapter one for detailed information). We propose here a new photoprotective mechanism; that Cyt c_{6A} functions as an electron sink under high light intensity to avoid over reduction of the PQ pool and thus to decrease PSII photodamage. We propose that Cyt c_{6A} accepts electrons directly from the PQ pool during high light intensities, or over-reduced PQ conditions, and donates electrons directly to Pc, thereby bypassing the Cyt b_6f complex. To test this hypothesis in plants we studied the model plant *A. thaliana*, using mutant and overexpressing lines of Cyt c_{6A} and measuring their growth performances under different light intensities, especially under high light conditions. Photosynthesis efficiencies were also measured using a PAM fluorimeter. We also attempted to confirm Cyt c_{6A} overexpression by immunoblot techniques. Fluorescence microscopy was also performed to test the predicted localisation of Cyt c_{6A} in the chloroplast. Finally we used $P700^+$ reduction kinetics experiments to measure the rate of PSI reduction in ΔCyt c_{6A} lines compared to wild type plants.

6.2 Immunoblot analysis

In order to interpret the results with overexpression lines, it was necessary to confirm that the Cyt c_{6A} protein is overexpressed. Three lines had been constructed. One was a fusion with EYFP at the C-terminus of Cyt c_{6A}. A second placed a myc-tag at the C-terminus of Cyt c_{6A} and the third used Cyt c_{6A} on its own. Fluorescence microscopy (see below) confirmed expression of the EYFP fusion. It was therefore decided to test the oeCyt c_{6A}-myc line for confirmation of overexpression, using anti-myc antibodies. Total leaf protein extract from 8 individual oeCyt c_{6A}-myc lines was loaded on an SDS gel. After electrophoresis the proteins were transferred to a PVDF membrane and probed with antibody to the Myc epitope. The antibody cross-reacted with a band of 17 kDa, and a second band of around 50 kDa. Stained gels (not shown) confirmed similar amounts of overall protein were present in lane 1 compared to the other lanes. It is not clear why the band at lowest Mr corresponds to 17 kDa, which is greater than expected, but this anomaly has been observed previously (C J Howe, pers. comm., Scharfenberg 2009). The results indicate that the Cyt c_{6A}-myc fusion had been successfully overexpressed. Given the fact that the second band corresponds to a protein of more than 2x17 kDa, we do not believe this to be evidence of a protein dimer (figure 6.1). The band could represent Cyt c_{6A} and a covalently interacting protein.

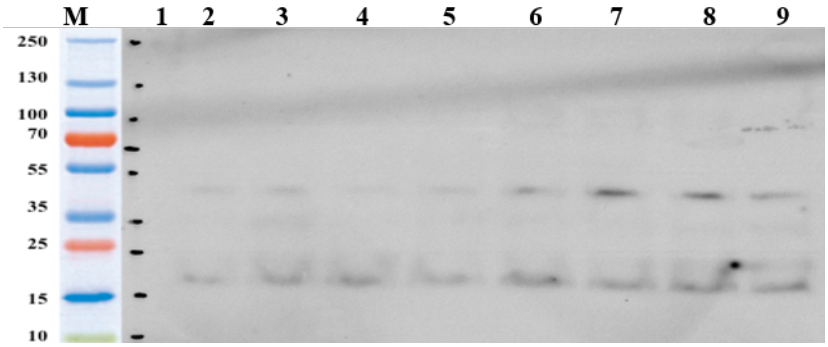

Figure 6.1: Detection of Cyt c_{6A} protein in Immunoblot analysis: Total leaf extract was loaded and probed with anti myc antibody after electrophoresis and blotting. The numbers on the left indicate the molecular mass (kDa) of the respective bands. Lane M: Molecular marker, Lane 1: Control extract from wild type plants, Lanes 2,3,4,5,6,7,8 and 9 different oeCyt c_{6A}-myc lines.

6.3 Protein localisation study

Several papers have speculated about the localisation of the Cyt c_{6A} in higher plants and algae (Gupta *et al*., 2002; Scharfenberg, 2011). Proteomic analysis of the thylakoid lumen has so far identified around 30 to 50 lumenal proteins and around 30 to 50 additional lumenal proteins have been predicted based on the presence of the TAT motif (Weigel *et al*., 2003a; Kleffmann *et al*., 2004; Peltier *et al*., 2002). Interestingly, Cyt c_{6A} has not been identified by proteomic analysis to be localised in the thylakoid lumen or in any other compartment, although Gupta *et al.,* reported a thylakoid location for overexpressed protein. Therefore an experiment was designed to tackle the question of where Cyt c_{6A} is located. An overexpression line of oeCyt c_{6A}-EYFP was generated (section 3.3.1) and Pc was picked as a positive control for lumenal proteins. A construct containing the cDNA sequence of the Pc major isoform fused at its 3' end with the EYFP coding sequence was generated and used to make an overexpression line in *A. thaliana* (section 3.3.3). Protein localisation experiments were performed using confocal fluorescence microscopy (section 2.14). oeCyt c_{6A}-EYFP showed a similar pattern to chlorophyll autofluorescence and the Pc fusion protein, indicating that it was indeed located in thylakoid of the chloroplast (figure 6.8). However, both the proteins showed heterogeneity in protein localization, with oeCyt c_{6A}-EYFP showing a particular marked concentration at the periphery of the thylakoid (figure 6.2), It is also interesting that the oeCyt c_{6A}-EYFP appeared to be located in a subset of chlorophyll-containing cells (figure 6.2, top left).

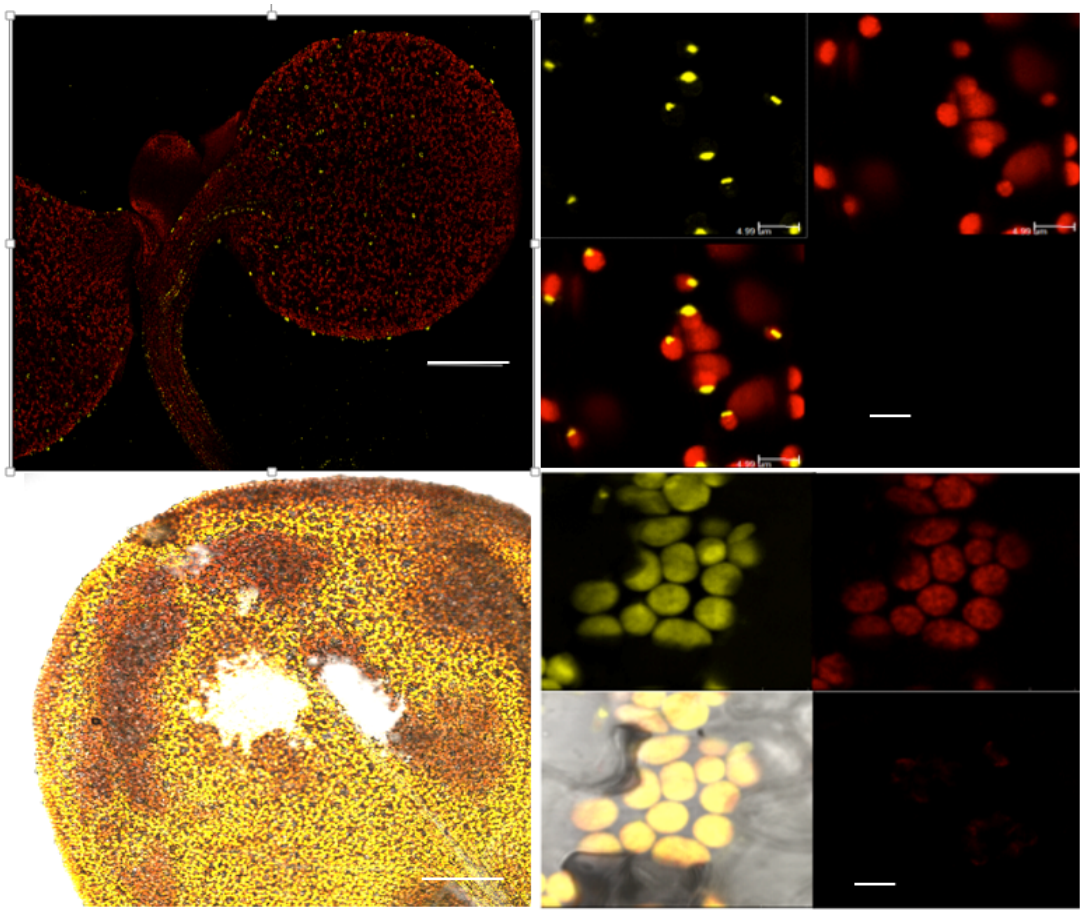

Figure 6.2: Localization of Cyt c_{6A} and Pc in plant chloroplasts: Upper panel left: Fluorescence microscopy to identify the location oeCyt c_{6A}-EYFP to the chloroplast of cotyledon and primordial leaf (bar 100 µm). Upper panel right shows different channel views, clockwise from bottom left: Merged view (bar 5 µm), EYFP channel, chlorophyll auto fluorescence and bright field view. Lower panel left: oePc-EYFP localised to the cotyledon (bar 100 µm). Lower panel right shows different channel views, clockwise from bottom left: Merged view (bar 5 µm), EYFP channel, chlorophyll auto fluorescence, and bright field view (bar 5 µm).

6.4 Growth characterisation of ΔCyt c_{6A} lines

An assessment of potential growth phenotypes in the Cyt c_{6A} mutant was performed to investigate the functional role of the protein in plants. Experiments on a knockout of a Cyt c_{6A} homologue, Cyt $c_{6C,}$ in the cyanobacterium *Synechococcus elongatus* PCC 7942 had revealed an impaired growth phenotype under high light conditions (See chapter 4 of this thesis). Therefore we analysed root growth, and leaf morphology and size for Cyt c_{6A} mutant lines, overexpression lines and wild type seedlings over time on MS agar plates.

We also characterised growth of mutant lines and wild type *A. thaliana* plants in the Plant Growth Facility, University of Cambridge (PGF) (section 2.7.2) Growth rates were measured over six weeks and the growth was compared to wild type plants.

6.4.1 Root and leaf growth phenotype in culture plates

As outlined above, we generated three different over expression lines, an overexpression line with a TAA translation terminator immediately after the open reading frame (hereafter oeCyt c_{6A}-TAA), an overexpression line with a C-terminal 4x myc epitope tag (hereafter oeCyt c_{6A}-myc), and an overexpression line with a C-terminal EYFP fusion (hereafter oeCyt c_{6A}-EYFP) (for detailed explanation refer to section 3.3 in chapter 3). Seeds of lines with Cyt c_{6A} mutations (652 & 66C), oeCyt c_{6A}-EYFP (randomly picked as a representative of the overexpression lines) and the wild type were sterilised and inoculated on MS agar plates (section 2.7), and growth was assessed under two different light intensities. The root length was measured every 24 hrs, for up to 13 days. Under 20 μE m^{-2} s^{-1} light intensity, no significant root or leaf growth difference was observed between wild type plants and the Cyt c_{6A} defective mutant lines. However, visibly reduced root growth and leaf size was observed in oeCyt c_{6A}-EYFP line compared to wild type and mutants (figure 6.3 A, C). Rosette leaves from 3 individual plants grown at 20 μE m^{-2} s^{-1} light intensity were carefully removed from the plants after 15 days and arranged size-wise and photographed (figure 6.3 E, each cluster representing a single plant).

Under 100 μE m^{-2} s^{-1} light intensity, both Cyt c_{6A} mutant lines and the wild type plants showed similar root growth rates, but the oeCyt c_{6A}-EYFP line showed significantly reduced root and leaf growth rate compared to the wild type plants and Cyt c_{6A} deficient mutant strains (figure 6.3 B, D). Rosette leaves from 4 individual plants grown at 100 μE m^{-2} s^{-1} light intensity were carefully removed from the plants after 15 days and arranged size-wise and photographed (Figure 6.3 F, each cluster representing a single plant).

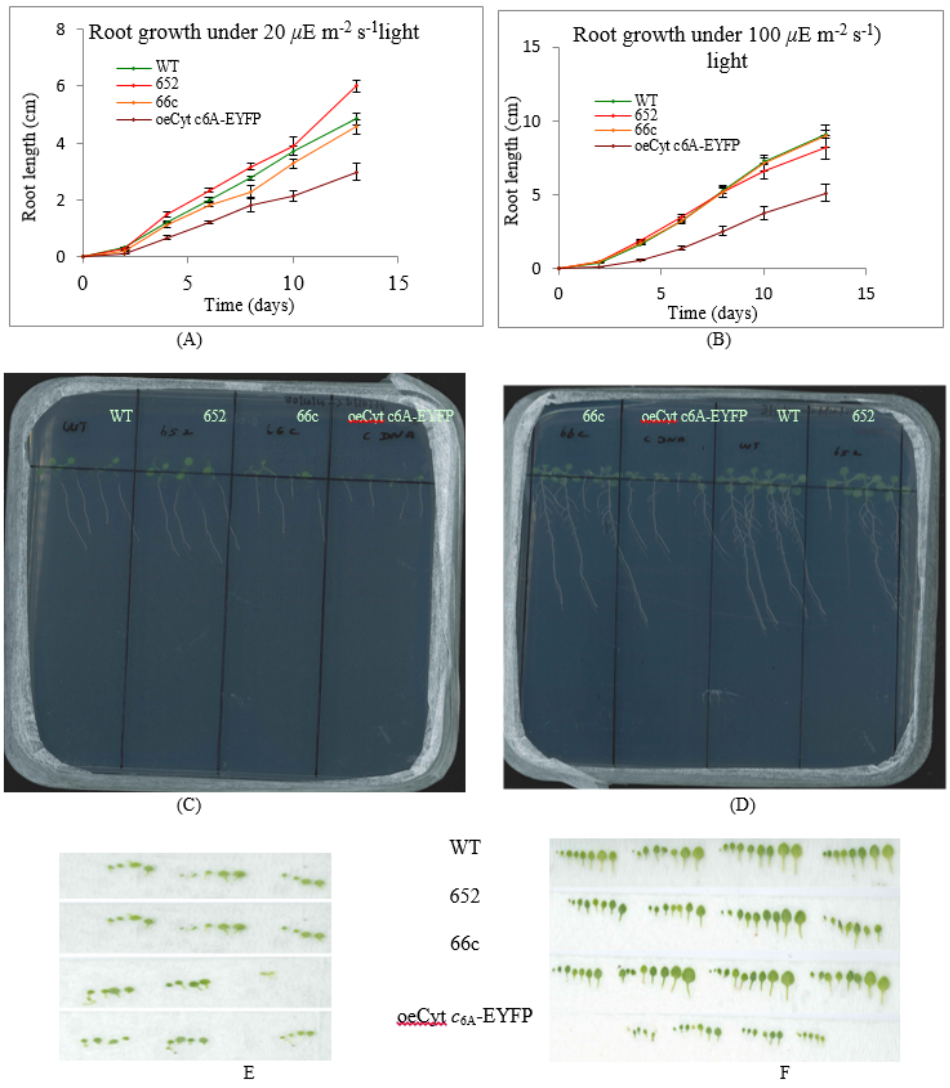

Figure 6.3: Growth analysis of Cyt c_{6A} mutants on agar plates: Cyt c_{6A} knockouts 652 and 665c, over expression mutant (oeCyt c_{6A}-EYFP) and the wild type were grown under 20 μE $m^{-2}s^{-1}$ (A) and 100 μE m^{-2} s^{-1} (B) conditions and their root growth rates were measured. 10 day old culture plates from 20 μE $m^{-2}s^{-1}$ (C) and 100 μE $m^{-2}s^{-1}$ (D) conditions show growth phenotype between strains. Rosette leaves from 3 individual plants grown under 20 μE $m^{-2}s^{-1}$ (E) and 4 individual plants from 100 μE $m^{-2}s^{-1}$ (F) were collected after 15 days and photographed. For detailed analysis refer to text. Each data point represents at least four independent plants and error bar indicates standard error (A&B)

Total numbers of leaves in different lines were counted and the result suggested that oeCyt c_{6A}-EYFP had fewer leaves compared to wild type and other mutants, with more or less similar leaf numbers found in wild type and mutant lines (figure 6.4A). The leaf areas of different lines grown at 100 μE m^{-2} s^{-1} light intensity were measured and the result

suggested that oeCyt c_{6A}-EYFP had highly reduced leaf areas compared to wild type and mutants, while more or less similar leaf surface areas were observed between mutants and wild type plant (figure 6.4B).

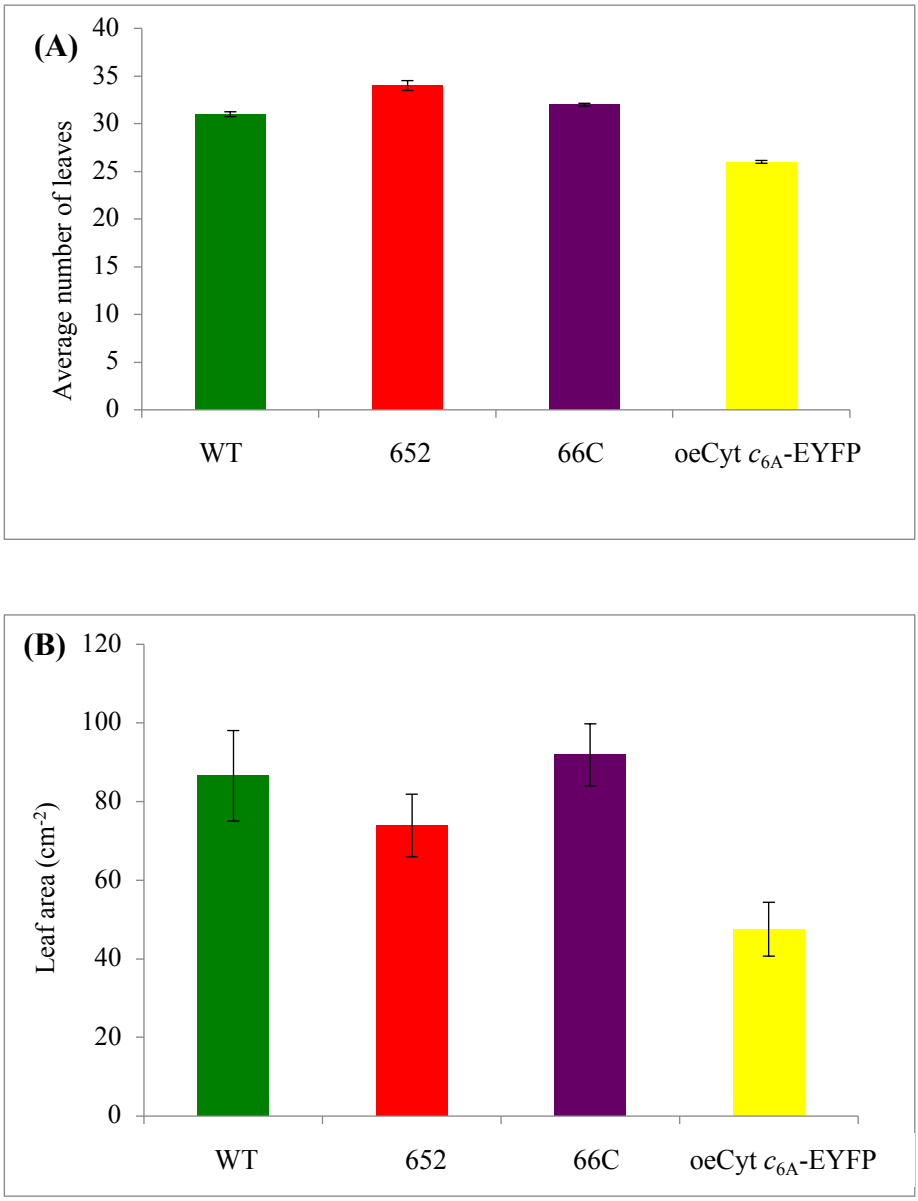

Figure 6.4: Average number of leaves and leaf areas of Cyt c_{6A} knockout lines, overexpression line and wild type seedlings. Average number of leaves in different lines grown for fifteen days under 100 μE m^{-2} s^{-1} light intensity (A) and average leaf surface areas of different lines grown under 100 μE m^{-2} s^{-1} light intensity (B). Each data point represents at least five independent plants. Error bar indicates standard error (A&B).

6.5 Characterisation of Cyt c_{6A} mutants under different light intensities in PGF

6.5.1 *A. thaliana* growth phenotype under different light intensities

We randomly selected Cyt c_{6A} mutant line 652 (hereafter ΔCyt c_{6A}) for a growth phenotype study in the PGF. Wild type, ΔCyt c_{6A} and overexpression lines (oeCyt c_{6A}-TAA, oeCyt c_{6A}-myc, oeCyt c_{6A}-EYFP) were grown under 150 and 300 μEm^{-2} s^{-1} light intensities in the PGF (section 2.7.2) and the growth rate of each line was determined. Plants were also grown at 500 μEm^{-2} s^{-1} and growth compared visually.

6.5.2. Growth phenotype under 150 μE m^{-2} s^{-1} light intensity

A. thaliana plants were grown under 150 μE m^{-2} s^{-1} light (section 2.7.2) and their shoot lengths were measured every 15 days. Under 150 μE m^{-2} s^{-1} light, a bleached phenotype was observed in ΔCyt c_{6A} plants after 15 days (figure 6.5, & 6.6.A 2).

Figure 6.5: Growth phenotype of Cyt c_{6A} mutant under 150 μE m^{-2} s^{-1} light intensity after 15 days. The bleaching phenotype was visible for ΔCyt c_{6A} compared to wild type Col-0 and oeCyt c_{6A}-myc.

ΔCyt c_{6A} shoot growth was similar to wild type plants after 30 and 45 days respectively (figure 6.6 C 1&2 and 6.6 E 1&2). However, a reduced shoot growth phenotype was noticed in all the overexpression line plants compared to wild type after 30 and 45 days

(figure 6.6 C 3, 4&5 and 6.6 E 3, 4&5 respectively). There were also differences in the magnitude of shoot growth among the overexpression lines. The shoot lengths were measured and the results suggested that the ΔCyt c_{6A} line grew at a similar rate to the wild type over 45 days, while the growth of the overexpression lines was significantly reduced compared to the wild type and ΔCyt c_{6A} lines, (figure 6.7A). Again, the different overexpression lines showed different degrees of growth impairment. Overall the shoot growth experiments in 150 μE m^{-2} s^{-1} light revealed that knocking out Cyt c_{6A} did not affect plant growth and development compared to wild type plants apart from the bleaching phenotype, whereas overexpression of Cyt c_{6A} impaired growth and development compared to wild type plants.

6.5.3. Growth phenotype under 300 and 500 μE m^{-2} s^{-1} light intensities

Under 300 μE m^{-2} s^{-1} light, no visible shoot growth phenotype was observed in the mutant plants after 15 days (figure 6.6B). Interestingly, the shoot growth pattern started to change subsequently. A clear shoot growth phenotype was observed in ΔCyt c_{6A} line plants after 30 days (figure 6.6.D 1&2), and a similarly reduced growth phenotype was also observed in all overexpression lines (figure 6.6.D 3,4&5). A more reduced growth phenotype was observed in ΔCyt c_{6A} lines after 45 days (figure 6.6 F 1&2). Interestingly, shoot growth in the overexpression lines increased after 30 days growth, and growth reached wild type levels at 45 days (figure 6.6.F 3,4&5 and figure 6.7B).

Further experimentation was attempted to test the shoot reduction growth phenotype in ΔCyt c_{6A} strains by growing them under 500 μE m^{-2} s^{-1} light intensity along with wild type and oeCyt c_{6A}-YFP line. The ΔCyt c_{6A} shoot growth and inflorescence spikes were visibly highly reduced compared to wild type and oeΔCyt c_{6A}-YFP strains after 45 days. Interestingly oeΔCyt c_{6A}-YFP showed a higher growth rate compared to the wild type and the ΔCyt c_{6A} strains. However, all the tested lines were highly brown pigmented (figure 6.8). The results confirmed that the reduced growth rate of ΔCyt c_{6A} strains seen under 300 μE m^{-2} s^{-1} light intensity was reproducible at 500 μE m^{-2} s^{-1} and suggested that overexpression might be protective at high light intensities.

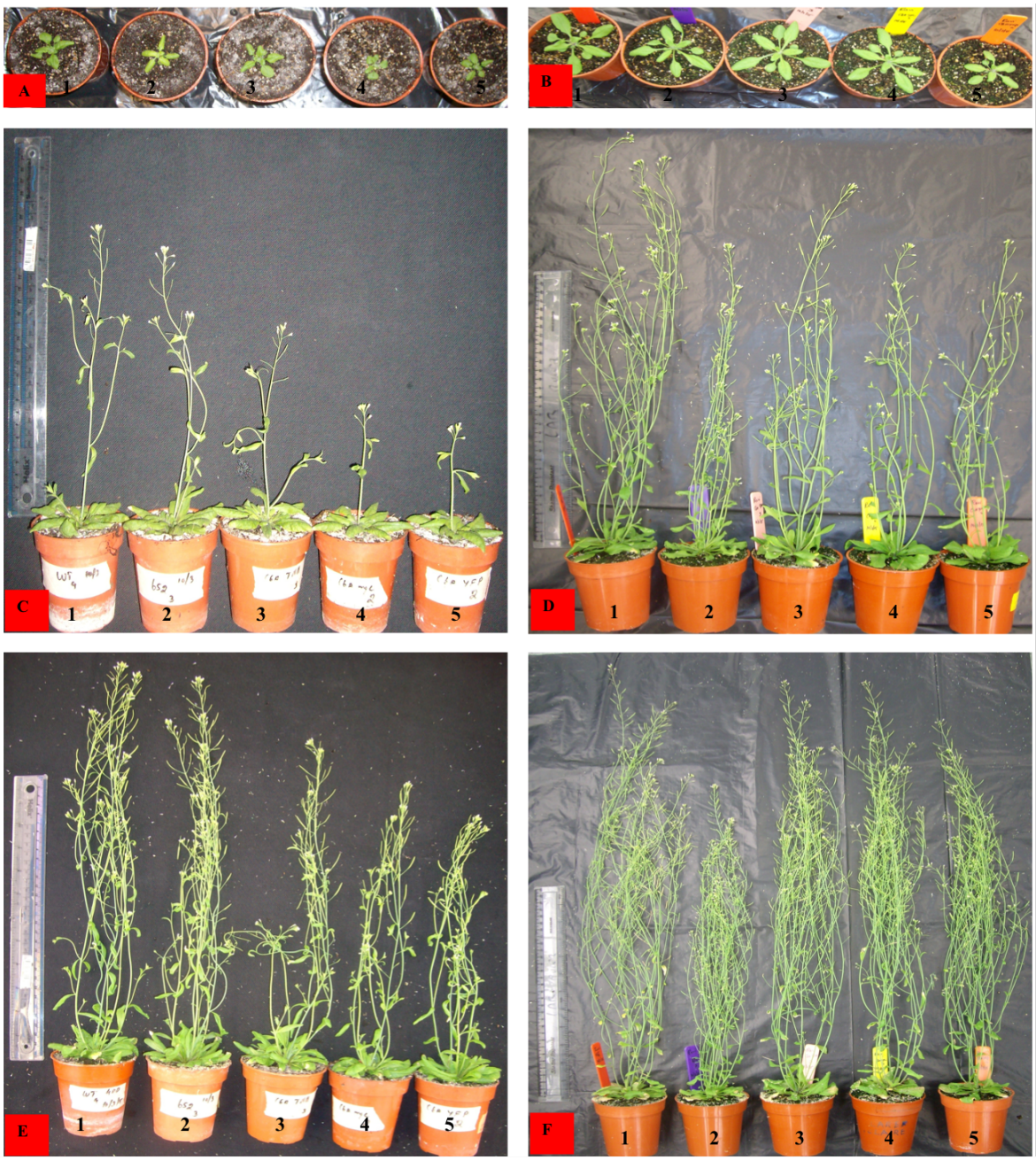

Figure 6.6: Cyt c_{6A} mutants and WT growth phenotype under different light intensities in plant growth facility: wild type (1), ΔCyt c_{6A}, (2), oeCyt c_{6A}-TAA (3), oeCyt c_{6A}-myc (4), and oeCyt c_{6A}-EYFP (5) strains were grown under 150 μE $m^{-2}s^{-1}$ (A,C and E) and 300 μE m^{-2} s^{-1} (B,D and F) conditions and their shoot lengths were measured to assess the growth rates among different strains. 15 days (A&B), 30 days (C&D) and 45 days (E&F).

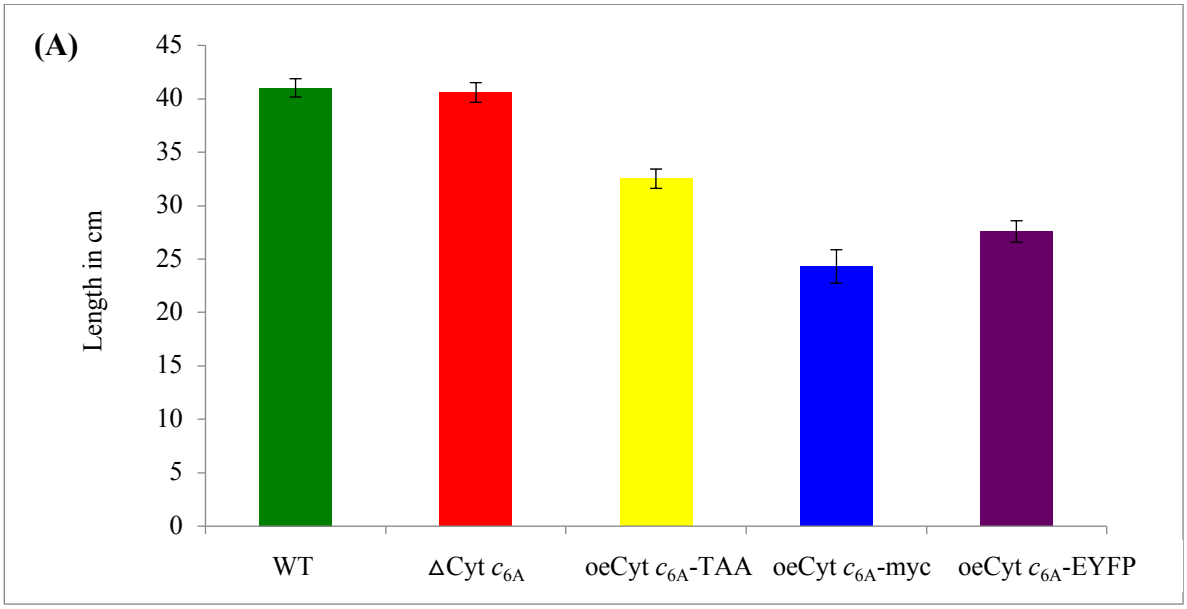

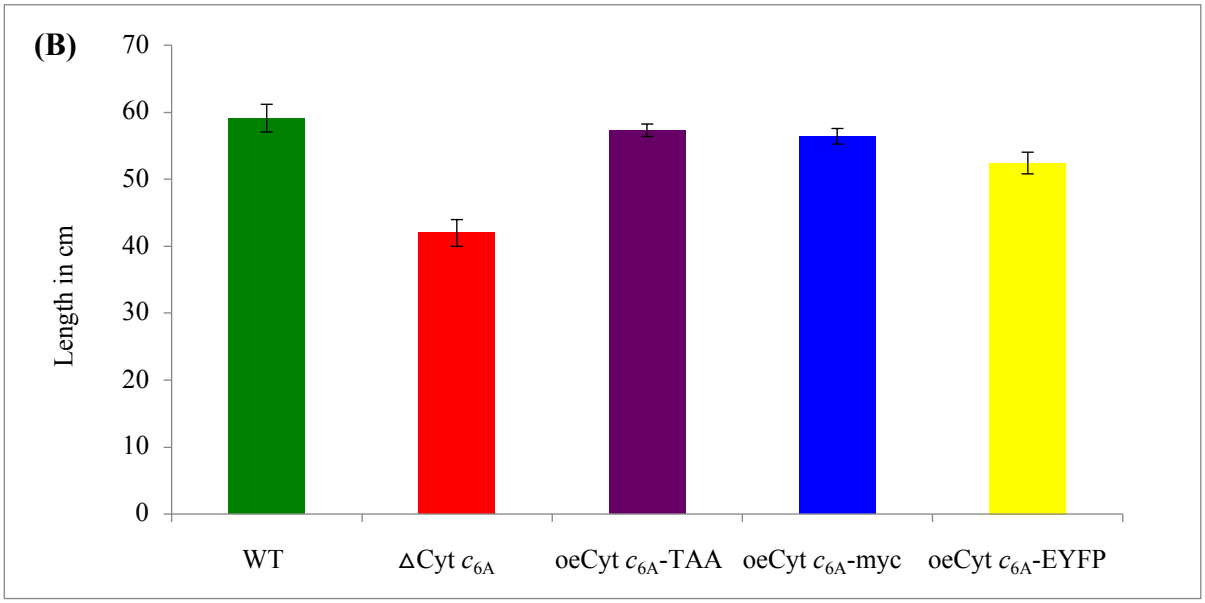

Figure 6.7: Shoot lengths under 150 and 300 μE m^{-2} s^{-1} light intensity after 45 days. Shoot growth phenotype of Cyt c_{6A} mutant and overexpression lines and wild type plants under 150 μE m^{-2} s^{-1} light intensity (A) and 300 μE m^{-2} s^{-1} light intensity (B). Each data point represents at least five independent plants. Error bar indicates standard error.

Wild type Col-0 **Δcyt c_{6A}** **oeΔCyt c_{6A}-EYFP**

Figure 6.8: Growth phenotype of ΔCyt c_{6A}, oeΔCyt c_{6A}-YFP and wild type plants under 500 μE m^{-2} s^{-1} light intensity. ΔCyt c_{6A} showed highly reduced shoots and inflorescence spike growth compared to wild type and oeΔCyt c_{6A}-YFP strains in 500 μE m^{-2} s^{-1} light intensity. Interestingly, oeΔCyt c_{6A}-YFP showed higher growth compared to wild type.

6.6 Physiological characterisation (Chlorophyll fluorescence measurement)

To try to understand the different behaviour of ΔCyt c_{6A} and wild type, we studied the photosynthetic electron transport chain under two different light intensities, by measuring chlorophyll fluorescence, and P700 reduction. Parameters such as *F*v/*F*m, ΦPSII yield and NPQ kinetics were measured under 245 and 975 μE $m^{-2}s^{-1}$ light intensities.

6.6.1 Physiological characterisation of ΔCyt c_{6A} under 245 μE m^{-2} s^{-1} light intensity

The photosynthetic energy transfer of the ΔCyt c_{6A} strain and wild type plants was assessed under 245 μE m^{-2} s^{-1} light intensity. Indistinguishable values of *F*v/*F*m were observed between wild type and ΔCyt c_{6A}, which imply that the maximum fluorescence yield in the dark adapted state was not affected by the Cyt c_{6A} mutation (figure 6.9 A). ΦPSII yield was similar to the wild type up to 200 seconds, after which a slightly lower yield but not statistically significant was observed for ΔCyt c_{6A} (figure 6.9B). NPQ for ΔCyt c_{6A} strain was similar to wild type for 100 sec, after which a lower value was seen for the mutant than wild type (figure 6.9C).

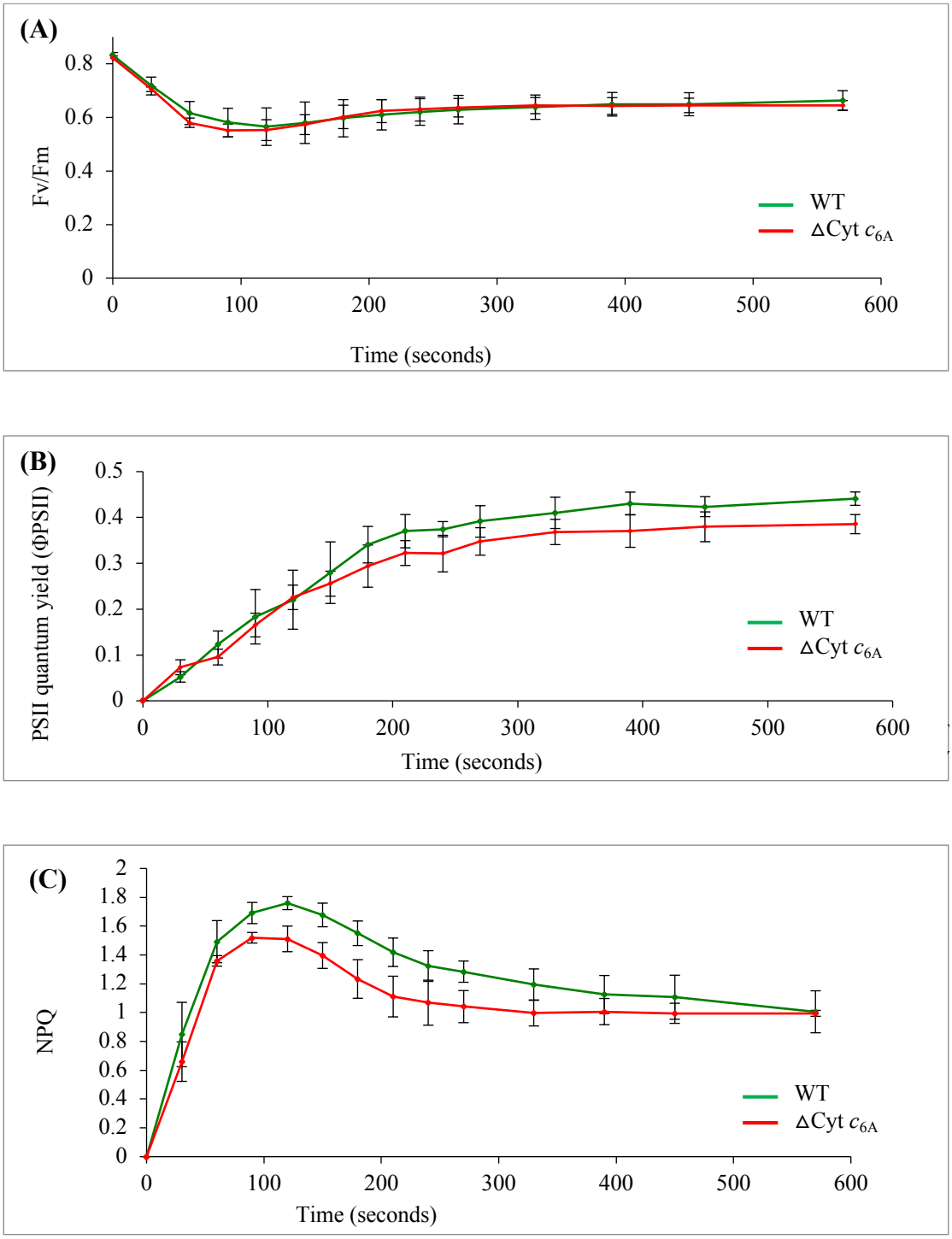

Figure 6.9: Measurement of photosynthetic efficiency of ΔCyt c_{6A} and wild type in 245 μE m^{-2} s^{-1} light intensity. *Fv*/*Fm* (A) was not affected and ΦPSII yield (B) was same for the first 200 sec, after which a slightly lower yield was observed for ΔCyt c_{6A} compared to wild type plants. A lower level of NPQ was observed in ΔCyt c_{6A} compared to wild type (C). Each data point represents at least five independent plants. Error bar indicates standard error. These data were generated in collaboration with Dr. Iskander Ibrahim in Professor John F Allen lab, Queen Mary University of London, UK.

6.6.2 Physiological characterisation of ΔCyt c_{6A} under 975 μE m^{-2} s^{-1} light intensity

Figure 6.10 shows the photosynthetic performances of ΔCyt c_{6A} mutant and wild type in 975 μE m^{-2} s^{-1} light intensity. *F*v/*F*m and ΦPSII yield of ΔCyt c_{6A} were similar to Col-0 wild type (figure 6.10 A&B). Interestingly a clear difference in NPQ was observed in ΔCyt c_{6A} lines compared to wild type plants (figure 6.10 C). The level of NPQ for ΔCyt c_{6A} and wild type was similar for 60 seconds, after which ΔCyt c_{6A} strains showed lower NPQ than wild type.

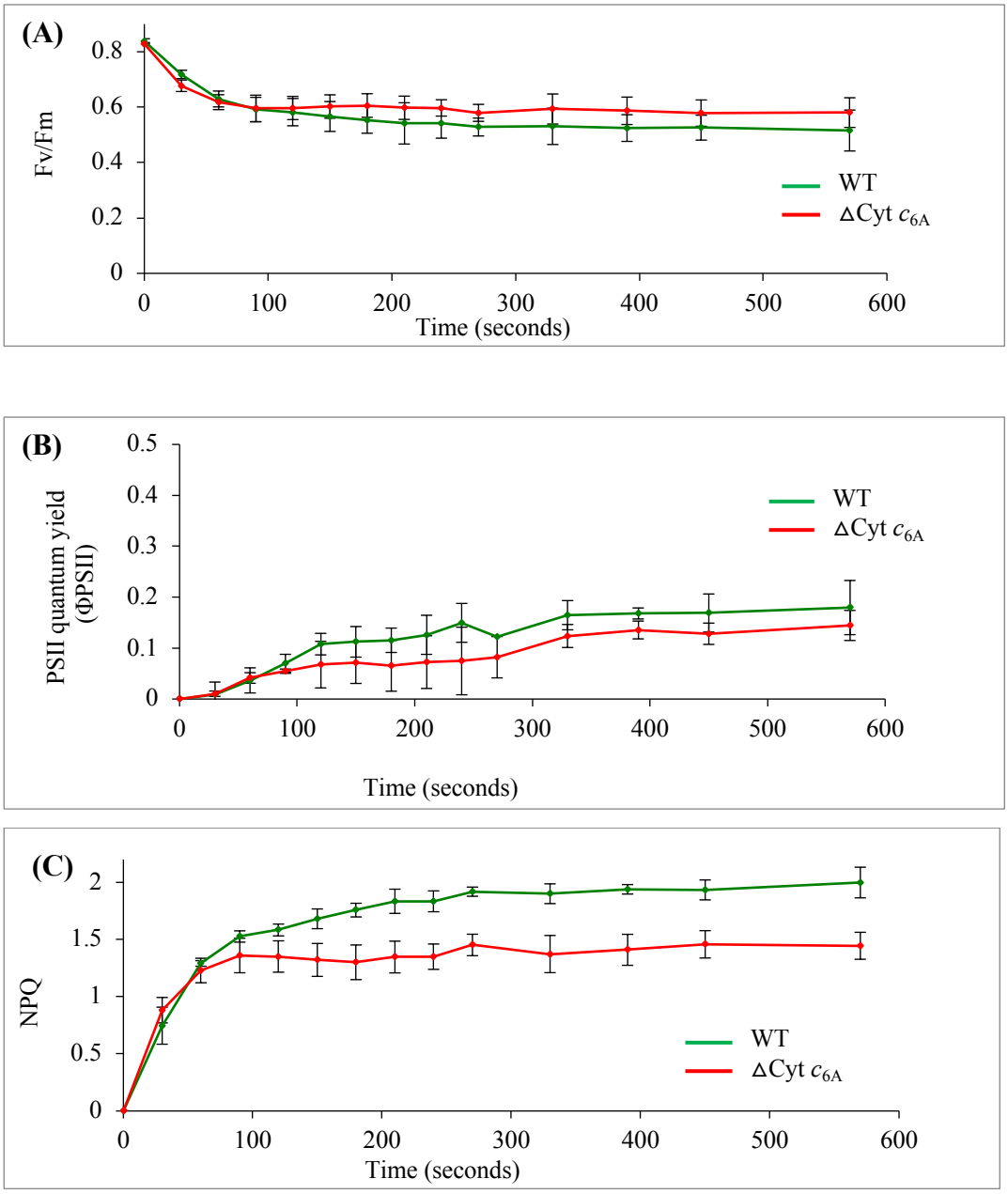

Figure 6.10: Photosynthetic performance of ΔCyt c_{6A} and wild type in 975 μE m^{-2} s^{-1} light conditions: Knocking out of Cyt c_{6A} did not alter the *F*v/*F*m (A) and ΦPSII yield (B). Interestingly a lower rate of NPQ was observed in ΔCyt c_{6A} compared to wild type (C). Each data point represents at least five independent plants. Error bar indicates standard error. These data were generated in collaboration with Dr. Iskander Ibrahim in Professor John F Allen lab, Queen Mary University of London, UK.

6.6.3 $P700^+$ reduction kinetics in ΔCyt c_{6A} and wild type plants

$P00^+$ dark reduction kinetics of wild type plants and ΔCyt c_{6A} line were measured. PSI was excited for 5 mins using far-red light. The light was switched off and immediately followed by 100 ms of a single saturating pulse (4500 μE m^{-2} s^{-1}) to complete oxidation of $P700^+$. Dark reduction of $P700^+$ was then recorded (section 2.13). Figure 6.11 shows the dark reduction rate of $P700^+$ for wild type and the ΔCyt c_{6A} strain. The reduction rate of $P700^+$ for the ΔCyt c_{6A} strain was significantly slower than wild type; we observed only 40% reduction in 2.5 sec compared to 75% in wild type. Complete reduction (100%) of $P700^+$ was observed in wild type in 7 sec, but only 80% reduction was observed in the ΔCyt c_{6A} strain, and we failed to observe 100% during the entire experiment (figure 6.11).

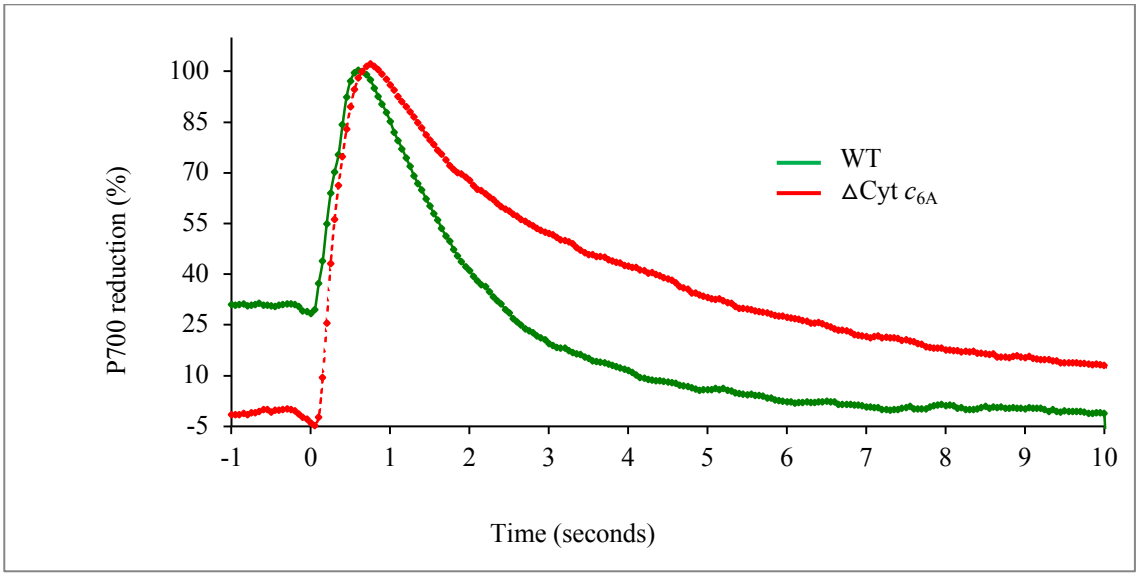

Figure 6.11: $P700^+$ reduction kinetics: ΔCyt c_{6A} and WT. A value of 100% indicates complete oxidation of P700. Lower values indicate the amount remaining oxidized at a given time. P700 reduction kinetics of WT was significantly faster than for the ΔCyt c_{6A} strain. Each data point represents at least four independent plants. This data was generated in collaboration with Dr. Iskander Ibrahim in Professor John F Allen lab, Queen Mary University of London, UK.

6.7 General Discussion of Cyt c_{6A} function

Since the discovery of Cyt c_{6A} in 2002, several studies have been published regarding the function of Cyt c_{6A} in higher plants. However, few of them reported *in vivo* experiments, which encouraged us to study the protein's functions *in vivo*. Several Cyt c_{6A} overexpression lines were generated (section 3.3) and 2 of them were confirmed for overexpression. The growth performance of these lines was tested, along with the ΔCyt c_{6A} lines and wild type plants, in culture plates and in the PGF. The oeCyt c_{6A}-EYFP line was used for localization by fluorescence microscopy. Finally we studied the electron transport chain of ΔCyt c_{6A} and wild type under two different light intensities, by measuring chlorophyll fluorescence, and $P700^+$ reduction. Parameters such as Fv/Fm, ΦPSII yield and NPQ kinetics were measured under 245 and 975 $\mu E\ m^{-2}s^{-1}$ light intensities.

Immunoblot analysis confirmed the expression of oeCyt c_{6A}-myc, and also indicated an additional band (figure 6.1). Based on the molecular weight, this does not represent either a dimer or interaction with the lumenal immunophilin FKBP13. It may represent an interaction with a higher molecular weight protein, which is possibly covalent or at least resistant to SDS-PAGE. Further experiments, such as purification and mass spectroscopic analysis are needed to identify the interacting partner. Confocal fluorescence microscopy confirmed expression of the EYFP fusion, and demonstrated that Cyt c_{6A} was located in the chloroplast, and possibly in the thylakoid lumen (figure 6.2). Although overexpression of untagged protein was not tested, it seems reasonable to assume overexpression, as the same expression signals were used as for the other constructs.

Under 20 and 100 $\mu E\ m^{-2}\ s^{-1}$ light intensities in culture plates, the wild type and ΔCyt c_{6A} plants were visibly indistinguishable whilst the oeCyt c_{6A}-EYFP line had much smaller

leaves, and reduced root lengths (figure 6.3), number of leaves (figure 6.4) and leaf surface areas compared to wild type plants. When plants were grown under 150 μE m^{-2} s^{-1} light intensity in the PGF, we observed similar shoot growth between ΔCyt c_{6A} line and wild type plants. However, the ΔCyt c_{6A} lines showed a bleached phenotype (figure 6.5), whilst all the over expression lines showed significantly reduced shoot growth phenotype compared to wild type plants (figure 6.6 A, C&E and figure 6.7A). However, different expression lines showed differences in the extent of growth retardation compared to wild type. In 300 μE m^{-2} s^{-1} light intensity the shoot growth rate of ΔCyt c_{6A} was highly reduced compared to wild type, and the growth of over expression lines growth was similar to wild type (figure 6.6 B,D&F and 6.7B) in contrast to growth at 150 μE m^{-2} s^{-1}. At 500 μE m^{-2} s^{-1} light, ΔCyt c_{6A} showed significantly reduced growth phenotype compared to wild type and overexpression lines (figure 6.8). Interestingly, enhanced growth was observed in 500 μE m^{-2} s^{-1} light intensity when the protein was overexpressed. Chlorophyll fluorescence measurements indicated lower levels of NPQ at 245 μE m^{-2} s^{-1} (figure 6.9) and 975 μE m^{-2} s^{-1} light (figure 6.10), and slower reduction of $P700^{+}$ (figure6.11)

A phenotype of impaired growth in high light was also observed in non photochemical quenching 4 and 1 (*npq*4 *& npq*1) mutants, which lack PsbS and zeaxanthin respectively (Roach *et al.,* 2012; Ciszak *et al.,* 2015; Bonfils *et al*., 2000; Müller *et al.,* 2001; Li *et al*., 2002; Dong *et al*., 2015), proton gradient regulatory protein 5 (*pgr*5) mutants (DalCorso *et al.,* 2008; Gollan *et al.,* 2015; Munekage *et al.,* 2002; Nandha *et al*., 2007; Tikkanen *et al.,* 2014; Müller *et al.,* 2001; Sugimoto *et al*., 2013; Allahverdiyeva e*t al*., 2015b), and proton gradient regulatory 5-like protein 1 (*pgrl*1) mutants in *Arabidopsis* (Müller *et al*., 2001; Suorsa *et al*., 2015; DalCorso *et al*., 2008).

These results presented here support the proposed hypothesis that Cyt c_{6A} is located in the thylakoid lumen and transfers electrons from the PQ pool to PSI, probably via Pc. According to this hypothesis, the low light intensity used was below the saturation of photosynthetic electron flow, the PQ pool was in a steady state, and linear electron flow occurred in wild type plants and ΔCyt c_{6A} lines. However, in over expression lines, the linear electron flow was disrupted by oeCyt c_{6A} accepting electrons directly from the PQ pool and donating to Pc, bypassing the Cyt b_6f complex, thus resulting in reduction of Pc and PSI, and leading to enhanced cyclic electron flow around PSI via PGR5 and PGRL1 (Tikkanen *et al*., 2015; Suorsa *et al*., 2015; Nandha *et al*., 2007). The high rate of cyclic

electron flow would lead to an increased *trans*-thylakoid proton gradient (ΔpH) and consequently also increased thermal dissipation of energy (NPQ) even at low light intensities. Thus, relatively high rates of NPQ and CEF resulted in reduced growth in oeCyt c_{6A} lines compared to wild type and ΔCyt c_{6A} under low light intensities. Another plausible explanation is that, when the oeCyt c_{6A} lines are grown at low light intensity, if Cyt c_{6A} accepts electrons directly from the PQ pool and donates them to PSI via Pc bypassing the Cyt b_6f complex, there will be less electron flow through the Cyt b_6f complex. This may result in a smaller proton gradient across the thylakoid membrane and less ATP production, leading to a reduction in growth in oeCyt c_{6A} lines compared to the wild type and mutant.

When the light intensity increases, the rate of photosynthetic electron transport becomes saturated, as the light is in excess of the requirement for the maximum photosynthetic rate (Erickson *et al*., 2015). In wild type plants, the excess light absorbed by the antenna proteins of PSII is dissipated as heat through PsbS mediated NPQ. This mechanism is activated by low lumenal pH resulting from cyclic electron flow through PGR5 and PGRL1 (Suorsa *et al*., 2015), which have thiol groups that can accept electrons from ferredoxin (Hertle *et al*., 2013; Tikkanen *et al*., 2015). Under high light intensity, PGR5 and PGRL1 may sense the redox state of PSI electron acceptors and mediate the cyclic electron transfer pathway from ferredoxin to the PQ pool via Ferredoxin –PQ oxidoreductase ((FQR) (Johnson 2011; Tikkanen *et al*., 2015). Through this mechanism PGR5 and PGRL 1 are expected to enhance the generation of ΔpH and NPQ. As the PQ pool gets increasingly reduced, PsbS protein dissipates excess energy as heat and the Cyt c_{6A} functions as an electron sink, accepting excess electrons from the PQ pool and donating them to Pc/PSI bypassing the Cyt b_6f complex. In ΔCyt c_{6A} the bypassing pathway is eliminated, which makes the system less able to sustain CEF, with consequently less NPQ. Thus the ΔCyt c_{6A} mutant could not dissipate excess excitation energy as heat compared to wild type. This, together with the more reduced PQ pool, may in turn result in reactive oxygen species that will damage the photosystems and other components of the cell, and lead to reduced growth compared to wild type plants in high light intensities. This imply that PsbS alone cannot dissipate the excess energy as heat it needs Cyt c_{6A}'s support to get rid of excess electrons from the PQ pool. These results therefore suggest an important role for Cyt c_{6A} under high light intensities for normal plant growth and development. The oeCyt c_{6A} lines showed similar growth to wild type in 300

μE m^{-2} s^{-1} light intensity and better growth compared to wild type in 500 μE m^{-2} s^{-1} light intensity. This may have resulted from an enhanced ability to reoxidise PQ in the overexpression lines.

The measurements of the $P700^+$ reduction kinetics of ΔCyt c_{6A} and wild type plants are consistent with Cyt c_{6A} transferring electrons to PSI via plastocyanin. The fact that the rate of $P700^+$ reduction in ΔCyt c_{6A} was relatively slower than in wild type, suggests an involvement of Cyt c_{6A} in PSI reduction.

Our findings therefore indicate that Cyt c_{6A} has an important function in the plant. Gupta el al 2002 reported that Cyt c_{6A} mutant plants did not show a visible phenotype (figure 6.12). However, we observed a clearly visible growth phenotype in the Cyt c_{6A} knockout mutant at 150 μE m^{-2} $s^{-1}$and greater light intensities. Gupta *et al*., 2002 and Weigel *et al*., (2003b) also did not report the growth performance of ΔCyt c_{6A} mutant under high light conditions to test for a growth impairment of ΔCyt c_{6A} mutant.

Gupta *et al*., 2002 reported a growth impairment in a Pc RNAi line in a wild type background where there is a normal level of Cyt c_{6A} expression (figure 6.12. 3), and that plants lacking both Pc and Cyt c_{6A} failed to grow photoautotrophically. Based on these results they claimed that Cyt c_{6A} replaces Pc under normal growth condition. However, Weigel *et al*., (2003b) demonstrated that knocking out individual *petE* genes (*petE1* and *petE2*) causes a growth phenotype and the Pc double knockout (*petE1:petE2*) mutant failed to grow photoautotrophically, although it could be grown in axenic culture on medium supplemented with sucrose. Weigel *et al*., (2003b) also tried to increase the level of Cyt c_{6A} in a Pc double knockout mutant but found that the former failed to perform as an electron carrier under normal conditions. Based on these data they suggested Pc is indispensible for photosynthetic electron transport in *Arabidopsis thaliana*.

It is likely that residual Pc expression takes place in the Pc RNAi line of Gupta *et al*., 2002, because of leakiness in gene silencing (Weigel *et al*., 2003). This residual Pc RNAi line might have retained enough Pc to support the residual level of photosynthesis. If Cyt c_{6A} can only transfer electrons to Pc, it is not clear why loss of Cyt c_{6A} in the Pc-deficient background would be lethal. However, it may be that inefficient electron transfer from

Cyt c_{6A} to PSI directly contributes to viability, in which case Cyt c_{6A} loss in a Pc-deficient background would be lethal.

A schematic model showing different routes of electron transfer chain in the WT, and ΔCyt $c_{6A,}$ oeCyt c_{6A} and *pgr5* lines in a range of light conditions is given in Figure 6.13.

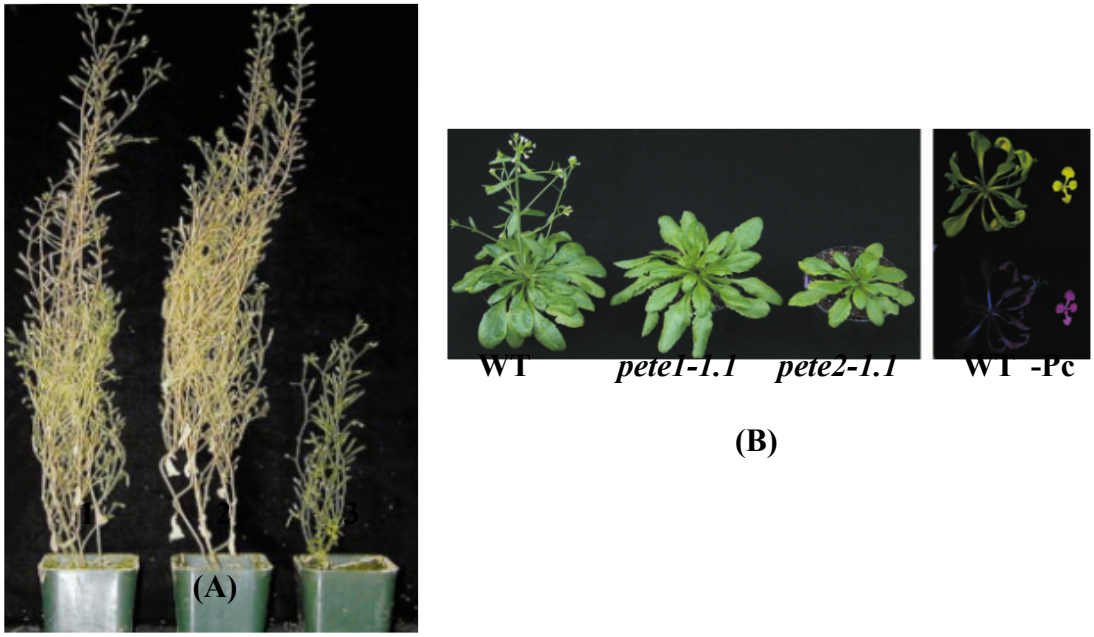

Fig.6.12: Growth characterization of plastocyanin and ΔCyt c_{6A} knockout mutants generated by Gupta *et al.,* 2002 (A), Wild type (1), ΔCyt c_{6A} (2), Pc RNAi line (3) and Weigel *et al*., 2003b (B), WT (wild type), pete-1.1 9 (*Δpete1*), *pete2*-1.1 (*Δpete2*) –Pc (*pete* double knockout).

≤ Growth Light (WT, ΔCyt c_{6A}, and *pgr*5)

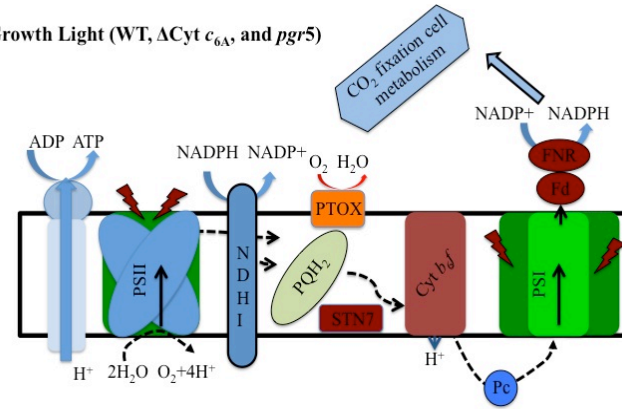

≤ Growth Light (oeCyt c_{6A})

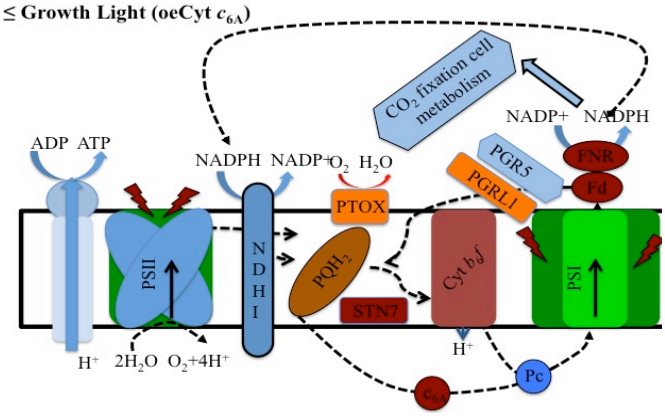

High Light (WT)

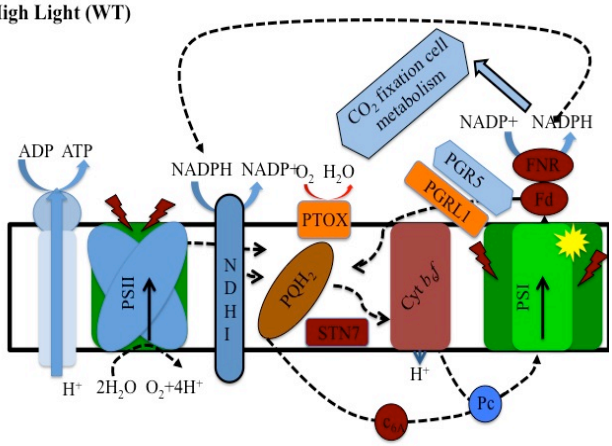

High Light (*pgr*5)

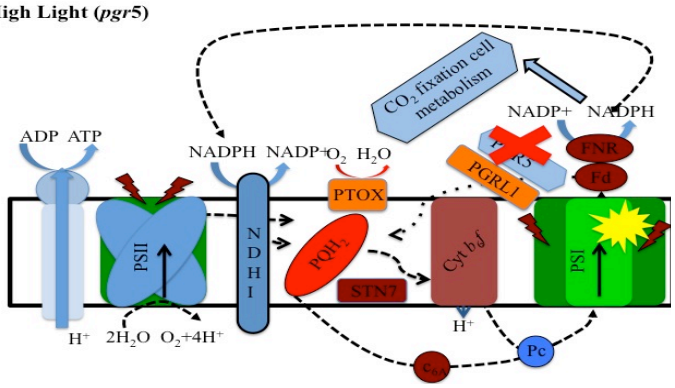

High Light (ΔCyt c_{6A})

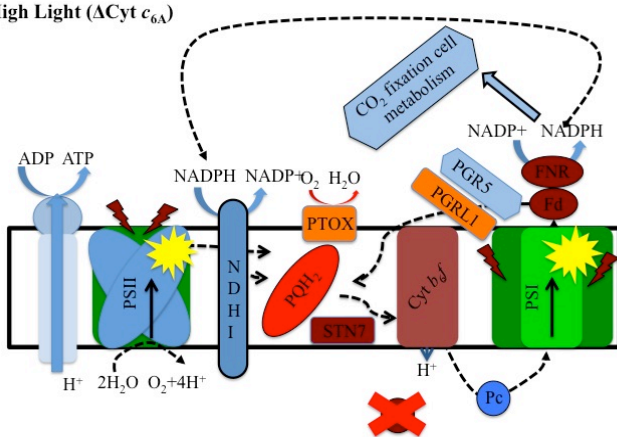

High Light (oeCyt c_{6A})

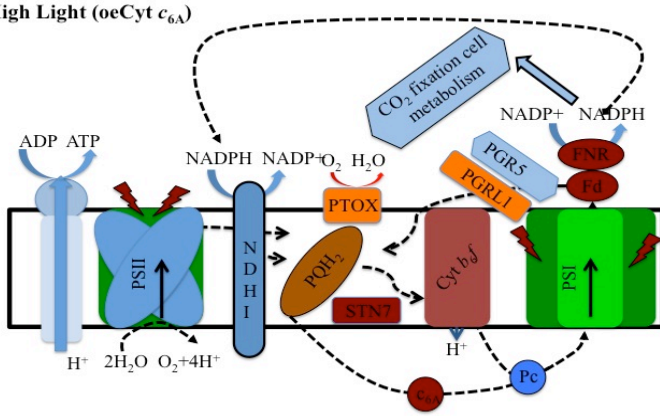

Figure 6.12: Schematic model showing different routes of electron transfer chain in WT, ΔCyt c_{6A}, and *pgr5* mutants and Cyt c_{6A} overexpression lines in growth light (20-150 μE m^{-2} s^{-1} light intensities) and high light intensities (300 & 500 μE m^{-2} s^{-1} and above). At growth light or below the growth light intensity WT, ΔCyt c_{6A} and *pgr5* could keep the intersystem electron transfer chain optimally oxidized, but in the over expression line the linear electron flow is disrupted and cyclic electron flow would more active. An increase in light intensity enhances ΔpH in WT, but not in ΔCyt c_{6A} and *pgr5*. Increased ΔpH slows down electron flow via Cyt b_6f in WT, but induces NPQ only in WT. In WT, NPQ prevents the over-reduction of Plastoquinone (PQ) pool and slows down the Cyt b_6f leading to oxidation of plastocyanin (Pc) and photosystem I (PSI). In ΔCyt c_{6A} that is unable to sustain a ΔpH of the same size, upon increasing light intersystem electron transfer chain becomes over reduced. Similar results can also seen in *pgr5* mutant that cannot increase the ΔpH upon increase in light intensity; the entire electron transfer chain becomes over-reduced. This results from the inability to slow down the Cyt b_6f rather than from the low level of NPQ.

CHAPTER 7 OVERALL DISCUSSIONS AND SUGGESTIONS FOR FUTURE EXPERIMENTS

7.1 Cyt c_{6C}/c_{6B} and Cyt c_M in cyanobacteria and Cyt c_{6A} in plants

Several low molecular weight redox proteins are present in cyanobacteria or plants. These are Cyt c_{6C}/c_{6B} (chapter 4), Cyt c_M (chapter 5) – all in cyanobacteria - and Cyt c_{6A} (chapter 6) in plants. The presence of modified forms of Cyt c_6 (Cyt c_{6A}) in plants and algae was reported in 2002. Genes for Cyt c_{6C}/c_{6B} were discovered from phylogenetic analysis and found in most cyanobacteria, and Cyt c_M is found in almost all cyanobacteria (Bialek *et al*., 2008; Cramer and Kallas 2016). The widespread distribution of genes for these cytochromes in cyanobacteria suggests important roles under certain circumstances. Cyt c_{6C}/c_{6B}, Cyt c_{6A} and Cyt c_M proteins have low redox midpoint potentials from 148 ± 1.7 mV to +199 mV range, which are too low to substitute effectively for Cyt c_6 or PC in electron transfer from the Cyt b_6f complex to PSI (Cho *et al*., 2000; Bialek *et al*., 2008; Reyes-Sosa *et al*., 2011; Zatwarnicki *et al*., 2014 Cramer and Kallas 2016).

In this thesis, we addressed the roles of these low molecular weight redox proteins under different light conditions. We successfully and individually knocked out Cyt c_{6C} and Cyt c_M coding genes in *S. elongatus* PCC 7942. Using the knockout lines we performed growth characterization studies under different light levels and RNA was extracted from cells grown under two different light levels to investigate the transcriptomes. Finally we studied the electron transport chain of ΔCyt $c_{6C,}$ and ΔCyt c_M along with wild type, with regard to the rate of oxygen evolution, respiration, and $P700^+$ reduction. Parameters such as *F*v/*F*m, ΦPSII yield and NPQ kinetics were also measured. Our findings have suggested the presence of new alternative electron transport pathways in cyanobacteria. According to the model proposed here, under extreme light conditions Cyt c_{6C} accepts electrons directly from the PQ pool and donates them to PC or directly to PSI bypassing the Cyt b_6f complex, and Cyt c_M accepts electron directly from the PQ pool, donating them to cytochrome oxidase.

After the surprising discovery of Cyt c_{6A} in 2002, several reports were published regarding the function of Cyt c_{6A} in higher plants. However, few of them reported *in vivo* experiments, which encouraged us to study the protein's functions *in vivo*. For this thesis,

Cyt c_{6A} overexpression lines were generated and confirmed for overexpression. Growth characterisation of these lines, along with ΔCyt c_{6A} lines and wild type plants, was tested in culture plates and in a plant growth facility. The oeCyt c_{6A}-EYFP line was used for localization by fluorescence microscopy. Finally we studied the electron transport chain of ΔCyt c_{6A} and wild type under two different light intensities, by measuring chlorophyll fluorescence, and $P700^+$ reduction. Parameters such as Fv/Fm, ΦPSII yield and NPQ kinetics were measured under 245 and 975 $\mu E\ m^{-2}s^{-1}$ light intensities. Based on our findings we proposed the hypothesis that Cyt c_{6A} is located in the thylakoid lumen and transfers electrons from the PQ pool to PSI, probably via PC bypassing the Cyt b_6f complex.

7.2 Possible future experiments

We successfully and individually knocked out Cyt c_{6C} and Cyt c_M coding genes in the cyanobacterium *S. elongatus* PCC 7942. However, because of the inability of the transgenic lines to undergo further transformation, we could not achieve double knockouts. Current advances in synthetic biology research have been underpinned by the exponential increase of advanced multigene editing and gene silencing tools. CRISPR/Cpf1 provides an excellent opportunity to generate multiplex gene knockouts and gene silencing (Zetsche *et al*., 2017; Tang *et al*., 2017; Wang *et al*., 2017; Kim *et al*., 2017). Such tools have been adapted for cyanobacterial gene knockout, knock-in and multiplex gene silencing (Yao *et al*., 2016; Behler *et al*., 2018; Ungerer and Pakrasi 2016; Wendt *et al*., 2016; Vasudevan *et al*., 2019). Generating double knockouts of Cyt c_{6C} and Cyt c_M is essential to understand the roles of these protein, especially under high light conditions and to test the proposed hypothesis. Double knockouts of Cyt c_{6C} & PC, Cyt c_M & PC, Cyt c_6 & Cyt c_M would possibly also be useful for further understanding and testing the proposed alternative electron transport routes. Tagging Cyt c_{6C} and Cyt c_M with His or myc tags would allow for protein pulldown analyses and studies on protein-protein interactions, although these would be limited by the possibly transient nature of the redox interactions. Generating Cyt c_{6C} and Cyt c_M over-expression lines with inducible promoters in knockout backgrounds would be useful to fine tune the functionality of the alternative pathways in cyanobacteria.

Photosynthetic electron transport inhibitor studies using DCMU (3-(3,4-dichlorophenyl)-1,1-dimethylurea), a specific sensitive inhibitor that inhibits the plastoquinone binding

site of PSII, and DBMIB (2,5-dibromo-3-methyl-6-isopropylbenzoquinone), which inhibits electron flow through the Cyt b_6f complex, would allow characterization of an alternative electron transport route from the PQ pool to PSI or Cyt oxidase in cyanobacteria. Investigation of the exoelectrogenic activity of ΔCyt c_{6C} and ΔCyt c_M lines would help to understand how the cell copes with excess electrons, so it would be interesting to measure current outputs in these two mutants.

The Cyt c_{6A}-EYFP fusion experiment demonstrated that Cyt c_{6A} was located in the chloroplast and possibly in the thylakoid lumen. However, protein aggregation was seen in the chloroplast, so immunogold labeling without overexpression would help to confirm the location of Cyt c_{6A} in thylakoid lumen. At 300 μE m^{-2} s^{-1} light intensity, we observed that growth of the ΔCyt c_{6A} line was highly reduced compared to wild type, and the growth of over expression lines was similar to wild type. At 500 μE m^{-2} s^{-1} light, the ΔCyt c_{6A} showed significantly reduced growth phenotype compared to wild type and overexpression lines. Interestingly, enhanced growth was observed in 500 μE m^{-2} s^{-1} light intensity when the protein was overexpressed. Doing RNAseq analysis of ΔCyt c_{6A} and oeCyt c_{6A} and wild type at 300 and 500 μE m^{-2} s^{-1} would help to understand the role of Cyt c_{6A} under high light conditions.

Bibliography

Adir, N., Zer, H., Shochat, S., Ohad, I. (2003). Photoinhibition – a historical perspective. *Photosynthesis Research*, *76*, 343–370.

Albarrán, C., Navarro, J. A., Molina-Heredia, F. P., Murdoch, P. D. S., De La Rosa, M. A., Hervás, M. (2005). Laser flash-induced kinetic analysis of cytochrome f oxidation by wild-type and mutant plastocyanin from the cyanobacterium Nostoc sp. PCC 7119. *Biochemistry*, *44*(34), 11601–11607. https://doi.org/10.1021/bi050917g

Allahverdiyeva, Y., Isojärvi, J., Zhang, P., Aro, E.-M. (2015a). Cyanobacterial Oxygenic Photosynthesis is Protected by Flavodiiron Proteins. *Life (Basel, Switzerland)*, *5*(1), 716–743. https://doi.org/10.3390/life5010716

Allahverdiyeva, Y., Suorsa, M., Tikkanen, M., Aro, E. M. (2015b). Photoprotection of photosystems in fluctuating light intensities. *Journal of Experimental Botany*, *66*(9), 2427–2436. https://doi.org/10.1093/jxb/eru463

Allen, J. F., de Paula, W. B. M., Puthiyaveetil, S., Nield, J. (2011). A structural phylogenetic map for chloroplast photosynthesis. *Trends in Plant Science*, *16*(12), 645–655. https://doi.org/10.1016/j.tplants.2011.10.004

Anders, S., & Huber, W. (2013). Differential expression of RNA-Seq data at the gene level – the DESeq package. *Bioconductor Package Vignette*.

Bailey, S., Grossman, A. (2008). Photoprotection in cyanobacteria: Regulation of light harvesting. In *Photochemistry and Photobiology* (Vol. 84, pp. 1410–1420). https://doi.org/10.1111/j.1751-1097.2008.00453.x

Baker, N. R. (2008). Chlorophyll fluorescence: a probe of photosynthesis in vivo. *Annual Review of Plant Biology*, *59*, 89–113. https://doi.org/10.1146/annurev.arplant.59.032607.092759

Behler, J., Vijay, D., Hess, W. R., Akhtar, M. K. (2018). CRISPR-Based Technologies for Metabolic Engineering in Cyanobacteria. *Trends in Biotechnology*, *xx*. https://doi.org/10.1016/j.tibtech.2018.05.011

Bellafiore, S., Barneche, F., Peltier, G., Rochaix, J.-D. (2005). State transitions and light adaptation require chloroplast thylakoid protein kinase STN7. *Nature*, *433*(7028), 892–895. https://doi.org/10.1038/nature03286

Bendtsen, J. D., Nielsen, H., Widdick, D., Palmer, T., Brunak, S. (2005). Prediction of twin-arginine signal peptides. *BMC Bioinformatics*, *6*(167). https://doi.org/10.1186/1471-2105-6-167

Bernroitner, M., Tangl, D., Lucini, C., Furtmüller, P. G., Peschek, G. A., Obinger, C. (2009). Cyanobacterial cytochrome c_M: Probing its role as electron donor for CuA of cytochrome c oxidase. *Biochimica et Biophysica Acta - Bioenergetics*, *1787*(3), 135–143. https://doi.org/10.1016/j.bbabio.2008.12.003

Bersanini, L., Battchikova, N., Jokel, M., Rehman, A., Vass, I., Allahverdiyeva, Y., Aro, E.-M. (2014). Flavodiiron protein Flv2/Flv4-related photoprotective mechanism dissipates excitation pressure of PSII in cooperation with phycobilisomes in Cyanobacteria. *Plant Physiology*, *164*(2), 805–818. https://doi.org/10.1104/pp.113.231969

Berry, S., Schneider, D., Vermaas, W. F. J., Rögner, M. (2002). Electron Transport Routes in Whole Cells of Synechocystis sp. Strain PCC 6803: The Role of the Cytochrome bd -Type Oxidase. *Biochemistry*, *41*(10), 3422–3429. https://doi.org/10.1021/bi011683d

Bialek, W., Nelson, M., Tamiola, K., Kallas, T., Szczepaniak, A. (2008). Deeply branching c_6-like cytochromes of cyanobacteria. *Biochemistry*, *47*(20), 5515–5522. https://doi.org/10.1021/bi701973g

Bombelli, P., Bradley, R. W., Scott, A. M., Philips, A. J., Mccormick, A. J., Cruz, S. M., … Fisher, A. C. (2011). Quantitative analysis of the factors limiting solar power

transduction by Synechocystis sp. PCC 6803 in biological photovoltaic devices. *Energy & Environmental Science*, *4*, 4690–4698. https://doi.org/10.1039/c1ee02531g

Bonfils, M. H. J., Lu, C., Niyogi, K. K. (2000). Photodamage of the Photosynthetic Apparatus and Its Dependence on the Leaf Developmental Stage in the. *Society*, *124*(September), 273–284.

Bovy, A., Devrieze, G., Borrias, M., Weisbeek, P. (1992). Transcriptional Regulation of the Plastocyanin and Cytochrome-c553 Genes from the Cyanobacterium Anabaena Species PCC-7937. *Mol Microbiol*, *6*, 1507–1513.

Brettel, K. (1997). Electron transfer and arrangement of the redox cofactors in photosystem I. *Biochimica et Biophysica Acta - Bioenergetics*, *1318*(3), 322–373. https://doi.org/10.1016/S0005-2728(96)00112-0

Campbell, D., Hurry, V., Clarke, A. K., Gustafsson, P., Oquist, G. (1998). Chlorophyll fluorescence analysis of cyanobacterial photosynthesis and acclimation. *Microbiology and Molecular Biology Reviews : MMBR*, *62*(3), 667–683.

Cooley, J. W., Vermaas, W. F. J. (2001). Succinate dehydrogenase and other respiratory pathways in thylakoid membranes of Synechocystis sp. strain PCC 6803: Capacity comparisons and physiological function. *Journal of Bacteriology*, *183*, 4251–4258. https://doi.org/10.1128/JB.183.14.4251-4258.2001

Chang, L., Liu, X., Li, Y., Liu, C.-C., Yang, F., Zhao, J., Sui, S.-F. (2015). Structural organization of an intact phycobilisome and its association with photosystem II. *Cell Research*, *25*(6), 726–737. https://doi.org/10.1038/cr.2015.59

Chauvat, F., Vries, L., Ende, A. (1986). A host-vector system for gene cloning in the cyanobacterium Synechocystis PCC 6803. *Molecular and General Genetics*, 185–191. https://doi.org/10.1007/BF00330208

Cho, Y. S., Pakrasi, H. B., Whitmarsh, J. (2000). Cytochrome $c_{(M)}$ from *Synechocystis*

6803: Detection in cells, expression in Escherichia coli, purification and physical characterization. *European Journal of Biochemistry*, *267*(4), 1068–1074. https://doi.org/10.1046/j.1432-1327.2000.01092.x

Chida, H., Yokoyama, T., Kawai, F., Nakazawa, A., Akazaki, H., Takayama, Y., … Oku, T. (2006). Crystal structure of oxidized cytochrome c6A from Arabidopsis thaliana. *FEBS Letters*, *580*(15), 3763–3768. https://doi.org/10.1016/j.febslet.2006.05.067

Chukhutsina, V., Bersanini, L., Aro, E. M., Van Amerongen, H. (2015). Cyanobacterial flv4-2 operon-encoded proteins optimize light harvesting and charge separation in photosystem II. *Molecular Plant*, *8*(5), 747–761. https://doi.org/10.1016/j.molp.2014.12.016

Ciszak, K., Kulasek, M., Barczak, A., Grzelak, J., Maćkowski, S., Karpiński, S. (2015). PsbS is required for systemic acquired acclimation and post-excess-light-stress optimization of chlorophyll fluorescence decay times in *Arabidopsis*. *Plant Signaling & Behavior*, *10*(1), e982018. https://doi.org/10.4161/15592324.2014.982018

Clough, S. J., Bent, A. F. (1998). Floral dip: A simplified method for Agrobacterium-mediated transformation of *Arabidopsis thaliana*. *Plant Journal*, *16*(6), 735–743. https://doi.org/10.1046/j.1365-313X.1998.00343.x

Cramer, W. A., Kallas, T. (2016). *Including Bioenergy and Related Processes Cytochrome Complexes : Evolution , Structures , Energy Transduction , and Signaling*.

DalCorso, G., Pesaresi, P., Masiero, S., Aseeva, E., Schünemann, D., Finazzi, G., Leister, D. (2008). A Complex Containing PGRL1 and PGR5 Is Involved in the Switch between Linear and Cyclic Electron Flow in *Arabidopsis*. *Cell*, *132*(2), 273–285. https://doi.org/10.1016/j.cell.2007.12.028

Dexter, J., Fu, P. (2009). Metabolic engineering of cyanobacteria for ethanol production.

Energy & Environmental Science, *2*(8), 857. https://doi.org/10.1039/b811937f

Durán, R. V., Hervás, M., De La Rosa, M. A., Navarro, J. A. (2004). The Efficient Functioning of Photosynthesis and Respiration in Synechocystis sp. PCC 6803 Strictly Requires the Presence of either Cytochrome c6 or Plastocyanin. *Journal of Biological Chemistry*, *279*(8), 7229–7233. https://doi.org/10.1074/jbc.M311565200

Dong, L., Tu, W., Liu, K., Sun, R., Liu, C., Wang, K., Yang, C. (2015). The PsbS protein plays important roles in photosystem II supercomplex remodeling under elevated light conditions. *Journal of Plant Physiology*, *172*, 33–41. https://doi.org/10.1016/j.jplph.2014.06.003

Ebenhöh, O., Fucile, G., Finazzi, G., Rochaix, J., Ebenho, O., Goldschmidt-Clermont, M. (2014). Short-term acclimation of the photosynthetic electron transfer chain to changing light : a mathematical model Short-term acclimation of the photosynthetic electron transfer chain to changing light : a mathematical model Author for correspondence :

Eberhard, S., Finazzi, G., Wollman, F.-A. (2008). The dynamics of photosynthesis. *Annual Review of Genetics*, *42*, 463–515. https://doi.org/10.1146/annurev.genet.42.110807.091452

Eisenhut, M., Georg, J., Klähn, S., Sakurai, I., Mustila, H., Zhang, P., Aro, E. M. (2012). The antisense RNA As1-flv4 in the cyanobacterium *Synechocystis* sp. PCC 6803 prevents premature expression of the flv4-2 operon upon shift in inorganic carbon supply. *Journal of Biological Chemistry*, *287*(40), 33153–33162. https://doi.org/10.1074/jbc.M112.391755

Erickson, E., Wakao, S., Niyogi, K. K. (2015). Light stress and photoprotection in *Chlamydomonas reinhardtii. The Plant Journal*, n/a-n/a. https://doi.org/10.1111/tpj.12825

Forstner, K. U., Vogel, J., & Sharma, C. M. M. (2014). READemption - A tool for the computational analysis of deep-sequencing-based transcriptome data. *bioRxiv*, 0–2.

http://doi.org/10.1101/003723

Frank, K., Sippl, M. J. (2008). High-performance signal peptide prediction based on sequence alignment techniques. *Bioinformatics (Oxford, England)*, *24*(19), 2172–2176. https://doi.org/10.1093/bioinformatics/btn422

Fujimori, T., Hihara, Y., Sonoike, K. (2005). PsaK2 subunit in photosystem I is involved in state transition under high light condition in the cyanobacterium *Synechocystis* sp. PCC 6803. *Journal of Biological Chemistry*, *280*(23), 22191–22197. https://doi.org/10.1074/jbc.M500369200

Golden, S. S. (1995). Light-responsive gene expression in cyanobacteria. *Journal of Bacteriology*, *177*(7), 1651–1654.

Gollan, P. J., Tikkanen, M., Aro, E.-M. (2015). Photosynthetic light reactions: integral to chloroplast retrograde signalling. *Current Opinion in Plant Biology*, *27*, 180–191. https://doi.org/10.1016/j.pbi.2015.07.006

González, L., Bolaño, C., Pellissier, F. (2003). Use of Oxygen Electrode in Measurements of Photosynthesis and Respiration. *Handbook of Plant Ecophysiology Techniques*, (Figure 1), 141–153. https://doi.org/10.1007/0-306-48057-3_9

Grieco, M., Tikkanen, M., Paakkarinen, V., Kangasjarvi, S., Aro, E.-M. (2012). Steady-state phosphorylation of light-harvesting complex II proteins preserves Photosystem I under fluctuating white light. *Plant Physiology*, *160*(December), 1896–1910. https://doi.org/10.1104/pp.112.206466

Gupta, R., He, Z., Luan, S. (2002). Functional relationship of cytochrome c(6) and plastocyanin in *Arabidopsis*. *Nature*, *417*(6888), 567–571. https://doi.org/10.1038/417567a

Hart, S. E., Schlarb-Ridley, B. G., Bendall, D. S., Howe, C. J. (2005). Terminal oxidases of cyanobacteria. *Biochemical Society Transactions*, *33*(Pt 4), 832–835.

https://doi.org/10.1042/BST0330832

Helman, Y., Tchernov, D., Reinhold, L., Shibata, M., Ogawa, T., Schwarz, R., Kaplan, A. (2003). Genes encoding A-type flavoproteins are essential for photoreduction of O2 in cyanobacteria. *Current Biology*, *13*(3), 230–235. https://doi.org/10.1016/S0960-9822(03)00046-0

Hertle, A. P., Blunder, T., Wunder, T., Pesaresi, P., Pribil, M., Armbruster, U., Leister, D. (2013). PGRL1 Is the Elusive Ferredoxin-Plastoquinone Reductase in Photosynthetic Cyclic Electron Flow. *Molecular Cell*, *49*(3), 511–523. https://doi.org/10.1016/j.molcel.2012.11.030

Hiraide, Y., Oshima, K., Fujisawa, T., Uesaka, K., Hirose, Y., Tsujimoto, R., Fujita, Y. (2015). Loss of Cytochrome c_M Stimulates Cyanobacterial Heterotrophic Growth in the Dark. *Plant and Cell Physiology*, *56*(2), 334–345. https://doi.org/10.1093/pcp/pcu165

Ho, K. K., Kerfeld, C. A., Krogmann, D. W. (2011). The Water-Soluble Cytochromes of Cyanobacteria. *Group*, 515–540. https://doi.org/10.1007/978-94-007-0388-9

Hohmann-Marriott, M. F., Blankenship, R. E. (2011). Evolution of photosynthesis. *Annual Review of Plant Biology*, *62*, 515–548. https://doi.org/10.1146/annurev-arplant-042110-103811

Howe, C. J., Schlarb-Ridley, B. G., Wastl, J., Purton, S., Bendall, D. S. (2006). The novel cytochrome c_6 of chloroplasts: A case of evolutionary bricolage? *Journal of Experimental Botany*, *57*(1), 13–22. https://doi.org/10.1093/jxb/erj023

Howe, C. J., Nimmo, R. H., Barbrook, A. C., Bendall, D. S. (2016). Cytochrome c_{6A} of Chloroplasts (pp. 701–712). Springer, Dordrecht. https://doi.org/10.1007/978-94-017-7481-9_33

Howitt, C. A., Vermaas, W. F. (1998). Quinol and cytochrome oxidases in the cyanobacterium Synechocystis sp. PCC 6803. *Biochemistry*, *37*(51), 17944–17951.

Retrieved from http://www.ncbi.nlm.nih.gov/pubmed/9922162

Johnson, G. N. (2011). Reprint of: Physiology of PSI cyclic electron transport in higher plants. *Biochimica et Biophysica Acta - Bioenergetics*, *1807*(8), 906–911. https://doi.org/10.1016/j.bbabio.2011.05.008

Kanazawa, A., Kramer, D. M. (2002). In vivomodulation ofnonphotochemical exciton quenching (NPQ) by regulation of the chloroplast ATP synthase. Proc. Natl. Acad. Sci. U.S.A. 99, 12789–12794. doi: 10.1073/pnas.182427499.

Kim, H. K., Song, M., Lee, J., Menon, A. V., Jung, S., Kang, Y. M., … Kim, H. (2017). In vivo high-throughput profiling of CRISPR-Cpf1 activity. *Nature Methods*, *14*(2), 153–159. https://doi.org/10.1038/nmeth.4104

King, J. D., Liu, H., He, G., Orf, G. S., Blankenship, R. E. (2014). Chemical activation of the cyanobacterial orange carotenoid protein. *FEBS Letters*, *588*(24), 4561–4565. https://doi.org/10.1016/j.febslet.2014.10.024

Kingsford, C. L., Ayanbule, K., Salzberg, S. L. (2007). Rapid, accurate, computational discovery of Rho-independent transcription terminators illuminates their relationship to DNA uptake. *Genome Biology*, *8*(2), R22.1-R22.12. https://doi.org/10.1186/gb-2007-8-2-r22

Kiirats, O., Cruz, J. A., Edwards, G. E., Kramer, D. M. (2009). Feedback limitation of photosynthesis at high CO2 acts by modulating the activity of the chloroplast ATP synthase. *Functional Plant Biology*, *36*(11), 893–901. https://doi.org/10.1071/FP09129

Kleffmann, T., Russenberger, D., Von Zychlinski, A., Christopher, W., Sjölander, K., Gruissem, W., Baginsky, S. (2004). The *Arabidopsis thaliana* chloroplast proteome reveals pathway abundance and novel protein functions. *Current Biology*, *14*(5), 354–362. https://doi.org/10.1016/j.cub.2004.02.039

Kramer, D. M., Sacksteder, C. A., Cruz, J. A. (1999). How acidic is the lumen ?

Photosynth. Res., *60*, 151–163.

Laisk, A., Eichelmann, H., Oja, V., Peterson, R. B. (2005). Control of cytochrome b_6f at low and high light intensity and cyclic electron transport in leaves, *1708*, 79–90. https://doi.org/10.1016/j.bbabio.2005.01.007

Lange, C., Herv, M., Rosa, M. A. De. (2003). Analysis of the stability of cytochrome c 6 with an improved stopped-flow protocol. *BIOCHEMICAL AND BIOPHYSICAL RESEARCH COMMUNICATIONS*, *310*, 215–221. https://doi.org/10.1016/j.bbrc.2003.09.010

Larkin, M. A., Blackshields, G., Brown, N. P., Chenna, R., McGettigan, P. A., McWilliam, H., Higgins, D. G. (2007). Clustal W and Clustal X version 2.0. *Bioinformatics (Oxford, England)*, *23*(21), 2947–2948. https://doi.org/10.1093/bioinformatics/btm404

Latifi, A., Ruiz, M., Zhang, C. C. (2009). Oxidative stress in cyanobacteria. *FEMS Microbiology Reviews*, *33*(2), 258–278. https://doi.org/10.1111/j.1574-6976.2008.00134.x

Lea-Smith, D. J., Ross, N., Zori, M., Bendall, D. S., Dennis, J. S., Scott, S. A., Howe, C. J. (2013). Thylakoid Terminal Oxidases Are Essential for the Cyanobacterium *Synechocystis* sp. PCC 6803 to Survive Rapidly Changing Light Intensities. *Plant Physiology*, *162*(1), 484–495. https://doi.org/10.1104/pp.112.210260

Lea-Smith, D. J., Bombelli, P., Vasudevan, R., Howe, C. J. (2015). Photosynthetic, respiratory and extracellular electron transport pathways in cyanobacteria. *Biochimica et Biophysica Acta (BBA) - Bioenergetics*, *1857*(3), 1–9. https://doi.org/10.1016/j.bbabio.2015.10.007

Lea-Smith, D.J., Vasudevan, R., Howe, C.J. (2016). Generation of Marked and Markerless Mutants in Model Cyanobacterial Species. *J. Vis. Exp.* (111), e54001, doi:10.3791/54001.

Li, X.-P., Muller-Moule, P., Gilmore, A. M., Niyogi, K. K. (2002). PsbS-dependent enhancement of feedback de-excitation protects photosystem II from photoinhibition. *Proceedings of the National Academy of Sciences of the United States of America*, *99*(23), 15222–15227. https://doi.org/10.1073/pnas.232447699

Li, Xiao Ping, Gilmore, Adam M., Caffarri, Stefano., Bassi, Roberto., Golan, Talila., Kramer, David., Krishna K. Niyogi. (2004). Regulation of photosynthetic light harvesting involves intrathylakoid lumen pH sensing by the PsbS protein. *Journal of Biological Chemistry*. 279, (22), 22866–22874.

Liu, L., Bryan, S. J., Huang, F., Yu, J., Nixon, P. J., Rich, P. R. (2012). Control of electron transport routes through redox-regulated redistribution of respiratory complexes, *109*(28). https://doi.org/10.1073/pnas.1120960109

Lucini, C. (2008). CuA and cytochrome Cm from the cyanobacterium Nostoc PCC 7120. PhD thesis.

Malakhov, M. P., Wada, H., Los, D. A., Semenenko, V. E., Murata, N. (1994). A New Type of Cytochrome c from *Synechocystis* PCC6803. *Journal of Plant Physiology*, *144*(3), 259–264. https://doi.org/http://dx.doi.org/10.1016/S0176-1617(11)81183-1

Malakhov, M. P., Malakhova, O. a., Murata, N. (1999). Balanced regulation of expression of the gene for cytochrome $c_{(M)}$ and that of genes for plastocyanin and cytochrome c6 in Synechocystis. *FEBS Letters*, *444*(2–3), 281–284. https://doi.org/10.1016/S0014-5793(99)00074-5

Manna, P., Vermaas, W. (1997). Lumenal proteins involved in respiratory electron transport in the cyanobacterium *Synechocystis* sp. PCC6803. *Plant Molecular Biology*, *35*, 407–416. https://doi.org/10.1023/A:1005875124387

Marcaida, M. J., Schlarb-Ridley, B. G., Worrall, J. a R., Wastl, J., Evans, T. J., Bendall, D. S., … Howe, C. J. (2006). Structure of cytochrome c_{6A}, a novel dithio-cytochrome of Arabidopsis thaliana, and its reactivity with plastocyanin: implications for function. *Journal of Molecular Biology*, *360*(5), 968–977.

https://doi.org/10.1016/j.jmb.2006.05.065

Mason, J. M., Bendall, D. S., Howe, C. J., Worrall, J. A. R. (2012). The role of a disulfide bridge in the stability and folding kinetics of Arabidopsis thaliana cytochrome $c_{(6A)}$. *Biochimica et Biophysica Acta*, *1824*(2), 311–318. https://doi.org/10.1016/j.bbapap.2011.10.015

Maxwell, K., Johnson, G. N. (2000). Chlorophyll fluorescence--a practical guide. *J. Exp. Bot.*, *51*(345), 659–668. https://doi.org/10.1093/jexbot/51.345.659

Molina-Heredia, F. P., Balme, A., Hervás, M., Navarro, J. a., De la Rosa, M. a. (2002). A comparative structural and functional analysis of cytochrome c_M, cytochrome c_6 and plastocyanin from the cyanobacterium Synechocystis sp. PCC 6803. *FEBS Letters*, *517*(1–3), 50–54. https://doi.org/10.1016/S0014-5793(02)02576-0

Molina-Heredia, F. P., Jürgen, Wastl, José A.Navarro, D. S. B., Manuel Hervás, Christopher J.Howe, A. D. la R. (2003). A new function for an old cytochrome? *Nature*, *424*(6944), 33–34. https://doi.org/10.1038/424033a

Müller, P., Li, X. P., Niyogi, K. K. (2001). Non-photochemical quenching. A response to excess light energy. *Plant Physiology*, *125*(4), 1558–1566. https://doi.org/10.1104/pp.125.4.1558

Mullineaux, C. W., Allen, J. F. (1990). State 1-State 2 transitions in the cyanobacterium *Synechococcus* 6301 are controlled by the redox state of electron carriers between Photosystems I and II. *Photosynthesis Research*, *23*(3), 297–311. https://doi.org/10.1007/BF00034860

Mullineaux, C. W., Emlyn-Jones, D. (2005). State transitions: An example of acclimation to low-light stress. *Journal of Experimental Botany*, *56*(411), 389–393. https://doi.org/10.1093/jxb/eri064

Mulo, P., Sicora, C., Aro, E. M. (2009). Cyanobacterial psbA gene family: Optimization of oxygenic photosynthesis. *Cellular and Molecular Life Sciences*, *66*(23), 3697–

3710. https://doi.org/10.1007/s00018-009-0103-6

Munekage, Y., Hojo, M., Meurer, J., Endo, T., Tasaka, M., Shikanai, T. (2002). PGR5 Is Involved in Cyclic Electron Flow around Photosystem I and Is Essential for Photoprotection in Arabidopsis. *Cell*, *110*, 361–371.

Muramatsu, M., Hihara, Y. (2012). Acclimation to high-light conditions in cyanobacteria: From gene expression to physiological responses. *Journal of Plant Research*, *125*(1), 11–39. https://doi.org/10.1007/s10265-011-0454-6

Nandha, B., Finazzi, G., Joliot, P., Hald, S., Johnson, G. N. (2007). The role of PGR5 in the redox poising of photosynthetic electron transport. *Biochimica et Biophysica Acta - Bioenergetics*, *1767*(10), 1252–1259. https://doi.org/10.1016/j.bbabio.2007.07.007

Nelson, N., Ben-Shem, A. (2004). The complex architecture of oxygenic photosynthesis. *Nature Reviews. Molecular Cell Biology*, *5*(12), 971–982. https://doi.org/10.1038/nrm1525

Nelson, N., Yocum, C. F. (2006). Structure and function of photosystems I and II. *Annual Review of Plant Biology*, *57*, 521–565. https://doi.org/10.1146/annurev.arplant.57.032905.105350

Nishio, J. N., Whitmarsh, J. (1993). Dissipation of the Proton Electrochemical Potential in lntact Chloroplasts ' II . The pH Gradient Monitored by Cytochrome f Reduction Kinetics. *Plant Physiology*, 89–96.

Otto, C., Stadler, P. F., & Hoffmann, S. (2014). Lacking alignments? The next-generation sequencing mapper segemehl revisited. *Bioinformatics*, *30*(13), 1837–1843. http://doi.org/10.1093/bioinformatics/btu146

Peltier, J.-B., Emanuelsson, O., Kalume, D. E., Ytterberg, J., Friso, G., Rudella, A., Van Wijk, K. J. (2002). Central functions of the lumenal and peripheral thylakoid proteome of *Arabidopsis* determined by experimentation and genome-wide

prediction. *The Plant Cell*, *14*(1), 211–236. https://doi.org/10.1105/tpc.010304

Petersen, T. N., Brunak, S., von Heijne, G., Nielsen, H. (2011). SignalP 4.0: discriminating signal peptides from transmembrane regions. *Nature Methods*, *8*(10), 785–786. https://doi.org/10.1038/nmeth.1701

Rahman, O., Cummings, S. P., Harrington, D. J., Sutcliffe, I. C. (2008). Methods for the bioinformatic identification of bacterial lipoproteins encoded in the genomes of Gram-positive bacteria. *World Journal of Microbiology and Biotechnology*, *24*(11), 2377–2382. https://doi.org/10.1007/s11274-008-9795-2

Renato, M., Pateraki, I., Boronat, A., Azcón-bieto, J. (2014). Tomato Fruit Chromoplasts Behave as Respiratory Bioenergetic Organelles during Ripening. *Plant Physiology*, *166*(October), 920–933. https://doi.org/10.1104/pp.114.243931

Reyes-Sosa, F. M., Gil-Martínez, J., Molina-Heredia, F. P. (2011). Cytochrome c6-like protein as a putative donor of electrons to photosystem I in the cyanobacterium *Nostoc* sp. PCC 7119. *Photosynthesis Research*, *110*(1), 61–72. https://doi.org/10.1007/s11120-011-9694-5

Ripley, B. D. (2001). The R project in statistical computing. *MSOR Connections*, (January), 23–25. http://doi.org/10.11120/msor.2001.01010023

Rippka, D., Deruelles, J., Watterbury, J. B., Herdman, S., Stanier, R. Y. (1979). Generic Assignments , Strain Histories and Properties of Pure Cultures of Cyanobacteria. *Journal of General Microbiology*, *110*(2), 1–61.

Roach, T., Krieger-Liszkay, A. (2012). The role of the PsbS protein in the protection of photosystems i and II against high light in *Arabidopsis thaliana*. *Biochimica et Biophysica Acta - Bioenergetics*, *1817*(12), 2158–2165. https://doi.org/10.1016/j.bbabio.2012.09.011

Robinson, C., Matos, C. F. R. O., Beck, D., Ren, C., Lawrence, J., Vasisht, N., Mendel, S. (2011). Biochimica et Biophysica Acta Transport and proofreading of proteins

by the twin-arginine translocation (Tat) system in bacteria. *Biochimica et Biophysica Acta*, *1808*, 876–884. https://doi.org/10.1016/j.bbamem.2010.11.023

Scharfenberg, M., Pesaresi, P., Weigel, M., Granlund, I., Schröder, W. P., Finazzi, G., … Leister, D. (2009). Mutants, overexpressors, and interactors of arabidopsis plastocyanin isoforms: Revised roles of plastocyanin in photosynthetic electron flow and thylakoid redox state. *Molecular Plant*, *2*(2), 236–248. https://doi.org/10.1093/mp/ssn041

Scharfenberg, M. (2011). Cytochromes c_{6A} – Functional Evolution of a Plastidial Protein, (October). PhD thesis

Schlarb-Ridley, B. G., Nimmo, R. H., Purton, S., Howe, C. J., Bendall, D. S. (2006). Cytochrome c_{6A} is a funnel for thiol oxidation in the thylakoid lumen. *FEBS Letters*, *580*(9), 2166–2169. https://doi.org/10.1016/j.febslet.2006.03.052

Scholes, G., Fleming, G., Olaya-Castro, A, van Grondelle, R. (2011). Lessons from nature about solar light harvesting. *Nature Publishing Group*, *3*(10), 763–774. https://doi.org/10.1038/nchem.1145

Schönberg, A., Baginsky, S. (2012). Signal integration by chloroplast phosphorylation networks: an update. *Frontiers in Plant Science*, *3*(November), 256. https://doi.org/10.3389/fpls.2012.00256

Schöttler, M. A., Tóth, S. Z., Boulouis, A., Kahlau, S. (2015). Photosynthetic complex stoichiometry dynamics in higher plants: Biogenesis, function, and turnover of ATP synthase and the cytochrome b_6f complex. *Journal of Experimental Botany*, *66*(9), 2373–2400. https://doi.org/10.1093/jxb/eru495

Schultze, M., Forberich, B., Rexroth, S., Dyczmons, N.G., Roegner, M., Appel, J., 2009. Localization of cytochrome b(6)f complexes implies an incomplete respiratory chain in cytoplasmic membranes of the cyanobacterium Synechocystis sp PCC 6803.

Shapiguzov, A., Ingelsson, B., Samol, I., Andres, C., Kessler, F., Rochaix, J.-D., Goldschmidt-Clermont, M. (2010). The PPH1 phosphatase is specifically involved in LHCII dephosphorylation and state transitions in *Arabidopsis*. *Proceedings of the National Academy of Sciences of the United States of America*, *107*(10), 4782–4787. https://doi.org/10.1073/pnas.0913810107

Sharkey, T. D., Vanderveer, P. J. (1989). Stromal Phosphate Concentration Is Low during Feedback Limited Photosynthesis1. *Plant Physiology*, *91,* 679–684.

Shimada, T. L., Shimada, T., Hara-Nishimura, I. (2010). A rapid and non-destructive screenable marker, FAST, for identifying transformed seeds of *Arabidopsis thaliana*: TECHNICAL ADVANCE. *Plant Journal*, *61*(3), 519–528. https://doi.org/10.1111/j.1365-313X.2009.04060.x

Shestakov, S. V, Khyen, N. T. (1970). Evidence for Genetic Transformation in Blue-Green Alga Anacystis nidulans. *Molecular General Genetics MGGGene Expression under Low-Oxygen Conditions in the Cyanobacterium Synechocystis Sp . PCC 6803 Demonstrates Hik31-Dependent and -Independent Responses*, *375*, 372–375.

Shestakov, S., Grigorieva, G. (1982). Transformation in the cyanobacterium Synechocystis sp . 6803. *FEMS Microbiology Letters*, *13*, 367–370.

Shimakawa, G., Shaku, K., Nishi, A., Hayashi, R., Yamamoto, H., Sakamoto, K., Miyake, C. (2015). FLAVODIIRON2 and FLAVODIIRON4 proteins mediate an oxygen-dependent alternative electron flow in *Synechocystis* sp. PCC 6803 under CO2-limited conditions. *Plant Physiology*, *167*(2), 472–480. https://doi.org/10.1104/pp.114.249987

Shuvalov, V. a, Allakhverdiev, S. I., Sakamoto, a, Malakhov, M., Murata, N. (2001). Optical study of cytochrome c_M formation in *Synechocystis*. *IUBMB Life*, *51*(2), 93–97. https://doi.org/10.1080/15216540118716

Sievers, F., Wilm, A., Dineen, D., Gibson, T. J., Karplus, K., Li, W., Higgins, D. G.

(2011). Fast, scalable generation of high-quality protein multiple sequence alignments using Clustal Omega. *Molecular Systems Biology*, *7*(539), 1–6. https://doi.org/10.1038/msb.2011.75

Solovyev, V., Salamov, A. (2010). Automatic Annotation of Microbial Genomes and Metagenomic Sequences. In R. W. Li (Ed.), *Metagenomics and its Applications in Agriculture, Biomedicine and Environmental Studies* (pp. 61–78).

Sugimoto, K., Okegawa, Y., Tohri, A., Long, T. A., Covert, S. F., Hisabori, T., Shikanai, T. (2013). A single amino acid alteration in PGR5 confers resistance to antimycin a in cyclic electron transport around PSI. *Plant and Cell Physiology*, *54*(9), 1525–1534. https://doi.org/10.1093/pcp/pct098

Summerfield, T. C., Nagarajan, S., Sherman, L. A. (2011). Gene expression under low-oxygen conditions in the cyanobacterium Synechocystis sp . PCC 6803 demonstrates Hik31-dependent and -independent responses. *Microbiology*, (157), 301–312. https://doi.org/10.1099/mic.0.041053-0

Suorsa, M., Järvi, S., Grieco, M., Nurmi, M., Pietrzykowska, M., Rantala, M., Aro, E.-M. (2012). PROTON GRADIENT REGULATION5 is essential for proper acclimation of *Arabidopsis* photosystem I to naturally and artificially fluctuating light conditions. *The Plant Cell*, *24*(7), 2934–2948. https://doi.org/10.1105/tpc.112.097162

Suorsa, M., Rossi, F., Tadini, L., Labs, M., Colombo, M., Jahns, P., Pesaresi, P. (2015). PGR5-PGRL1-dependent cyclic electron transport modulates linear electron transport rate in Arabidopsis thaliana. *Molecular Plant*, (February), 271–288. https://doi.org/10.1016/j.molp.2015.12.001

Takizawa, K., Cruz, J. A., Kanazawa, A., Kramer, D. M. (2007). The thylakoid proton motive force in vivo. Quantitative, non-invasive probes, energetics, and regulatory consequences of light-induced pmf. *Biochimica et Biophysica Acta - Bioenergetics*, *1767*(10), 1233–1244. https://doi.org/10.1016/j.bbabio.2007.07.006

Tang, X., Lowder, L. G., Zhang, T., Malzahn, A. A., Zheng, X., Voytas, D. F., … Qi, Y. (2017). A CRISPR-Cpf1 system for efficient genome editing and transcriptional repression in plants. *Nature Plants*, *3*(February), 1–5. https://doi.org/10.1038/nplants.2017.18

Thurotte, A., Lopez Igual, R., Wilson, A., Comolet, L., Bourcier de Carbon, C., Xiao, F., Kirilovsky, D. (2015). Regulation of Orange Carotenoid Protein activity in cyanobacterial photoprotection. *Plant Physiology*, *169*(September), pp.00843.2015. https://doi.org/10.1104/pp.15.00843

Tikkanen, M., Mekala, N. R., Aro, E. M. (2014). Photosystem II photoinhibition-repair cycle protects Photosystem i from irreversible damage. *Biochimica et Biophysica Acta - Bioenergetics*, *1837*(1), 210–215. https://doi.org/10.1016/j.bbabio.2013.10.001

Tikkanen, M., Rantala, S., Aro, E.-M. (2015). Electron flow from PSII to PSI under high light is controlled by PGR5 but not by PSBS. *Frontiers in Plant Science*, *6*(July), 521. https://doi.org/10.3389/fpls.2015.00521

Ungerer, J., Pakrasi, H. B. (2016). Cpf1 Is A Versatile Tool for CRISPR Genome Editing Across Diverse Species of Cyanobacteria. *Scientific Reports*, *6*(December), 1–9. https://doi.org/10.1038/srep39681

Vasudevan, R., Gale, G. A. R., Schiavon, A. A., Puzorjov, A., Malin, J., Gillespie, M. D., … McCormick, A. J. (2019). CyanoGate: A modular cloning suite for engineering cyanobacteria based on the plant MoClo syntax. *Plant Physiology*, *180*(May), pp.01401.2018. https://doi.org/10.1104/pp.18.01401

Vermaas, W. (1996). Molecular genetics of the cyanobacterium Synechocystis sp . PCC 6803 : Principles and possible biotechnology applications. *Journal of Applied Phycology*, *8*, 263–273.

Vermaas, W. Photosynthesis and respiration in Cyanobacteria. ENCYCLOPEDIA OF LIFE SCIENCES © 2001, John Wiley & Sons, Ltd. www.els.net

Vincze, T. (2003). NEBcutter: a program to cleave DNA with restriction enzymes. *Nucleic Acids Research*, *31*(13), 3688–3691. https://doi.org/10.1093/nar/gkg526

Waasbergen, L. G. Van, Dolganov, N., Arthur, R., Grossman, A. R. (2002). nblS , a Gene Involved in Controlling Photosynthesis-Related Gene Expression during High Light and Nutrient Stress in *Synechococcus elongatus* PCC 7942 nblS , a Gene Involved in Controlling Photosynthesis-Related Gene Expression during High Light and Nutri, *184*(9), 2481–2490. https://doi.org/10.1128/JB.184.9.2481

Wang, C., Yamamoto, H., Shikanai, T. (2015). Role of cyclic electron transport around photosystem I in regulating proton motive force. *Biochimica et Biophysica Acta*, *1847*(9), 931–938. https://doi.org/10.1016/j.bbabio.2014.11.013

Wang, M., Mao, Y., Lu, Y., Tao, X., Zhu, J. kang. (2017). Multiplex Gene Editing in Rice Using the CRISPR-Cpf1 System. *Molecular Plant*, *10*(7), 1011–1013. https://doi.org/10.1016/j.molp.2017.03.001

Wastl, Jürgen., Derek S. Bendall., Howe, C. J. (2002). Higher plants contain a modified cytochrome c_6. *Trends in Plant Science*, *7*(6), 244–245.

Weigel, M., Pesaresi, P., Leister, D. (2003a). Tracking the function of the cytochrome c_6-like protein in higher plants. *Trends in Plant Science*, *8*(11), 513–517.

Weigel, M., Varotto, C., Pesaresi, P., Finazzi, G., Rappaport, F., Salamini, F., Leister, D. (2003b). Plastocyanin is indispensable for photosynthetic electron flow in *Arabidopsis thaliana*. *The Journal of Biological Chemistry*, *278*(33), 31286–31289. https://doi.org/10.1074/jbc.M302876200

Wendt, K. E., Ungerer, J., Cobb, R. E., Zhao, H., Pakrasi, H. B. (2016). CRISPR/Cas9 mediated targeted mutagenesis of the fast growing cyanobacterium Synechococcus elongatus UTEX 2973. *Microbial Cell Factories*, *15*(1), 1–8. https://doi.org/10.1186/s12934-016-0514-7

Worrall, J. a R., Luisi, B. F., Schlarb-Ridley, B. G., Bendall, D. S., Howe, C. J. (2008).

Cytochrome c_{6A}: discovery, structure and properties responsible for its low haem redox potential. *Biochemical Society Transactions*, *36*(Pt 6), 1175–1179. https://doi.org/10.1042/BST0361175

Worrall, J. a R., Schlarb-Ridley, B. G., Reda, T., Marcaida, M. J., Moorlen, R. J., Wastl, J., Howe, C. J. (2007). Modulation of heme redox potential in the cytochrome c_6 family. *Journal of the American Chemical Society*, *129*(30), 9468–9475. https://doi.org/10.1021/ja072346g

Yao, L., Cengic, I., Anfelt, J., Hudson, E. P. (2016). Multiple Gene Repression in Cyanobacteria Using CRISPRi. *ACS Synthetic Biology*, *5*(3), 207–212. https://doi.org/10.1021/acssynbio.5b00264

Zatwarnicki, P., Barciszewski, J., Krzywda, S., Jaskolski, M., Kolesinski, P., Szczepaniak, A. (2014). Cytochrome c_{6B} of Synechococcus sp. WH 8102 - Crystal structure and basic properties of novel c6-like family representative. *Biochemical and Biophysical Research Communications*, *443*(4), 1131–1135. https://doi.org/10.1016/j.bbrc.2013.10.167

Zetsche, B., Heidenreich, M., Mohanraju, P., Fedorova, I., Kneppers, J., Degennaro, E. M., … Zhang, F. (2017). Multiplex gene editing by CRISPR-Cpf1 using a single crRNA array. *Nature Biotechnology*, *35*(1), 31–34. https://doi.org/10.1038/nbt.3737

Zhang, X., Henriques, R., Lin, S. S., Niu, Q. W., Chua, N. H. (2006). Agrobacterium-mediated transformation of *Arabidopsis thaliana* using the floral dip method. *Nature Protocols*, *1*(2), 641–646. https://doi.org/10.1038/nprot.2006.97

Zhang, P., Allahverdiyeva, Y., Eisenhut, M., Aro, E.-M. (2009). Flavodiiron proteins in oxygenic photosynthetic organisms: photoprotection of photosystem II by Flv2 and Flv4 in *Synechocystis* sp. PCC 6803. *PloS One*, *4*(4), e5331. https://doi.org/10.1371/journal.pone.0005331

Zhang, H., Liu, H., Niedzwiedzki, D. M., Prado, M., Jiang, J., Gross, M. L., Blankenship, R. E. (2014). Molecular mechanism of photoactivation and structural location of the cyanobacterial orange carotenoid protein. *Biochemistry*, *53*(1), 13–19. https://doi.org/10.1021/bi401539w

Appendix-A

Reagents medias compositions used for the current experiments

Culture mediums

LB liquid Medium	25 g of Luria Broth Miller (Sigma-Aldrich) powder in dH_2O to 1L Sterilized by autoclave.
LB Agar medium	25 g of LB powder, 15 g of agar in 1L dH_2O Sterilized by autoclave.
MS medium solid	Dissolving ½ strength MS salt in 0.8% plant agar.

Nucleic acid loading dye

6x DNA loading dye	30% (v/v) glycerol, 0.25% (w/v) bromophenol blue, 0.25% (w/v) xylene cyanol FF. (Store at 4°C).

Northern Blot buffer solution

20 X SSC Stock	3 M NaCl, 300 mM Sodium citrate, pH 7.0
2 X SSC	Dilute 20 X stock solution in 1:10 with DEPC treated water
Wash Buffer	0.1 M Maleic acid, 0.15 M NaCl (pH 7.5 at 20°C), 0.3% (V/V) Tween 20.
Maleic acid buffer:	0.1 M Maleic acid, 0.15 M NaCl adjust with NaOH (solid) to pH 7.5 at 20°C.

Detection buffer:	0.1 M Tris-HCl. 0.1M NaCl, adjust of pH to 9.5 (20°C).

Western Blot buffer solutions

10 X SDS-PAGE Running Buffer	30.24 g Tris (Trizma)**,** 144 g Glycine**,** 10 g SDS**,** dH_2O to 1L.
5 x SDS loading buffer	10% (w/v) of SDS, 10 mM DTT, 20% (v/v) glycerol, 0.2M Tris-HCl pH 6.8 0.005% Bromophenol blue.
Lysis buffer	8 M Urea, 10mM Tris pH8, 5mM MgAcetate, 4% CHAPS Before use, warm the solution to 40°C to dissolve the urea.
Laemmli 2X buffer	4% SDS, 10% b-mercaptoethanol, 20% glycerol, 0.004% bromophenol blue, 0.125 M Tris-HCl, Check the pH and adjust pH to 6.8.
PBST	150 mM NaCl**,** 5.2 mM Na2HPO4**,** 1.7 mM KH2PO4**,** 0.2% Tween 20**,** Check the pH, should be about pH 7.4.
Blocking buffer	5% milk or BSA (bovine serum albumin) in PBST, Mix well and filter. Failure to filter can lead to “spotting” where tiny dark grains will contaminate the blot during color development.

Appendix-B

PCR parameters used to amplify genes open reading frames and gene fragments from genomic DNA of *S. elongatus*

Parameter Name	Temperature	Time	N. of cycle
Hold	98 °C	Preheat	1 cycle
Initial denaturation	98 °C	60 s	1 cycle
Denaturation	98 °C	30 s	
Annealing	58/60 °C	30 s	
Extension	72 °C	1 min/kb	30 cycle
Final extension	72 °C	5 min	1 cycle
Hold	4 °C	Indefinite	1 cycle

PCR parameters used to check knockouts in *S. elongatus*

Parameter Name	Temperature	Time	N. of cycle
Hold	95 °C	Preheat	1 cycle
Initial denaturation	95 °C	60 s	1 cycle
Denaturation	95 °C	30 s	
Annealing	58/60 °C	30 s	
Extension	72 °C	1 min/kb	30 cycle
Final extension	72 °C	5 min	1 cycle
Hold	4 °C	Indefinite	1 cycle

PCR parameters used to amplify cytochrome c_{6A} cDANs from *Arabidopsis* cDNA

Parameter Name	**Temperature**	**Time**	**N. of cycle**
Hold	98 °C	Preheat	1 cycle
Initial denaturation	98 °C	60 s	1 cycle
Denaturation	98 °C	30 s	
Annealing	52to 62 °C	30 s (Step down)	
Extension	72 °C	1 min/kb	30 cycle
Final extension	72 °C	5 min	1 cycle
Hold	4 °C	Indefinite	1 cycle

PCR parameters used to check T DNA mutation in *Arabidopsis* seedlings.

Parameter Name	**Temperature**	**Time**	**N. of cycle**
Hold	95 °C	Preheat	1 cycle
Initial denaturation	95 °C	60 s	1 cycle
Denaturation	95 °C	30 s	
Annealing	58/60 °C	30 s	
Extension	72 °C	1 min/kb	30 cycle
Final extension	72 °C	5 min	1 cycle
Hold	4 °C	Indefinite	1 cycle

APPENDIX C		
Cytochrome c_{6C} Primers		
Knockout primers		
S.No	**Primers Name**	**Sequence**
1	7942 cyt c_{6C} k/O left for *Eco*RI	GCTGGAATTCTGTAAGGCCAATTCGTAGGG
2	7942 cyt c_{6C} k/O left rev *kpn*I	ATCA GGTACC TCTGTCCAGCCTGTGTCAAG
3	7942 cyt c_{6C} k/O right for *Xba*I	GGAATCTAGAGCGATAGTCAGCCCACAAAT
4	7942 cyt c_{6C} K/O right rev *Hind*III	AAGAAAGCTTAGGGAATCGACTCCTGCTCT
Knockout checking primers		
S.No	**Primers Name**	**Sequence**
5	7942 cyt c_{6C} K/O for	GCTGGAATTCTGTAAGGCCAATTCGTAGGG
6	7942 cyt c_{6C} k/O rev	AAGAAAGCTTAGGGAATCGACTCCTGCTCT
Cytochrome c_M Primers		
Cyt c_M knockout primers		
S.No	**Primers Name**	**Sequence**
7	7942 cyt c_M left for *Eco*RI	GTACGAATTCGGATAGCCCTCTAGGCGAAT
8	7942 cyt c_M left rev *Bam*HI	GTACGGATCCACCTCTTGCGCTACCTTGAA
9	7942 cyt c_M right for *Bam*HI	GTACGGATCCCTGTCAGTCGTTTGCAGGAC
10	7942 cyt c_M right rev *Xba*I	GTACTCTAGATTTTGTCACCCAAGTTGCAG
Cyt c_M knockout checking primers		
S.No	**Primers Name**	**Sequence**
11	7942 cyt c_M K/O for	CCGTCGCTACGGCAGTAC
12	7942 cyt c_M K/O rev	CAAAGTGGTTGTCCATCTCGCC
Cytochrome c_{6A} Primers		
Primers used to amplify cyt c_{6A} cDNA to over express in Arabidopsis thaliana wild type background		

S.No	Primers Name	Sequence
13	Cyt c_{6A} cDNA for *Eco*RI:*Sal*I	CAGAGAATTCGTCGACCAAACAGTTAAAAGGAAAAAAAAAAAAAATTCTTTGAG
14	Cyt c_{6A} cDNA rev *Cla*I:*Pst*I	ATCTGCTGCAGATCGATGTCCGTAGATACAGTTGGCCA
Primers used to amplify plastocyanin major isoform (*pete2*) cDNA to over express in Arabidopsis thaliana wild type background for control study		
S.No	**Primers Name**	**Sequence**
15	Plas major cDNA for *Eco*RI:*Sla*I	CAGAGAATTCGTCGACCCACATAAAAACTCATAAACTCGATCGA
16	Plas major cDNA rev *Cla*I:*Pst*I	ATCTGCTGCAGATCGATGTTAACGGTGACTTTACCGACCA
Primers Used for qRT-PCR		
S.No	**Primers Name**	**Sequence**
19	7942 16s rRNA for	CAGCTCGTGTCGTGAGATGT
20	7942 16s rRNA rev	AAGGGGCATGATGACTTGAC
21	7942 c_{6C} RTPCR for	GGGCAAAACCCTACAACTCA
22	7942 c_{6C} RTPCR rev	GAAACGATCGCAATTTCCTC
23	7942 cytM RTPCR for	CTCCTGGCAACTGCTGTC
24	7942 cytM RTPCR rev	AGCCGGCACAGTTGATTT

	Appendix table 4.1: Transcript analysis of Δcyt c_{6C} type cultures compared to 3 different light conditions													
Number of genes percompomnents	**Gene simbol**	**Gene finder**	**Cyt c_{6C} 150 vs WT 150**			**Cyt c_{6C} 500 vs WT 500**			**Cyt c_{6C} 500 vs Cyt c_{6C} 150**			**WT500 vs WT150**		
PS II	**PS II**	**Gene annotation**	**Log2 values**	**Fold change**	**P Values**	**Log2 values**	**Fold change**	**P Values**	**Log2 values**	**Fold change**	**P Values**	**Log2 values**	**Fold change**	**P Values**
1	*psbA1*	Synpcc7942_0424	1.1	2.2	0.01	-0.4	-1.3	0.41	-1.3	-2.5	0.00	0.2	1.2	0.59
2	*psbA2*	Synpcc7942_1389	0.5	1.4	0.57	0.6	1.5	0.36	3.5	11.6	0.00	3.5	11.0	0.00
3	*psbA3*	Synpcc7942_0893	0.6	1.5	0.48	1.3	2.5	0.01	0.9	1.9	0.06	0.2	1.1	0.73
4	*psbB*	Synpcc7942_0697	-0.4	-1.3	0.64	-0.1	-1.1	0.88	2.4	5.5	0.00	2.2	4.5	0.00
5	*psbC*	Synpcc7942_0656	-0.0	-1.0	0.99	-0.1	-1.1	0.90	2.9	7.6	0.00	3.0	7.9	0.00
6	*psbD1*	Synpcc7942_0655	-0.2	-1.1	0.84	0.0	1.0	0.99	3.6	11.9	0.00	3.4	10.5	0.00
7	*psbD2*	Synpcc7942_1637	-0.2	-1.2	0.78	0.0	1.0	0.98	3.6	12.3	0.00	3.4	10.3	0.00
8	*psbE*	Synpcc7942_1177	0.1	1.0	0.97	-0.1	-1.1	0.85	0.6	1.5	0.15	0.8	1.7	0.04
9	*psbF*	Synpcc7942_1176	0.1	1.1	0.95	-0.1	-1.1	0.90	0.7	1.6	0.11	0.8	1.8	0.03
10	*psbH*	Synpcc7942_0225	-0.5	-1.5	0.35	0.3	1.3	0.50	-0.9	-1.9	0.01	-1.8	-3.5	0.00
11	*psbI*	Synpcc7942_1705	-0.4	-1.3	0.60	-1.0	-2.0	0.04	-2.4	-5.1	0.00	-1.8	-3.4	0.00
12	*psbJ*	Synpcc7942_1174	0.1	1.1	0.90	-0.1	-1.0	0.92	0.4	1.3	0.35	0.6	1.5	0.12
13	*psbK*	Synpcc7942_0456	-0.7	-1.7	0.35	-0.6	-1.5	0.39	-3.0	-8.0	0.00	-3.2	-9.0	0.00
14	*psbL*	Synpcc7942_1175	0.1	1.1	0.89	0.1	1.0	0.92	0.4	1.3	0.36	0.5	1.4	0.24
15	*psbM*	Synpcc7942_0699	-0.4	-1.4	0.64	1.4	2.7	0.02	-2.6	-5.9	0.00	-4.4	-21.4	0.00
16	*psbN*	Synpcc7942_0224	-0.1	-1.1	0.93	-0.0	-1.0	0.98	1.2	2.3	0.01	1.1	2.2	0.01
17	*psbO*	Synpcc7942_0294	0.1	1.1	0.92	-0.3	-1.2	0.68	1.4	2.7	0.01	1.9	3.6	0.00
18	*psbP*	Synpcc7942_1038	0.1	1.1	0.91	1.6	3.0	0.00	1.2	2.3	0.00	-0.2	-1.2	0.65
19	*psbQ*	Synpcc7942_1678	0.1	1.0	0.97	-1.3	-2.5	0.00	1.4	2.6	0.00	2.7	6.6	0.00
20	*psbTc*	Synpcc7942_0696	-0.1	-1.1	0.87	-0.2	-1.1	0.77	1.6	3.1	0.00	1.6	3.1	0.00
21	*psbU*	Synpcc7942_1882	0.0	1.0	0.99	0.7	1.6	0.18	1.1	2.2	0.01	0.5	1.4	0.30
22	*psbV*	Synpcc7942_2010	-0.5	-1.4	0.57	-1.1	-2.2	0.04	0.6	1.5	0.23	1.2	2.4	0.00
23	*psbW*	Synpcc7942_1679	-0.4	-1.3	0.59	0.8	1.8	0.14	1.5	2.9	0.00	0.3	1.2	0.53
24	*psbX*	Synpcc7942_2016	-0.9	-1.9	0.08	-0.4	-1.3	0.51	-1.9	-3.9	0.00	-2.5	-5.7	0.00

25	*psbY*	Synpcc7942_1962	-0.7	-1.6	0.25	0.0	1.0	0.95	-2.7	-6.4	0.00	-3.4	-10.5	0.00
26	*psbZ*	Synpcc7942_2245	-0.6	-1.5	0.46	-0.9	-1.9	0.10	-1.8	-3.5	0.00	-1.5	-2.7	0.00
27	*psb27*	Synpcc7942_0343	-0.1	-1.0	0.95	-0.8	-1.7	0.07	1.3	2.4	0.00	2.0	4.0	0.00
28	*psb28*	Synpcc7942_2478	0.1	1.1	0.97	0.3	1.2	0.85	-0.6	-1.5	0.54	-0.8	-1.7	0.42
29	*psb29*	Synpcc7942_1555	0.4	1.3	0.61	0.4	1.4	0.38	1.8	3.6	0.00	1.8	3.4	0.00
30	*psb30*	Synpcc7942_2134	0.9	1.8	0.29	0.4	1.3	0.48	3.0	8.1	0.00	3.5	11.2	0.00
31	*ftsH (1)*	Synpcc7942_0297	-0.1	-1.1	0.91	0.5	1.4	0.37	2.3	5.0	0.00	1.7	3.2	0.00
32	*ftsH (2)*	Synpcc7942_0942	-0.1	-1.1	0.89	0.3	1.3	0.48	1.7	3.2	0.00	1.2	2.3	0.00
33	*ftsH (3)*	Synpcc7942_0998	-0.2	-1.1	0.87	0.3	1.2	0.55	0.3	1.2	0.47	-0.2	-1.1	0.72
34	*fstH-2*	Synpcc7942_1314	0.1	1.0	0.97	-0.7	-1.6	0.27	1.9	3.8	0.00	2.7	6.5	0.00
PS I	**PS I**	**Gene annotation**	**Log2 values**	**Fold change**	**P Values**	**Log2 values**	**Fold change**	**P Values**	**Log2 values**	**Fold change**	**P Values**	**Log2 values**	**Fold change**	**P Values**
1	*psaA*	Synpcc7942_2049	0.1	1.1	0.90	-1.6	-3.1	0.00	0.8	1.7	0.05	2.6	5.9	0.00
2	*psaB*	Synpcc7942_2048	-0.0	-1.0	0.97	-1.1	-2.2	0.02	1.3	2.5	0.00	2.4	5.2	0.00
3	*psaC*	Synpcc7942_0535	0.7	1.7	0.23	0.5	1.4	0.43	0.1	1.1	0.84	0.4	1.3	0.37
4	*psaD*	Synpcc7942_1002	0.5	1.4	0.47	-0.9	-1.9	0.05	-0.9	-1.9	0.04	0.5	1.5	0.19
5	*psaE*	Synpcc7942_1322	0.3	1.2	0.76	-0.3	-1.2	0.61	-0.8	-1.8	0.05	-0.3	-1.2	0.52
6	*psaF*	Synpcc7942_1250	-0.4	-1.3	0.72	-1.3	-2.4	0.03	0.8	1.7	0.15	1.7	3.2	0.00
7	*psaI*	Synpcc7942_2343	0.2	1.2	0.82	-0.3	-1.2	0.68	-0.9	-1.9	0.06	-0.4	-1.3	0.40
8	*psaJ*	Synpcc7942_1249	-0.1	-1.1	0.93	-1.1	-2.2	0.03	-1.2	-2.3	0.01	-0.2	-1.1	0.73
9	*psaK1*	Synpcc7942_0407	1.2	2.3	0.03	-0.3	-1.2	0.60	-0.9	-1.9	0.04	0.6	1.5	0.16
10	*psaK2*	Synpcc7942_0920	1.6	3.0	0.00	0.4	1.3	0.53	-0.7	-1.6	0.17	0.5	1.4	0.30
11	*psaL*	Synpcc7942_2342	0.5	1.4	0.55	-0.8	-1.7	0.13	-0.4	-1.3	0.39	0.9	1.8	0.04
12	*bptA*	Synpcc7942_2513	-0.1	-1.1	0.95	-0.7	-1.6	0.17	-0.8	-1.8	0.04	-0.3	-1.2	0.55
13	*ycf3*	Synpcc7942_2321	-0.3	-1.3	0.74	-1.6	-3.1	0.00	0.6	1.5	0.27	1.9	3.7	0.00
14	*ycf4*	Synpcc7942_0654	0.0	1.0	0.98	0.1	1.1	0.81	2.2	4.5	0.00	2.1	4.2	0.00
Cyt b_6f complex	**Cyt b_6f complex**	**Gene annotation**	**Log2 values**	**Fold change**	**P Values**	**Log2 values**	**Fold change**	**P Values**	**Log2 values**	**Fold change**	**P Values**	**Log2 values**	**Fold change**	**P Values**
1	*petA*	Synpcc7942_1231	-0.4	-1.3	0.64	0.2	1.1	0.81	1.5	2.9	0.00	1.0	2.0	0.01
2	*petB*	Synpcc7942_2331	0.3	1.2	0.78	1.3	2.5	0.02	1.7	3.3	0.00	0.7	1.6	0.15
3	*petC*	Synpcc7942_1232	-0.3	-1.2	0.73	0.1	1.1	0.83	1.7	3.3	0.00	1.3	2.4	0.00

4	*petD*	Synpcc7942_2332	0.2	1.1	0.87	0.3	1.2	0.62	0.6	1.5	0.18	0.5	1.4	0.28
5	*petG*	Synpcc7942_1479	0.1	1.0	0.96	0.5	1.5	0.25	-1.9	-3.7	0.00	-2.4	-5.2	0.00
6	*petL*	Synpcc7942_0113	0.6	1.5	0.39	0.9	1.9	0.06	-0.1	-1.1	0.75	-0.5	-1.4	0.24
7	*petM*	Synpcc7942_2426	-0.3	-1.2	0.73	1.9	3.7	0.00	-1.0	-2.0	0.02	-3.2	-9.4	0.00
8	*petN*	Synpcc7942_0475	0.1	1.1	0.88	-0.1	-1.1	0.89	-0.3	0.8	0.50	-0.1	-1.0	0.90
ATP synthase	**ATP synthase**	**Gene annotation**	**Log2 values**	**Fold change**	**P Values**	**Log2 values**	**Fold change**	**P Values**	**Log2 values**	**Fold change**	**P Values**	**Log2 values**	**Fold change**	**P Values**
1	*atpA*	Synpcc7942_0336	0.1	1.1	0.95	1.6	3.0	0.00	1.6	3.1	0.00	0.1	1.1	0.80
2	*atpB*	Synpcc7942_2315	0.0	1.0	0.97	0.9	1.8	0.05	1.4	2.6	0.00	0.6	1.5	0.13
3	*atpC/E*	Synpcc7942_2316	-0.1	-1.1	0.95	1.5	2.7	0.00	2.3	4.9	0.00	0.8	1.7	0.05
4	*atpD*	Synpcc7942_0335	0.5	1.4	0.53	1.6	3.1	0.00	2.0	4.1	0.00	0.9	1.9	0.04
5	*atpF*	Synpcc7942_0334	0.1	1.1	0.92	1.6	3.0	0.00	2.1	4.4	0.00	0.6	1.6	0.10
6	*atpG*	Synpcc7942_0333	-0.1	-1.0	0.97	1.3	2.5	0.00	1.6	3.0	0.00	0.2	1.1	0.71
7	*atpH*	Synpcc7942_0332	0.4	1.3	0.64	1.8	3.6	0.00	1.9	3.8	0.00	0.5	1.4	0.26
Phycobiliproteins	**Phycobiliproteins**	**Gene annotation**	**Log2 values**	**Fold change**	**P Values**	**Log2 values**	**Fold change**	**P Values**	**Log2 values**	**Fold change**	**P Values**	**Log2 values**	**Fold change**	**P Values**
1	*apcA*	Synpcc7942_0327	0.3	1.2	0.80	-1.0	-2.0	0.15	-0.3	-1.2	0.65	1.0	2.0	0.06
2	*apcB1/apcF*	Synpcc7942_2158	0.3	1.2	0.79	-0.6	-1.6	0.33	0.7	1.6	0.15	1.1	2.1	0.01
3	*apcB*	Synpcc7942_0326	0.5	1.4	0.59	-0.1	-1.1	0.85	-0.5	-1.4	0.38	0.6	1.6	0.20
4	*apcD*	Synpcc7942_0240	-0.3	-1.2	0.88	-0.7	-1.6	0.52	0.6	1.5	0.52	1.0	2.0	0.24
5	*cpcA1*	Synpcc7942_1048	0.4	1.3	0.70	-1.1	-2.1	0.06	-2.2	-4.5	0.00	-0.7	-1.6	0.15
6	*cpcA2*	Synpcc7942_1053	0.4	1.3	0.69	-1.0	-2.0	0.01	-1.8	-3.4	0.00	-0.4	-1.3	0.47
7	*cpcB1*	Synpcc7942_1047	0.3	1.2	0.76	-1.1	-2.2	0.04	-2.4	-5.4	0.00	-1.0	-2.0	0.03
8	*cpcB2*	Synpcc7942_1052	0.4	1.3	0.67	-1.0	-2.0	0.01	-1.5	-2.9	0.00	-0.2	-1.1	0.76
9	*cpcE*	Synpcc7942_1054	0.4	1.3	0.71	-2.0	-4.0	0.00	-0.8	-1.7	0.15	1.6	3.0	0.00
10	*cpcF*	Synpcc7942_1055	-0.0	-1.0	NA	-0.7	-1.7	0.34	0.4	1.3	0.54	1.1	2.2	0.06
11	*cpcG*	Synpcc7942_2030	0.4	1.3	0.63	-0.2	-1.1	0.82	-0.6	-1.5	0.19	-0.1	-1.0	0.91
12	*cpcH*	Synpcc7942_1049	0.4	1.4	0.58	-1.5	-2.8	0.00	-1.7	-3.2	0.00	0.3	1.2	0.59
13	*cpcI1*	Synpcc7942_1050	0.4	1.3	0.68	-1.8	-3.6	0.00	-1.4	-2.7	0.00	0.8	1.7	0.08
14	*cpcI2/cpcD*	Synpcc7942_1051	0.4	1.3	0.65	-0.7	-1.7	0.20	-0.7	-1.6	0.19	0.5	1.4	0.31
High light	**High light**	**Gene annotation**	**Log2**	**Fold**	**P Values**	**Log2**	**Fold**	**P Values**	**Log2**	**Fold**	**P Values**	**Log2**	**Fold**	**P Values**

inducible gene	inducible gene		values	change		values	change		values	change		values	change	
1	*nblA1*	Synpcc7942_2127	1.2	2.4	0.05	5.1	33.8	0.00	2.9	7.7	0.00	-0.9	-1.9	0.05
2	*nbIB*	Synpcc7942_1823	0.3	1.2	0.71	-0.3	-1.2	0.64	0.3	1.3	0.44	0.9	1.9	0.02
3	*nbIB2*	Synpcc7942_1721	-0.6	-1.5	0.35	0.5	1.4	0.38	1.1	2.2	0.01	0.1	1.1	0.87
4	hliA	Synpcc7942_1997	0.5	1.4	0.42	3.4	10.9	0.00	-0.5	-1.4	0.23	-3.4	-10.8	0.00
5	*hliC*	Synpcc7942_0243	0.5	1.4	0.50	1.2	2.4	0.01	2.1	4.3	0.00	1.4	2.6	0.00
6	*hliP1*	Synpcc7942_1331	0.5	1.4	0.49	1.0	2.0	0.04	1.1	2.1	0.01	0.6	1.5	0.19
7	*hliP2*	Synpcc7942_1759	0.3	1.3	0.71	1.2	2.4	0.02	0.6	1.6	0.19	-0.2	-1.2	0.63
8	*isiA/cp43'*	Synpcc7942_1542	-0.6	-1.5	0.74	2.3	5.0	0.01	5.8	56.7	0.00	2.9	7.6	0.00
Electron carrier	**Electron carrier**	**Gene annotation**	**Log2 values**	**Fold change**	**P Values**	**Log2 values**	**Fold change**	**P Values**	**Log2 values**	**Fold change**	**P Values**	**Log2 values**	**Fold change**	**P Values**
2	*petJ1*	Synpcc7942_1630	2.2	4.7	0.00	0.6	1.5	0.43	-0.0	-1.0	0.96	1.6	3.1	0.00
3	*petJ1iso*	Synpcc7942_0239	-0.2	-1.2	0.88	0.2	1.1	0.83	2.0	4.0	0.00	1.7	3.1	0.00
1	*petE*	Synpcc7942_1088	-0.6	-1.5	0.31	-0.3	-1.2	0.54	2.6	6.2	0.00	2.4	5.1	0.00
4	*petJ2*	Synpcc7942_2542										1.8	3.4	0.00
5	*cytM*	Synpcc7942_1478	0.3	1.2	0.72	1.3	2.4	0.00	-0.4	-1.3	0.36	-1.4	-2.6	0.00
Respiration	**Respiration**	**Gene annotation**	**Log2 values**	**Fold change**	**P Values**	**Log2 values**	**Fold change**	**P Values**	**Log2 values**	**Fold change**	**P Values**	**Log2 values**	**Fold change**	**P Values**
1	*cydA*	Synpcc7942_1767	0.0	1.0	0.99	0.3	1.2	0.02	4.6	23.5	0.00	4.3	19.4	0.00
2	*cydB*	Synpcc7942_1766	0.1	1.0	0.97	0.5	1.4	0.04	3.6	11.9	0.00	3.1	8.5	0.00
3	*ctaA*	Synpcc7942_2601	-1.4	-2.7	0.00	-1.6	-2.9	0.00	2.5	5.8	0.00	2.7	6.3	0.00
4	*cox*	Synpcc7942_2603	-1.2	-2.4	0.06	-1.7	-3.2	0.00	2.4	5.4	0.00	2.9	7.3	0.00
5	*ctaC*	Synpcc7942_2602	-0.8	-1.7	0.26	-1.2	-2.3	0.03	2.8	7.1	0.00	3.2	9.2	0.00
6	*ctaE*	Synpcc7942_2604	-1.3	-2.4	0.03	-1.8	-3.4	0.00	0.7	1.7	0.14	1.2	2.3	0.01
NDH II	**NDH II**	**Gene annotation**	**Log2 values**	**Fold change**	**P Values**	**Log2 values**	**Fold change**	**P Values**	**Log2 values**	**Fold change**	**P Values**	**Log2 values**	**Fold change**	**P Values**
1	*ndbA*	Synpcc7942_0101	-0.6	-1.5	0.46	-0.1	-1.1	0.92	0.9	1.9	0.05	0.4	1.3	0.36
2	*ndbB*	Synpcc7942_2508	0.6	1.5	0.33	1.3	2.5	0.00	2.2	4.4	0.00	1.5	2.8	0.00
3	*ndbC*	Synpcc7942_0198	0.7	1.6	0.31	-0.7	-1.6	0.20	3.1	8.7	0.00	4.5	22.3	0.00
SDH	**SDH**	**Gene annotation**	**Log2 values**	**Fold change**	**P Values**	**Log2 values**	**Fold change**	**P Values**	**Log2 values**	**Fold change**	**P Values**	**Log2 values**	**Fold change**	**P Values**
1	*sdhA*	Synpcc7942_0641	0.1	1.1	0.89	0.7	1.6	0.17	1.4	2.7	0.00	0.9	1.8	0.03

2	*sdhB*	Synpcc7942_1533	0.1	1.1	0.94	0.1	1.1	0.85	-1.3	-2.5	0.00	-1.3	-2.5	0.00
NADH 1	**NADH 1**	**Gene annotation**	**Log2 values**	**Fold change**	**P Values**	**Log2 values**	**Fold change**	**P Values**	**Log2 values**	**Fold change**	**P Values**	**Log2 values**	**Fold change**	**P Values**
1	*ndhA*	Synpcc7942_1343	0.4	1.3	0.71	1.0	2.0	0.01	4.2	18.5	0.00	3.6	11.8	0.00
2	*ndhB*	Synpcc7942_1415	0.5	1.4	0.49	1.4	2.7	0.00	3.2	9.0	0.00	2.3	4.8	0.00
3	*ndhC*	Synpcc7942_1180	-0.0	-1.0	0.97	1.4	2.6	0.00	2.8	6.8	0.00	1.3	2.5	0.00
4	*ndhD*	Synpcc7942_1976	0.1	1.1	0.96	-2.8	-7.1	0.00	-0.5	-1.4	0.31	2.4	5.3	0.00
5	*ndhD2*	*Synpcc7942_1439*	1.8	3.5	0.00	1.6	3.0	0.00	0.9	1.8	0.08	0.8	1.7	0.08
6	*ndhD3*	Synpcc7942_2092	1.0	2.1	0.16	1.4	2.6	0.02	5.3	39.8	0.00	5.0	32.0	0.00
7	*ndhD4*	Synpcc7942_0609	0.2	1.2	0.79	1.0	2.0	0.02	1.5	2.9	0.00	0.7	1.7	0.04
8	ndhD5	Synpcc7942_1473	0.0	1.0	0.99	1.7	3.2	0.00	0.9	1.9	0.08	-0.7	-1.7	0.14
9	*ndhE*	Synpcc7942_1346	0.0	1.0	0.99	0.3	1.3	0.54	2.3	4.8	0.00	1.9	3.8	0.00
10	ndhF1	Synpcc7942_1977	0.5	1.4	0.48	1.4	2.7	0.00	3.5	11.1	0.00	2.5	5.8	0.00
11	ndhF3	Synpcc7942_2091	1.3	2.4	0.06	2.0	3.9	0.00	4.3	19.4	0.00	3.6	11.9	0.00
12	ndhF4	Synpcc7942_0309	0.6	1.5	0.49	-0.9	-1.8	0.19	1.5	2.8	0.01	2.9	7.7	0.00
13	*ndhG*	Synpcc7942_1345	-0.1	-1.1	0.95	0.6	1.5	0.26	3.5	10.9	0.00	2.7	6.7	0.00
14	*ndhH*	Synpcc7942_1743	-0.2	-1.2	0.80	0.8	1.8	0.13	3.7	12.9	0.00	2.6	6.2	0.00
15	*ndhI*	*Synpcc7942_1344*	0.1	1.1	0.95	0.4	1.3	0.54	3.6	12.0	0.00	3.3	10.0	0.00
16	*ndhJ*	*Synpcc7942_1182*	0.1	1.1	0.93	0.8	1.8	0.05	2.6	5.9	0.00	1.8	3.5	0.00
17	*ndhK*	*Synpcc7942_1181*	0.0	1.0	0.99	1.1	2.1	0.02	3.4	10.3	0.00	2.3	5.0	0.00
18	*ndhL*	Synpcc7942_0413	0.9	1.8	0.16	2.2	4.6	0.00	2.2	4.5	0.00	0.8	1.8	0.05
19	*ndhM*	Synpcc7942_1982	0.7	1.7	0.17	1.8	3.5	0.00	1.5	2.9	0.00	0.5	1.4	0.22
20	*cmpR*	*Synpcc7942_1310*	0.2	1.1	0.91	-0.9	-1.9	0.17	2.3	5.0	0.00	3.4	10.6	0.00
21	*cupA*	Synpcc7942_2093	0.1	1.1	0.92	0.5	1.4	0.44	4.3	19.3	0.00	3.9	15.3	0.00
22	*cupB*	*Synpcc7942_0308*	0.6	1.5	0.41	-0.4	-1.3	0.47	1.4	2.7	0.00	2.4	5.3	0.00

Appendix table 5.1: Transcript analysis of Δcyt c_M cultures compared to 3 different light conditions

S.No	Components	Gene finder	Cyt c_M 150 vs WT 150			Cyt c_M 600 vs WT 600			Cyt c_M 600 vs Cyt *cM* 150			WT600 vs WT150		
PS II	PS II	Gene annotation	Log_2 values	Fold change	P Values	Log_2 values	Fold change	P Values	Log_2 values	Fold change	P Values	Log_2 values	Fold change	P Values
1	*psb*A1	Synpcc7942_0424	0.5	1.4	0.06	0.0	1.0	0.91	-2.1	-4.2	0.00	-1.6	-3.0	0.00
2	*psb*A2	Synpcc7942_1389	2.3	5.1	0.00	0.2	1.1	0.69	-0.9	-1.8	0.05	1.3	2.5	0.00
3	*psb*A3	Synpcc7942_0893	1.7	3.2	0.00	0.3	1.3	0.26	-1.6	-2.9	0.00	-0.2	-1.2	0.44
4	*psb*B	Synpcc7942_0697	0.4	1.3	0.25	-0.7	-1.7	0.06	-0.7	-1.7	0.19	0.4	1.4	0.23
5	*psb*C	Synpcc7942_0656	1.2	2.4	0.00	-0.6	-1.5	0.08	-0.6	-1.5	0.22	1.2	2.4	0.00
6	*psb*D1	Synpcc7942_0655	2.0	4.1	0.00	-0.4	-1.3	0.20	-0.7	-1.6	0.12	1.8	3.4	0.00
7	*psb*D2	Synpcc7942_1637	2.1	4.3	0.00	-0.3	-1.2	0.40	-0.7	-1.6	0.11	1.7	3.3	0.00
8	*psb*E	Synpcc7942_1177	-1.7	-3.3	0.00	-0.9	-1.9	0.01	-0.3	-1.2	0.70	-1.1	-2.2	0.00
9	*psb*F	Synpcc7942_1176	-1.9	-3.6	0.00	-0.9	-1.9	0.01	-0.3	-1.2	0.77	-1.2	-2.3	0.00
10	*psb*H	Synpcc7942_0225	-2.1	-4.3	0.00	-0.6	-1.6	0.02	-0.4	-1.3	0.40	-1.8	-3.6	0.00
11	*psb*I	Synpcc7942_1705	-2.8	-6.8	0.00	-0.4	-1.3	0.29	0.0	-1.0	0.99	-2.4	-5.2	0.00
12	*psb*J	Synpcc7942_1174	-2.0	-4.0	0.00	-0.9	-1.9	0.01	-0.1	-1.1	0.93	-1.2	-2.3	0.00
13	*psb*K	Synpcc7942_0456	-4.1	-16.9	0.00	-0.7	-1.7	0.11	-0.5	-1.4	0.54	-3.9	-14.6	0.00
14	*psb*L	Synpcc7942_1175	-2.4	-5.4	0.00	-0.9	-1.9	0.01	-0.1	-1.1	0.96	-1.6	-3.0	0.00
15	*psb*M	Synpcc7942_0699	-4.5	-23.0	0.00	-0.8	-1.8	0.09	0.0	-1.0	0.99	-3.7	-13.2	0.00
16	*psb*N	Synpcc7942_0224	0.8	1.7	0.03	-0.5	-1.4	0.18	0.1	1.1	0.96	1.4	2.6	0.00
17	*psb*O	Synpcc7942_0294	0.4	1.3	0.38	-0.8	-1.8	0.10	-0.8	-1.8	0.30	0.4	1.4	0.35
18	*psb*P	Synpcc7942_1038	-1.0	-2.0	0.00	-0.6	-1.5	0.02	0.5	1.4	0.15	0.1	1.1	0.72
19	*psb*Q	Synpcc7942_1678	0.6	1.5	0.02	-0.8	-1.7	0.01	0.1	1.1	0.95	1.5	-0.4	0.00
20	*psb*Tc	Synpcc7942_0696	-1.2	-2.3	0.00	-0.8	-1.7	0.04	-0.3	-1.2	0.78	-0.7	-1.6	0.02
21	*psb*U	Synpcc7942_1882	-1.4	-2.6	0.00	-1.1	-2.1	0.01	-0.3	-1.2	0.82	-0.6	-1.5	0.12
22	*psb*V	Synpcc7942_2010	-2.0	-4.1	0.00	-1.0	-2.0	0.02	-0.5	-1.5	0.48	-1.6	-2.9	0.00
23	*psb*W	Synpcc7942_1679	0.1	1.1	0.66	-0.5	-1.4	0.11	-0.3	-1.2	0.64	0.4	1.3	0.23
24	*psb*X	Synpcc7942_2016	-3.2	-9.3	0.00	-1.0	-2.0	0.01	-0.3	-1.2	0.78	-2.5	-5.6	0.00
25	*psb*Y	Synpcc7942_1962	-4.1	-16.9	0.00	-0.9	-1.8	0.02	0.1	1.0	0.98	-3.2	-9.0	0.00
26	*psb*Z	Synpcc7942_2245	-2.0	-4.1	0.00	-1.0	-2.0	0.02	-0.6	-1.5	0.44	-1.6	-3.0	0.00
27	*psb*27	Synpcc7942_0343	-0.1	-1.1	0.78	-0.9	-1.9	0.00	0.0	1.0	1.00	0.8	1.8	0.00

28	*psb*28	Synpcc7942_2478	-3.9	-15.0	0.00	0.5	1.4	0.52	1.3	2.4	0.22	-3.1	-8.7	0.00
29	*psb*29	Synpcc7942_1555	1.5	2.8	0.00	-0.8	-1.8	0.00	-0.3	-1.2	0.50	2.0	4.1	0.00
30	*psb*30	Synpcc7942_2134	2.5	5.7	0.00	-0.1	-1.1	0.78	0.3	1.2	0.50	2.9	7.5	0.00
31	*ftsH*	Synpcc7942_0297	1.1	2.2	0.00	-0.3	-1.2	0.39	-0.3	-1.2	0.76	1.2	2.3	0.00
32	*ftsH*	Synpcc7942_0942	1.0	2.0	0.00	-0.1	-1.1	0.85	-0.1	-1.1	0.94	0.9	1.9	0.00
33	*ftsH*	Synpcc7942_0998	-0.7	-1.6	0.00	-0.7	-1.7	0.01	0.3	1.2	0.60	0.3	1.3	0.17
34	*fstH-2*	Synpcc7942_1314	-1.3	-2.4	0.00	-0.7	-1.6	0.01	0.0	-1.0	1.00	-0.3	-1.3	0.66
PS II	**PS II**	**Gene annotation**	**Log_2 values**	**Fold change**	**P Values**	**Log_2 values**	**Fold change**	**P Values**	**Log_2 values**	**Fold change**	**P Values**	**Log_2 values**	**Fold change**	**P Values**
1	*psa*A	Synpcc7942_2049	-1.0	-2.0	0.02	-0.9	-1.9	0.05	-0.5	-1.4	0.57	-0.5	-1.5	0.20
2	*psa*B	Synpcc7942_2048	-1.2	-2.4	0.00	-0.9	-1.8	0.04	-0.5	-1.4	0.51	-0.9	-1.8	0.02
3	*psa*C	Synpcc7942_0535	-0.1	-1.1	0.68	-0.9	-1.9	0.01	-0.2	-1.2	0.82	0.5	-0.7	0.10
4	*psaD*	Synpcc7942_1002	-2.0	-4.0	0.00	-1.1	-2.1	0.01	-0.5	-1.4	0.53	-1.4	-2.6	0.00
5	*psa*E	Synpcc7942_1322	-2.3	-5.0	0.00	-1.2	-2.3	0.00	-0.4	-1.3	0.65	-1.5	-2.8	0.00
6	*psaF*	Synpcc7942_1250	-0.7	-1.6	0.10	-1.9	-3.8	0.00	-0.7	-1.7	0.32	0.5	1.4	0.26
7	*psaI*	Synpcc7942_2343	-2.5	-5.5	0.00	-1.6	-3.1	0.00	-0.7	-1.6	0.28	-1.5	-2.9	0.00
8	*psaJ*	Synpcc7942_1249	-3.4	-10.8	0.00	-1.8	-3.4	0.00	-0.5	-1.4	0.54	-2.2	-4.5	0.00
9	*psaK*1	Synpcc7942_0407	0.6	1.5	0.10	-1.6	-3.1	0.00	-1.3	-2.5	0.00	0.9	1.9	0.01
10	*psaK*2	Synpcc7942_0920	-0.5	-1.4	0.22	-1.6	-3.0	0.00	-0.5	-1.4	0.54	0.6	1.5	0.18
11	*psaL*	Synpcc7942_2342	-1.6	-3.1	0.00	-1.7	-3.2	0.00	-0.7	-1.6	0.23	-0.6	-1.6	0.06
12	*bptA*	Synpcc7942_2513	1.2	2.4	0.00	-0.9	-1.8	0.00	-0.8	-1.7	0.01	1.4	2.6	0.00
13	*ycf3*	Synpcc7942_2321	-1.6	-3.0	0.00	-0.6	-1.5	0.13	-0.3	-1.2	0.70	-1.3	-2.5	0.00
14	*ycf4*	Synpcc7942_0654	0.9	1.9	0.00	-0.1	-1.0	0.88	0.2	1.1	0.87	1.2	2.3	0.00
Cyt *b6f* comp	**PS II**	**Gene annotation**	**Log_2 values**	**Fold change**	**P Values**	**Log_2 values**	**Fold change**	**P Values**	**Log_2 values**	**Fold change**	**P Values**	**Log_2 values**	**Fold change**	**P Values**
1	*pet*A	Synpcc7942_1231	0.1	1.0	0.89	-1.0	-2.0	0.02	-0.5	-1.4	0.55	0.6	1.5	0.12
2	*pet*B	Synpcc7942_2331	1.1	2.2	0.00	-0.3	-1.3	0.40	-0.5	-1.4	0.51	1.0	2.0	0.00
3	*pet*C	Synpcc7942_1232	1.3	2.5	0.00	-0.8	-1.8	0.05	-0.7	-1.7	0.18	1.4	2.6	0.00
4	*pet*D	Synpcc7942_2332	-0.8	-1.8	0.02	-0.7	-1.6	0.12	-0.6	-1.5	0.40	-0.8	-1.7	0.03
5	*pet*G	Synpcc7942_1479	-1.7	-3.3	0.00	-0.6	-1.5	0.06	-0.1	-1.1	0.93	-1.2	-2.3	0.00
6	*pet*L	Synpcc7942_0113	-0.7	-1.6	0.08	-0.8	-1.7	0.05	-0.2	-1.1	0.92	0.0	-1.0	0.93
7	*pet*M	Synpcc7942_2426	-2.2	-4.7	0.00	-0.4	-1.3	0.40	-0.3	-1.2	0.85	-2.1	-4.3	0.00
8	*pet*N	Synpcc7942_0475	0.1	1.1	0.76	-0.7	-1.6	0.03	-0.1	-1.1	0.91	0.6	1.6	0.02

ATP Synthase	**ATP Synthase**	**Gene annotation**	**Log_2 values**	**Fold change**	**P Values**	**Log_2 values**	**Fold change**	**P Values**	**Log_2 values**	**Fold change**	**P Values**	**Log_2 values**	**Fold change**	**P Values**
1	*atpA*	Synpcc7942_0336	-0.3	-1.2	0.55	-0.6	-1.5	0.19	0.0	-1.0	1.00	0.3	1.3	0.43
2	*atpB*	Synpcc7942_2315	-0.3	-1.3	0.33	-0.8	-1.7	0.04	-0.1	-1.0	0.98	0.4	1.3	0.28
3	*atpC/E*	Synpcc7942_2316	0.6	1.5	0.04	-0.8	-1.8	0.02	-0.2	-1.1	0.89	1.3	2.4	0.00
4	*atpD*	Synpcc7942_0335	0.7	1.6	0.09	-0.7	-1.6	0.12	0.0	-1.0	0.99	1.3	2.5	0.00
5	*atpF*	Synpcc7942_0334	1.1	2.2	0.00	-0.7	-1.6	0.08	-0.3	-1.2	0.79	1.5	2.9	0.00
6	*atpG*	Synpcc7942_0333	1.2	2.3	0.00	-0.7	-1.7	0.07	-0.4	-1.3	0.63	1.6	3.0	0.00
7	*atpH*	Synpcc7942_0332	1.6	3.0	0.00	-0.6	-1.5	0.11	-0.3	-1.3	0.68	1.9	3.7	0.00
Phycobili proteins	***Phycobil iproteins***	**Gene annotation**	**Log_2 values**	**Fold change**	**P Values**	**Log_2 values**	**Fold change**	**P Values**	**Log_2 values**	**Fold change**	**P Values**	**Log_2 values**	**Fold change**	**P Values**
1	*apc*A	Synpcc7942_0327	0.4	1.4	0.36	-1.1	-2.1	0.04	-1.0	-2.0	0.13	0.5	1.4	0.29
2	*apcB1/apcF*	Synpcc7942_2158	0.6	1.5	0.11	-1.1	-2.2	0.00	-0.6	-1.5	0.38	1.1	2.2	0.00
3	*apcB*	Synpcc7942_0326	-0.8	-1.8	0.05	-1.1	-2.1	0.03	-0.9	-1.9	0.19	-0.6	-1.6	0.16
4	*apc*D	Synpcc7942_0240	0.0	-1.0	0.93	-0.8	-1.8	0.11	-1.1	-2.1	0.11	-0.2	-1.1	0.70
5	*cpc*A1	Synpcc7942_1048	-2.0	-4.1	0.00	-1.4	-2.6	0.00	-1.5	-2.9	0.00	-2.2	-4.6	0.00
6	*cpcA*2	Synpcc7942_1053	-1.8	-3.6	0.00	-1.4	-2.6	0.00	-1.4	-2.7	0.00	-1.9	-3.7	0.00
7	*cpc*B1	Synpcc7942_1047	-1.4	-2.7	0.00	-1.4	-2.7	0.00	-1.7	-3.2	0.00	-1.7	-3.3	0.00
8	*cpc*B2	Synpcc7942_1052	-1.1	-2.1	0.00	-1.4	-2.7	0.00	-1.4	-2.6	0.00	-1.1	-2.1	0.00
9	*cpcE*	Synpcc7942_1054	0.4	1.3	0.36	-0.7	-1.7	0.12	-1.5	-2.9	0.00	0.6	1.5	0.20
10	*cpcF*	Synpcc7942_1055	1.1	2.1	0.01	-0.6	-1.5	0.11	-0.6	-1.5	0.48	1.4	2.6	0.00
11	*cpc*G	Synpcc7942_2030	-0.7	-1.6	0.05	-1.4	-2.6	0.00	-0.3	-1.2	0.77	-0.2	-1.1	0.69
12	*cpc*H	Synpcc7942_1049	-0.8	-1.7	0.05	-1.2	-2.3	0.01	-0.9	-1.9	0.07	-1.4	-2.6	0.00
13	*cpc*I1	Synpcc7942_1050	0.0	1.0	0.94	-1.0	-2.1	0.01	-1.8	-3.4	0.00	-0.7	-1.6	0.06
14	*cpc*I2/cpcD	Synpcc7942_1051	-0.6	-1.5	0.15	-1.1	-2.1	0.02	-1.7	-3.3	0.00	-0.9	-1.9	0.02
Electron carrier	**Electron carrier**	**Gene annotation**	**Log_2 values**	**Fold change**	**P Values**	**Log_2 values**	**Fold change**	**P Values**	**Log_2 values**	**Fold change**	**P Values**	**Log_2 values**	**Fold change**	**P Values**
1	*petE*	Synpcc7942_1088	0.6	1.5	0.07	-1.2	-2.3	0.00	-0.4	-1.3	0.62	1.4	2.7	0.00
2	*petJ1*	Synpcc7942_1630	1.6	3.1	0.00	-2.0	-4.1	0.00	-0.3	-1.2	0.69	3.4	10.3	0.00
3	*petJ1iso*	Synpcc7942_0239	0.9	1.9	0.01	-0.8	-1.7	0.02	-0.1	-1.1	0.96	1.6	3.0	0.00
4	*petJ2*	Synpcc7942_2542	1.0	2.0	0.00	0.3	1.2	0.24	0.2	1.1	0.83	0.8	1.8	0.00
5	*cytM*	Synpcc7942_1478										0.4	1.3	0.20
High light inducible gene	**High light inducible gene**	**Gene annotation**	**Log_2 values**	**Fold change**	**P Values**	**Log_2 values**	**Fold change**	**P Values**	**Log_2 values**	**Fold change**	**P Values**	**Log_2 values**	**Fold change**	**P Values**
1	*nbl*A1	Synpcc7942_2127	0.3	1.2	0.49	-0.4	-1.4	0.31	1.3	2.4	0.00	2.0	4.0	0.00

2	*nbIB*	Synpcc7942_1823	0.2	1.2	0.34	-0.4	-1.3	0.10	-0.1	-1.0	0.96	0.6	1.5	0.01
3	*nbIB2*	Synpcc7942_1721	-1.1	-2.2	0.00	-0.7	-1.6	0.03	0.0	-1.0	0.98	-0.5	0.7	0.09
4	hliA	Synpcc7942_1997	-1.1	-2.1	0.00	0.3	1.3	0.35	1.2	2.3	0.00	-0.2	-1.2	0.54
5	*hliC*	Synpcc7942_0243	-0.4	-1.3	0.18	0.0	-1.0	0.98	1.2	2.3	0.00	0.8	1.7	0.01
6	*hliP*	Synpcc7942_1331	0.6	1.5	0.02	0.1	1.1	0.72	0.0	1.0	0.98	0.5	1.4	0.03
7	*hliP*	Synpcc7942_1759	-0.4	-1.4	0.12	-0.1	-1.1	0.81	0.3	1.2	0.73	-0.1	-1.1	0.76
8	*isiA/cp43'*	Synpcc7942_1542	3.0	8.0	0.00	0.6	1.5	0.21	1.0	2.1	0.11	3.4	10.6	0.00
Respiration	**Respiration**	**Gene annotation**	**Log_2 values**	**Fold change**	**P Values**	**Log_2 values**	**Fold change**	**P Values**	**Log_2 values**	**Fold change**	**P Values**	**Log_2 values**	**Fold change**	**P value**
1	*cydA*	Synpcc7942_1767	1.1	2.2	0.00	0.4	1.3	0.32	0.6	1.5	0.35	1.3	-0.4	0.00
2	*cydB*	Synpcc7942_1766	-0.8	-1.7	0.07	0.3	1.2	0.53	0.7	1.7	0.30	-0.3	-1.3	0.45
3	*ctaA*	Synpcc7942_2601	-1.9	-3.7	0.00	1.4	2.6	0.00	1.9	3.7	0.00	-1.4	-2.6	0.00
4	*cox*	Synpcc7942_2603	-2.8	-7.0	0.00	1.5	2.9	0.00	1.8	3.6	0.00	-2.5	-5.6	0.00
5	*ctaC*	Synpcc7942_2602	-2.7	-6.4	0.00	1.7	3.2	0.00	1.9	3.9	0.00	-2.4	-5.4	0.00
6	*ctaE*	Synpcc7942_2604	-4.3	-19.4	0.00	1.6	3.0	0.00	1.8	3.4	0.00	-4.1	-17.5	0.00
NDH II	**NDH II**	**Gene annotation**	**Log_2 values**	**Fold change**	**P Values**	**Log_2 values**	**Fold change**	**P Values**	**Log_2 values**	**Fold change**	**P Values**	**Log_2 values**	**Fold change**	**P Values**
1	*ndbA*	Synpcc7942_0101	-0.7	-1.6	0.01	-0.9	-1.9	0.00	0.1	1.1	0.94	0.6	1.5	0.02
2	*ndbB*	Synpcc7942_2508	1.9	3.8	0.00	-0.1	-1.1	0.60	0.3	1.2	0.46	2.4	5.1	0.00
3	*ndbC*	Synpcc7942_0198	1.5	2.9	0.00	0.2	1.2	0.54	1.1	2.1	0.00	2.4	5.2	0.00
SDH	**SDH**	**Gene annotation**	**Log_2 values**	**Fold change**	**P Values**	**Log_2 values**	**Fold change**	**P Values**	**Log_2 values**	**Fold change**	**P Values**		**Fold change**	**P Values**
1	*sdhA*	Synpcc7942_0641	0.7	1.6	0.00	-0.3	-1.2	0.15	0.3	1.2	0.36	1.3	2.5	0.00
2	*sdhB*	Synpcc7942_1533	-1.2	-2.3	0.00	-0.5	-1.4	0.17	-0.1	-1.1	0.96	-0.8	-1.8	0.00
NADH 1	**NADH 1**	**Gene annotation**	**Log_2 values**	**Fold change**	**P Values**	**Log_2 values**	**Fold change**	**P Values**	**Log_2 values**	**Fold change**	**P Values**	**Log_2 values**	**Fold change**	**P Values**
1	*ndh*A	Synpcc7942_1343	1.6	2.9	0.00	0.8	1.7	0.09	1.4	2.7	0.00	2.2	4.6	0.00
2	*ndhB*	Synpcc7942_1415	0.6	1.6	0.06	0.3	1.2	0.44	0.5	1.5	0.39	0.9	1.8	0.01
3	*ndh*C	Synpcc7942_1180	1.4	2.6	0.00	0.2	1.1	0.53	0.7	1.6	0.04	1.9	3.6	0.00
4	*ndhD*	Synpcc7942_1976	-0.4	-1.4	0.18	0.7	1.6	0.06	-0.1	-1.0	0.97	-1.2	-2.2	0.00
5	*ndhD2*	*Synpcc7942_1439*	0.9	1.9	0.01	-1.0	0.5	0.02	1.9	3.6	0.00	3.7	13.2	0.00
6	*ndh*D3	Synpcc7942_2092	2.8	-0.1	0.00	0.4	-0.8	0.45	0.9	1.8	0.24	3.2	9.4	0.00
7	*ndh*D4	Synpcc7942_0609	-0.1	-1.1	0.77	-0.3	0.8	0.26	0.2	1.2	0.75	0.5	1.4	0.07
8	*ndhD5*	Synpcc7942_1473	-3.3	-10.1	0.00	1.2	2.3	0.04	2.5	5.7	0.00	-2.0	-4.0	0.00
9	*ndhE*	Synpcc7942_1346	-1.0	0.5	0.00	0.6	-0.6	0.12	1.2	-0.4	0.00	-0.4	-1.3	0.28

10	*ndhF1*	Synpcc7942_1977	2.1	4.2	0.00	-0.3	0.8	0.43	-0.1	1.0	0.97	2.3	4.9	0.00
11	*ndhF3*	Synpcc7942_2091	2.4	5.4	0.00	0.5	-0.7	0.41	1.0	2.0	0.19	3.0	7.9	0.00
12	*ndhF4*	Synpcc7942_0309	1.3	2.4	0.00	-0.5	0.7	0.09	-0.1	0.9	0.95	1.7	3.3	0.00
13	*ndhG*	Synpcc7942_1345	0.4	1.3	0.42	0.7	1.6	0.14	1.2	2.3	0.02	0.9	1.8	0.03
14	*ndhH*	Synpcc7942_1743	0.9	1.8	0.01	0.1	1.1	0.74	1.0	1.9	0.04	1.7	3.2	0.00
15	*ndh*I	*Synpcc7942_1344*	0.8	1.7	0.05	0.8	1.7	0.10	1.2	2.3	0.02	1.2	2.3	0.00
16	*ndh*J	*Synpcc7942_1182*	0.8	1.8	0.00	0.2	1.1	0.41	0.7	1.6	0.01	1.3	2.5	0.00
17	*ndh*K	*Synpcc7942_1181*	1.2	2.3	0.00	0.1	-0.9	0.62	0.8	1.8	0.01	1.9	3.7	0.00
18	*ndh*L	Synpcc7942_0413	0.6	1.5	0.04	-0.1	-1.1	0.78	0.3	1.2	0.62	1.0	2.0	0.00
19	*ndhM*	Synpcc7942_1982	0.4	1.3	0.18	-0.5	-1.4	0.09	0.2	1.1	0.86	1.0	2.1	0.00
20	*cmpR*	*Synpcc7942_1310*	-0.2	-1.1	0.48	-0.1	-1.1	0.69	0.2	1.1	0.84	0.1	1.1	0.72
21	*cupA*	Synpcc7942_2093	0.3	1.3	0.45	0.4	1.4	0.35	1.0	2.0	0.08	0.9	1.9	0.03
22	*cupB*	*Synpcc7942_0308*	0.1	1.1	0.73	-0.3	-1.3	0.25	0.0	-1.0	0.98	0.4	1.3	0.13

	Appendix table 6.1: Transcript analysis of wild type cultures compared to 2 different light conditions							
S.No	Components Name	Gene annotation	WT500 vs WT150			WT600 vs WT150		
PS II	**PS II**	**Gene annotation**	**Log_2 values**	**Fold change**	**P Values**	**Log_2 values**	**Fold change**	**P Values**
1	*psb*A1	Synpcc7942_0424	0.222131383	1.166455591	0.5885000	-1.587115317	-3.004479997	0.0000000
2	*psb*A2	Synpcc7942_1389	3.461574115	11.01634785	0.0000000	1.308303732	2.476501907	0.0000000
3	*psb*A3	Synpcc7942_0893	0.181025168	1.13368919	0.7306000	-0.220796977	-1.165377189	0.4360000
4	*psb*B	Synpcc7942_0697	2.179158148	4.528892038	0.0000000	0.435719371	1.352585104	0.2316000
5	*psb*C	Synpcc7942_0656	2.988878641	7.93856718	0.0000000	1.239291912	2.360826323	0.0000000
6	*psb*D1	Synpcc7942_0655	3.389739789	10.48125661	0.0000000	1.784268667	3.444438137	0.0000000
7	*psb*D2	Synpcc7942_1637	3.369956759	10.33851277	0.0000000	1.701565711	3.252537546	0.0000000
8	*psb*E	Synpcc7942_1177	0.775773165	1.712107353	0.0395000	-1.108107505	-2.155626914	0.0001000
9	*psb*F	Synpcc7942_1176	0.842384663	1.793011403	0.0252000	-1.176184306	-2.259783101	0.0000000
10	*psb*H	Synpcc7942_0225	-1.802644928	-3.488592115	0.0000000	-1.831343343	-3.558682794	0.0000000
11	*psb*I	Synpcc7942_1705	-1.772295162	-3.415969662	0.0000000	-2.373066795	-5.180411837	0.0000000
12	*psb*J	Synpcc7942_1174	0.587033351	1.502154652	0.1232000	-1.205215303	-2.305716765	0.0000000
13	*psb*K	Synpcc7942_0456	-3.166292999	-8.977370886	0.0000000	-3.867120766	-14.59215209	0.0000000
14	*psb*L	Synpcc7942_1175	0.466622578	1.381870649	0.2430000	-1.587790855	-3.005887166	0.0000000
15	*psb*M	Synpcc7942_0699	-4.42201377	-21.43674224	0.0000000	-3.718979966	-13.16814266	0.0000000
16	*psb*N	Synpcc7942_0224	1.107914623	2.155338736	0.0076000	1.363514457	2.573112361	0.0000000
17	*psb*O	Synpcc7942_0294	1.85190041	3.609753718	0.0000000	0.445668685	1.361945228	0.3488000
18	*psb*P	Synpcc7942_1038	-0.223603951	-1.167646808	0.6470000	0.101455376	1.072855202	0.7214000
19	*psb*Q	Synpcc7942_1678	2.730021723	6.634656265	0.0000000	1.489370792	-0.356167852	0.0000000
20	*psb*Tc	Synpcc7942_0696	1.61874991	3.071088123	0.0000000	-0.722259793	-1.649764151	0.0210000
21	*psb*U	Synpcc7942_1882	0.450564362	1.366574737	0.3012000	-0.5646846	-1.479064123	0.1229000
22	*psb*V	Synpcc7942_2010	1.24955726	2.377684445	0.0032000	-1.554164847	-2.936636803	0.0000000
23	*psb*W	Synpcc7942_1679	0.299643186	1.230839959	0.5256000	0.362475026	1.285629578	0.2328000
24	*psb*X	Synpcc7942_2016	-2.503382676	-5.670133394	0.0000000	-2.489388181	-5.615397617	0.0000000
25	*psb*Y	Synpcc7942_1962	-3.394498531	-10.51588621	0.0000000	-3.171488921	-9.009761528	0.0000000
26	*psb*Z	Synpcc7942_2245	-1.455371251	-2.742271192	0.0003000	-1.588842253	-3.008078576	0.0000000
27	*psb*27	Synpcc7942_0343	1.989927019	3.972169038	0.0000000	0.831183191	1.779143885	0.0013000
28	*psb*28	Synpcc7942_2478	-0.79164512	-1.731047269	0.4167000	-3.117177844	-8.676888823	0.0000000
29	*psb*29	Synpcc7942_1555	1.774802272	3.421911082	0.0000000	2.048586817	4.137005332	0.0000000

30	*psb*30	Synpcc7942_2134	3.479388657	11.15322214	0.0000000	2.914227347	7.53823801	0.0000000
31	*ftsH*	Synpcc7942_0297	1.678493032	3.200934226	0.0000000	1.190690532	2.282619724	0.0000000
32	*ftsH*	Synpcc7942_0942	1.213734367	2.31937222	0.0001000	0.944966061	1.925143597	0.0007000
33	*ftsH*	Synpcc7942_0998	-0.158687572	-1.116271198	0.7154000	0.341379948	1.266967878	0.1721000
34	*fstH-2*	Synpcc7942_1314	2.694919593	6.475176836	0.0000000	-0.34218384	-1.267674049	0.6632000
PS II	**PS I**	**Gene annotation**	**Log_2 values**	**Fold change**	**P Values**	**Log_2 values**	**Fold change**	**P Values**
1	*psa*A	Synpcc7942_2049	2.57016383	5.938768641	0.0000000	-0.546212865	-1.46024745	0.1979000
2	*psa*B	Synpcc7942_2048	2.391583914	5.247331423	0.0000000	-0.867431839	-1.824412347	0.0189000
3	*psa*C	Synpcc7942_0535	0.396068791	1.315917269	0.3687000	0.536089603	-0.689637628	0.0993000
4	*psaD*	Synpcc7942_1002	0.541107686	1.455089291	0.1943000	-1.395502528	-2.630801737	0.0000000
5	*psa*E	Synpcc7942_1322	-0.277608726	-1.212184017	0.5181000	-1.492644821	-2.814043872	0.0000000
6	*psaF*	Synpcc7942_1250	1.685684527	3.216929963	0.0002000	0.490603548	1.405032545	0.2561000
7	*psaI*	Synpcc7942_2343	-0.403434838	-1.322653202	0.4014000	-1.544080768	-2.916182013	0.0000000
8	*psaJ*	Synpcc7942_1249	-0.17509478	-1.129038576	0.7310000	-2.184354354	-4.54523332	0.0000000
9	*psaK*1	Synpcc7942_0407	0.594813991	1.51027785	0.1587000	0.891144109	1.854646342	0.0064000
10	*psaK*2	Synpcc7942_0920	0.496911251	1.41118903	0.2997000	0.559768146	1.474032308	0.1806000
11	*psaL*	Synpcc7942_2342	0.850150652	1.802689159	0.0385000	-0.647958577	-1.566949383	0.0637000
12	*bptA*	Synpcc7942_2513	-0.255409457	-1.193674476	0.5468000	1.368959615	2.582842399	0.0000000
13	*ycf3*	Synpcc7942_2321	1.897212644	3.724928269	0.0000000	-1.323993362	-2.503581398	0.0000000
14	*ycf4*	Synpcc7942_0654	2.064715081	4.183513472	0.0000000	1.170265864	2.250531666	0.0001000
Cyt *b6f* complex	**Cyt b_6f**	**Gene annotation**	**Log_2 values**	**Fold change**	**P Values**	**Log_2 values**	**Fold change**	**P Values**
1	*pet*A	Synpcc7942_1231	0.986906229	1.981930303	0.0120000	0.567057069	1.481498401	0.1173000
2	*pet*B	Synpcc7942_2331	0.67916585	1.601213684	0.1473000	1.007479178	2.010395264	0.0035000
3	*pet*C	Synpcc7942_1232	1.273833176	2.41803173	0.0024000	1.374190296	2.592223831	0.0001000
4	*pet*D	Synpcc7942_2332	0.468167224	1.383350965	0.2763000	-0.78176392	-1.719231618	0.0325000
5	*pet*G	Synpcc7942_1479	-2.375555173	-5.189354784	0.0000000	-1.22146477	-2.331833485	0.0000000
6	*pet*L	Synpcc7942_0113	-0.493263734	-1.407625675	0.2403000	-0.03487688	-1.024469391	0.9345000
7	*pet*M	Synpcc7942_2426	-3.227141354	-9.364106574	0.0000000	-2.093885553	-4.268962688	0.0000000
8	*pet*N	Synpcc7942_0475	-0.057364974	-1.040563476	0.8964000	0.642225352	1.560734731	0.0194000
ATP Synthase	**ATP synthase**	**Gene annotation**	**Log_2 values**	**Fold change**	**P Values**	**Log_2 values**	**Fold change**	**P Values**
1	*atpA*	Synpcc7942_0336	0.136714947	1.099398905	0.8028000	0.326469814	1.2539413	0.4349074
2	*atpB*	Synpcc7942_2315	0.571711857	1.486286106	0.1341000	0.367514114	1.290127914	0.2762601
3	*atpC/E*	Synpcc7942_2316	0.760112252	1.693622396	0.0515000	1.257703819	2.391148647	0.0000114

4	*atpD*	Synpcc7942_0335	0.906477379	1.87446304	0.0350000	1.349054236	2.547450717	0.0003847
5	*atpF*	Synpcc7942_0334	0.645522303	1.564305514	0.0965000	1.530574923	2.88900945	0.0000034
6	*atpG*	Synpcc7942_0333	0.166898705	1.122642596	0.7122000	1.578778365	2.987167973	0.0000037
7	*atpH*	Synpcc7942_0332	0.476007061	1.390888779	0.2551000	1.883937589	3.690810303	0.0000000
Phycobili proteins	**Phycobili proteins**	**Gene annotation**	**Log_2 values**	**Fold change**	**P Values**	**Log_2 values**	**Fold change**	**P Values**
1	*apc*A	Synpcc7942_0327	1.019818346	2.027663634	0.0610000	0.501633141	1.415815369	0.2858000
2	*apcB1/apF*	Synpcc7942_2158	1.092737709	2.132783773	0.0103000	1.105180461	2.151257856	0.0008000
3	*apcB*	Synpcc7942_0326	0.644340214	1.563024307	0.2044000	-0.634386364	-1.552277364	0.1560000
4	*apc*D	Synpcc7942_0240	0.984237533	1.978267518	0.2403000	-0.199827922	-1.148561352	0.7004000
5	*cpc*A1	Synpcc7942_1048	-0.708584105	-1.634199488	0.1452000	-2.200192393	-4.595406207	0.0000000
6	*cpcA*2	Synpcc7942_1053	-0.380184992	-1.301508733	0.4695000	-1.872817468	-3.662471335	0.0000000
7	*cpc*B1	Synpcc7942_1047	-0.991850462	-1.988734191	0.0252000	-1.702638451	-3.254956924	0.0000000
8	*cpc*B2	Synpcc7942_1052	-0.164234532	-1.120571365	0.7620000	-1.057292262	-2.081022065	0.0038000
9	*cpcE*	Synpcc7942_1054	1.591695453	3.014033502	0.0005000	0.555292823	1.46946686	0.2026000
10	*cpcF*	Synpcc7942_1055	1.13005934	2.188677424	0.0598000	1.384046415	2.609993864	0.0004000
11	*cpc*G	Synpcc7942_2030	-0.059132614	-1.041839192	0.9074000	-0.159313461	-1.116755578	0.6860000
12	*cpc*H	Synpcc7942_1049	0.256268479	1.194385436	0.5924000	-1.358843383	-2.56479476	0.0004000
13	*cpc*I1	Synpcc7942_1050	0.780114529	1.717267193	0.0760000	-0.667394084	-1.588201633	0.0559000
14	*cpc*I2/cpcD	Synpcc7942_1051	0.483584757	1.398213585	0.3084000	-0.90928222	-1.878110855	0.0222000
Electron carrier	**Electron carrier**	**Gene annotation**	**Log_2 values**	**Fold change**	**P Values**	**Log_2 values**	**Fold change**	**P Values**
1	*petE*	Synpcc7942_1088	2.356313355	5.120601735	0.0000000	1.42422682	2.683706348	0.0000000
2	*petJ1*	Synpcc7942_1630	1.637866366	3.11205243	0.0016000	3.363570969	10.29285262	0.0000000
3	*petJ1iso*	Synpcc7942_0239	1.651403741	3.141391476	0.0005000	1.598600479	3.028493844	0.0000000
4	*petJ2*	Synpcc7942_2542	1.756053243	3.377728203	0.0001000	0.849336161	1.801671717	0.0045000
5	*cytM*	Synpcc7942_1478	-1.385377619	-2.61240327	0.0000000	0.354228658	1.27830195	0.2012000
High light inducible gene	**High light inducible gene**	**Gene annotation**	**Log_2 values**	**Fold change**	**P Values**	**Log_2 values**	**Fold change**	**P Values**
1	*nbl*A1	Synpcc7942_2127	-0.89727963	-1.862550613	0.0502000	1.98530056	3.959451421	0.0000000
2	*nbIB*	Synpcc7942_1823	0.898138459	1.86365971	0.0162	0.606943546	1.523029141	0.0092
3	*nbIB2*	Synpcc7942_1721	0.075055114	1.053401277	0.8733	-0.478043035	-1.392853028	0.0934
4	*hliA*	Synpcc7942_1997	-3.435062058	-10.8157519	0.0000000	-0.216179186	-1.161653003	0.5371000
5	*hliC*	Synpcc7942_0243	1.350932744	2.550769868	0.0003000	0.781689345	1.71914275	0.0091000

6	*hliP*	Synpcc7942_1331	0.556383498	1.470578194	0.1922000	0.533791892	1.447729323	0.0319000
7	*hliP*	Synpcc7942_1759	-0.249452894	-1.188756223	0.6296000	-0.100496767	-1.072142573	0.7560000
8	*isiA/cp43'*	Synpcc7942_1542	2.930783043	7.625241568	0.0001000	3.405084614	10.59333256	0.0000000
Respiration	**Respiration**	**Gene annotation**	**Log_2 values**	**Fold change**	**P Values**	**Log_2 values**	**Fold change**	**P value**
1	cydA	Synpcc7942_1767	4.276352278	19.37806051	0.0000000	1.322646938	-0.399800744	0.0001000
2	cydB	Synpcc7942_1766	3.088506083	8.506148744	0.0000000	-0.334865686	-1.261259981	0.4471000
3	*ctaA*	Synpcc7942_2601	2.662280293	6.330328173	0.0000000	-1.401444438	-2.641659349	0.0003000
4	cox	Synpcc7942_2603	2.872546537	7.323567211	0.0000000	-2.486894382	-5.605699395	0.0000000
5	*ctaC*	Synpcc7942_2602	3.205048679	9.221801929	0.0000000	-2.427208378	-5.378516775	0.0000000
6	*ctaE*	Synpcc7942_2604	1.207739006	2.30975368	0.0055000	-4.129423475	-17.50170385	0.0000000
NDH II	**NDH II**	**Gene annotation**	**Log_2 values**	**Fold change**	**P Values**	**Log_2 values**	**Fold change**	**P Values**
1	*ndbA*	Synpcc7942_0101	0.428965641	1.346268006	0.3646000	0.596802633	1.512361086	0.0245000
2	*ndbB*	Synpcc7942_2508	1.467049043	2.76455839	0.0000000	2.358484076	5.128312141	0.0000000
3	*ndbC*	Synpcc7942_0198	4.476192304	22.25707811	0.0000000	2.387887676	5.233904773	0.0000000
SDH	**SDH**	**Gene annotation**	**Log_2 values**	**Fold change**	**P Values**	**Log_2 values**	**Fold change**	**P Values**
1	*sdhA*	Synpcc7942_0641	0.863630954	1.819612126	0.0339000	1.308996648	2.477691639	0.0000000
2	*sdhB*	Synpcc7942_1533	-1.326147959	-2.507323172	0.0001000	-0.835286368	-1.784211161	0.0043000
NADH 1	**NADH 1**	**Gene annotation**	**Log_2 values**	**Fold change**	**P Values**	**Log_2 values**	**Fold change**	**P Values**
1	*ndh*A	Synpcc7942_1343	3.562460071	11.81428218	0.0000000	2.205726352	4.613067338	0.0000000
2	*ndhB*	Synpcc7942_1415	2.25616148	4.777187426	0.0000000	0.87590675	1.835161143	0.0074000
3	*ndh*C	Synpcc7942_1180	1.316158617	2.490022221	0.0002000	1.859592088	3.629050387	0.0000000
4	*ndhD*	Synpcc7942_1976	2.401666529	5.284132083	0.0000000	-1.156100946	-2.228543228	0.0001000
5	*ndhD2*	*Synpcc7942_1439*	0.793418705	1.73317665	0.0762000	3.722805514	13.20310654	0.0000000
6	*ndh*D3	Synpcc7942_2092	5.002212092	32.04910341	0.0000000	3.232211506	9.397073325	0.0000000
7	*ndhD4*	Synpcc7942_0609	0.744203806	1.675049588	0.0392000	0.489526565	1.403984069	0.0738000
8	*ndhD5*	Synpcc7942_1473	-0.723962399	-1.651712281	0.1360000	-1.996511149	-3.990338538	0.0000000
9	*ndhE*	Synpcc7942_1346	1.940990791	3.839692535	0.0000000	-0.404543799	-1.323670281	0.2808000
10	*ndhF1*	Synpcc7942_1977	2.544074173	5.832337364	0.0000000	2.298356808	4.918971881	0.0000000
11	*ndhF3*	Synpcc7942_2091	3.573228604	11.90279602	0.0000000	2.976626132	7.871432065	0.0000000
12	*ndhF4*	Synpcc7942_0309	2.943269512	7.691524158	0.0000000	1.742393739	3.345898635	0.0000000
13	*ndhG*	Synpcc7942_1345	2.734601025	6.655748986	0.0000000	0.876219995	1.835559646	0.0302000
14	*ndhH*	Synpcc7942_1743	2.625119543	6.169354479	0.0000000	1.687435821	3.22083738	0.0000000
15	*ndh*I	*Synpcc7942_1344*	3.325216752	10.02282123	0.0000000	1.219249513	2.328255704	0.0015000
16	*ndh*J	*Synpcc7942_1182*	1.825959221	3.545426581	0.0000000	1.307659091	2.475395576	0.0000000

17	*ndh*K	*Synpcc7942_1181*	2.321366287	4.998053301	0.0000000	1.901245154	3.735354466	0.0000000
18	*ndh*L	Synpcc7942_0413	0.812749466	1.756555872	0.0456000	0.964702957	1.951661644	0.0002000
19	*ndhM*	Synpcc7942_1982	0.451073627	1.367057217	0.2224000	1.045634306	2.064273753	0.0000000
20	*cmpR*	*Synpcc7942_1310*	3.401999562	10.57070404	0.0000000	0.108704186	1.07825932	0.7166000
21	*cupA*	Synpcc7942_2093	3.935698698	15.30253431	0.0000000	0.914896852	1.885434265	0.0269000
22	*cupB*	*Synpcc7942_0308*	2.414751709	5.332276933	0.0000000	0.403537144	1.322746998	0.1281000